Neuropilins, relevant targets for the treatment of clear cell Renal Cell Carcinoma

Aurore Dumond

UNIVERSITÉ CÔTE D'AZUR

ÉCOLE DOCTORALE
SCIENCES DE LA VIE ET DE LA SANTÉ

THÈSE DE DOCTORAT

Les Neuropilines : des cibles pertinentes dans le traitement du cancer du rein à cellules claires

Aurore DUMOND

Centre Scientifique de Monaco

Présentée en vue de l'obtention du grade de docteur en Science de la vie et de la santé SVS

Spécialité : Recherche Clinique et Thérapeutique

d'Université Côte d'Azur

Dirigée par : Dr Gilles Pagès / Dr Renaud Grépin

Soutenue le : 04 décembre 2020

Devant le jury, composé de :

Dr Patrick Auberger, Directeur de Recherche, C3M

Dr Sergio Cantoreggi, Directeur scientifique, Helsinn

Pr Christian Cavé, Professeur CNRS, Université Paris-Saclay

Pr Christiane Garbay, Professeur CNRS, Université Paris-Descartes

Dr Renaud Grépin, Chargé de Recherche, Centre Scientifique de Monaco

Pr Agnès Noel, Professeur, Université de Liège

Dr Gilles Pagès, Directeur de Recherche, Centre Scientifique de Monaco / IRCAN

Dr Fabrice Soncin, Directeur de Recherche CNRS, Université de Lille

CSM CENTRE SCIENTIFIQUE DE MONACO

HELSINN
Building quality cancer care together

Les Neuropilines : des cibles pertinentes dans le traitement du cancer du rein à cellules claires

Jury :

Président du jury :

Dr Patrick Auberger, Directeur de Recherche, C3M

Rapporteurs :

Pr Agnès Noel, Professeur, Université de Liège
Pr Christian Cavé, Professeur CNRS, Université Paris-Saclay

Examinateurs :

Pr Christiane Garbay, Professeur CNRS, Université Paris-Descartes
Dr Fabrice Soncin, Directeur de Recherche CNRS, Université de Lille

Invité :

Dr Sergio Cantoreggi, Directeur scientifique, Helsinn

Directeurs de thèse :

Dr Renaud Grépin, Chargé de Recherche, Centre Scientifique de Monaco
Dr Gilles Pagès, Directeur de Recherche, Centre Scientifique de Monaco / IRCAN

RESUME

Les cancers du rein à cellules claires (ccRCC) représentent 80% des cancers du rein. Environ 80% des ccRCC présentent une inactivation/ mutation du gène de *Von Hippel-Lindau* (*VHL*), entraînant la stabilisation des facteurs inductibles d'hypoxie 1 et 2 alpha (HIF1 et 2α) et la surexpression de leurs gènes cibles tels que "le facteur de croissance vasculaire endothélial (VEGF)", le principal facteur d'angiogenèse.

Ainsi les ccRCC sont les cancers les plus vascularisés et représentent un paradigme pour les traitements anti-angiogéniques (AAT). Aujourd'hui, 15 différents AAT ont obtenu l'approbation de la FDA et de l'EMA. Ils sont divisés en trois familles :

- les anticorps ciblant les VEGFs

- les inhibiteurs de tyrosine-kinase (TKi), qui ciblent les récepteurs impliqués dans la néo-angiogenèse, tel que le sunitinib

- les récepteurs « leurres » qui piègent le VEGFA et le PlGF tel que l'aflibercept.

La surexpression du VEGF (impliqué dans l'angiogenèse), et des autres membres de la famille du VEGF, le VEGFC (impliqué dans la lymphangiogenèse) est un phénomène clé dans la tolérance immune. Ainsi, des inhibiteurs de points de contrôle immunitaire (anti PD-1, anti PD-L1 et anti CTLA-4) ont aussi obtenu l'approbation des autorités de santé pour le traitement des ccRCC.

En revanche, une rechute après quelques mois de traitement par les TKi est souvent observée et les inhibiteurs de points de contrôle immunitaire présentent une efficacité sur seulement 20% des patients. Ainsi, le ccRCC reste incurable chez une majorité de patients et de nouvelles stratégies thérapeutiques ciblant à la fois l'angiogenèse, la lymphangiogenèse et la tolérance immune sont nécessaires.

Les Neuropilines (NRP1 et NRP2) sont des corécepteurs de VEGF et de VEGFC et sont exprimés sur les cellules endothéliales vasculaires et lymphatiques, sur les cellules tumorales et sur les cellules du système immunitaire. Ainsi, les Neuropilines sont de nouvelles cibles pertinentes pour le traitement du ccRCC.

Ma thèse décrit la pertinence du ciblage des voies de signalisation NRP1 et NRP2 dans les ccRCC par une approche génétique (invalidation des deux gènes par CRISPR/Cas9) et par une approche pharmacologique (développement d'un inhibiteur des NRPs). Les résultats précliniques générés représentent une première étape essentielle pour l'initiation d'essais cliniques de phase précoce pour les patients en échec thérapeutique.

Mots clés : Neuropilines, Micro-environnement tumoral, Oncologie, Immunologie, Cancers

ABSTRACT

Clear cell Renal Cell Carcinoma (ccRCC) represent 80% of kidney cancers. Around 80% of ccRCC present an inactivation of the *von Hippel-Lindau gene* (*VHL*) gene, leading to the stabilization the Hypoxia Inducible Factors 1 and 2 alpha (HIF-1 and 2α) and to the overexpression of their targeted genes such as the « Vascular Endothelial Growth Factor (VEGF) », the principal angiogenic factor. Thus, ccRCC are one of the most vascularized cancers and represent a paradigm for anti-angiogenic treatments (AAT). Currently,15 different AAT have obtained FDA and EMA approval. They are divided in three different families:

- antibodies targeting VEGF
- tyrosine-kinase inhibitors (TKi) that target receptors involved in neo-angiogenesis such as the current reference therapy, sunitinib
- decoy receptors that trap VEGFA and PlGF such as aflibercept.

Overexpression of VEGF (involved in angiogenesis) and of the other member of the VEGF family, VEGFC (involved in lymphangiogenesis) is also a key phenomenon of immune tolerance. Therefore, immune-checkpoint inhibitors (anti PD-1, anti PD-L1 and anti CTLA-4) also obtained an approval for the treatment of ccRCC.

However, relapse on TKi are frequently observed after a few months and immune-checkpoint inhibitors present a long-lasting effect only in 20% of patients. Hence, ccRCC is still an uncurable disease and new therapeutic strategies targeting concomitantly angiogenesis/lymphangiogenesis and immune tolerance are urgently needed. Neuropilins (NRP1 and NRP2) are co-receptors of VEGF and VEGFC and are expressed on vascular and lymphatic endothelial cells, on tumor cells and on immune cells. Hence, they may represent ideal targets to inhibit the drivers of ccRCC aggressiveness.

My thesis describes the relevance of targeting the NRP1 and NRP2 signaling pathways in ccRCC by a genetic (invalidation of the two genes by CRISPR/Cas9) and by a pharmacological approach (development of a NRPs inhibitor). The preclinical results generated represent an essential first step for the initiation of early phase clinical trials for patients with treatment failure.

Keywords: Neuropilins, Tumoral microenvironment, Oncology, Immunology, Cancers

A mon Grand-père,

Et à ma Famille.

REMERCIEMENTS

Voilà 3 ans de passés (enfin même presque 4 avec le stage de Master)… DEJA ! La thèse c'est une très belle aventure enrichissante, professionnellement et personnellement ! Et tout ça grâce à VOUS tous qui m'avez entourée tout au long de ces 4 années (et même depuis plus longtemps pour certains !).

Je voudrais commencer par remercier tous les membres du jury d'avoir accepté d'évaluer ce travail.

Mon cher **Renaud**, merci pour tout ! Tout d'abord, de m'avoir pris sous ton aile dès mon stage de master 2 et de m'avoir clairement tout appris alors que je ne partais qu'avec 4 mois de théorie en Bio… Qu'est-ce qu'on aura rigolé en tout cas ! Sans toi, je n'en serai pas là… Certes tu m'as « abandonné » mais je sais que tu l'as fait parce que tu me faisais confiance et donc je ne pouvais pas te décevoir ! Beaucoup continueront de dire que tu m'as abandonnée, mais s'ils savaient à quels points tu as continué à être présent, ils changeraient très vite d'avis ! Quelle chance j'ai eu et j'ai de t'avoir eu sur mon chemin, que ce soit pour le boulot ou personnellement, tu es une personne formidable ! Merci d'avoir toujours été là professionnellement et personnellement (quel courage quand même haha !!!), d'avoir toujours le mot pour me faire rire et je sais que ce n'est pas sur le point de s'arrêter !!

Gilles, merci pour ta disponibilité et pour avoir su répondre présent lorsque j'en avais besoin. Merci pour toutes ces conversations à se casser la tête pour comprendre le pourquoi du comment on avait certains résultats et pour nos débats très enrichissants… Merci pour ton soutien, ton aide et tous tes bons conseils !

Luc, merci de m'avoir permis, dès mon master 2, de continuer à faire un peu de chimie au milieu de toute cette biologie, de m'avoir aussi accueilli pour faire des séminaires chez les parisiens et pour toutes nos conversations de chimistes ! Je me souviendrai du congrès JJC de Paris et de la belle organisation avec la croisière en péniche sur la Seine… Merci aussi de m'avoir présenté de nombreuses personnes qui ont participé à ce projet : **Etienne Brachet, Yves Lepelletier, Christiane Garbay, Nathalie Lagarde, Mathieu Montes, Françoise Raynaud, Philippe Belmont,** et je dois en oublier, désolée…

Mes compagnons de bureau/labo : **les deux équipes de BioMed** du CSM, ceux qui sont devenus un peu plus que de simples collègues, grâce à qui j'ai travaillé dans la bonne humeur et avec qui j'ai partagé beaucoup d'apéros !

Marina, la joie de vivre, la gentillesse et la chanteuse du labo. Quel plaisir de travailler avec toi dans la bonne humeur.
Valérie, merci pour ton aide sur certaines manips, heureusement que tu étais là et surtout c'est un plaisir de travailler avec toi, toujours aux petits soins !
Merci à toutes les deux pour votre présence, de m'avoir supporté pendant la rédaction et même en général d'ailleurs, faut me suivre des fois !!
Merci à **Sandy** aussi. Partie un peu plus tôt, donc déjà merci pour ton bureau 😉. Merci pour tes conseils scientifiques et la relecture de ce manuscrit !
Merci à toutes les trois, vous êtes devenues des amies sur qui je peux compter. Et où que j'aille après ma thèse, on se réservera des journées/soirées à chaque fois que je reviendrai dans le sud pour des vacances, c'est promis ! Vous me manquerez, ça c'est sûr !

Vincent, la force tranquille du labo, toujours prêt pour l'apéro ! Je garderai de bons souvenirs de ces apéros au son de votre musique, d'un certain retour à Nice en bateau… Merci aussi pour tes conseils scientifiques et ta relecture du manuscrit 😊 !

Jérôme, merci pour ton aide au labo, les CRISPR, le FACS qui ne veut jamais fonctionner quand il faut et surtout pour les manips souris avec **Chris.** Merci pour ta sympathie et ta gentillesse 😊. Et vive le NF 😉.

Miliça, Boutaina, **Giuditta** and **Scott,** who have been my office's companions for a long time and my companions for Fiesta and Apéroooo! **Miliça, Bou** and **Giu** I will remember all our nights out and our trip to Barcelona! Many adventures together 😉! Thank you to have been a part of my PhD life!

Chris, Shamir et **Guillaume,** votre arrivée a marqué un grand changement au labo ! Merci pour votre bonne humeur et vos jolis compliments quotidiens (ça fait toujours plaisir !). En tout cas j'aurai bien rigolé avec vous !!

Doria et **Willian,** les derniers arrivés au labo qui ont amené leur sympathie aux deux équipes.

Renaud (Grover)**,** tu mérites d'être intégré aux paragraphes de la BioMed 😉, toujours là pour les bons plans, apéros et toujours de bonne humeur ! Merci pour tous ces bons moments !

Merci à **Jacques Pouysségur** pour sa présence et les discussions que nous avons pu avoir sur le projet lors des différentes présentations.

Enfin un grand merci à tout le CSM pour l'accueil durant ces 4 années ! Notamment **Denis** et **Alexandra,** pour leur présence dès que j'en avais besoin.

Un merci aussi à l'**Institut de Chimie de Nice** pour leur accueil lors de mes manips de chimie et notamment à l'équipe du **Dr Rachid Benhida** : **Cyril, Lou** et **Marie** particulièrement !

I would like to thank **HELSINN Company** for their financial support and, most of all, the persons I have met who contributed to the project's progress: **Roberto De Ponti, Sandra Van Essche, Sergio Cantoreggi, Emmanuelle Rampal, Marianne Bjørdal** and **Mr Riccardo Braglia.**

Pour finir, un énorme merci à toute ma famille : **Papa, Maman, Mémé**. Je ne serai pas là sans vous, merci pour votre soutien de toujours, pour votre confiance et votre amour ! Je ne vous remercierai jamais assez pour tout ça… Je vous aime !
Karine, ma sœur, merci pour ta présence ! C'était cool de pouvoir vous voir toi et les « petits » tous les mercredis, ça me manquera !

Merci à tous mes amis présents et qui m'ont soutenu durant ces 4 ans et depuis même plus longtemps aussi ! **Claire,** qui a même partagé quelques mois au CSM avec moi, merci pour ton soutien quotidien indéfectible ; **Marine** et **Patricia**, les copines d'enfance et toujours là ; **Bastien, Thibaut, Thizy, Xavier, Annaëlle, Pauline, Séb, Claire** et **Max,** les copains lyonnais, nos week-ends retrouvailles étaient toujours des bouffées d'oxygène ; **Mathilde,** le soutien indéfectible même du Japon. Et tous les autres qui ont toujours été présents, ont toujours eu des petits mots et des pensées pour moi : **Emma, Marion, Léa, Sophie, Alicia…**

Et enfin un énorme merci à mon chéri, **Jojo**, merci pour tout, pour ton soutien, pour m'avoir supporté au quotidien et j'avoue que ça ne devait pas être facile tous les jours surtout sur la fin de cette thèse ! Merci d'avoir toujours été aux petits soins pour moi ! Le meilleur reste à venir pour tous les deux ! Je t'aime.

Je m'excuse pour ceux que j'aurai oublié… !

Mais Merci à vous tous qui avez contribué de près comme de loin à tout ça !

TABLE OF CONTENT

TABLE OF CONTENT
TABLE OF CONTENT **13**
TABLE OF FIGURES **17**
ABBREVIATIONS **19**
PART I: INTRODUCTION **21**
I) Clear cell Renal Cell Carcinoma (ccRCC) **23**
1) Statistics 23
2) Risk factors 23
3) Diagnosis 23
4) Treatments 23
II) Tumoral angiogenesis **25**
1) Vascular organization 25
1.1 Vasculogenesis 26
1.2 Angiogenesis 26
1.3 Principal mechanisms of angiogenesis 27
1.4 Tumoral angiogenesis 29
2) VEGFA 30
3) The VEGF receptors 31
3.1 Receptor structure 31
3.2 VEGFR1 32
3.3 VEGFR2 32
4) Current anti-angiogenic treatments or immunotherapies for ccRCC 33
4.1 Choice of the treatments ***(Figure 6)*** 33
4.2 First-line treatments 34
4.3 Second-line treatments 34
4.4 Third-line treatments 35
4.5 Overview of the treatments' efficacy and safety 35
4.6 Anti-angiogenics and immunotherapies combinations 38
4.7 Conclusion on current treatments 38
5) Resistance mechanisms to targeted therapies 39
5.1 Redundant angiogenic pathways 39
5.2 Hypoxia 41
5.3 Increased lymphatic network 43
III) Tumoral lymphangiogenesis **44**

1) Lymphatic system 44
2) Lymphangiogenesis 44
3) VEGFC and VEGFR3 45
4) Tumor lymphangiogenesis ***(Figure 9)*** 45
5) Lymphangiogenesis role in resistance to sunitinib 46
IV) Neuropilins: Generalities 48
1) Genomic organization and protein structure 48
2) The phenotype of knock-out mice 49
3) Neuropilins' ligands and interactors 49
3.1 SEMA3/Plexin 49
3.2 VEGF/VEGFR 49
3.3 PlGF/VEGFR 50
3.4 HGF/cMET 50
3.5 TGFβ1/TGFβR 50
3.6 PDGF/PDGFR 51
3.7 FGF/FGFR2 51
3.8 Galectins 51
3.9 EGF/EGFR 51
3.10 Hedgehog signaling pathway 51
3.11 Integrins 52
3.12 Conclusion on NRPs' ligands ***(Figure 11)*** 52
V) Neuropilins and the immune system *(Figure 12)* 53
1) Dendritic cells (DC) 53
2) Macrophages 53
3) T cells 54
3.1 Cytotoxic T cells (T $CD8^+$) 54
3.2 Helper T cells (T $CD4^+$) 54
3.3 NKT cells 54
3.4 Regulatory T cells (Treg) 54
VI) Neuropilins and cancers 58
1) Functions of NRPs in cancer 58
2) Role in cancer stem cells 59
3) Role in cancer-associated fibroblasts (CAF) 59
4) Prognostic role of NRP1 and NRP2 pathways 60
5) Role in the therapeutic response 60
5.1 Resistance to chemo- and radiotherapies 60

5.2 Resistance to targeted therapies 60
VII) NRPs inhibitors 62
1) MNRP-1685A antibody 62
2) Peptides and pseudo-peptides 62
2.1 Structural basis to determine NRP1 and NRP2 chemical inhibitors 62
2.2 A7R heptapeptide and its derivates 63
2.3 EG3287 and its derivates 63
3) Non-peptidic inhibitors selected by multi-step screening 64
3.1 Identification of the Chembridge compound (ID: 7739526), not tested *in-vivo* 64
3.2 NRPa-47 and NRPa-308, two non-peptidic NRP1 antagonists active *in-vivo* 64
VIII) NRPa-308 66
1) Screening of NRPa-47 and NRPa-308 66
2) Screening that has led to the selection of NRPa-308 66
3) Docking experiments of NRPa-308 67
4) Functional evaluation of NRPa-308 67
PART II: OBJECTIVES 69
PART III: RESULTS 73
ARTICLE 1 75
I) Scientific context and objectives 77
II) Results 78
1) NRPa-308 synthesis optimisation 78
2) NRPa-308 3D structure 79
3) NRPa-308 stability 79
III) Conclusion and perspectives 80
ARTICLE 2 103
I) Scientific context and objectives 105
II) Results 106
1) NRPs' down-regulation by shRNA 106
2) NRPs knock-out by CRISPR/Cas9 107
3) NRPs inhibition by NRPa-308 107
III) Conclusion and perspectives 108
PART IV: DISCUSSION 161
I) Current ccRCC treatments 163
II) Hallmarks of Cancer 163
III) Neuropilins: new target involved in many cancer hallmarks 165
IV) Genetic modulation by shRNA and CRISPR/Cas9 165

1) NRPs genetic down-regulation by shRNA 165
2) NRP genetic invalidation by CRISPR/Cas9 166
3) Conclusion 166
V) Inhibition by NRPa-308 compound 167
1) NRPa-308 *in-vitro* efficacy on ccRCC cells 167
2) NRPa-308 *in-vivo* effects on breast cancer cells 168
3) NRPa-308 *in-vivo* effects on ccRCC cancer cells 168
4) On what depends NRPa-308 efficacy? 168
5) Conclusion 171
VI) Effects of NRPa-308 on the immune system response 171
1) *In-vivo* tests with NRPa-308 171
2) Conclusion 172
VII) Combination of NRPa-308 with immune checkpoints inhibitors 172
VIII) *In-vivo* ccRCC metastatic models 173
IX) *In-vivo* ccRCC angiogenic models 176
X) NRPa-308 *in-vivo* bioavailability at the tumor 177
XI) Targeting specifically NRP1 177
XII) Parallel studies on NRPa-47 178
PART V: CONCLUSION 181
REFERENCES 185
APPENDICES 197
Appendix 1. ccRCC treatments' chemical structure. 199
Appendix 2. NRPs inhibitors' chemical structure. 201
Appendix 3. Article 3 203
Appendix 4. Review 1. 219
Appendix 5. Review 2. 231
Appendix 6. Patent: New anti-VEGFC antibodies and uses thereof. 243

TABLE OF FIGURES

Figure 1. ccRCC one of the most vascularized cancers 25
Figure 2. Angiogenesis mechanisms 29
Figure 3. Tumoral angiogenesis. 30
Figure 4. VEGFA's different splicing. 31
Figure 5. Anti-angiogenics's year of approval by the authorities 33
Figure 6. ccRCC treatments choice 35
Figure 7. Redundant angiogenic pathways. 40
Figure 8. Lysosomal sequestration of tyrosine-kinase inhibitors. 43
Figure 9. Tumoral lymphangiogenesis 46
Figure 10. Neuropilins' different isoforms. 48
Figure 11. mRNA levels of NRPs' ligands in ccRCC and in normal kidney tissues [93] 52
Figure 12. Role of NRPs in the activation or suppression of the immune system 57
Figure 13. NRPa-308 synthesis route 77
Figure 14. Optimisation of NRPa-308 synthesis route 78
Figure 15. NRPa-308 chemical structure. 79
Figure 16. mRNA levels of VEGFA, VEGFC, NRP1 and NRP2 in kidney and breast cancer cell lines. 169
Figure 17. Influence of NRP2 protein level on NRPa-308 effects 170
Figure 18. NRPa-47 inhibitor 178
Figure 19. NRPa-47 structure optimizations 179

All the images from the figures come from Servier Medical Art.

ABBREVIATIONS

ABCB1	ATP-binding cassette, sub-family B, member 1
AKT	Protein kinase B
Ang1	Angiopoietin 1
ATCC	American Type Culture Collection
BSA	Bovine Serum Albumine
CAF	Cancer Associated Fibroblast
CAM	Chorioallantoic Membrane
ccRCC	clear cell Renal Cell Carcinoma
c-KIT	Stem cell growth factor receptor
CSC	Cancer Stem Cells
CSF1R	Colony Stimulation Factor 1 receptor
CTLA-4	Cytotoxic T Lymphocyte Associated protein 4
CXCL	C-X-C motif chemokine
CXCR	C-X-C motif chemokine receptor
DC	Dendritic cells
DNA	Desoxyribonucleic acid
EGF	Endothelial Growth Factor
EMA	European Medical Agency
EMT	Endothelial-Mesenchymal Transition
EPC	Endothelial Progenitor Cells
ERK	MAP Kinase/Extracellular signal regulated kinase
FAK	Focal Adhesion Kinase
FDA	Food and Drug Agency
FGF	Fibroblast Growth Factor
FGFR	Fibroblast Growth Factor Receptor
Flk1	Fetal Liver Kinase 1
Gal-1	Galectin-1
GAM	Glioma Associated Macrophages
GFP	Green Fluorecent Protein
HDF	Normal Dermal Fibroblast
HGF	Hepatocyte Growth Factor
HIF	Hypoxia Inducible Factor
HRP	Horseradish Peroxidase
IC_{50}	Half maximal inhibitory concentration
IFNα	Interferon α
IGF	Insulin like Growth Factor
IL	Interleukine
IMDC	International Metastatic Renal Cell Carcinoma Database Consortium
Kd	Constance de dissociation
KO	Knockout
Luc	Luciferase
MAPK	Mitogen-Activated Protein Kinases
mccRCC	metastatic clear cell Renal Cell Carcinoma

MET	Mesenchymal-Epithelial Transition
MHC	Class I Major Histocompatibility Complex
mRNA	messenger Ribonucleic Acid
mTOR	mechanistic Target Of Rapamycin
NRP	Neuropilin
OS	Overall Survival
PBS	Phosphate Buffered Saline
PD-1	Programmed-Death 1 receptor
PDGF	Platelet-derived Growth Factor
PDGFR	Platelet-derived Growth Factor Receptor
PD-L1	Programmed Death Ligand 1
PDX	Patients Derived Xenograft
PEI	Polyethylenimine
PFS	Progression-Free Survival
PlGF	Placenta Growth Factor
PPC	Pericytes Progenitor Cells
Prox1	Prospero homeobox 1
qPCR	quantitative Polymerase Chain Reaction
RECIST	Response Evaluation Criteria In Solid Tumors
SDF1	Stromal cell-Derived Factor 1
SEMA	Semaphorin
sgRNA	single guide Ribonucleic Acid
shRNA	short-hairpin Ribonucleic Acid
SI	Selectivity Index
T CD4+	Helper T cells
T CD8+	Cytotoxic T cells
TAM	Tumor Associated Macrophages
TBS	Tris-Buffered Saline
TCGA	The Cancer Genome Atlas
TGFβ	Transforming Growth Factor beta
TGFβR	Transforming Growth Factor beta Receptor
Tki	Tyrosine Kinase inhibitor
TNFα	Tumor Necrosis Factor alpha
Treg	Regulatory T cells
VEGF	Vascular Endothelial Growth Factor
VEGFR	Vascular Endothelial Growth Factor Receptor
VHL	Von-Hippel Lindau
WDFY1	WD-repeat and FYVE-domain-containing protein 1
α SMA	α Smooth-Muscle Actin

PART I: INTRODUCTION

INTRODUCTION

I) Clear cell Renal Cell Carcinoma (ccRCC)

1) Statistics

Kidneys are mainly involved in blood filtration to eliminate waste and toxins from the organism. Only one form of pediatric kidney cancer exist: nephroblastoma or Wilms tumor, which concerns around 120 new cases every year in France. Then, most of kidney cancers developed in adults with around 12000 new cases per year in France and 350000 in the world, represent the seventh type of most frequent cancer and ninth cause of death from cancer. Two third of cases are men of 40 years old and more and the frequency of diagnoses increases with the age. Different forms of kidney cancers exist, among them the clear cell Renal Cell Carcinoma that represent around 80% of kidney cancers [1]. ccRCC owns a clear cytoplasm resulting from accumulated glycogen, phospholipids and neutral lipids [2]. This accumulation of glycogen is notably correlated to patient's poor prognosis [3].

2) Risk factors

Different factors can increase a person's cancer risk:

- The personal history: renal failure or dialysis increase the kidney cancer's risk of about 10 times [1];
- Smoking (risk increased by 2) [1] or environmental factors: professional exposition to cadmium, hydrocarbon for example [1]
- Family predispositions: most of kidney cancers has no hereditary origin but around 1 to 2% of ccRCC involve heredity factors with the mutation of the *Von Hippel-Lindau* (*VHL)* gene [1].

3) Diagnosis

The first stages of kidney cancer are asymptomatic. Thus, the diagnosis comes lately in the development of the disease and most of the time following abdominal echography carried out for another reason [1]. Later, imaging (scanner or magnetic resonance imaging) and pathological exams confirm the cancerous nature of the mass detected by imaging, the subgroup of RCC and the presence of metastases [1].

4) Treatments

For non-metastatic patients (M0), surgery by cyto-reductive nephrectomy is carried out followed by regular scanner monitoring [1].

ccRCC are radio- and chemo-resistant, which could be explained by the decrease, in most ccRCC, of p53 (transcription factor involved in cell cycle regulation, autophagy and apoptosis) expression through the stabilisation of HIF-2α [4].

For patients with metastatic (M1) ccRCC (mccRCC), surgery was the rule since recently. However, the dogma is changing since surgery does not improve either progression free survival (PFS) nor overall survival (OS) [5]. Thus, M1 patients are treated by immunotherapies or anti-angiogenics, that are chosen according to the patient's prognostic [1]. This part will be developed later *(II-4)Current anti-angiogenic treatments or immunotherapies for ccRCC)*.

II) Tumoral angiogenesis

ccRCC is one of the most vascularized cancers. In around 80% of the cases, the *von Hippel Lindau* gene (*VHL*) is inactivated leading to the stabilization of Hypoxia Inducible Factor 1α and 2α (HIF1/2 α). After dimerization with HIF1β, the resulting HIF stimulates the transcription of target genes such as the main pro-angiogenic factor Vascular Endothelial Growth Factor A (VEGFA), the immune suppressive Programmed Death Ligand 1 (PD-L1) and the Platelet-derived Growth Factor (PDGF) ***(Figure 1)*.**

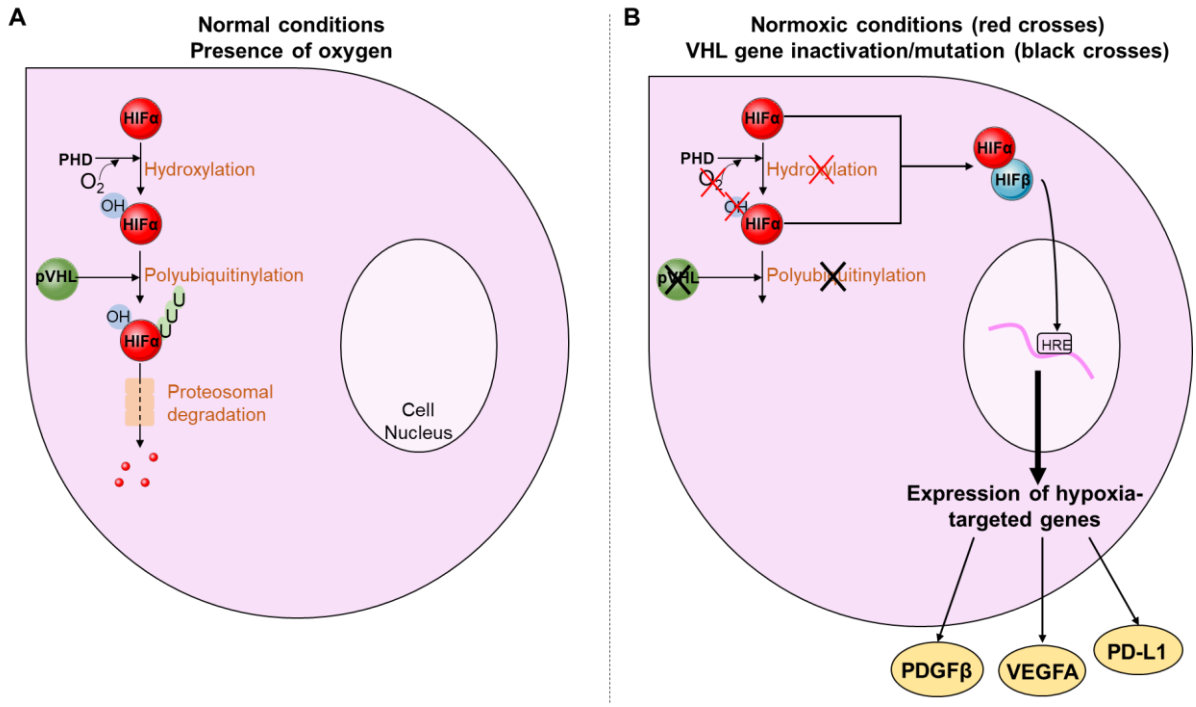

Figure 1. ccRCC one of the most vascularized cancers. **A.** In normal condition, the hypoxia inducible factor α (HIFα) is hydroxylated and the Von-Hippel-Lindau factor induces its degradation by the proteasome. **B.** In normoxic conditions (red crosses) or when the *von Hippel-Lindau* gene is inactivated (black crosses), HIFα is no more hydroxylated or does not undergo polyubiquitination. Thus, HIFα is stabilized and forms a complex with HIFβ. The resulting active transcription factor induces the expression of its target genes such as VEGFA, PD-L1 and PDGFβ.

1) Vascular organization

Blood vessels are organized in arteries, veins and capillaries, that have different morphologies according to their functions. During early embryonic development, cells from the mesoderm differentiate into hemangioblasts: multipotent precursor cells of hematopoietic and endothelial cells forming the blood vessels [6]. Blood vessels are composed of endothelial and mural cell: blood vessels' wall is composed of endothelial cells forming a monolayer. Their cohesion is mediated by VE-cadherins enabling cell-cell adhesion [6]. Endothelial cells are bound to a basal membrane and mural cells, such as pericytes covering the vessels, prevent hyperpermeability

and vascular leakage [7]. Already at this stage, capillaries differentiate in arteries or veins [6]. Arteries are formed by multiple concentric layers of vascular smooth muscle cells to support the high-pressure mediated by the transport of blood to the capillaries. However, veins, that are exposed to a lower blood pressure, are formed by thinner smooth muscle cells' layers [7]. Blood vessels of a smaller diameter, such as arterioles, capillaries or venules, are covered by support cells such as pericytes. They are involved in the blood vessels' maturation and stabilization and in endothelial cells' differentiation and proliferation [7]. The formation of blood vessels is an essential physiological mechanism. During embryogenesis, tissue growth needs oxygen and nutrients. Thus, vasculogenesis is set up and enables the formation of the primary vascular network [7]. Blood vessels are also involved in organs morphogenesis and in the elimination of metabolic waste. The vascular network formation is also important during post-natal development and in adults during wound healing, menstrual cycle and placenta's formation. However, it plays a key pathological role in cancers [7]. Two distinct mechanisms exist: vasculogenesis and angiogenesis.

1.1 Vasculogenesis

During the development, vasculogenesis is the formation of primitive blood vessels from angioblastic precursors. Vasculogenesis is the differentiation of hemangioblasts to angioblasts that will differentiate in endothelial cells. Endothelial cells will form a primary vascular plexus composed of blood vessels interconnected with homogenised size [6]. Vasculogenesis occurs in extra- and intra-embryonic tissues. The migration capacities of endothelial cells and of the angioblastic precursors are essential for the formation of the first blood vessels in the embryo. Vasculogenesis needs soluble growth factors such as VEGFA and the Fibroblast Growth Factor 2 (FGF2). Vasculogenesis is not only observed during embryogenesis but it occurs also in adults physiologically and pathologically. Indeed, in the adults, new blood vessels originate from bone marrow endothelial progenitors.

1.2 Angiogenesis

Angiogenesis is the formation of new blood vessels from the existing vascular network during the development but also in adults. During embryogenesis, the primary vascular plexus is modified by budding to form a mature vascular network. In adults, physiological angiogenesis occurs during wound healing, menstrual cycle or muscular exercise. Thus, angiogenesis is a transient phenomenon that is regulated by a fragile balance between pro- and anti-angiogenic factors [6]. This balance is deregulated in ischemic heart diseases (decreased angiogenesis) or

in cancers (up-regulated angiogenesis). Angiogenesis is involved in around seventy different pathologies.

The principal pro-angiogenic factor VEGFA induces angiogenesis by stimulating VEGF receptors (VEGFR1/2), and VEGF co-receptors, the Neuropilins 1 and 2 (NRP1/2).

1.3 Principal mechanisms of angiogenesis

1.3.1 Budding angiogenesis ***(Figure 2)***

Budding angiogenesis occurs through pro- and anti-angiogenic factors and through different cellular types. Neovessels' growth necessitates four steps from pre-existing vessels' sides or extremities.

- Vasodilatation and vascular permeabilization

The interactions between the endothelial cells, the extracellular matrix and the pericytes become weaker. Thus, endothelial cells are more sensitive to growth factors produced by cells, such as the VEGFA. The VEGFA induces vessels dilatation and vascular permeability by redistributing intracellular molecules like VE-cadherins. It enables endothelial cell migration through vascular wall. Furthermore, matrix metalloproteases and proteases from the plasminogen-protease activator system enable the degradation of the extracellular matrix and of the basal membrane.

- Endothelial cell activation and proliferation

The degradation of the extracellular matrix and of the basal membrane induces the release of FGF2 and VEGFA. They trigger cell proliferation and migration through a VEGFA gradient and chemotaxis [6]. The migration of endothelial cells also involves integrins (αvβ3, αvβ5, α5β1). To prevent the formation of an anarchic vascular network, only few endothelial cells initiate the angiogenic expansion from the capillaries. These "tip-cells" occupy the leading position to initiate angiogenesis. When tip-cells are stimulated by angiogenic factors, they acquire invasion and migration capacities but they secrete also proteases enabling the destruction of the adjacent basement membrane [6]. The selection of tip-cell is regulated by [6]:

- **VEGFA** expression that will activate the angiogenic stimuli and affects endothelial cells
- Tip-cells' characteristics are obtained by endothelial cells that do not express **Notch1**. Indeed, the activation by Dll4 of endothelial cells expressing Notch1 inhibits their transition to the activated state and so limits the number of tip-cells to prevent anarchic vessel formation. Thus, Dll4 or Notch1 lower expression results in the formation, branching and fusion of newly formed vessels. Then tip-cells sprout towards VEGFA gradient.

- Vascular tubules formation

Then, endothelial cells adhere to each other to form the new vessels. VEGFA and angiopoietin 1 (Ang1) are involved in regulating the new tubule diameter. The integrins αvβ3 and α5β1 enable interactions between endothelial cells and the extracellular matrix.

- Vascular stabilisation

The new vessels are stabilized by the recruitment of accessory and mural cells (pericytes and smooth muscle cells) and by the formation of a common extracellular matrix between endothelial and mural cells [6]. Pericytes are present around the capillaries and smooth muscle cells next to arterioles and venules and inhibit endothelial cells proliferation and migration [6]. These two cell types form multiple layers around the endothelial lining and control the vasodilatation and the blood pressure [6]. Blood vessel stabilization is also regulated by several factors: PDGFβ, whose secretion is stimulated by VEGFA. It is highly expressed by tip-cells. The stimulation of its receptor PDGFR-β induces mural cell proliferation and migration [6]. TGFβ1 induces the contact between endothelial cells and pericytes. It inhibits tip-cells proliferation and migration and consequently the stabilization of the newly-formed vessels [6]. Ang-1, expressed by pericytes and smooth muscle cells, stimulates its receptor Tie2, present on endothelial cells. Tie2 activation stabilizes the interactions between mural and endothelial cells during the formation of the vascular tubule [6]. Finally, Notch is involved in the maintenance of vessel integrity by enabling the vessels' coverage by smooth muscles cells [7].

1.3.2 Other mechanisms

Some tumors develop in vascularized organs, like the brain. In this case, they do not rely on angiogenesis for oxygen and nutrient supply. Indeed, the astrocytoma surround the blood vessels and develop invasive but non-angiogenic tumors. The blood vessels in contact with the tumor are reduced and tumoral ischemic zones appear. The resulting hypoxia stimulates the production of the growth factors VEGFA and FGF2 and of classical angiogenesis.

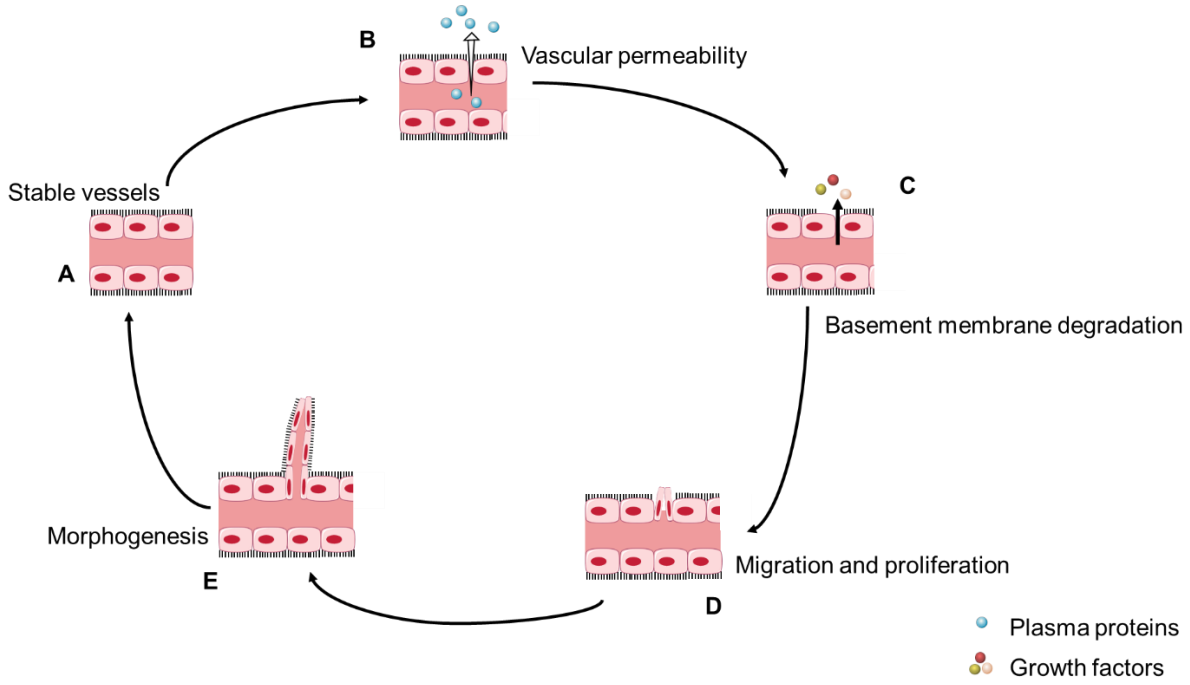

Figure 2. Angiogenesis mechanisms. Stable vessels **(A)** undergo vascular permeability, which induces plasma proteins' release **(B)**. The degradation of the membrane **(C)** decreases pericytes and endothelial cells contact and releases growth factors. Tip-cells proliferate and migrate according to the VEGFA gradient **(D)** and new vessels are formed **(E)** and stabilized with mural cells. *Adapted from B. A. Bryan et P. A. D'Amore **[8]**.*

1.4 Tumoral angiogenesis

To grow over a few millimetres, tumors need oxygen and nutrients. By providing these essential elements, tumoral angiogenesis is an important contributor of tumor development [6]. Thus, peri-tumoral angiogenesis stimulates tumor growth and dissemination and participates in the elimination of metabolic wastes. Angiogenesis enables the tumor to metastasize, but it does not give its malignant characteristic. Indeed, an aggressive tumor can present a low vascularization and a tumor of low grade can present an important vascularization. This suggests that after tumoral angiogenesis induction, the neo-vascularisation depends on a finely regulated production of pro-angiogenic factors by tumor cells and cells of the microenvironment [9,10].

During the angiogenic switch, tumor cells produce pro-angiogenic factors, such as VEGFA, FGF2, TGFβ, EGF or TNFα, that stimulate endothelial cell proliferation, migration and differentiation needed for vessel formation. The angiogenic switch occurs only when tumors produce more pro-angiogenic factors than anti-angiogenic factors ***(Figure 3)***. This imbalance occurs following genetic modifications of tumor cells (oncogene activation) or during environment changes (hypoxia or inflammation for example).

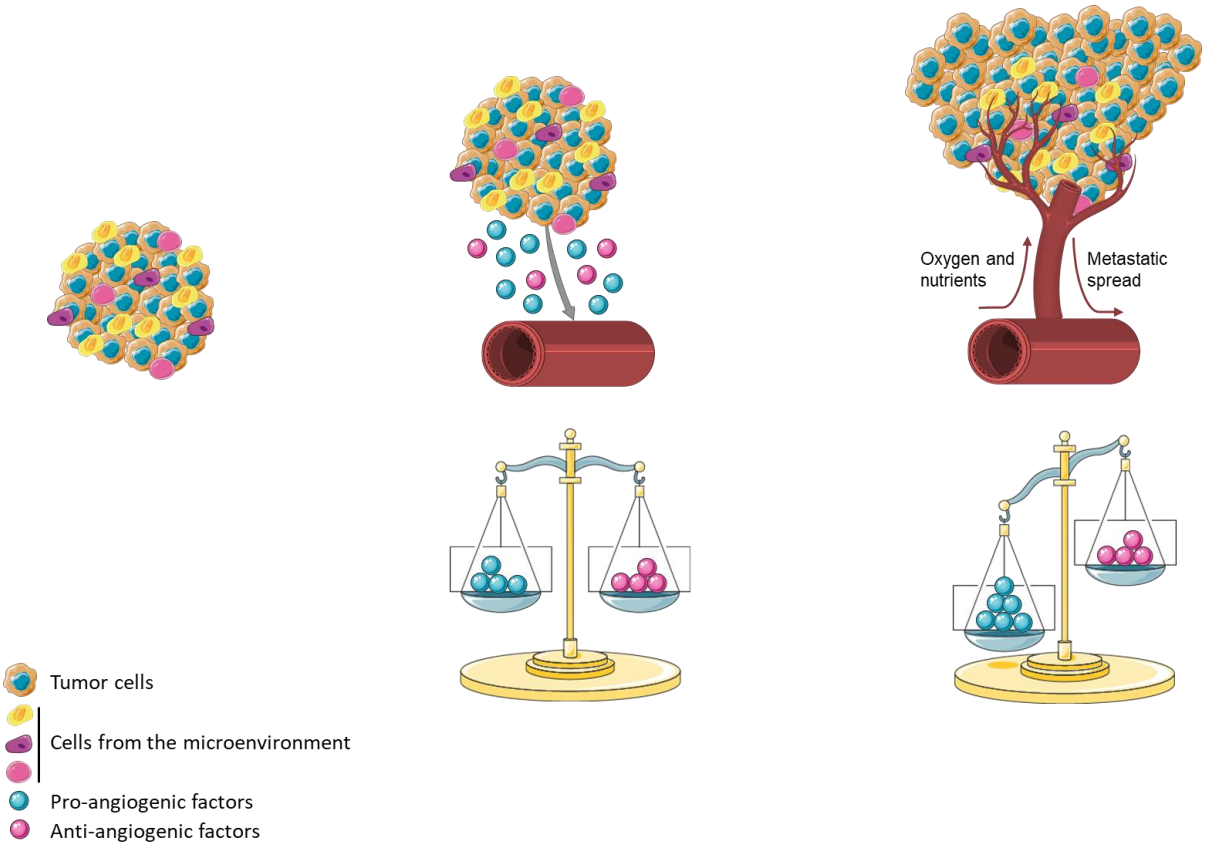

Figure 3. Tumoral angiogenesis. The production of pro-angiogenic factors by tumor cells deregulates the angiogenic balance. The resulting angiogenic switch enables the transport of oxygen and nutrients to the tumors leading to its growth and its metastatic spread through the newly formed blood vessels.

2) VEGFA

Several factors are known as positive activators of angiogenesis, but the VEGFA is the critical regulator [6]. In healthy people, VEGFs are involved in wound healing and vascular homeostasis. However, a high level of VEGFs promotes tumor angiogenesis and lymphangiogenesis (the formation of lymphatic vessels) and is synonymous of poor prognosis in cancers [11]. In most of ccRCC cases, inactivation of the *VHL* gene leads to the upregulation of HIF1/2 target genes such as, VEGFA. The VEGFA gene is composed of 8 exons: exons 1 to 5 code for the binding domain to VEGFRs and exons 7 and 8 encode the binding domain to the co-receptors, Neuropilins (NRPs) [6]. Different splices occur in exons 6, 7 and 8 giving rise to different isoforms. Furthermore, exon 8a generates pro-angiogenic isoforms whereas exon 8b generates anti-angiogenic isoforms ***(Figure 4)*** [12]. Four predominant forms of VEGFA exist: VEGF121, VEGF189, VEGF206 and the more abundant and active in many cancers, the VEGF165 [6]. VEGF165 binds to VEGFR1 (Kd= 2-10pM) and to VEGFR2 (Kd= 75-125pM), expressed by endothelial cells in the tumor microenvironment. Their stimulation activates the MAP Kinase/Extracellular signal regulated kinase (ERK) and protein kinase B (AKT) signaling pathways that enhances proliferation and consequently angiogenesis [6]. VEGFA stimulates

also the differentiation of hemangioblasts to hematopoietic cells [6]. VEGFA also binds to NRPs and preferentially to NRP1 (Kd= 0.2nM) as compared to NRP2 (Kd= 0.5nM). Thus, many anti-angiogenic treatments target the VEGFA/VEGFR pathway to reduce tumoral angiogenesis and to decrease tumor progression. The different existing anti-angiogenic treatments will be described later *(4) Current anti-angiogenic treatments or immunotherapies for ccRCC)*.

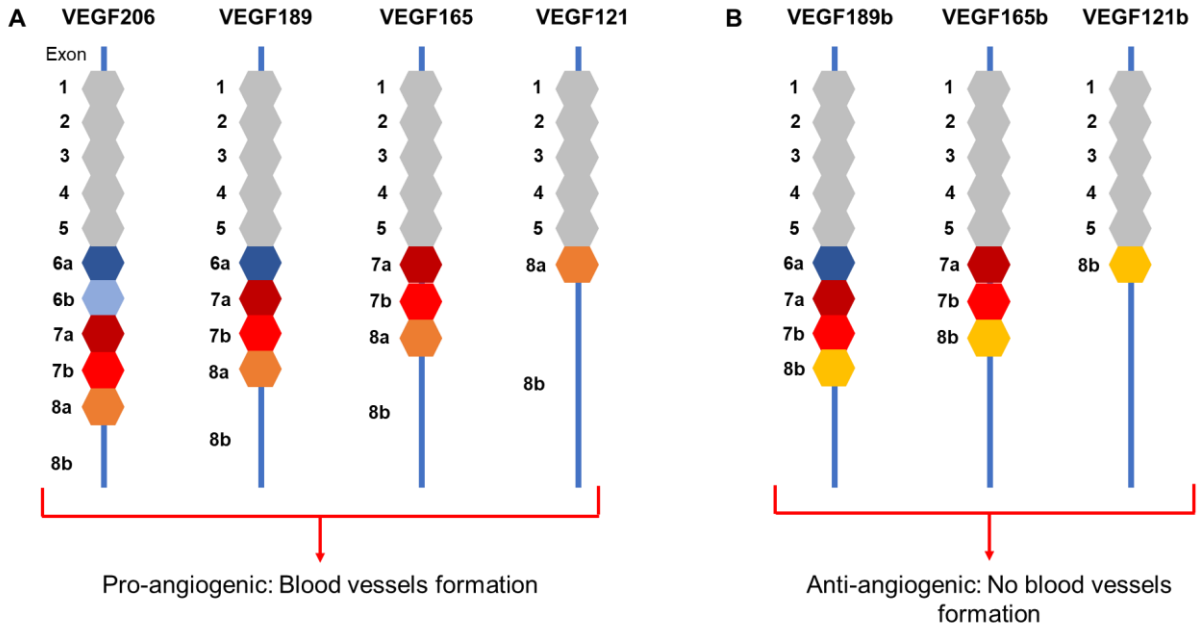

Figure 4. VEGFA's different splicing. VEGFA undergoes different splicing in exons 6 to 8 giving different forms of VEGFA, the main one being the VEGF165. **A.** VEGFA forms expressing the exon 8a are pro-angiogenic. **B.** VEGFA forms expressing the exon 8b are anti-angiogenic.

3) The VEGF receptors

Three VEGF receptors exist: VEGFR1 (Flt1), VEGFR2 (KDR) and VEGFR3 (Flt4). All of them participate in angiogenesis, but only VEGFR2 and 3 stimulate lymphangiogenesis.

3.1 Receptor structure

The VEGFRs are composed of [6]:

- An extracellular domain formed by seven immunoglobulin-like loops on which VEGFA binds
- A transmembrane domain mediating dimer formation
- A tyrosine-kinase activity intracellular domain separated in two fragments TK-1 and TK-2 by an inter-kinase insert
- A C-terminal extremity inducing signaling pathways activation

VEGFA binding on one of these receptors induces their homo- or heterodimerisation stabilized by contacts between the immunoglobulin-like domains. Dimerization stimulate trans-phosphorylation of the intracellular domains and an optimal phosphorylation of the intracellular substrates [13,14]. These phosphorylation events activate different signaling pathways such as the ERK and AKT pathways involved in survival, proliferation or migration phenomena [15].

3.2 VEGFR1

VEGFR1 or Flt1 (fms-like tyrosine kinase) is expressed by the endothelial cells, monocytes, macrophages, dendritic cells and by different cancer cells such as breast cancers. VEGFR1 knock-out (KO) mice die at the embryonic age of 9 days due to the formation of an anarchic and dysfunctional vascular network. The VEGFA, VEGFB and PlGF bind to the VEGFR1 but only the VEGFA can bind both VEGFR1 and VEGFR2.

The VEGFA has a better affinity for VEGFR1 as compared to VEGFR2 [16]. However, VEGFA stimulates a very weak VEGFR1 autophosphorylation [6] and VEGFR1 tyrosine-kinase activity is less important [17]. Its high affinity for VEGFA, the presence of VEGFR1 soluble forms and the VEGFR1's capacity to form heterodimers with the VEGFR2 make VEGFR1 a natural down-regulator of the VEGFR2 signaling pathway [18]. After VEGFA binding to VEGFR1, two signaling pathways are activated: ERK involved in proliferation and in p53 phosphorylation and AKT implicated in reducing apoptosis, and consequently, in angiogenesis and inflammation. Following its stimulation, VEGFR1 is internalized and degraded.

3.3 VEGFR2

VEGFR2 or KDR (kinase insert domain receptor) or Flk1 (fetal liver kinase 1) is principally expressed by vascular endothelial cells, but also, at lower levels, by ductal pancreatic, retinal progenitor, hematopoietic cells and by some cancer cells, for example colon or breast cancers. VEGFR2 levels are 3 to 5 times more important in tumor vessels than in normal ones [19]. In endothelial cells, *VEGFR2* gene expression is stimulated by VEGFA, which further enhances their proliferation [20]. A soluble form of VEGFR2, sVEGFR2, binds to VEGFC preventing its interaction to VEGFR3, which decreases lymphangiogenesis [21]. sVEGFR2 plasmatic levels decrease by 30% in ccRCC patients treated by one of the current reference therapies, sunitinib [22]. VEGFR2 KO mice die at the embryonic age of 8.5/9.5 days due to a hematopoietic system and endothelial cells defects [6]. VEGFR2-dependent signaling pathways are involved in mitosis, migration and survival [6].

The third VEGFA receptor, VEGFR3, is mainly involved in lymphangiogenesis. Its role will be discussed in the corresponding chapter (3) *VEGFC and VEGFR3*).

Thus, ccRCC is one of the most vascularized cancer due to its overexpression of VEGFA factor involved in many steps on angiogenesis, as explained in this part. Thus, today ccRCC treatments are mainly anti-angiogenics, which are targeting the VEGF/VEGFR pathways.

4) Current anti-angiogenic treatments or immunotherapies for ccRCC

4.1 Choice of the treatments ***(Figure 6)***

Interleukin-2 and/or interferon α (IFNα) were the first treatments used to treat metastatic ccRCC (mccRCC) but only few patients (about 11 to 17%) were responsive [23]. They are considered now as “old” immunotherapies. Despite their high vascularization, ccRCC became eligible for anti-angiogenic drugs in 2007 after colon, lung and breast cancers. Different families of treatments including anti-angiogenics or next generation immunotherapies are approved for mccRCC:

- Tyrosine-kinase inhibitors (TKi)
- mTOR inhibitors
- Anti VEGF antibodies (combined with immunotherapies)
- Immunotherapies

These treatments are used up to the fourth line after relapse and increase survival, but long-term remissions are still rare. During the last 15 years, up to 15 treatments have been approved by the competent authorities ***(Figure 5)***.

.

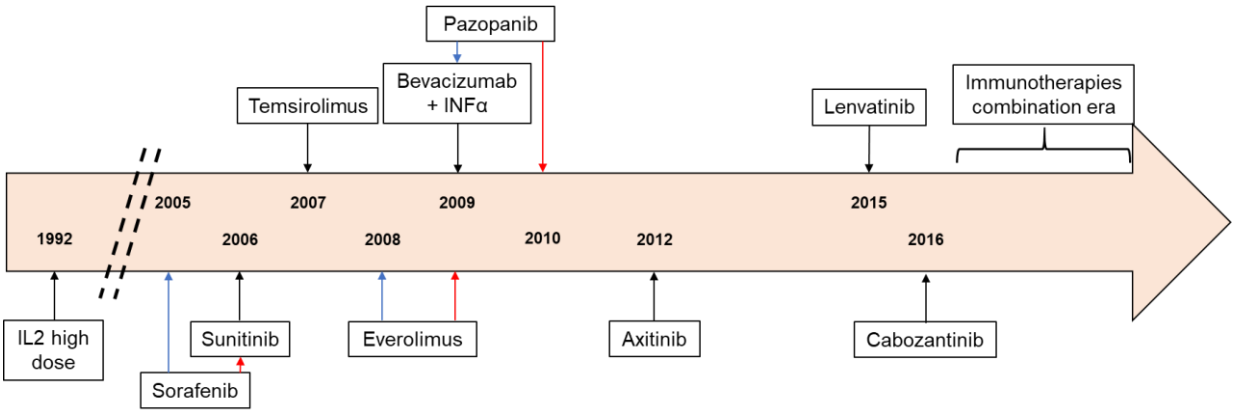

Figure 5. Anti-angiogenics’s year of approval by the authorities. Food and Drug Administration (FDA) ***[24]*** (blue arrows) or European Medical Agency (EMA) ***[25]*** (red arrows) sites for the dates of approval. Black arrows indicate the same year of approval for both agencies.

The optimal treatment is chosen according to a score established by the International Metastatic Renal Cell Carcinoma Database Consortium (IMDC) [26]:

- Karnofsky Performance Status Scale, which represents the patient's capacity to carry out all the daily tasks
- Less than a year passed between the diagnosis and the start of mccRCC treatment
- Calcium rate is abnormally high
- Number of blood cells lower than normal
- Number of platelets superior to normal
- Neutrophils rate abnormally high

From these parameters, a good (0 parameter), intermediate (1 to 2 parameters) or bad (3 to 6 parameters) prognostic is established.

4.2 First-line treatments

Patients with good or intermediate prognostic: bevacizumab treatment (monoclonal antibody targeting the VEGFA) combined to IFNα, or tyrosine-kinase inhibitors (sunitinib [27], pazopanib [28] and sorafenib [29]) increase progression free survival (PFS) compared to IFNα. Other options exist as a newly developed TKi, tivozanib [30] or high dose of interleukine-2 [31].

Patients with a poor prognosis: temsirolimus (mTOR specific inhibitor) has an effect on overall survival (OS) in comparison to IFNα, with a median of 10.9 months against 7.3 months [32]. The TKi such as sunitinib, sorafenib or pazopanib are still an option [31].

However, a clinical study on 1096 patients with good or intermediate prognosis highlighted the efficacy of targeting two immune checkpoints, the nivolumab (anti PD-1) and the ipilimumab (anti CTLA-4), in comparison to sunitinib (longer progression free survival; 11.6 months against 8.4 months) [33].

Two recent phase III clinical trial show the relevance of combining an anti-angiogenic (axitinib, VEGFR2 inhibitor) with an anti PD-1 (pembrolizumab) [34] or an anti PD-L1 (avelumab) [35]. The combination pembrolizumab/axitinib increases the PFS of 15.1 months as compared to 11.1 months for the sunitinib and the combination with avelumab increased PFS of 13.8 months as compared to 7.2 months for sunitinib. Only the combination pembrolizumab/axitinib increases the OS.

4.3 Second-line treatments

Treatments targeting the VEGFA/VEGFR pathway became references for the first-line but also for the second-line with the axitinib [36], the cabozantinib [37] or the everolimus [38] with an important improvement of the PFS [31].

Two clinical trials highlighted an improvement of the overall survival (OS) with the nivolumab (25 months) or the everolimus (19.6 months), that can be used after TKi's failure in comparison to everolimus [39].

4.4 Third-line treatments

Everolimus is the most used third-line treatment but sunitinib, sorafenib, pazopanib, temsirolimus and axitinib are also proposed. Generally, patients with a good or intermediate prognosis have an OS extended by third-line treatments of, respectively, 29.9 months and 15.5 months against 5.5 months for patients with poor prognosis [40].

The same treatments can be proposed in the fourth-line with benefits on the OS [41]. Another option is to include patients in clinical trials.

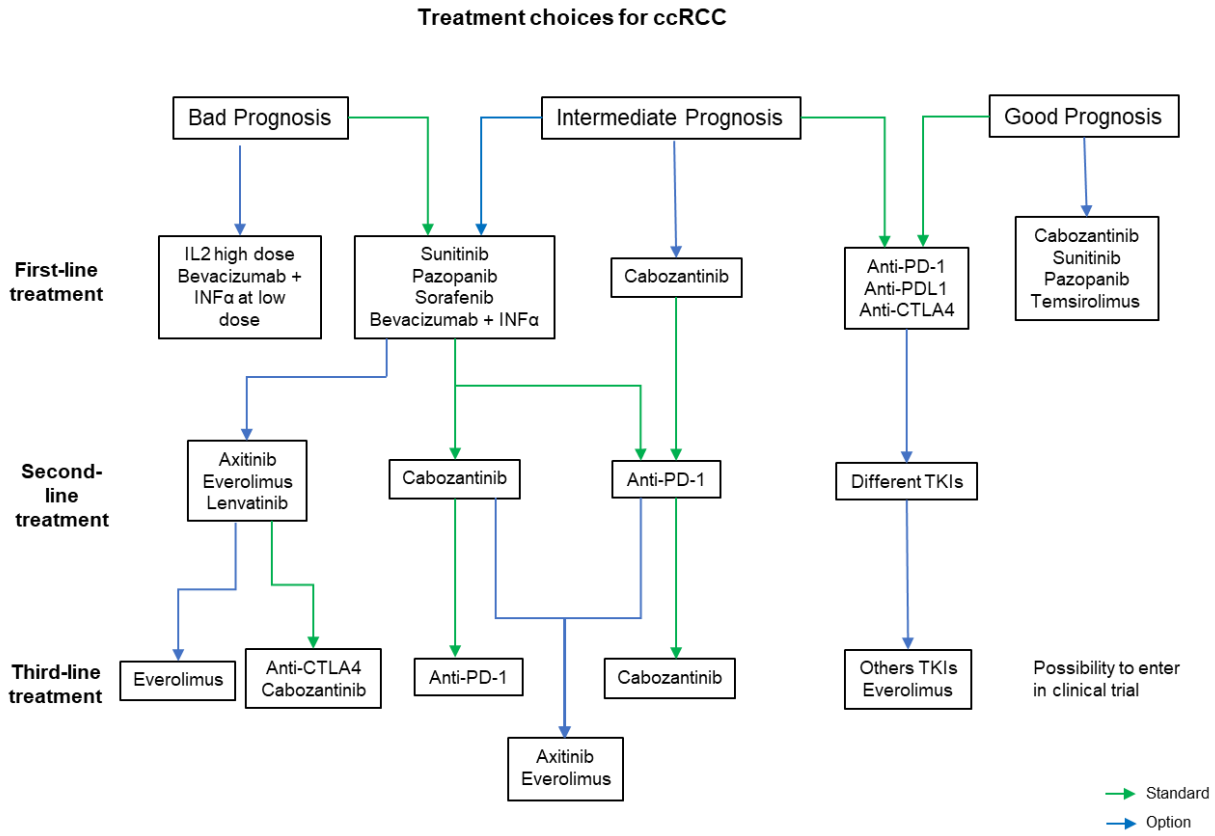

Figure 6. ccRCC treatments choice. Summary of how treatments are chosen according to patient's prognosis.

4.5 Overview of the treatments' efficacy and safety

4.5.1 Anti-angiogenic treatments

The existing anti-angiogenics treatments are presented in the order of their acceptance date by the authorities.

a) Sorafenib

It targets VEGFR1, 2 and 3, PDGFRβ, stem cell growth factor receptor (c-Kit) and B-Raf. It was the first inhibitor approved by the FDA and the EMA for the treatment of advanced RCC in, respectively, 2005 and 2006 [42]. Its anti-tumoral efficacy is linked to its antiproliferative and anti-angiogenic effects. The sorafenib is an option for the first-line treatment. The clinical trial SWITCH-II on 377 patients highlighted that the treatment by pazopanib followed by sorafenib is more efficient than the treatment by sorafenib followed by pazopanib with a median PFS of 12.9 months versus 8.6 months, respectively [43].

b) Sunitinib

It inhibits VEGFR1, 2 and 3, PDGFRα or β, c-KIT, fms like tyrosine kinase 3 (FLT3), and Colony Stimulation Factor 1 receptor (CSF1R). It has been approved in 2006 by FDA and EMA [44]. In a combined retrospective study on 4543 mccRCC patients, a median PFS of 9.4 months and a median OS of 18.7 months have been obtained [45]. Three categories of patients (from the most to the less frequent) were identified: i) patients responsive to treatment but who relapse after approximatively one year, ii) patients unresponsive to the treatment and iii) patients who respond to treatment during many years. These characteristics illustrate the need to identify predictive markers to determine treatment efficacy in the different patients.

c) Temsirolimus

It is a derivate of rapamycin, a mTOR serine/threonine kinase inhibitor. It inhibits mTORC1 by binding the intracellular receptor protein FKBP12 [32]. Temsirolimus improved OS in patients with poor prognosis mccRCC in a phase III clinical trial compared to interferon α (10.9 months vs. 7.3 months). However, the combination of temsirolimus with interferon α did not improve survival [32].

d) Everolimus

As temsirolimus, it is a derivate of rapamycin and it inhibits mTORC1 by binding the intracellular receptor protein FKBP12 but it is not converted to rapamycin *in-vivo* [46]. A phase II clinical trial highlights that everolimus is not efficient as first-line treatment. However, a phase III clinical trial demonstrated that everolimus, used as a second- or third-line therapy after the failure of previous therapies such as TKi, improves the median PFS of about 2 months compared to placebo [46]. More recently, the combination of everolimus plus lenvatinib has shown a better efficacy compared to everolimus alone (see paragraph *h) Lenvatinib*). Furthermore, the presence of S6RP, a downstream effector of mTORC1 signaling pathway, might be a good predictive marker of the patients' positive response to everolimus [46]. Finally, compared to sorafenib and axitinib, everolimus presents a better safety profile [46].

e) Bevacizumab

This humanized monoclonal antibody targeting the VEGFA was one of the first treatment used for mccRCC in association with IFNα. Its efficacy is inferior to that of tyrosine-kinase inhibitors and it lost its approval in 2016. Today, it is used in combination with an immune checkpoint inhibitor (*4.5.2 Immune checkpoints inhibitors*) [47].

f) Pazopanib

It targets the VEGFR1, 2 and 3, PDGFRα and β and c-Kit. It has been approved by FDA in 2009 and by EMA in 2010 as first-line treatment for advanced ccRCC. It improves the PFS as compared to placebo, with median PFS and OS of, respectively, 8.3 to 13.7 months and 19 to 29.1 months [44]. However, it induces asymptomatic hepatotoxicity in some patients.

g) Axitinib

It targets VEGFR1, 2 and 3, PDGFR and c-Kit. In 2010, the phase III Axis clinical trial (NCT00678392) highlighted that axitinib did not modify the OS but improved the PFS compared to sorafenib as second-line treatment for patients with advanced ccRCC [48]. Axitinib is, today, mainly combined with immunotherapies *(4.6* Anti-angiogenics and immunotherapies combinations*).*

h) Lenvatinib

It targets VEGFRs, PDGFR, Fibroblast growth factor receptor (FGFR), c-Kit and RET receptor tyrosine-kinase. It was first developed for thyroid carcinoma non-responsive to standard therapy [49]. A phase II clinical trial was performed on 153 patients with advanced (metastatic or unresectable) ccRCC after a first treatment by anti-angiogenic therapy. Lenvatinib combined with everolimus, but also lenvatinib alone, increased patients' PFS compared to everolimus alone (14.6 months vs. 5.5 months), in patients who have progressed after a first anti-angiogenic treatment [50].

i) Cabozantinib

It targets the VEGFR2, the mesenchymal-epithelial transition factor receptor (cMET), and the AXL tyrosine-kinase receptor. It has been approved by EMA and FDA as a second-line treatment after progression under anti-angiogenic therapy [37]. A phase III clinical trial, on 658 patients treated by one or more TKi, has highlighted an OS of 21.4 months for the cabozantinib against 16.5 months for everolimus. In patients with advanced ccRCC with poor or intermediate risk, the phase II clinical trial CABOSUN showed a benefit of the use of cabozantinib in the first-line as compared to sunitinib with a median PFS of 8.6 months versus 5.3 months [51]. Thus,

the cabozantinib has been added to first-line treatments possibilities for patients with poor or intermediate risk.

4.5.2 Immune checkpoints inhibitors

In addition to being one of the most vascularized cancers, ccRCC is also immunogenic with the expression of immune checkpoints factors such as PD-L1 and CTLA-4 [52], immune checkpoint inhibitors are developed and tested on ccRCC.

The programmed-death 1 receptor (PD-1) and the cytotoxic T lymphocyte associated protein 4 (CTLA-4) are involved at different steps of the immune response. Their inhibition improves the intratumor infiltration of the $CD8^+$ T lymphocytes and induces a more important antitumoral efficacy [44]. The phase III clinical trial CheckMate-214 highlighted the efficacy of the combination of nivolumab (anti PD-1) plus ipilimumab (anti CTLA-4) [33]. Thus in 2018, the FDA approved the use of the combination nivolumab/ipilimumab in the first line for patients with intermediate and high risk. The phase III clinical trial IMmotion-151, in patients with advanced ccRCC, showed the efficacy of the combination of atezolizumab with bevacizumab on PFS in PD-L1 positive patients as compared to sunitinib with, respectively, 11.2 months and 7.7 months [47].

4.6 Anti-angiogenics and immunotherapies combinations

Several trials combining inhibitors of the VEGFA/VEGFR signaling pathways and of the immune checkpoints showed promising results. In patients with positive PD-L1 tumors, a median PFS of 13.8 months was obtained with the combination avelumab/axitinib against 7.2 months for sunitinib and an OS of 11.6 months against 10.7 months for sunitinib [35]. For the association pembrolizumab/axitinib, a PFS of 15.1 months was observed versus 11.1 months for sunitinib. The estimated percentage of patients who were alive at 12 or 18 months after treatment was higher in the pembrolizumab/axitinib group (median survival not reached for both arms of treatment) [34]. A phase III CLEAR study is evaluating the efficacy of the combination pembrolizumab/lenvatinib, which has already shown Phase I and II antitumor activity in ccRCC, compared to sunitinib as first-line therapy for advanced ccRCC [53].

4.7 Conclusion on current treatments

Besides the multiplication of the therapeutics options that improved the kidney cancer care, mccRCC are still incurable with the relapse of patients after a few months of treatments and the different resistance mechanisms established by tumor cells.

The current challenges consist in:

i) identifying predictive markers of treatments' response to select the best one. These markers need to be easily detectable on samples obtained by a non-invasive method in the patients;

ii) proposing new therapeutic options, other than VEGFA/VEGFR targeting agents and immune checkpoints inhibitors to prevent tumor cells' resistance mechanisms establishment.

*See **Appendix 1** for ccRCC treatments' chemical structure.*

5) Resistance mechanisms to targeted therapies

The response to targeted therapies is determined by the Response Evaluation Criteria In Solid Tumors (RECIST), which represents the disease progression during treatment. Two types of resistance to targeted therapies exist:

i) intrinsic, which is the immediate failure of the treatment. It can be related to the presence of resistant tumor clones;

ii) acquired, characterized by tumor growth after initial tumor regression. Thus, different factors involved in resistance mechanisms have been identified.

This part on the resistance mechanisms to targeted therapies will particularly focus on sunitinib, the standard of care of mccRCC for the last ten years.

5.1 Redundant angiogenic pathways

Angiogenesis redundancy is one of the earliest mechanisms leading to resistance to anti-angiogenic treatments. As explained before, VEGFA is the main pro-angiogenic factor, and, together with its receptors, the principal target of anti-angiogenic treatments. However, many other growth factors induce angiogenesis such as angiopoietins (ANG), epidermal growth factor (EGF), fibroblasts growth factor (FGF), hepatocyte growth factor (HGF), transforming growth factor (TGF), placental growth factor (PlGF) and stromal cell-derived factor 1 (SDF1) but also interleukine 6 and 8 (IL-6 and 8). PlGF binds to the VEGF receptors, but all the other growth factors bind to different receptors expressed by endothelial cells. This diversity of factors/receptors involved in angiogenesis gives tumors many available ways to form blood vessels. Indeed, when VEGFA or VEGFR are inhibited by anti-angiogenic treatments, these different pathways act as substitutes to maintain vessel formation [54]. Furthermore, anti-angiogenic treatments targeting VEGFA and VEGFR increase the expression of these diverse growth factors inducing angiogenesis [55]. These growth factors, under anti-angiogenic treatments, are produced by different cells from the tumor microenvironment: tumor cells, bone marrow-derived cells, tumor associated macrophages, tumor-associated fibroblasts and cells

from healthy tissues ***(Figure 7)***. This angiogenic switch is responsible for the tumor revascularization and relapse under anti-angiogenic treatments [54].

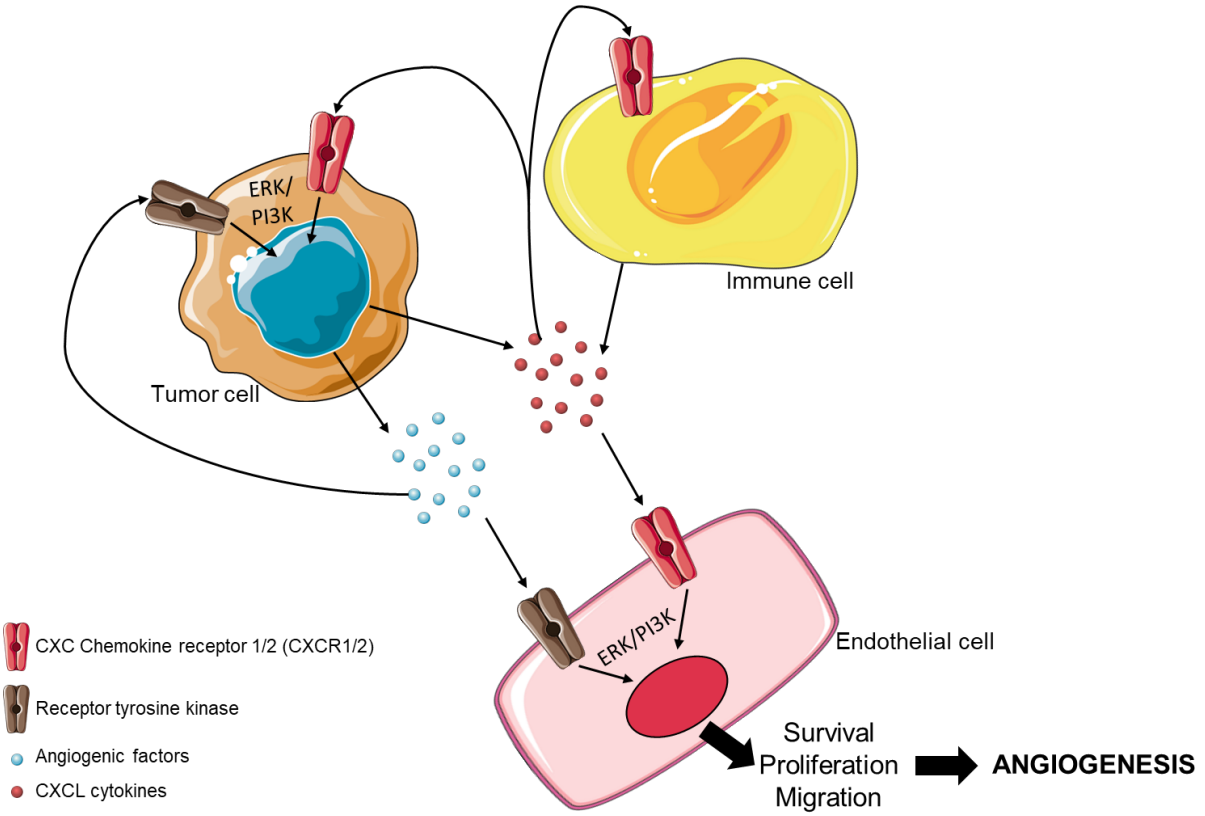

Figure 7. Redundant angiogenic pathways. The production of angiogenic factors and of CXCL cytokines by the cells from the microenvironment (immune cells) and by the tumor itself, enable to compensate the anti-angiogenic treatments effects by activating other proliferative and migrative signaling pathways that induce angiogenesis. *Adapted from S. Giuliano **[54]**.*

As explained before, different splices of VEGFA exist, with pro- and anti-angiogenic forms. Thus, according to the presence of anti- or pro-angiogenic VEGFA forms, patients might relapse or not to their treatment [54]. For example, the presence of $VEGF_{xxxb}$ forms (anti-angiogenic forms) decreased bevacizumab anti-tumoral effects in ccRCC [56,57].

High IL-6 or 8 expression are markers of resistance to anti-angiogenic treatments, associated with shorter PFS and OS for patients receiving sunitinib or pazopanib [58]. On the one side, IL-8 by binding to CXCR2 promotes VEGFA expression, which leads to autocrine activation of VEGFR2 and angiogenesis leading to treatment resistance [58]. Inhibition of IL-8 reduces tumor growth in sunitinib-resistant tumors [59]. On the other hand, IL-6 is overexpressed during sorafenib, sunitinib or pazopanib treatments, which induces activation of AKT/mTOR signaling, increases VEGFA expression and resistance to anti-angiogenic treatments [58].

5.2 Hypoxia

Anti-angiogenic drugs, by destroying the vascular network, may enhance hypoxia in the tumor microenvironment as an immediate early response. Hypoxia induces a hostile environment from which tumors try to escape by increasing tumor invasiveness and metastatic spread [54].

5.2.1 Aggressive cell selection

HIF1 and 2α enable the cell adaptation to hypoxia [60] and as explained before, HIF1 and 2α are stabilized due to the mutation/inactivation of the *VHL* gene in most ccRCC cases. A selective HIF-2α antagonist, PT2399, targeting the PAS-B domain of HIF-2α subunit was developed and tested in human ccRCC. It inhibits tumor progression and is active in sunitinib resistant-cells. However, some ccRCC are still resistant to this combination, which could be explained by a mutation of HIF2α, preventing its dimerization, observed after long exposure with PT2399 [61] and also by mutations of the p53 gene, present in many cancers and generating pro-tumoral functions [60].

5.2.2 Cancer stem cells selection

Hypoxia enables the maintenance of a cancer stem cells (CSC) niche. CSCs enable tumor's adaptation to hypoxia induced by anti-angiogenic treatments and induce tumor invasiveness and metastasis spread. In glioblastoma and in breast cancer xenografts, hypoxia increases the CSC pool and tumor growth after sunitinib or bevacizumab treatment [54]. During treatment, most of CSCs stay in a TGFβ -mediated quiescent state in which they are undetectable. Moreover, treatments generally target the highly proliferative but not the quiescent cells. If the treatment is stopped, CSCs participate to the regeneration of the tumor and induce cancer relapse [62]. Different CSC targeted therapies are currently developed [63]:

- The signaling pathways used by CSC (Hedgehog with vismodegib, Notch with demcizumab, Wnt with OMP54F28, TGFβ with fresolimumab): studies on the efficacy of these strategies and on stratification of patients that could benefit of them are ongoing;
- The surface markers expressed by CSC with antibodies. However, the main issue is the presence of these markers on CSC but also on normal cells inducing adverse effects. Still, some treatments targeting, for example, CD123 (Talacotuzumab), CD44 (RO5429083), CD47 (Hu5F9-G4) or EpCAM (Catumaxomab) are in clinical trials;
- Targeting the microenvironment like CXCR4 involved in CSC quiescent state (plerixafor), CXCR1 that binds to IL8 promoting self-renewal and tumor progression (reparixin), FAK which is maintaining stemness (defactinib);

- CSC's metabolism by targeting the glutathione balance, Bcl2 (venetoclax) to reduce oxidative phosphorylation.

5.2.3 Lysosomal sequestration of tyrosine-kinase inhibitors

Lysosomes contain hydrolases that are active at an acidic pH between 4.6 to 5 [58]. Lysosomal sequestration is the phenomenon by which hydrophobic weak bases accumulate into the acidic lysosomes driven by the large pH gradient. The greater is the pH gradient, more basic drugs will be sequestrated. Their hydrophobic characteristic enables them to pass easily through the lysosomes' membrane [58]. As soon as these weak bases enter the acidic lysosome, they become protonated and can no more exit the lysosome. This phenomenon is irreversible and induces therapy resistance. The hydrophobic weak base profile of several TKis, such as sunitinib, pazopanib and erlotinib provokes their lysosomal sequestration [58]. Such lysosomal trapping prevents their accessibility to the kinase domain of receptors present in the cytoplasm. Furthermore, cancer cells undergo, over again, formation of lysosomes upon chronic exposure to lysosomotropic drugs. Lysosomotropic drugs also stimulate the expression of ABCB1 (ATP-binding cassette, sub-family B [MDR/TAP], member 1), enhancing the accumulation of the drug in lysosomes and its export out of the cells [64]. Therapies that undergo lysosomal sequestration have common physicochemical characteristics: ClogP > 2 and a basic pKa between 6.5 and 11. Sunitinib, which was the main reference treatment for years for mccRCC, with pKa of 8.95 and ClogP of 5.2 undergoes lysosomal sequestration [64]. As explained before, the pH gradient allows sunitinib to accumulate in lysosomes, by passing through their membrane thanks to its hydrophobic property. In the lysosome, sunitinib is protonated and becomes membrane impermeable, which results in lysosome sequestration and to the unavailability of sunitinib to its tyrosine kinase receptors target localised at the plasma membrane ***(Figure 8)*** [64]. Giuliano S et *al*. also observed that the amine group added to sunitinib to improve its solubility is responsible of its basic property [64]. An optimisation of sunitinib molecule was carried out by the chemist from Institute of Chemistry of Nice but it does not prevent its lysosomal trapping. The combination of lysosomal destabilizing agents and of an inhibitor of the ABCB1 transporter (overexpressed under sunitinib treatment) efficiently increases the death of cell lines but also of cells from patients who progressed under sunitinib. However, the important toxic effects of lysosomal destabilizing agents prevent their use in the clinic. However, ABCB1 transporter inhibition is currently tested in clinical trials [64]. The lysosomal sequestration of sunitinib leads to a NFκB-dependent inflammatory response through the activation of MSK1 and the downstream of p38/MAPK and ERK signals [65]. One of the chemokines produced by this inflammatory response is CXCL5. CXCL5 represents a relevant marker for patients' unresponsiveness. It could serve as a surrogate marker of resistance mechanisms enabling the administration of an optimal second-line treatments with non-lysosomotropic drugs [65].

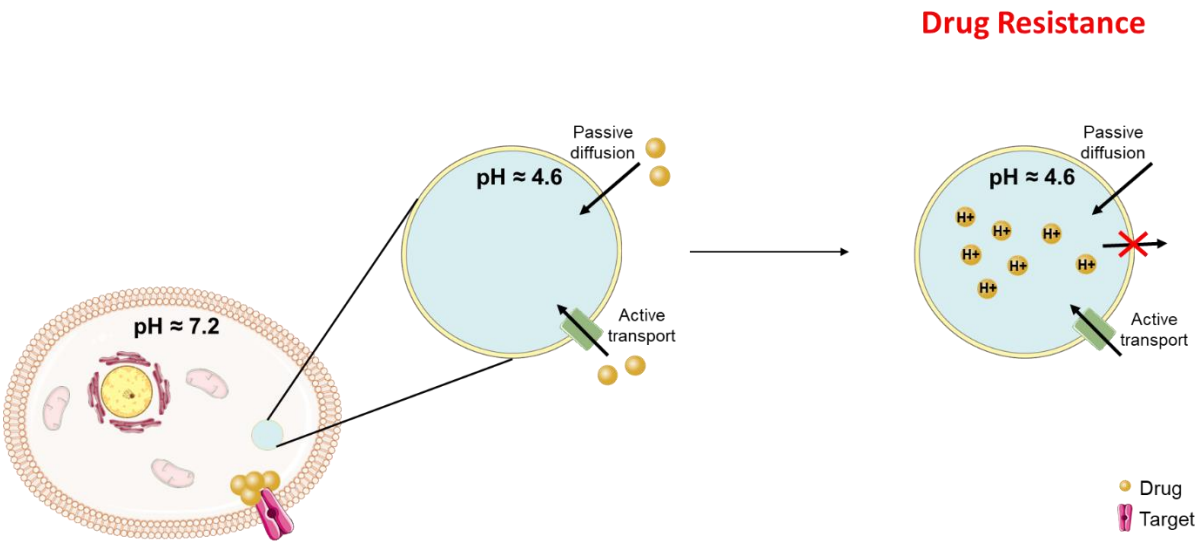

Figure 8. Lysosomal sequestration of tyrosine-kinase inhibitors. Hydrophobic weak base drugs, presenting ClogP > 2 and a basic pKa between 6.5 and 11, are sequestrated by lysosomes, which possess an acidic pH. Sequestrated drugs are then protonated which prevents their export out of the lysosomes. Thus, cells become resistant to the drugs. *Adapted from Dr Sandy Giuliano.*

5.2.4 Recruitment of vascular progenitors

Anti-angiogenic treatments enhance the production of inflammatory cytokines, which promotes tumor cell extravasation and the recruitment of angio-competent cells. Indeed, HIF1α promotes the production of pro-angiogenic factors such as VEGFA, VEGFR1, PDGFB, FGF2 and angiopoietins by healthy tissue and tumor cells [54]. These cytokines induce angiogenesis by activating vascular cell proliferation and migration, vascular progenitors and vascular modulator cells (tumor-associated macrophages and immature monocytes for example). These progenitors include: i) endothelial progenitor cells (EPC) that are present in the vasculature and differentiate into endothelial cells; ii) pericytes progenitor cells (PPC) that envelop blood vessels and mature into pericytes and vascular smooth muscle cells [54]. Pericytes' infiltration participates in resistance mechanism to anti-angiogenic therapies. Indeed, an enhancement of pericytes' infiltration increases endothelial cell survival and induces tumor growth [54].

5.3 Increased lymphatic network

Anti-angiogenic treatments destroy blood vessels. This stress stimulates the formation of a lymphatic network. Tumors from sunitinib-treated RCC patients present increased lymphatic vessels and increased lymph node invasion. These mechanisms depend mainly on the overexpression of VEGFC after sunitinib treatment [66]. This will be discussed more specifically in the next part.

III) Tumoral lymphangiogenesis

1) Lymphatic system

Lymphatic system has a major role in immunity, liquids homeostasis and absorption of dietary fats. Lymphangiogenesis is the formation of new lymphatics vessels from the existing lymphatic network. A genetical or traumatic lymphatic anomaly can induce oedemas, dysfunction in immunity defence and/or an accumulation of dietary fat. The systemic capillary endothelium is normally impermeable to big size proteins (> 70 kDa). However, a minimal protein leakage occurs and, if not compensated, leads to a protein accumulation in the extravascular media and an oncotic oedema [67]. In normal conditions, all the proteins that go out of the capillary endothelium are absorbed by the lymphatic network through the interstices between the endothelial cells [67]. Lymphatic capillaries have a thinner wall, do not contain pericyte and basal membrane. Their anatomic stability is maintained through anchor filaments between lymphatic capillaries and the extracellular matrix [67]. Lymphatic vessels also transport leucocytes, antigens and antigen presenting cells. Lymph nodes, on the path of lymphatic vessels, contain the immune cells and retain the different antigens. Thus, the immune response take place in the lymph nodes with the contact between naive T cells and antigen presenting cells [67].

2) Lymphangiogenesis

Lymphangiogenesis is induced after the budding of lymphatic endothelial cells from existing lymphatic vessels. Like angiogenesis, normal lymphangiogenesis occurs during embryonic development and transiently in adult tissues during wound healing and the menstrual cycle. However, pathological lymphangiogenesis occurs during inflammation and metastatic dissemination. During embryonic development, the vascular system develops first. Then, lymphatic endothelial cells differentiate from the blood vascular endothelium by activation of lymphatic-specific transcription factors like prospero homeobox 1 (Prox1) [68]. Prox1 is necessary for the differentiation and the budding of lymphatic endothelial cells. Indeed, Prox1 stimulates the expression of other lymphangiogenic factors such as VEGFR3 and integrin α9. The lymphatic endothelial cells expressing Prox1 migrate from veins to the adjacent mesenchyme where they can form the lymphatic plexus. This migration is modulated by VEGFC [68]. The primary lymphatic network, by VEGFR3- and VEGFC-dependent sprouting, enhances lymphangiogenesis and the formation of a bigger lymphatic network. The lymphatic vessels, thus formed, acquire basement membrane, smooth muscle cell coverage and valves through the expression of transcription factors Foxc2 and NAFTc1 [68].

The main lymphangiogenic factors are the VEGFA, B, C and D, the PlGF and their receptors VEGFR2 and 3. Activation of these receptors induces lymphatic endothelial cell migration, proliferation and survival. However, in normal and pathological conditions, the principal pro-

lymphangiogenic factor is the VEGFC. The role of VEGFD is minor in lymphangiogenesis. After activation of the VEGFC/VEGFR3 signaling pathway, the FGF2, the IGF1 and 2 (insulin like growth factor), the HGF (hepatocyte growth factor), the lymphotoxin α (TNF family) and the PDGFβ also participate in lymphangiogenesis in different experimental models [67]. Angiopoietins 1 and 2 and their receptors Tie1 and 2 control blood vessels stability, permeability and survival [67].

3) VEGFC and VEGFR3

VEGFR3, the main pro-lymphangiogenic receptor, is expressed on blood vessels and is essential for the blood system formation. It limits excessive VEGFR2-induced angiogenesis. However, when the vascular system formation is completed, VEGFR3 is principally expressed in the lymphatic system and the binding to its ligand is necessary to be activated [68]. VEGFR3 does not bind VEGFA but two other VEGF factors, VEGFC and D [6].

VEGFC is an important regulator of lymphangiogenesis. VEGFC is a protein that becomes active after proteolytic maturation at its N- and C-terminal domains. Its mRNA expression is negatively controlled by HIF1α and HIF2α, but HIF2α (HIF oncologic form) indirectly enhances VEGFC protein expression [69]. VEGFC also binds to VEGFR co-receptors, the Neuropilins 1 and 2 that modulate the VEGFR signaling. VEGFC is also secreted by tumor and immune cells and cancer-associated fibroblasts. Its expression by tumor cells stimulates their proliferation, survival and metastatic dissemination.

In ccRCC, VEGFC expression increased in tumor cells according to their ability to form tumors in nude mice. Furthermore, VEGFC expression correlates to mccRCC tumor aggressiveness [66].

4) Tumor lymphangiogenesis ***(Figure 9)***

Lymphatic vessels vehiculate the tumor cell antigens to lymph nodes where they activate naive T cells and the anti-tumor immune response. However, in advanced tumors, cancer cells invade the sentinel lymph nodes. Highly aggressive tumor cells produce VEGFC, which participates in the formation of new lymphatic vessels bypassing the sentinel lymph nodes, and in the migration of tumor cells to other organs [69]. Thus, the lymphatic network is involved, through VEGFC expression, in metastatic dissemination. The lymphatic network presents two roles: i) in the initial phase of tumor development, it has beneficial effects by bringing the tumor antigens to the lymph nodes and by presenting them to naive T cells to activate the immune system; ii) when the lymphatic vessels are transporting tumor cells, it has detrimental effects through the VEGF-dependent formation of lymphatic vessels and the tumor dissemination. Tumor metastasis is the first sign of tumor progression. Furthermore, lymphatic vasculature correlates with metastasis. More precisely, the overexpression of VEGFC correlates with a more important lymphatic

network and with tumor dissemination through lymphatic vessels. Metastatic cells in the lymph node either enter in a dormant state or survive and proliferate [68]. VEGFC enables the dilatation of existing peritumoral lymphatic vessels and the sprouting of the new lymphatic vessels around the tumor [68].

However, ccRCC cells over-express VEGFC when they are exposed to an anti-angiogenic treatment.

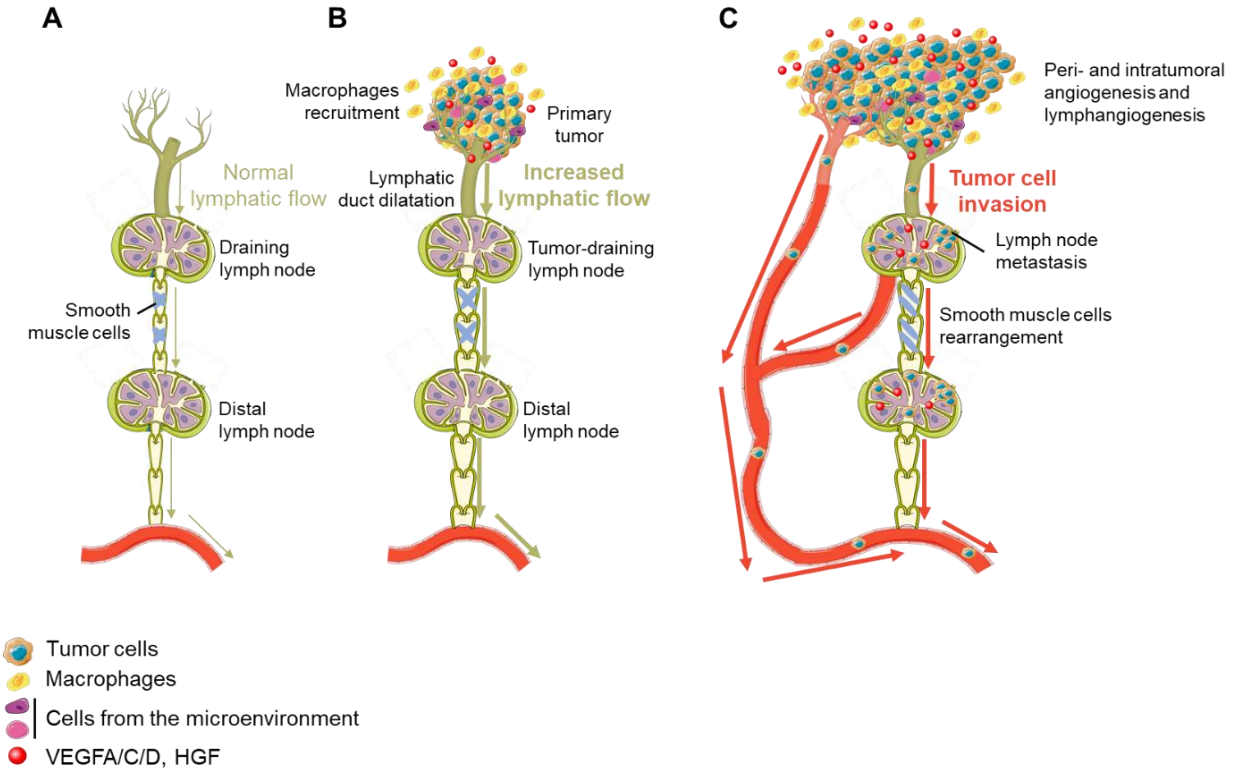

Figure 9. Tumoral lymphangiogenesis. A. Normal lymphatic drainage through the lymphatic capillaries and the lymph nodes. ***B.*** Primary tumor produces pro-lymphangiogenic factors (VEGFA/C/D and HGF for example) that are transported through the collecting lymphatics to the tumor-draining lymph node, where they induce lymphangiogenesis from the pre-existing lymphatic vessels in the lymph node. ***C.*** When tumor cells have started to metastasize in lymph node, they represent new sources of lymphatic factors, which induce the remodelling and smooth muscle cells rearrangement and lymphangiogenesis in distant lymphatic vessels and, thus, distant metastasis such as organ metastasis. *Adapted from S. Karaman and M. Detmar **[70]**.*

5) Lymphangiogenesis role in resistance to sunitinib

As stated before, sunitinib targets the pro-angiogenic pathway VEGFA/VEGFR on blood vessels. Sunitinib improves PFS but not OS and most patients relapse after a few months of treatment with increased metastasis. 80% of solid tumors disseminate through the lymphatic vessels, while the 20% left disseminate through the blood vessels [66]. Sunitinib increases the density of peri- and intratumor lymphatics vessels inducing lymphangiogenesis. This

observation was obtained on experimental tumors in mice treated by sunitinib [66]. The overexpression of VEGFC by tumor cells might be one of the causes of this sunitinib-induced lymphangiogenesis. Indeed, this VEGFC overexpression correlates with lymph nodes metastasis, lymphatic vessel density and organ metastasis [66]. Sunitinib induces VEGFC by activating HuR (VEGFC mRNA stabilization) through the p38 MAP kinase stress pathway. This phenomenon is only observed in tumor but not in normal cells.

Many anti-angiogenic treatments are available to treat ccRCC but in most of the cases, these treatments have transient effects with the relapse of patients after a few months. These transient effects are mainly due to established resistance mechanisms: redundant angiogenic pathways, cancer stem cells selection, lysosomotropic sequestration or lymphangiogenesis for example. Thus, today's objectives are either the development of predictive markers for patient's response to treatments or the discovery of new therapeutic targets that are involved in many cancer's hallmarks, which could prevent the establishment of resistance mechanisms. For that, we focussed on Neuropilins, which are the co-receptors of VEGF/VEGFR pathways.

IV) Neuropilins: Generalities

1) Genomic organization and protein structure

Neuropilins are type-1 membrane glycoproteins of 130-140 kDa. Two proteins of the same family coding by two genes on independent chromosomes (10p12 for NRP1 and 2q34 for NRP2), NRP1 and NRP2, share 44% of sequence homology. They are composed of a cytoplasmic domain of 43-44 amino acids, a transmembrane domain and a N-terminal extracellular domain composed of five subdomains: a1, a2, b1, b2 and c. The membrane and cytoplasmic parts are involved in the receptors' dimerization. Co-receptors are known to be cell surface molecules that do not contain intrinsic catalytic activity and only involved in enhancing their ligands/receptors signal. However, NRPs' cytoplasmic part contains a triplet of amino acids "serine, glutamic acid, alanine (SEA)", which enables NRPs to bind to a PDZ domain through the GIPC1 protein [71]. This PDZ domain attracts signaling proteins that enable the NRPs to signal after ligand binding even without the presence of their receptor. Some alternative NRPs splices give soluble forms of NRP1 and NRP2: sNRP1 and sNRP2 without transmembrane and cytoplasmic domains, and an isoform of NRP2 without the SEA amino acid triplet ***(Figure 10)***.

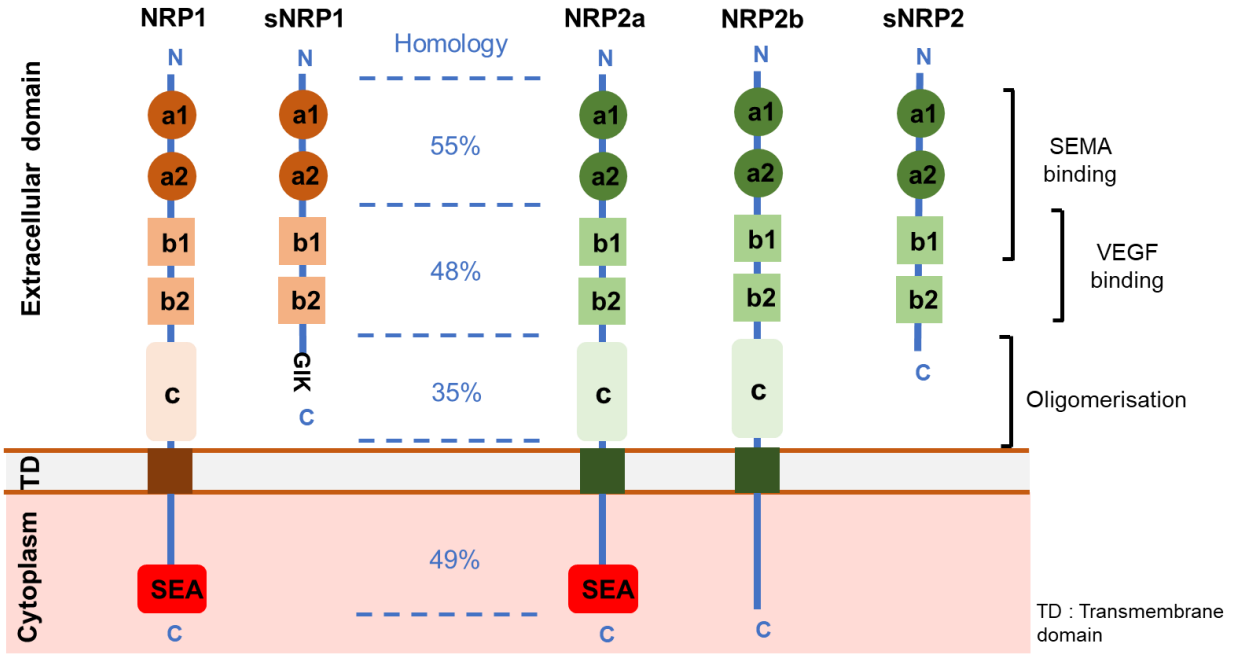

Figure 10. Neuropilins' different isoforms. Neuropilins share 44% of sequence homology. Different isoforms of Neuropilins exist: soluble NRP1 without its transmembrane and its cytoplasmic form (sNRP1), NRP2 with the SEA domain (NRP2b) and a soluble form of NRP2 (sNRP2).

2) The phenotype of knock-out mice

NRP1 gene invalidation (KO) generates vascular, nervous and cardiac networks defects responsible of an embryonic lethality between 10 and 12.5 days [72]. On the other hand, its overexpression is also lethal for embryos of about 12.5 days due to cardiac defects [73].

Instead, NRP2 KO is not lethal but a decrease of lymphatic vessels and some abnormalities during the neural development are observed [74].

Finally, NRP1 and NRP2 double KO gives rise to more severe vascular abnormalities and earlier embryos lethality at 8.5 days [75] with the presence of important avascular zones .

3) Neuropilins' ligands and interactors

Neuropilins bind to specific ligands and form heterodimers with ten different families of receptors. The ligands bind to NRPs homo- or heterodimers and to their receptors to form a complex that induces specific intracellular signals.

3.1 SEMA3/Plexin

NRPs were first described in neuronal guidance through their binding to semaphorins (SEMA), a family of proteins (seven classes) that guides axon growth and induces cell apoptosis, migration and tumor suppression. SEMA3A, less expressed during tumor development, is an angiogenic inhibitor and recruits pericytes to vessels [76]. SEMA3C is involved in cell apoptosis, invasion and metastasis and inhibits pathological angiogenesis. SEMAs bind to NRPs through the a1, a2, b1 and b2 domains and form a complex SEMAs/NRPs/Plexins (SEMA receptors) [77]. This complex enhances signal transduction during development, axon guidance and immunity. The SEMA3E/PlexinD1 pathway initiates the development of axon tracts in the forebrain and establishes functional neuronal networks. In axons that express plexinD1 but not NRP1, SEMA3E acts as a repellent. However, when axons express both plexinD1 and NRP1, SEMA3E acts as an attractant [78]. PlexinD1 is necessary for SEMA3E's effects on axonal guidance and NRP1 is necessary, its extracellular part being sufficient, to control the gating response of SEMA3E to induce a repulsive or an attractive axon growth [78]. Thus, any defect in the NRP1/SEMA3E signaling during neurodevelopment may induce neural disorder as it was suggested in a mouse model of schizophrenia [79].

3.2 VEGF/VEGFR

In healthy people, VEGFA-dependent effects are transient in physiological conditions. However, it is also involved in pathological angiogenesis and lymphangiogenesis. NRP1 binds the VEGFA and its receptors VEGFR1 and 2. VEGFA binding enhances this pathway leading to increased angiogenesis. NRP2 binds VEGFA and VEGFC, the main pro-lymphangiogenic factor, and forms a complex with its receptors VEGFR2 and 3 to induce angiogenesis and

lymphangiogenesis. The binding of VEGFA or C occurs through the b1 and b2 domains of the NRPs. Soluble NRPs are competitive forms for the binding of VEGFs to NRPs. VEGFRs' activation by VEGFs binding does not require NRPs. However, in the absence of VEGFRs, as it is the case in many tumors, NRPs alone can still induce cell migration and angiogenesis in a VEGFR-independent manner. Indeed, the binding of VEGFA to NRP1, independently of VEGFRs, activates RhoA and Ras, that are effectors of different pathways [76].
Thus, targeting the binding of VEGFs to NRPs is highly relevant in a therapeutic context.

3.3 PlGF/VEGFR

Placental growth factor (PlGF) belongs to the VEGFs family and binds to the VEGFR1. It was first described as an homodimeric protein produced by the placenta. Following different splices, three isoforms exist: PlGF1, 2 and 3. PlGF2 is the only form containing exon 6, coding for a heparin binding domain [80]. PlGF2 binds to NRP1 through exons 6 and 7 coding sequence, and PlGF1 binds to NRP1 through exon 7 coding sequence [80]. In breast cancer, overexpression of PlGF1 and NRP1 correlates with poor prognosis and cancer tissues overexpress PlGF2 as compared to normal tissues [81]. In melanoma, even in the absence of VEGFRs, the PlGFs/NRPs pathways are involved in tumor growth, angiogenesis, migration and metastasis [82]. Van Bergen *et al.* highlighted the relevance of targeting PlGFs in retinal diseases resistant to anti-VEGFs therapies [83]. In the Sonic Hedgehog medulloblastoma subgroup, PlGFs binds NRP1 resulting in the activation of the MAPK signaling and consequently to tumor growth and dissemination [84]. Finally, the PlGF/NRP signaling pathway plays a major role in the resistance to anti-angiogenic therapies [82].

3.4 HGF/cMET

Hepatocyte growth factor (HGF)/cMET (HGF receptor) signaling pathway stimulates endothelial cell survival, proliferation, migration and has a major role in tumor progression. NRP1 binding to cMET induces tumor invasion. HGF/cMET pathway also promotes immune tolerance by interacting with the programmed death ligand 1 (PD-L1) [85] and the interaction with NRP1 enhances this immune tolerance.

3.5 TGFβ1/TGFβR

TGFβ1/TGFβR signaling pathway stimulates the SMAD2/3 signal involved in physiological development, host immunity, inflammation, tumor progression and metastasis [86]. TGFβ binds to NRP1 through its b1 domain and form a ternary complex with TGFβRI, II and III. Activation of TGFβ1/TGFβR/NRP1 induces angiogenesis in a VEGFR2-independent manner and promotes T regulatory lymphocytes activity and immune tolerance.

3.6 PDGF/PDGFR

Four PDGFs' variants exist: PDGF A, B, C and D that binds to their tyrosine-kinase receptors PDGFRα and β. According to the nature of the ligand, the receptors will homo- or hetero-dimerize giving three possibilities: αα, αβ or ββ. PDGF/PDGFR complex activates MAPK/ERK and PI3K signaling pathways. Overexpression of PDGF and PDGFR on tumor vasculature enhances pathological angiogenesis [86], cell proliferation, differentiation and epithelial to mesenchymal transition [76]. NRP1 forms a complex with PDGF/PDGFR and enhances their downstream signaling pathways.

3.7 FGF/FGFR2

FGF/FGFR2 pathway induces cell migration, proliferation and angiogenesis. NRPs form a complex with FGFR2 amplifying the biological phenomena induced by FGF/FGFR2.

3.8 Galectins

Galectins, β-galactoside-binding proteins, induced the interaction between cell-cell and cell-matrix. Galectin-1 (Gal-1) is involved in tumor-associated endothelial cell proliferation, migration and adhesion through VEGFR2 phosphorylation and increased by Gal-1/NRP1 binding [87]. Indeed, Gal-1 activation of NRP1/VEGFR1-dependent AKT signal decreases endothelial-cadherin cell-cell junctions and increases vascular permeability [88].

3.9 EGF/EGFR

Epidermal growth factor receptor (EGFR) is a monomeric transmembrane protein. Mutations are observed in several forms of cancers, such as breast or lung cancers and it is overexpressed in many tumors. NRP1 extracellular domain induces EGFR-endocytosis and AKT-dependent cancer cell viability and tumor growth [89]. Moreover, NRP2 is also required to activate EGFR endocytosis, through the WDFY1 motif (WD-repeat and FYVE-domain-containing protein 1), in cancer cells and to maintain its activity [90].

3.10 Hedgehog signaling pathway

The Hedgehog signaling pathway is involved in embryogenesis, tissue healing, cell proliferation and differentiation but an overexpression or downregulation of its signal induces cancer development and epithelial-mesenchymal transition. SHH signaling pathway inhibition increases tumor cell differentiation [91]. NRPs are major regulators of the Hedgehog signaling pathway through a feedback loop existing between NRP1 and Hedgehog: Hedgehog induces NRP1 expression, which, in turn, promotes the activation of Hedgehog target genes [76].

3.11 Integrins

The α5β1 or α9β1 integrins expressed on endothelial cells, through their interaction with NRP2 expressed by tumor or endothelial cells induce tumor spreading and metastasis spread in an integrin-dependent manner [92].

3.12 Conclusion on NRPs' ligands ***(Figure 11)***

Neuropilins indirectly activate several pathways involved in cancer hallmarks such as: angiogenesis, lymphangiogenesis, tumor growth, migration or proliferation. TCGA analyzes highlighted that most of the actors involved in these different pathways are overexpressed in ccRCC confirming the implication of NRPs in cancer development. Therefore, NRPs represent relevant targets for the treatment of ccRCC.

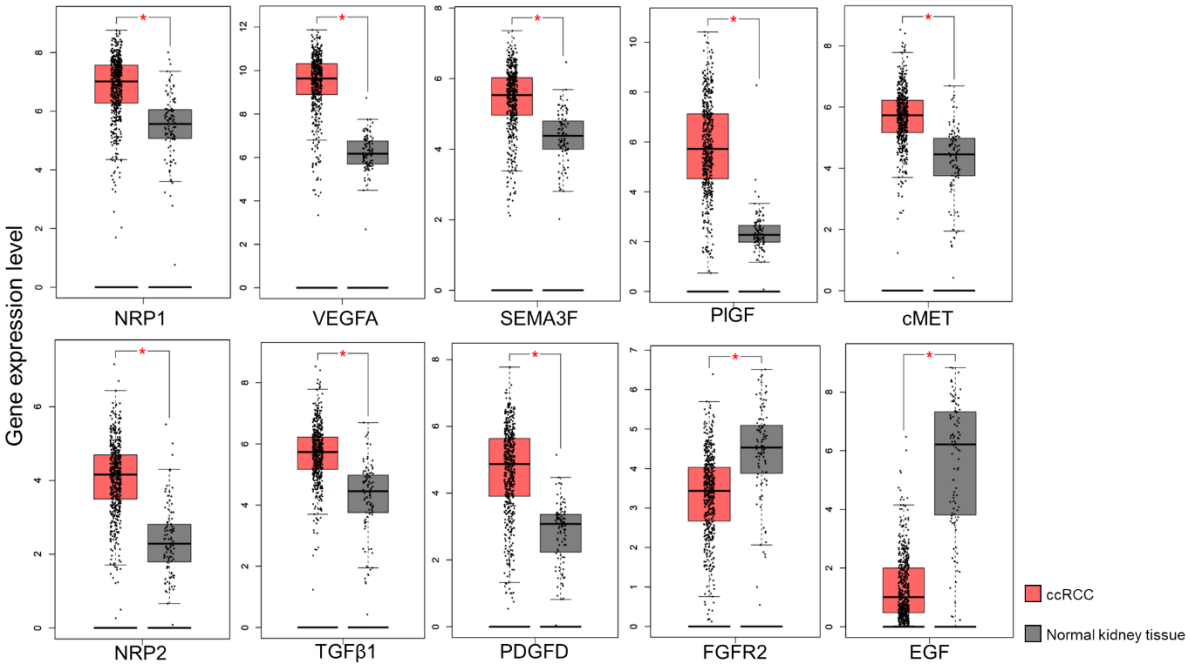

Figure 11. mRNA levels of NRPs' ligands in ccRCC and in normal kidney tissues ***[93]***.

V) Neuropilins and the immune system *(Figure 12)*

Neuropilins are expressed on many immune cells and are involved in the activation or the inactivation of the immune response by interacting with its ligand or receptors.

1) Dendritic cells (DC)

Dendritic cells are recruited to tumor sites. After their contact with the antigen, they are maturated and they migrate to the lymphoid organs to activate naive T cells for the induction of the primary immune response. Two types of DCs exist: i) myeloid DCs (mDC), which present the antigen to naive T cells; ii) plasmacytoid DCs (pDC), principally involved in immune suppression. Activated pDCs also activate naive T cells but to a lesser extent as compared to mDCs.

NRP1 is expressed on mature DC and on naive T cells. A NRP1/NRP1 homophilic interaction induces the formation of an immunological synapse between the two cell types. Thus, NRP1 promotes the antigen presentation by DCs through this synapse and activates the primary immune response [94,95]. NRP1 also rearranges the cytoskeleton allowing dendritic cells' transmigration to the lymphatics and lymphoid tissues to activate T cells. At a late T cell activation stage, SEMA3A is secreted. Its interaction with NRP1 expressed by T cells disrupts the formation of the immunological synapse with the DCs, decreasing naive T cell activation and increasing immune tolerance [96].

NRP2 expression on DCs increases during their differentiation from monocytes to dendritic cells [97]. Its sialylation protects DCs during their migration to lymph nodes. Then, in the lymph nodes, the polysialic acid is eliminated of NRP2 and DCs activate naive T cells [98,99].

2) Macrophages

They play a key role in the immune surveillance, cellular debris elimination and antigen presentation. Two types of macrophages exist: i) pro-inflammatory M1 macrophages; ii) pro-angiogenic, immunosuppressive, thus pro-tumoral particularly in hypoxic zones M2 macrophages. Hypoxia induces the overexpression of SEMA3A on tumor cells, which interacts with NRP1 and their receptors plexin A1 and A4, expressed on Tumor-associated macrophages (TAM). TAMs reside and exert their pro-tumoral role in the hypoxic zone. However, in a decreased NRP1 expression environment, TAM remain in the normoxic peripheric zones of the tumor, which suppress their pro-tumoral role [100,101]. In the microglia, NRP1 exerts an immune suppressive role by inducing a M2 phenotype but its expression on glioma-associated macrophages (GAM) has a pro-tumoral effect confirmed by NRP1 inhibition that decreases tumor growth and induces a macrophage polarization to an anti-tumoral role [102,103].

In the inflammatory zones, NRP2 expression increases during the differentiation of monocytes to macrophages [97]. NRP2 sialylation reduces macrophages' phagocytosis capacity [104], [105], promoting tumor progression [76].

3) T cells

T cells are involved in the adaptative immune response for the control and the elimination of pathogenic agents and of tumor cells. However, any dysfunctions or over-activation in their development induce auto-immune diseases and cancers. Four types of T cells exist:

3.1 Cytotoxic T cells (T $CD8^+$)

T $CD8^+$ recognize the specific antigen through the class I major histocompatibility complex (MHC) presented by infected cells and destroy them. This antigen recognition is enhanced through NRP1, whose expression is increased on effective T $CD8^+$ and memory T cells [77]. Furthermore, NRP1 expression, which correlates with PD1 expression on T $CD8^+$, represents a relevant biomarker to determine anti-PD1 immunotherapies efficacy. Indeed, patients with non-small cell lung cancer invaded with PD1-positive T $CD8^+$ are highly responsive to anti-PD1 immunotherapies and present a longer survival [106].

3.2 Helper T cells (T $CD4^+$)

Helper T cells are non-cytotoxic but produce interleukin 2 and interferon gamma that stimulate T and B cell proliferation. NRP1 is expressed on $CD4^+$ T cells and induces B cell differentiation [77].

$CD4^+$/$CD8^+$ T cells over-express NRP2 but NRP2 expression is lower on T cells expressing only CD8 or only CD4.

3.3 NKT cells

NKT cells link innate and adaptative immunity. Activated NKT cells lyse their targets and produce anti- and pro-inflammatory cytokines. NRP1 role on these cells is not yet described [77].

3.4 Regulatory T cells (Treg)

Treg are involved in immune homeostasis, allergic responses, auto-immune diseases, tumor immunity and graft rejection and their accumulation in tumors induces cancer progression and immune suppression [107]. NRP1 overexpression on activated Treg enhances their immunosuppressive role through its binding to SEMA4A expressed by dendritic cells. Indeed, NRP1/SEMA4A binding stabilizes Treg by recruiting PTEN (Phosphatase and tensin homolog)

and by inhibiting AKT phosphorylation and induces Treg migration to the tumors by secreting IL-10 and IL-35 (anti-inflammatory cytokine) Furthermore, the stimulation by tumors expressing VEGFA enhances $NRP1^{+}$ Treg infiltration to tumors and their immunosuppressive response [108].

Thus, the NRPs have different roles in the immune system either in cell migration, cell-cell interaction or in the regulation of the immune response.

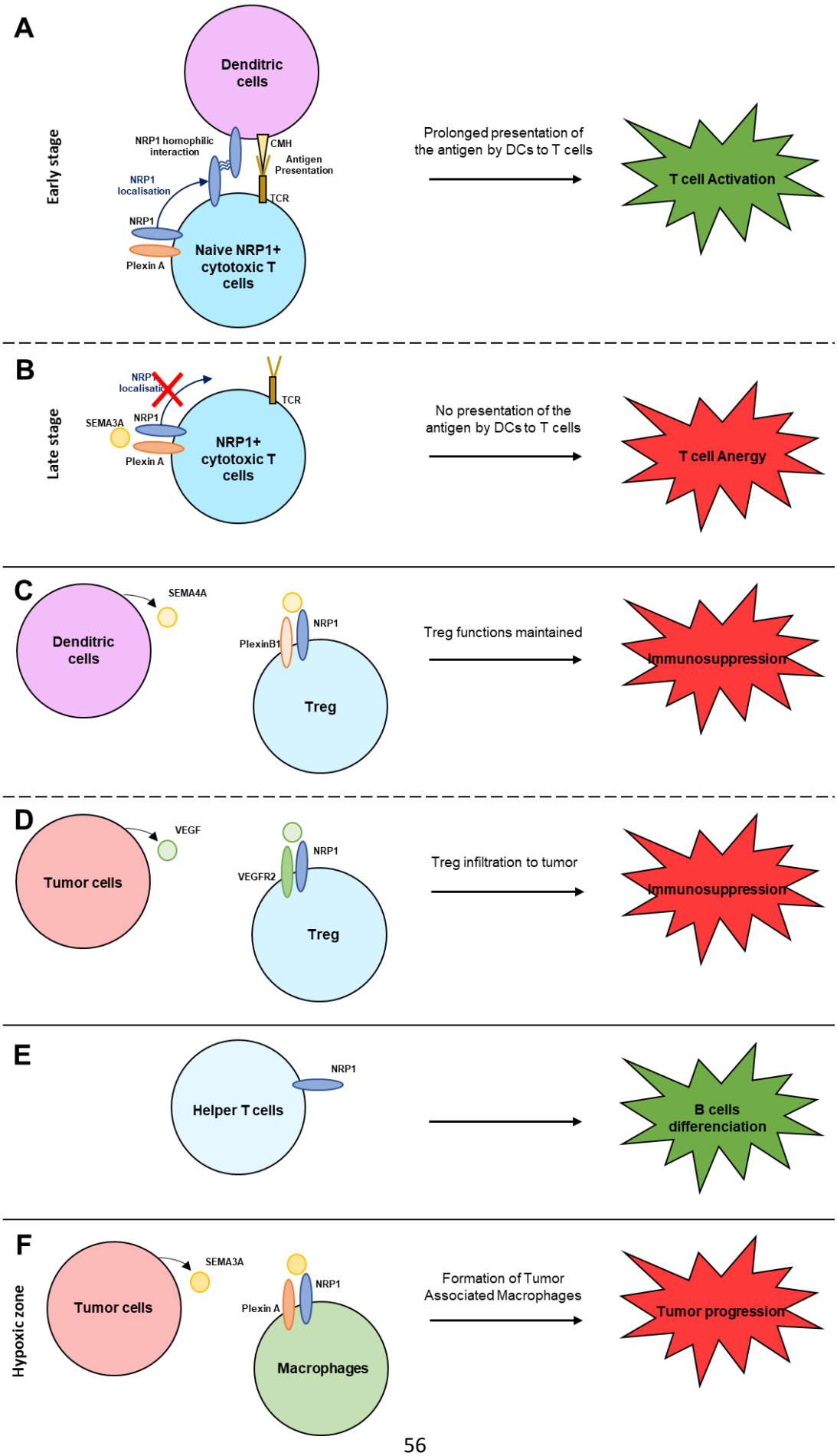
A
Early stage
Denditric cells
NRP1 homophilic interaction
CMH
Antigen Presentation
NRP1 localisation
TCR
NRP1
Plexin A
Naive NRP1+ cytotoxic T cells
Prolonged presentation of the antigen by DCs to T cells
T cell Activation
B
Late stage
NRP1 localisation
TCR
SEMA3A
NRP1
Plexin A
NRP1+ cytotoxic T cells
No presentation of the antigen by DCs to T cells
T cell Anergy
C
Denditric cells
SEMA4A
PlexinB1
NRP1
Treg
Treg functions maintained
Immunosuppression
D
Tumor cells
VEGF
VEGFR2
NRP1
Treg
Treg infiltration to tumor
Immunosuppression
E
Helper T cells
NRP1
B cells differenciation
F
Hypoxic zone
Tumor cells
SEMA3A
Plexin A
NRP1
Macrophages
Formation of Tumor Associated Macrophages
Tumor progression

Figure 12. Role of NRPs in the activation or suppression of the immune system. **A.** Naive cytotoxic T cells' NRP1/denditric cells' NRP1 homophilic interaction prolonged antigen presentation and induces T cell activation. **B.** SEMA3A, expressed by mature cytotoxic T cells inhibits NRP1 localisation inducing T cell anergy. **C.** T reg cells' NRP1/ Dendritic cells' SEMA4A interaction maintains Treg functions. **D.** Treg cells' NRP1/ Tumor cells' VEGF interaction enables Treg cells infiltration into the tumor and immunosuppression. **E.** $NRP1^{+}$ helper T cells induce immune response through B cells differentiation. **F.** Macrophages' NRP1/ tumor cells' SEMA3A induce the formation of tumor associated macrophages (TAM) and tumor progression.

VI) Neuropilins and cancers

The level of NRPs correlates with tumor growth, invasiveness, angiogenesis and poor prognosis and their overexpression is often observed in carcinoma, melanoma, glioblastoma, leukemia and lymphoma. Thus, studying the different functions of the NRPs in cancers is relevant to understand their role in cancer progression.

1) Functions of NRPs in cancer

As stated before, to grow over a few millimetres, tumors set a pro-angiogenic environment that induces the formation of new blood vessels form the existing vascular network. This new vascular network supplies oxygen and nutrients needed for tumor growth and survival. NRPs expressed on tumor cells and on cells of the microenvironment influence tumor angiogenesis [76]. Animal studies on prostate, colorectal, kidney, lung and breast human cancers highlighted that NRP1 expression correlates with exacerbated angiogenesis and with a poor prognosis [109]. Only in pancreatic cancer, a high expression of NRP1 reduces vascularized areas, tumor growth and improves survival [110]. NRP2 expression is principally correlated to tumor progression. In most cancers, NRP1 and NRP2 co-expression induces tumor growth and invasiveness [111]. SEMA3C, binding with equivalent affinity to NRP1 and NRP2, targets immature vessels sprouting and inhibits tumor lymphangiogenesis. However, its cleaved form p65-SEMA3C induces $NRP2^+$ cancer cells' tumor lymphangiogenesis and metastatic dissemination [112].

NRP1 expression on tumor cells stimulates cell viability, proliferation, migration, metastasis and enhances cancer cell stemness. Moreover, NRP1 promotes epithelial-mesenchymal transition through different pathways (TGFβ, Hedgehog, HGF…), which explains its pro-tumoral role. In breast cancer, NRP1 interaction with VEGFA inhibits apoptosis, which is counteracted by SEMA3B [109]. SEMA3F competes with VEGFA in binding to the NRPs and inhibits breast cancer cell migration. However, SEMA3F decreases membrane E-cadherin, promoting cell metastasis [109]. SEMA3A, expressed on endothelial cells, inhibits VEGFA effects and correlates with a good prognosis [113], but is generally lost during tumor progression [76]. Cells with a higher VEGFA expression compared to SEMA3A expression have pro-migratory characteristics, but in a $VEGFA^+/SEMA3A^+$ environment, NRP1 binds preferentially SEMA3A [114].

In colon cancer, NRP1 expression correlates with increased number of blood vessels and a poor prognosis. NRP2 over-expression stimulates tumor progression and its down-regulation reduces tumorigenesis and enhances apoptosis [115]. In prostate cancer, activation of VEGF-NRP1-c-MET signaling induces cancer cell survival [116]. In ccRCC, NRP1 down-regulation decreases migration, invasion and tumorigenesis [91], and NRP2 down-regulation inhibits cell

extravasation and metastatic spread in the lymphatic network [92]. In experimental model of lung cancer, NRP1 down-regulation reduces cell migration, invasion and metastasis [117].

2) Role in cancer stem cells

A tumor is composed of diverse cells with different morphologies, proliferation and metastatic capacities and resistance to therapeutic agents. Among these tumor microenvironment cells, only cancer stem cells (CSC) initiate a new primary tumor or metastasis. CSCs self-renew, induce the heterogeneous aspect of tumors and are resistant to chemo- and radiotherapies.

The role of the VEGFA/NRP1 pathway on stemness have been studied in two types of breast cancer cell lines: the MDA-MB-231 (triple negative breast cancer) and the MCF-7 (hormone sensitive breast cancer). MDA-MB-231 cells have stemness characteristics, but MCF-7 have low stemness properties. In these breast cancer cell lines, the level of stemness has been correlated to VEGFA and NRP1 expression [118]. Down-regulation of VEGFA and NRP1 in MDA-MB-231 cells and overexpression of VEGFA and NRP1 in MCF-7 confirmed the role of the VEGFA/NRP1 pathway in driving stemness properties [118]. VEGFA/NRP1 induces CSCs in breast cancers through the Wnt/β-catenin pathway [118]. VEGFA/NRP1 implication in glioma [119] and in medulloblastoma stemness properties [120] was also highlighted.

The VEGFC/NRP2 pathway is also involved in breast cancer stemness [121] through the activation of the YAP/TAZ signaling [122]. The interaction between NRP2 and α6β1 integrin induces the focal adhesion kinase (FAK) activation involved in tumorigenesis and associated to aggressive tumors [123].

3) Role in cancer-associated fibroblasts (CAF)

Fibroblasts are part of the tumor microenvironment and become myofibroblasts (normal activated fibroblasts) under tumoral conditions. The interaction between myofibroblasts and fibronectin induces fibronectin fibril assembly, a regulated determinant of matrix stiffness involved in tumor growth [124]. NRP1 induces fibronectin fibril assembly through α5β1 integrin. Indeed, NRP1 intracellular domain stimulates the intracellular kinase c-ABL, which activates small GTPases (Rac or Rho). These GTPases activate α5β1 integrin functions and increase fibronectin binding and assembly [124]. Furthermore, CAFs are one of the most prevalent cells in the tumor microenvironment and the principal source of TGFβ1. NRP1/TGFβ1 interaction induces endothelial-mesenchymal transition (EndMT), an important source of CAFs [125]. CAFs also induce tumor migration and invasion by promoting epithelial-mesenchymal transition (EMT) through Hedgehog signaling [126]. Thus, NRP1 expressed on CAF might also stimulate EMT, inducing tumor migration and invasion and worsening the prognosis.

4) Prognostic role of NRP1 and NRP2 pathways

In many cancers, NRPs correlate with poor prognosis. Some studies are presented here. NRP1 is overexpressed and correlates with poor prognosis in bladder cancer [127]. In osteosarcoma, NRP1 is a prognostic marker of shorter progression free survival (PFS) and of overall survival (OS) [128]. NRP2 is involved in laryngeal squamous cell carcinoma progression and represents a new therapeutic target [129]. In prostate adenocarcinoma, NRP2 is a marker of poor prognosis [130]. In non-metastatic kidney cancer, some activators of the NRP2 pathway, such as VEGFC, are described as markers of good prognosis. However, in metastatic kidney cancers, these activators are synonymous of shorter survival [69]. Thus, NRP2 and the level of expression of its partners must be determined to adapt a specific therapeutic strategy in kidney cancers at different step of their development: non-metastatic vs. metastatic.

5) Role in the therapeutic response

As stated before, one of the mechanisms of resistance to targeted therapies depends on the activation of alternative tyrosine-kinase signaling pathways mediated by the activation of several tyrosine-kinase receptors interacting with NRPs.

5.1 Resistance to chemo- and radiotherapies

In non-small cell lung cancer cells, a high NRP1 expression increases radio-resistance through an ABL-1-mediated up-regulation of RAD51 expression [131]. In pancreatic cancer, NRP1 enhances resistance to gemcitabine and 5-fluorouracil through the activation of ERK/MAP Kinase signaling pathway [132].

The NRP2/VEGFC pathway inhibiting mTOR complex 1 activity activates autophagy, which helps cancer cells to survive following treatment [133]. In adenocarcinoma, SEMA3F induces NRP2 overexpression, which decreases integrin αvβ3 and increases cell sensitivity to chemotherapy [134].

In some cancers, NRPs-targeted therapies decrease resistance to chemo/radiotherapies.

5.2 Resistance to targeted therapies

NRP1 activates the JNK signaling leading to the overexpression of EGFR and IGF1R, responsible of tumor growth and resistance to BRAF (melanoma targeted therapy), HER2 (breast cancer targeted therapy) and MET (stomach and lung carcinomas therapy) inhibitors [135].

NRP2 overexpression decreases EGFR expression in EGFR-addicted tumor cells, which reduces their resistance to MET-targeted therapies [136].

Thus, NRPs represent relevant biomarkers to determine patients' responsiveness to radio- or chemotherapies or to targeted therapies. Indeed, patients with low NRP1 expression present a better overall survival (OS) than patients with high NRP1 level [137,138].

To conclude, due to their implication in many hallmarks of cancer and in the immune response, targeting NRPs is a relevant therapeutic strategy, thus many inhibitors are developed.

VII) NRPs inhibitors

*See **Appendix 2** for NRPs inhibitors' chemical structure.*

1) MNRP-1685A antibody

MNRP-1685A (vesencumab) is a humanized monoclonal antibody specific of the NRP1 b1 and b2 extracellular domains. It inhibits the interaction of NRP1 with VEGFA. It was selected by phage display (method of antibody selection based on the random expression of antibodies fragments or of multiple peptides by bacteriophages) [139]. In preclinical models, MNRP-1685A exerts anti-tumoral effects on tumor growth, which are enhanced in the presence of a VEGFA specific antibody [140]. MNRP-1685A decreases vascular integrity and the number of pericytes, which explains the sensitivity of blood vessels to anti-VEGFA antibodies. MNRP-1685A, alone or in combination with bevacizumab (Avastin ®), has been tested on solid tumors after therapeutic failure in phase Ia and phase Ib clinical trials [140,141]. MNRP-1685A was well tolerated during dose escalation trials, but presented some adverse effects that were reduced with dexamethasone premedication. However, a high proteinuria observed in patients who received the two antibodies was fatal and resulted in the arrest of the clinical trials. Today's issue is to determine a therapeutic window for the administration of the anti-NRP1 antibody.

2) Peptides and pseudo-peptides

2.1 Structural basis to determine NRP1 and NRP2 chemical inhibitors

Many crystallographic structures of the tuftsin (TKPR tetrapeptide sequence miming the VEGFA C-terminal extremity), of the VEGFA and of the VEGFC, interacting with the NRP1 and NRP2 binding domains, have been obtained by X Rays [142]. The tuftsin and the VEGFA C-terminal extremities are binding to NRPs b1 and b2 domains through their terminal arginine. Other amino acids are involved in their binding through hydrogen bonds. Indeed, the asparagine in the position 320 (Asp-320) establishes two hydrogen bonds with the guanidinium motif on arginine's lateral chain, the tyrosine Tyr-353, Tyr-349 and serine Ser-346 interact with the terminal carboxyl motif. The binding pockets of NRP1 and NRP2 are mostly similar excepting a few amino acids, thus these differences might enable the synthesis of specific inhibitors of only one form of NRPs. The VEGFC is secreted in the form of an inactive pro-protein, thus, as explained before, to acquire its biological activity it goes through a proteolysis of its N- and C- terminal extremities. This proteolysis gives C-terminal a basic property with two arginine (SIIRR) enabling the binding to NRPs. The obtention by crystallography of the binding of the proteolyzed form of VEGFC with NRP2, present similar interactions than those observed for VEGFA with NRP1.

2.2 A7R heptapeptide and its derivates

The ATWLPPR (A7R) was the first peptide identified by phage display, inhibiting the interaction of the VEGFs to the NRPs. A7R inhibits VEGFA binding on VEGFR2, endothelial cell (HuVEC) proliferation and reduces tumoral vascular network, which blocks experimental breast cancer tumor growth [143]. The C-terminal arginine, the leucine in position 4 and the prolines in position 5 and 6 (LPRR) are essential for its binding and efficacy.

To label the A7R peptide, ^{99m}Tc (technetium 99m) has been introduced in its N-terminal part through a S-benzoyl-mercaptoacetic motif. In opposition to the original peptide, the labelled one could no more interact with NRP2, highlighting existing and important binding interactions between the N-terminal extremity of the peptide with NRP2.

In-vivo stable forms of A7R have been developed to be used in dynamic phototherapies [144] or by magnetic resonance imaging [145].

2.2.1 Glycosylated peptido-mimetics

Rigified peptido-mimetics derivates from A7R have been developed with a carbohydrate motif replacing the LPRR sequence [146]. The most efficient peptido-mimetic, owning a phenylsulfonamid motif and an arginine, inhibits VEGFA/NRP1 interaction and reduces tubulogenesis. Its stability in the NRP1 binding pocket is obtained by hydrogen bonds between its guanidinium motif and the Asp-320 of NRP1 and also by π-π or cation- π interaction involving its phenylsulfonamid motif.

2.2.2 Rigidified pentapeptides

Branched pseudo-peptides with the motif Lys(hArg)-AA^2-AA^3-Arg (AA stands for amino acids, and the number in superscript its position) have been developed [147]. The interactions between these pseudo-peptides and NRP1 are established through hydrogen bonds between the peptide's Lys(hArg) part and NRP1 Asp-320, the central part of the pseudo-peptide, but also through AA^2 and AA^3. Initially, AA^3 was a proline. Different optimisations have been carried out by replacing this proline by some of its isosteres. Its replacement by the 3,4-dehydroproline (ΔPro) or by the octahydroindole (Oic) induces the metabolic stability of the pseudo-peptide increasing its affinity to NRP1. Cyclic pseudo-peptides derivates from A7R, more stable *in-vivo* than linear peptides, have also been synthesized [147].

2.3 EG3287 and its derivates

NRP1 pseudo-peptides inhibitors based on the VEGFA C-terminal structure have been developed. These pseudo-peptides are focused on the VEGFA sub-domain between Ser-138 and Arg-165, stabilized by two disulfide bridges, an α helix and a β strand. EG3287, synthesized in 2006, is the bicyclic peptide corresponding to this sequence, [148]. EG3287 inhibits the

interaction between the VEGFA and NRP1^{+} porcine endothelial cells. A structural optimization of this bicyclic peptide gave a new “hit”: EG00229 [149]. This new peptide owns a guanidinium motif, miming the VEGFA C-terminal arginine, linked through a tiophen motif to a sulfonamide motif. The crystallographic structure showed that EG00229 is overlaying the tufstine binding mode in the NRP1 binding pocket [150]. The guanidinium motif forms hydrogen bonds with NRP1 Asp-320 and Ser-149. EG00229 inhibits the interaction between the VEGFA and the NRP1^{+} DU145 human prostate carcinoma cells, decreases pulmonary carcinoma cell viability and increases cytotoxic effects of paclitaxel and of 5-fluorouacil, first-line chemotherapies used in different cancers. EG01377, developed by the same team in 2018, is a NRP1 specific inhibitor. EG01377 inhibits HuVEC migration, VEGFA-induced microtubule formation and melanoma cell spheroids growth [151].

3) Non-peptidic inhibitors selected by multi-step screening

Multi-step screening, including virtual screening, use important compounds’ library to identify structures interacting with high affinity with the target. For NRP1, two screening have been carried out on 500000 compounds available in the *Chembridge Compound Collection* [152]. FAF-Drug2 software reduced the number of potential NRP1 inhibitors to 300000 by excluding molecules presenting toxic properties or bad pharmacological profiles.

3.1 Identification of the Chembridge compound (ID: 7739526), not tested *in-vivo*

Dockings from the crystallographic structure of tuftsin and NRP1 binding enabled the identification of 508 potential NRP1 inhibitors. Their inhibition capacity of VEGFA binding to NRP1 at 100µM was tested and 7 hits, with an inhibition over 40% were selected. Then, an *in-silico* screening was carried out to identify new molecules presenting structural similarities with the 7 hits. The new candidates were then tested for their inhibitory effects at 100µM. This was repeated three times. The best compound obtained with this approach (Chembridge ID: 7739526) inhibits VEGFA binding to NRP1 in a similar way as tuftsin [153]. As compared to the previous peptides, this molecule does not have a guanidinium motif. The binding prediction showed that the hydrogen from the hydroxyl motif of the inhibitor, forms a hydrogen bond with NRP1 Asp-320, and the oxygen of the inhibitor’s ether motif forms a hydrogen bond with NRP1 Glu-348. The effects on cells have not been determined yet.

3.2 NRPa-47 and NRPa-308, two non-peptidic NRP1 antagonists active *in-vivo*

We will focus on this screening in the next part. Indeed, this study was carried out by the chemist from University Paris-Descartes, with whom we are working with on this project.

As stated before, NRPs might be relevant oncology target to treat ccRCC due to their implication in many cancer hallmarks, thus many groups are working on the development of NRPs inhibitors. However, most of them are still in development or have not yet shown their anti-tumoral effects. Thus, our collaboration with the chemists from University Paris-Descartes gives us the opportunity to design NRPs inhibitors and improve their efficacy through biological tests.

VIII) NRPa-308

1) Screening of NRPa-47 and NRPa-308

During the virtual screening, 3000 potential candidates, small molecules without peptidic motif, were obtained. The *in-vitro* docking analysis of their binding to NRP1 selected 1317 molecules. A cellular-based screening carried out on endothelial cells reduced the list of potential antagonists to 158. A molecular screening selected 56 candidates according to their capacity to inhibit NRP1 and VEGFA interactions. Finally, the determination of these 56 compounds' inhibitory concentration 50 (IC_{50}) on human endothelial and on human breast cancer cells (MDA-MB231) pointed out two promising NRP1 inhibitors, NRPa-47 and NRPa-308 [153,154,155].
NRPa-47 owns a benzimidazole core connected through a carboxythioured spacer arm to a benzodioxane core. This inhibitor does not have a guanidinium motif, and the nitrogen from the benzimidazole forms a hydrogen bond with NRP1 Asp-320. The sulfur of the spacer arm and an oxygen from the benzodioxane forms hydrogen bonds with Tyr-291 (for the sulfur), Tyr-353 and Thr-349 (for the oxygen) from NRP1 binding pocket. The docking of NRPa-47 with NRP1 enabled to optimize its structure and a new NRP1 inhibitor has been obtained, NRPa-48, which presents similar anti-proliferative effects compared to the parent one.
The NRP1 inhibitor NRPa-308 will be described more precisely in the next part.
NRPa-47, NRPa-48 and NRPa-308 have anti-angiogenic effects, decrease endothelial cell migration and have cytotoxic effects on many cancer cell lines. However, the membrane cell crossing mechanisms is not yet elucidated but it could depend on the carrier's activity of NRPs.

The first study conducted on this NRPs inhibitor was on breast cancers. The results of this study are presented here **[154]**.

2) Screening that has led to the selection of NRPa-308

NRPa-308 owns three aromatic cores. During the screening, NRPa-308 presents an IC_{50} of 0.2µM in de-adhesion and viability assays on HuVEC. It was next tested on triple negative breast cancer cells (MDA-MB-231) and it exerts effects ten times stronger than the other candidates with an IC_{50} of 0.6µM. Moreover, NRPa-308 inhibits VEGFA/NRP1 binding with an IC_{50} of 42µM. To confirm that NRPa-308 effects on viability depend on NRP1, it was tested on MDA-MB-231 cells down-regulated for the expression of NRP1 by shRNA. In these cells, the IC_{50} for NRPa-308 increased (IC_{50} of 9µM), which was not the case in shVEGFA MDA-MB-231 cells used as negative control.

NRPa-308 effects on viability was tested on two triple negative breast cancer cell lines (MDA-MB-231 and BT-549) and on two kidney cancer cell lines (786-O and A498), NRPa-308 effects on viability were correlated to NRP1 levels on the different cell lines. NRPa-308 was also tested against 22 kinases, comprising the different forms of the VEGFA/VEGFR axis. No inhibitory effect was detected upon them.

3) Docking experiments of NRPa-308

The docking suggests that the ethyl ether is inserted in NRP1 binding pocket and interacts with NRP1 through π-stacking and through hydrogen bonds with the aromatic cores of Tyr-297 and Tyr-353. Furthermore, the oxygen from the amide and the azote from the sulfonamide of NRPa-308 establish hydrogen bonds with NRP1 Trp-301 and Glu-348.

4) Functional evaluation of NRPa-308

NRPa-308 exerts *in-vitro* anti-angiogenic (inhibition of HuVEC tubule formation under VEGFA stimulation) and anti-migration on HuVEC cells. NRPa-308 effects were also determined on MDA-MB-231 xenograft mouse model. The group treated by gavage with NRPa-308 at 50mg/kg, three times a week, presents a better survival and reduced tumor growth, vascular network, and metastasis.

PART II: OBJECTIVES

OBJECTIVES

Clear cell Renal Cell Carcinoma (ccRCC) being one of the most vascularized cancer with VEGFA overexpression. Hence, anti-angiogenic therapies were a turning point for ccRCC treatment, whereas the majority of patients relapses after a few months of treatment and some of them are even unresponsive to these anti-angiogenics.

Thus, the current main objectives for ccRCC treatment are:

i) To develop predictive markers that should be easily detectable with a non-invasive method for the response to treatments for each patient

ii) To develop new treatments that inhibit alternative proliferation mechanisms or/and that activate the immune system.

Neuropilins, described as VEGFR co-receptors, are expressed on endothelial, tumor and immune cells, thus they are drivers of several hallmarks of cancer: angiogenesis, lymphangiogenesis, tumor cell proliferation and (in)activation of the immune system.

Our principal objective was to determine the effects of each NRP (1 and 2) on ccRCC aggressiveness. For that purpose, we developed ccRCC cells down-regulated by shRNA and knocked-out by CRISPR-Cas9 for *NRP1* and *NRP2* genes. These methods enabled us to determine the specific role of NRP1 and NRP2 and to establish therapeutic strategies to target Neuropilins according to their expression level.

Our collaboration with chemists from University Paris-Descartes and Institute of Chemistry of Nice enabled us to test the Neuropilins inhibitor, NRPa-308. NRPa-308 was obtained through a screening among 500000 molecules carried out by our colleagues at University Paris-Descartes. NRPa-308 exerts *in-vitro* anti-proliferative and anti-angiogenic properties and *in-vivo* anti-tumoral effects in breast cancers.

Thus, our objective was to determine if NRPa-308 exerts biological effects also in ccRCC. The NRPs knocked-out cells were also useful there to determine the specificity of the inhibitor for NRP1 and/or 2 but also to establish its efficacy according to the NRPs expression level of cancer cells.

This study was important to determine if NRPa-308 might be a “hit” or if structure’s optimization is necessary to obtain better specificity and efficacy. My work paves also the way of a a therapeutic strategy for ccRCC treatment.

PART III: RESULTS

ARTICLE 1

ARTICLE 1

Synthesis, 3D-structure and stability analyses of NRPa-308, a new promising anti-cancer agent.

Etienne Brachet*, **Aurore Dumond***, Wang-Qing Liu*, Mari Fabre*, Mohamed Selkti, Françoise Raynaud, Olivier Hermine, Rachid Benhida, Philippe Belmont, Christiane Garbay, Yves Lepelletier, Cyril Ronco, Gilles Pagès, Luc Demange.

*Co-first authors

Article published in Bioorganic & Medicinal Chemistry Letters.

I) Scientific context and objectives

Our collaboration with the chemists from Université Paris-Descartes enabled us to work on the Neuropilin inhibitor, NRPa-308, obtained by a screening through 500000 molecules. Due to the orthogonality of the amide and sulphonamide bonds formation, NRPa-308 synthesis was challenging, 2 different synthesis were possible but both of them included 5 steps with different purification steps (**Figure 13. NRPa-308 synthesis route.** Reagents and conditions (a) $ClSO_3H$, 120°C, 4h; (b) 2N aq. HCl, $nBu_4N^+Br^-$, toluene, reflux overnight; (c) p-toluidine, DIEA, DMAP, CH_3CN, rt, overnight; (d) 2N aq. NaOH, MeOH, 3h, rt; (e) 2-ethoxyaniline, BOP, DIEA, DMF, rt, overnight; (f) $SOCl_2$, DMF, rt, overnight.***Figure 13***).

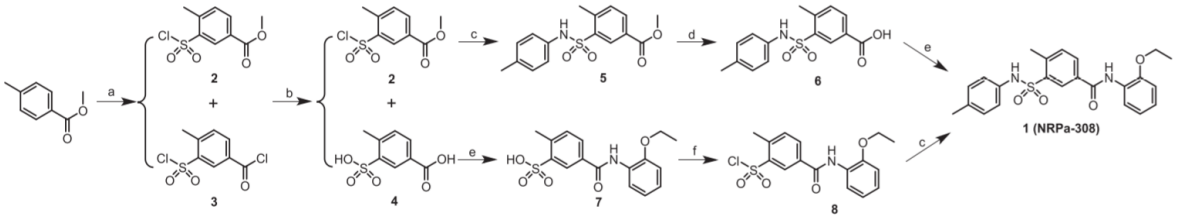

Figure 13. **NRPa-308 synthesis route.** Reagents and conditions (a) $ClSO_3H$, 120°C, 4h; (b) 2N aq. HCl, $nBu_4N^+Br^-$, toluene, reflux overnight; (c) *p*-toluidine, DIEA, DMAP, CH_3CN, rt, overnight; (d) 2N aq. NaOH, MeOH, 3h, rt; (e) 2-ethoxyaniline, BOP, DIEA, DMF, rt, overnight; (f) $SOCl_2$, DMF, rt, overnight.

The first limited step was step (a) with the sulfonylation of the methyl *p*-toluate which required time, our first approach was to carry this step with 1.1 equivalent of chlorosulfonic acic and

solvent-free at 120°C for 4 hours. However, a mix of three compounds: i) the expected sulfonyl chloride product **2**, ii) the dechlorinated compound **3** and iii) the remaining methyl *p*-toluate in a 1/1/3 ratio was obtained. Then the hydrolysation step (b) with 2N aqueous HCl in refluxing toluene, with tetrabutylammonium bromide as catalyst, were conditions that are supposed to hydrolyse selectively the carboxyl chloride compared to the sulfonyl chloride. However, a part of compound **2** has been totally hydrolysed giving the carboxyl-sulfonic diacid **4**. After some isolations and separations, the non-purified compound **2** was mixed with *p*-toluidine in the presence of the catalyst DMAP to obtain the sulfonamide compound **5**, acidification followed by saponification and some purifications give pure compound **6**. Finally, compound **6** coupling to 2-ethoxyaniline in presence of BOP/DIEA in DMF results in the final compound **1** NRPa-308 in 73% yield.

Compound **4** provided an alternative synthesis route, without any purification, but the yield was very low, not allowing any possible scale-up.

Thus, NRPa-308 synthesis route had to be optimised to reduce timing and purifications, which have an ecologic impact and also production costs.

II) Results

1) NRPa-308 synthesis optimisation

According to the synthesis route observed from compound **4**, starting from the commercially available *p*-methylbenzoic acid, NRPa-308 might be obtained with a three-steps synthesis (***Figure 14***).

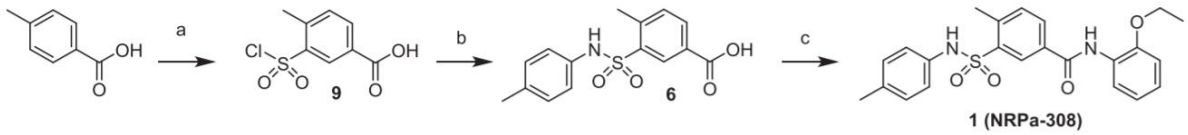

Figure 14. **Optimisation of NRPa-308 synthesis route.** Reagents and conditions (a) $ClSO_3H$, 100°C, 12h; (b) p-toluidine$^-$, DCM, 0°C – rt. 1h; (c) *o*-ethoxyaniline, EDCI, DIEA, DMF, rt, overnight.

The first step was the chlorosulfonylation of the *p*-methylbenzoic acid in chlorosulfonic acid at 100°C overnight. After neutralization by ice-quenched of the unreacted chlorosulfonic acid and some filtrations, compound **9** was obtained and was directly reacted with *p*-toluidine at 0°C for 1 hour to give the bi-aryl sulfonamide **6**. No purification was necessary at this step. Compound **6** was then mixed to 1.1 equivalent of *o*-ethoxyaniline with the presence of 1.1 equivalent of the coupling agent EDCI and 3.1 equivalent of the base diisopropylethylamine overnight to give, after treatment and purification, NRPa-308 in 64% yield.

With this new synthesis route, NRPa-308 is obtained in a shorter time and at a gram scale. Furthermore, no purification step was needed during the intermediate steps, which enables to reduce ecologic impacts and production costs, aspects that must be considered for future large-scale production.

2) NRPa-308 3D structure

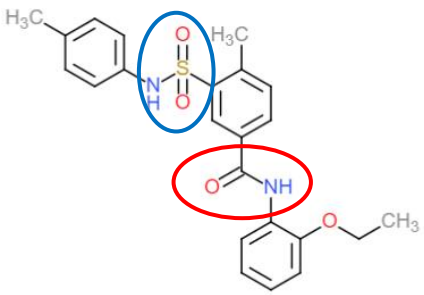

Figure 15. **NRPa-308 chemical structure.**

Crystallography assay enabled to determine the 3D structure of NRPa-308. The two aromatic rings linked by the amide bond (red circle) are coplanar, while the third one linked by the sulphonamide part (blue circle) is perpendicular to the rest of the molecule.

3) NRPa-308 stability

As stated before, NRPa-308 anti-proliferative effects correlated to its incubation times with the tumor cells, thus our objective was to determine if these effects are totally due to NRPa-308 itself or to one of its metabolites or degradation products. For that, NRPa-308 stability was determined by HPLC at three different pH (0.9, 7.4 and 8.4) and at two different temperatures (25°C and 37°C). After 16 days, NRPa-308 was fully stable under the different conditions. Then, we studied its stability in the cellular culture media in presence of the breast cancer cell lines, on which NRPa-308 exerts its anti-proliferative and anti-angiogenics effects: MDA-MB231 and

BT549 [154]. The two breast cancer cell lines were cultured in the presence of 2µmol/L of NRPa-308 for three days and the HPLC analysis of the supernatant showed that NRPa-308 was also stable in these conditions.

Thus, the anti-proliferative and anti-angiogenic effects observed previously on breast cancer cell lines [154] are totally due to NRPa-308 and not to its metabolite or degradation products.

III) Conclusion and perspectives

According to this study and to our collaboration with University Paris-Descartes, we optimized NRPa-308 synthesis route with a three-steps procedure that requires no intermediate purification and no expensive reactants. This result is highly interesting when thinking to future large-scale up production that will have its ecologic impact and its time of production reduced. Furthermore, we demonstrated NRPa-308 stability in different conditions, highlighting its striking cytotoxic effects against breast cancer cells.

ccRCC expressing NRP1 and NRP2 and current anti-angiogenic treatments presenting a transient efficacy and even sometimes inefficacy, our objective was to determine if Neuropilins were relevant oncology targets in this type of cancer and if NRPa-308 had also biological effects in ccRCC.

Bioorganic & Medicinal Chemistry Letters 29 (2019) 126710

Contents lists available at ScienceDirect

Bioorganic & Medicinal Chemistry Letters

journal homepage: www.elsevier.com/locate/bmcl

Synthesis, 3D-structure and stability analyses of NRPa-308, a new promising anti-cancer agent

Etienne Brachet[a,k], Aurore Dumond[b,k], Wang-Qing Liu[c,d,k], Marie Fabre[e,k], Mohamed Selkti[a], Françoise Raynaud[d], Olivier Hermine[f,g,h], Rachid Benhida[e,i], Philippe Belmont[a], Christiane Garbay[d], Yves Lepelletier[f,g,h], Cyril Ronco[e], Gilles Pagès[b,j,l], Luc Demange[a,l,]

[a] Université de Paris, CiTCoM, UMR 8038 CNRS, Faculté de Pharmacie, F-75006 Paris, France
[b] Centre Scientifique de Monaco, Biomedical Department, 8 quai Antoine Ier, MC-98000, Monaco
[c] Université de Paris, CiTCoM, UMR 8038 CNRS & U 1268 INSERM, Faculté de Pharmacie, F-75006 Paris, France
[d] Université de Paris, LCBPT, UMR 8601 CNRS, UFR Biomédicale des Saints-Pères, F-75006 Paris, France
[e] Université Côte d'Azur, ICN, UMR 7272 CNRS, F-06108 Nice, France
[f] INSERM UMR 1163, Laboratory of Cellular and Molecular Basis of Normal Hematopoiesis and Hematological Disorders: Therapeutical Implications, 24 boulevard Montparnasse, F-75015 Paris, France
[g] Université de Paris, Imagine Institute, 24 boulevard Montparnasse, F-75015 Paris, France
[h] CNRS ERL 8254, 24 boulevard Montparnasse, F-75015 Paris, France
[i] Mohamed VI Polytechnic University, UM6P, 43150 BenGuerir, Morocco
[j] Université Côte d'Azur, UMR 7284 CNRS and INSERM U 1081, Institute for Research on Cancer and Aging (IRCAN), Centre Antoine Lacassagne, 33 Avenue de Valombrose, F- 06189 Nice, France

ARTICLE INFO

Keywords:
Anti-cancer agents
Neuropilins
NRPa-308 synthesis
NRP-a308 stability

ABSTRACT

We report herein the synthesis of a newly described anti-cancer agent, NRPa-308. This compound antagonizes Neuropilin-1, a multi-partners transmembrane receptor overexpressed in numerous tumors, and thereby vali-dated as promising target in oncology. The preparation of NRPa-308 proved challenging because of the ortho-gonality of the amide and sulphonamide bonds formation. Nevertheless, we succeeded a gram scale synthesis, according to an expeditious three steps route, without intermediate purification. This latter point is of utmost interest in reducing the ecologic impact and production costs in the perspective of further scale-up processes. The purity of NRPa-308 has been attested by means of conventional structural analyses and its crystallisation allowed a structural assessment by X-Ray diffraction. We also reported the remarkable chemical stability of this molecule in acidic, neutral and basic aqueous media. Eventually, we observed for the first time the accumulation of NRPa-308 in two types of human breast cancer cells MDA-MB231 and BT549.

Tumor neoangiogenesis supplies cancer cells in oxygen and nutrients. Moreover, the neoformed blood vessels promote also the dissemination of malignant cells to healthy tissues. Therefore, tackling angiogenesis proved to be a relevant therapeutic option in oncology since more than 30 years.[1]

Tumor angiogenesis results from the over-expression of specific endothelial cell growth factors, among them the pro-angiogenic iso-forms of the Vascular Endothelial Growth Factor (e.g. VEGF-A_{165}), which bind simultaneously to the tyrosine kinase receptors VEGF-R1 or VEGF-R2, and to neuropilins (NRPs).[2] NRPs are multi-partners trans-membrane proteins with a non-catalytic cytosolic domain. Although NRPs have been initially described for binding the semaphorins and for their role in neuronal guidance, their involvement in tumor aggressiveness, angiogenesis, lymphangiogenesis and immune escape is now evidenced.[3] Moreover, NRPs overexpression is nowadays clinically related to a poor prognosis.

The currently marketed anti-angiogenic drugs, such as Avastin® (a monoclonal antibody directed towards VEGF-A) and Sunitinib® (an ATP mimic targeting the cytosolic domain of tyrosine-kinase involved in angiogenesis), prevents the interaction between VEGF-A_{165} and its receptors VEGF-R1 or VEGF-R2 or directly inhibits their kinase activity, respectively. However, despite indisputable transient benefits for

Corresponding author.
E-mail address: luc.demange@parisdescartes.fr (L. Demange).
[k] These authors contributed equally to this work.
[l] These authors co-directed the work.

https://doi.org/10.1016/j.bmcl.2019.126710 Received 15 July 2019; Accepted 17 September 2019
Available online 16 October 2019 0960-894X/

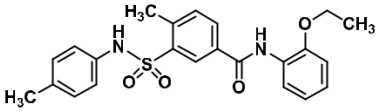

1 (NRPa-308)

NRPa-308 anti-proliferative activity :

IC_{50} (48h)	MDA-MB231 : 4.9 µM BT549 : 2.1 µM	IC_{50} (72h)	MDA-MB231 : 0.2 µM BT549 : 0.1 µM

Sunitinib anti-proliferative activity :

IC_{50} (48h)	MDA-MB231 : 2.6 µM BT549 :2.2 µM	IC_{50} (72h)	MDA-MB231 : 3.7 µM BT549 : 3.5 µM

Chart 1. Structure of NRPa-308, and its antiproliferative activity against two breast cancer cell lines (MDA-MB-231 and BT549) measured after 48 h and 72 h treatment and compared to these of the marketed drug Sunitinib®. These values have been reported by us in ref. [7].

patients, these therapies are not curative; tumors always relapse and become more aggressive, highlighting the real need for alternative therapeutic strategies.[4] Thereby, in the continuation of our ongoing research in the development of new and potent anticancer agents,[5] we have focused our attention on NRPs as targets,[6] and we have recently disclosed NRPa-308 (Chart 1, Compound **1**), a small-sized antagonist of the interaction between VEGF-A_{165} and NRPs.[7] NRPa-308 exerts remarkable anti-angiogenic and anti-proliferative effects *in vitro* (IC_{50} in the 10 nM range against a large panel of solid and hematological malignancies). Moreover, in our experimental models of nude mice xenografted with human triple negative breast cancer cells (MDA-MB231), NRPa-308 reduces the tumor growth by more than 60%, and enhances significantly animal survival. In addition, this molecule has no acute toxicity in treated animals.[7]

Altogether, these results underline the high potential of NRPa-308 for opening new avenues in anticancer strategies. Thus, we report herein a straightforward synthesis allowing a gram scale production of this molecule. Interestingly, this optimized process does not require intermediate time-consuming purification steps. We also demonstrate the chemical stability of this promising anticancer agent and its significant accumulation in two types of human breast cancer cells (MDA-MB231 and BT549).

Although NRPa-308 may be described as a “simple” molecule (MW = 424 g/mol, three aromatic rings connected by sulphonamide and amide linkages), it is noteworthy that its large-scale synthesis faces difficulties. This challenge is mainly due to similar synthetic pathways for accessing amide and sulphonamide bonds. Therefore, we decided to smoothly condense successively the required substituted anilines to the central ring, using the commercially available methyl *p*-toluate as starting material.

Our initial approach is outlined in Scheme 1; the first step consists in the sulfonylation of the methyl *p*-toluate. In fact, despite its apparent chemical simplicity, this reaction is poorly exploited due to its experimental difficulty.[8] To illustrate this paradox, one can mention the recent work of Singh and co-workers who reported a three-steps process of *p*-toluate sulfonylation through a time-consuming pathway, in-cluding successive saponification and re-esterification.[9] However, we decided to react commercially available methyl *p*-toluate with one equivalent of chlorosulfonic acid under solvent-free conditions to in-tend the mono-sulfonyl chloride derivative **2**. Different experimental conditions have been tested. We studied the influence of the load of chlorosulfonic acid (from 1.5 eq. until 0.5 eq.) and the influence of the temperature (from 50 °C to 130 °C, since methyl *p*-toluate melts at 35 °C). The best conversion was observed by heating methyl *p*-toluate with 1.1 eq. of chlorosulfonic acid at 120 °C for 4 h. Nevertheless, this sulfonylation has always led to a mixture of compounds difficult to separate, which consisted of: (i) the expected sulfonyl chloride product **2**; (ii) the dichlorinated compound **3**, and (iii) the remaining unreacted methyl *p*-toluate. With these optimized conditions, the analytic mon-itoring allowed to estimate the ratio methyl *p*-toluate/**2**/**3** as about 1/ 1/3.

This crude material was hydrolysed overnight using 2 N aqueous HCl in refluxing toluene with tetrabutylammonium bromide as a phase-transfer catalyst.[10] Although this method is known to hydrolyse selectively a carboxyl chloride *vs* a sulfonyl chloride, this was not the case here since a part of compound **2** has been fully hydrolysed, affording the carboxyl-sulfonic diacid **4**, which was isolated from the aqueous layer (49% yield). On the other hand, evaporation of the remaining organic layer provided a mixture of a solid containing compound **2** and the unreacted methyl *p*-toluate (20% yield), and compound **3** as an oil. The two layers were separated by filtration. Unpurified compound**2** was coupled with *p*-toluidine using catalytic amounts of DMAP to afford sulfonamide **5**,[11] which was then saponified to provide **6** after acid-ification. The *p*-toluic acid resulting from the unreacted methyl *p*-tol-uate was removed at this step by repeated trituration in diethyl ether affording compound **6** as a pure white solid (31% yield). The coupling of **6** with *2*-ethoxyaniline using BOP/DIEA in DMF led to the final ex-pected compound **1** (NRPa-308) in 73% yield.

According to this process, the recycling of **4** provided an alternative route to compound **1** (Scheme 1). Indeed, compound **4** was treated with *o*-ethoxyaniline in presence of BOP/DIEA. The resulting compound **7** was obtained in 62% yield, and treated with thionyl chloride at room temperature;[12] it afforded a chloro-sulfonic acid derivative, which was directly condensed with *p*-toluidine in the presence of catalytic DMAP. Following this pathway, compound **1** was obtained in 24% yield (over two steps). Although this process does not require any purification step, which is very important to speed up a synthesis, it does not allow any scale-up, since the desired product was obtained in less than 10% yield from the commercial starting material.

Therefore, we have considered the alternative synthetic route out-lined in Scheme 2. According to this second pathway, the target com-pound **1** may be obtained in only three steps from *p*-methylbenzoic acid as commercially available starting material. The chlorosulfonylation has been conveniently performed by heating *p*-methylbenzoic acid in chlorosulfonic acid at 100 °C. The reaction occurs overnight, however the subsequent work-up requires a sustained attention. Indeed, the mixture should be cautiously ice-quenched to avoid an exothermic behaviour leading to the formation of side-products. After the

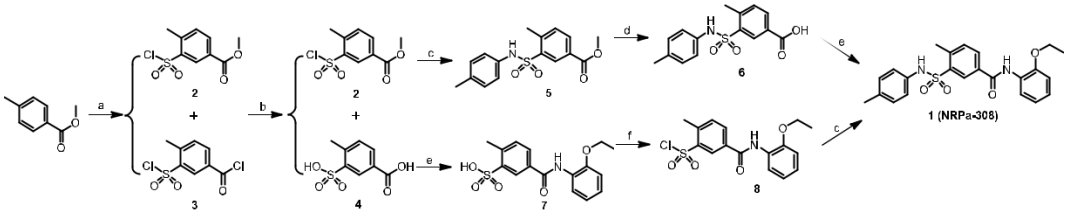

Scheme 1. Reagents and conditions (a): $ClSO_3H$, 120 °C, 4 h; (b): 2 N aq. HCl, $nBu_4N^+Br^-$, toluene, reflux overnight; (c): *p*-toluidine, DIEA, DMAP, CH_3CN, R.T. overnight; (d) 2 N aq. NaOH, MeOH, 3 h, R.T; (e): *2*-ethoxyaniline, BOP, DIEA, DMF, R.T. overnight; (f): $SOCl_2$, DMF, rt, overnight.

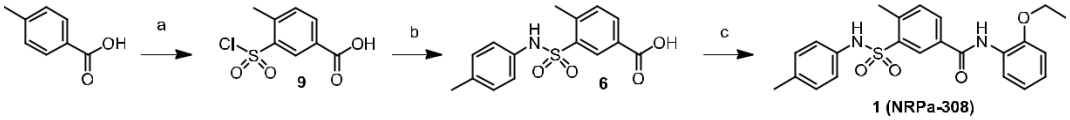

Scheme 2. Reagents and conditions (a): $ClSO_3H$, 100 °C, 12 h; (b): p-toluidine$^-$, DCM, 0 °C – rt. 1 h; (c): *o*-ethoxyaniline, EDCI, DIEA, DMF, R.T. overnight.

neutralization of the unreacted chlorosulfonic acid, conventional fil-tration and water washing afforded**9** as a white solid in 84% yield. The unpurified product was directly reacted at 0 °C in dichloromethane with *p*-toluidine for one hour to afford the bi-aryl sulfonamide **6**. The ex-pected product was isolated as a pure solid after acidic treatment and extraction (78% yield). ^{1}H NMR provided evidence that no purification was required at this step. Eventually, compound **6** has been reacted according to a conventional process with *o*-ethoxyaniline (1.1 eq.) in the presence of EDCI (1.1 eq) as coupling agent and diisopropylethy-lamine (3.1 eq.) as base. This last reaction has been completed over-night, and it afforded after treatment and purification by flash chro-matography the expected NRPa-308 (**1**) as a pure white solid (64% yield).

To summarize, this second synthetic route afforded NRPa-308 **1** in shortened reaction times and at the gram scale (global yield from the commercially available starting material: 42%). Another key feature is the absence of intermediate purifications, which reduces the ecologic impact and the production costs of the synthesis (no use of large amount of toxic solvents requiring recycling).

In addition, single crystals of NRPa-308 **1** were obtained from hot toluene, and a suitable one was selected for X-Ray 3-D structure de-termination. The experimental procedure is depicted in the Supporting Information section. Briefly, the structure was solved by direct method using SHELXS[13] refinement, based on F^2 was carried out by full matrix least squares using SHELXL-2018[14] software with anisotropic dis-placement parameters for all non-hydrogen atoms. Hydrogen atoms were located on a difference Fourier map and introduced into that calculations as a riding model with isotropic thermal parameters. All calculations were performed by using the Crystal Structure crystal-lographic software package WINGX.[15]

NRPa-308 **1** has a molecular structure built from entities, depicted in Fig. 1.[16] The crystal data collection and refinement parameters are collected in Table S1 (Supporting Information section). CCDC-1939102 contains the supplementary crystallographic data for this paper, which can be obtained free of charge from the Cambridge Crystallographic Data centre.

Briefly, at the single molecular level, the two aromatic rings linked thanks to the amide bond appear rather coplanar, while the third one, connected by the sulphonamide linker, is twisted, rather perpendicular to the central aromatic ring. At the supramolecular architecture level, neutral molecules are associated in the crystal essentially via NeH···O hydrogen bonds in a three-dimensional way. More precisely, two hy-drogen bonds involving three close molecules are evidenced in this structure: (i) the first involves the NH “amide” of the “central” mole-cule, and an oxygen of the sulfoxide linker belonging to an adjacent molecule; (ii) the second takes place between the NH “sulfonamide” of the “central” molecule and the oxygen of the amide belonging to a third molecule. In the continuation of this structural analysis, we plan now to crystalize NRPa-308 **1** with NRP-1 to decipher the close contacts be-tween the antagonist and its receptor.

We next focused our attention on NRPa-308 **1** chemical stability. Interestingly, we reported formerly that the anti-proliferative activities of NRPa-308 are deeply related to its incubation times with the tumor cells (Chart 1).[7] Thus, our purpose was to unambiguously demonstrate that these anti-proliferative effects are solely due to NRPa-308, and not to one of its potential metabolites or one of its degradation products.

First, the chemical stability of NRPa-308 was assayed by HPLC analysis at three different pH (0.9, 7.4 and 8.4) and at two temperatures

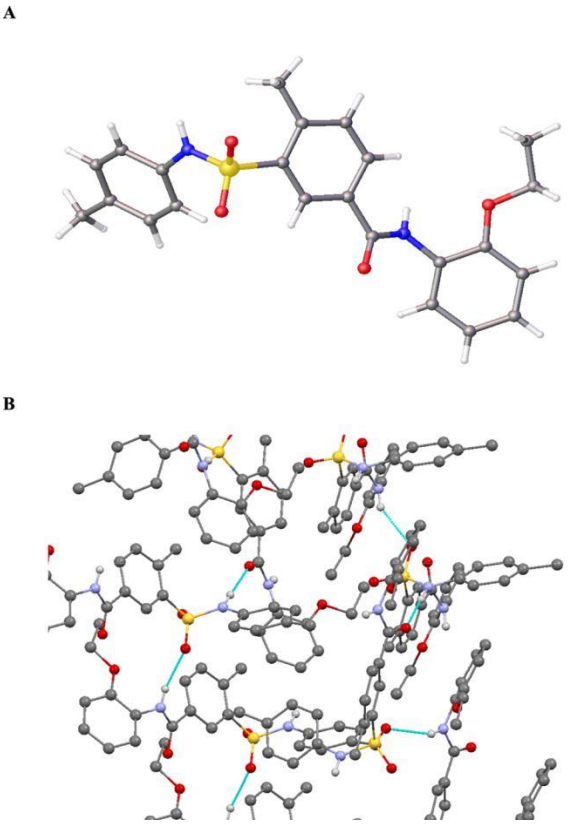

Fig. 1. Structure of NRPa-308 **1** analysed by X Ray. Please refer to reference [16], and to the Supporting Information section for more details. **A**: Single crystal of Nrp-a308 **1**; **B:** Supramolecular arrangement of Nrp-a308 **1**.

(25 °C and 37 °C). After 16 days, the compound proved fully stable under all these conditions (Fig. 2, the detailed experimental procedures are given in the Supporting Information section).

Next, we studied the stability of NRPa-308 in cellular culture media, in presence of malignant cells. To this end, MDA-MB-231 and BT-549 breast cancer cells were cultured in the presence of 2 µmol of NRPa-308 for three days, and the HPLC analyses of the supernatant revealed that NRP-a308 was not degraded (Fig. S1, Supporting Information section). Then, the cells were washed and lysed with methanol. The lysates were extracted with $CHCl_3$/MeOH, 9/1, v/v and quantitatively analysed by HPLC. In both cases, NRPa-308 proved stable, with no other peak de-tected (Fig. 3, the detailed experimental procedures are given in the Supporting Information section). Therefore, the *in vitro* antiproliferative activities, already measured by us (Chart 1), are due to compound **1** and not due to one of its metabolites or degradation products.

In addition, the quantitative dosage revealed a significant accu-mulation of NRPa-308 in cells, with respectively 5.14 ± 0.06.10^{-9} mol and 1.40 ± 0.01.10^{-9} mol calculated in MDA-MB231 and BT549 cells, after three days. Indeed, NRPa-308 mimics the interaction be-tween NRP-1 and the endogenous tetrapeptide TKPR, so-called tuftsin.

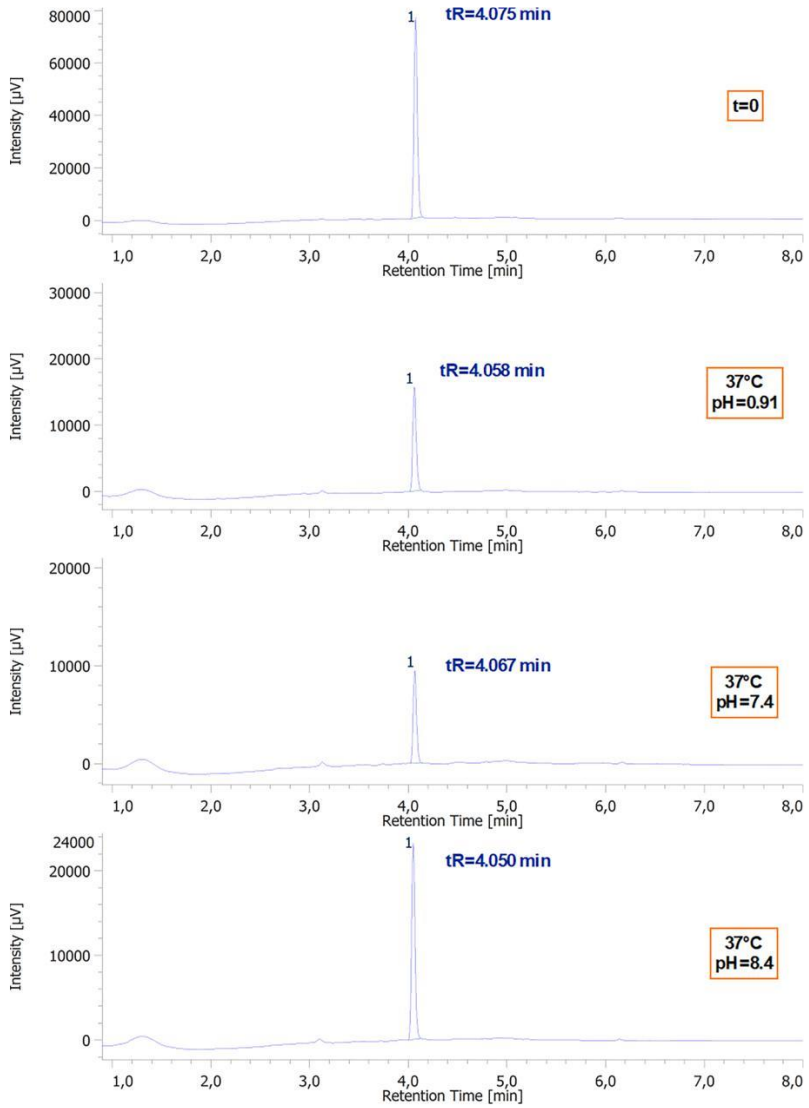

Fig. 2. Chromatograms showing the stability of NRPa-308 in aqueous buffers at pH 0.9, 7.4 and 8.4 after 16 days incubation at 37 °C.

Tuftsin has been used as model for the development of penetrating peptides able to interact with the VEGF-A_{165}/NRP-1 hotspot.[17b] The tufstin-derivative penetrating peptides respect the C-terminus sequence R/K/XXR/K (so called: C-end rule or CendR). They interact thereby with NRP-1, and are internalized into the cells thanks to the NRP-1 transmembrane trafficking. Based on this mechanism, peptide carriers (iRGD peptides) for selective drugs delivery have been recently disclosed. The iRGDs carriers are short-sized cyclic peptides, whose cleavage by integrins deliver a “C-end rule” sequence, able to be internalized into cells by NRP-1.[18] The iRGDs are used to selectively address inside malignant cells potential therapeutic agents, such as small-sized molecules (e.g. doxorubicin) or siRNAs.[19] However, at the best of our knowledge, non-peptidic small-sized NRP-1 antagonists have ever been reported for a potential “iRGD” like vectorization process. Thus, this result might constitute a way for the development of a new class of non-peptidic compounds able to selectively address therapeutic agents into the tumor cells through NRP-1.

To conclude, we report herein an expeditious synthesis for the newly identified anti-cancer agent NRPa-308. Our strategy is based on a three steps procedure, and it requires neither intermediate purification nor use of expensive reactants, which is of utmost interest for the de-velopment of further large-scale production. The structure of this mo-lecule has been unambiguously characterised thanks to X-Ray crystal-lography, and the three-dimensional supramolecular architecture of the crystal is granted by NeH···O hydrogen bonds between three adjacent molecules. We also observed the acute stability of this molecule in different media, which proved that its remarkable cytotoxic effects against cancer cells is not imputable to any of its potential metabolites. Lastly, we report the significant accumulation of NRPa-308 into cancer cells, which might be related to the transmembrane trafficking prop-erties of NRP-1.

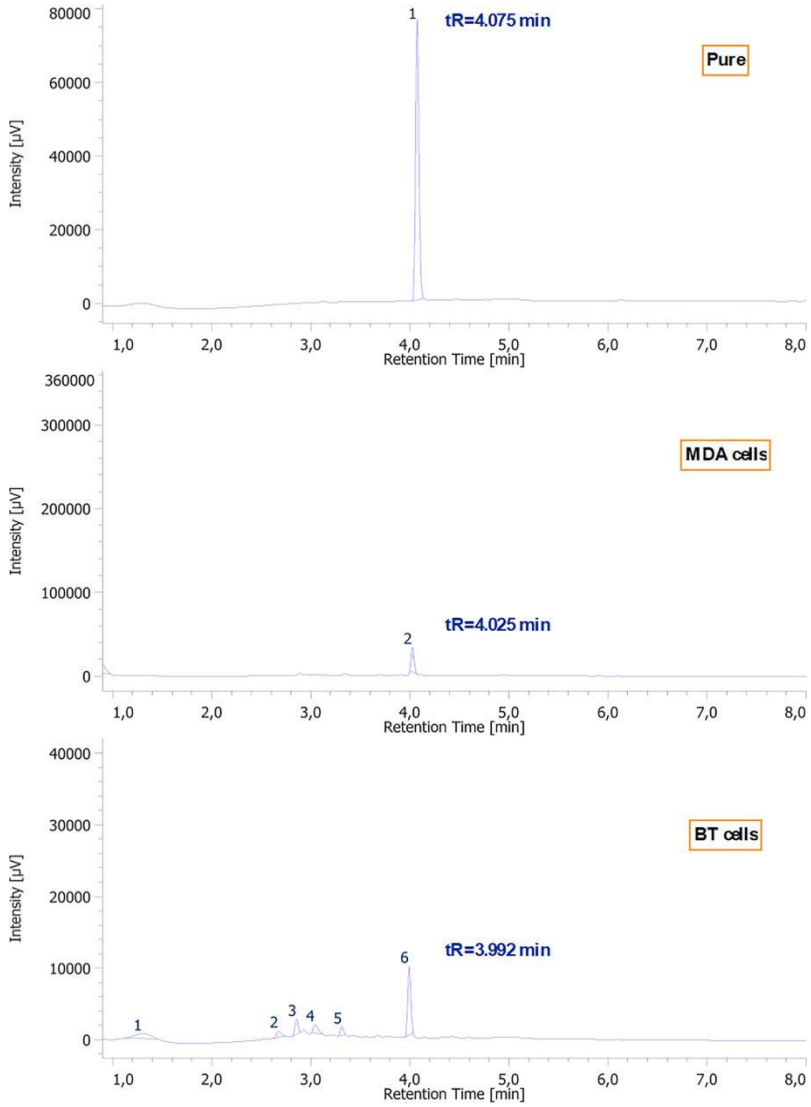

Fig. 3. Chromatograms showing the metabolism of NRPa-308 in MDA-MB231 and BT549 cells after three days incubation at 37 °C.

Acknowledgements

This work has been supported by the French Government through the UCA^{JEDI} investments, and through the National Research Agency (ANR), with the reference number ANR "TARMAC" ANR-17-CE17-0011-03 (MF PhD grant). Also, we are grateful to the financial support from ANR "GOLDWAR" ANR-16-CE07-0006-02. This study was conducted as part of the Centre Scientifique de Monaco Research Program, funded by the Government of the Principality of Monaco. This work was supported by the Helsinn company (AD PhD grant) (https://www.helsinn.com/). This article is based upon work form COST Action CA15135, supported by COST.

Appendix A. Supplementary data

Supplementary data to this article can be found online at https://doi.org/10.1016/j.bmcl.2019.126710.

References

1. a) Arezumand R, Alibakhshi A, Ranjbari J, Ramazani A, Muyldermans S. *Front Immunol.* 2017;8:1746/1–1746/13;
   b) Martin AR, Ronco C, Demange L, Benhida R. *Med Chem Commun.* 2017;8:21–52;
   c) Frandsen S, Kopp S, Wehland M, Pietsch J, Infanger M, Grimm D. *Curr Pharm Des.* 2016;22:5927–5942.
2. a) Bergantino F, Guariniello S, Raucci R, et al. *Biochim Biophys Acta.* 1854;2015:410–425;
   b) Horowitz A, Seerapu HR. *Cell Signal.* 2012;24:1810–1820;
   c) Ferrara N, Gerber HP, LeCouter J. *Nat Med.* 2003;9:669–676.
3. a) Roy S, Bag AK, Singh RK, Talmadge JE, Batra SK, Datta K. *Front Immunol.* 2017;8:1228/1–1228/27;
   b) Guo HF, Vander Kooi CW. *J Biol Chem.* 2015;290:2912–2916;
   c) Prud'homme GJ, Glinka Y. *Oncotarget.* 2012;3:921–939;
   d) Jubb AM, Strickland L, Liu SD, Mak J, Schmidt M, Koeppen H. *J Pathol.* 2012;226:50–60;
   e) Koch S. *Biochem Soc Trans.* 2012;40:20–25;
   f) Grandclement C, Borg C. *Cancers.* 2011;3:1899–1928.
4. a) Spanheimer PM, Lorenzen AW, De Andrade JP, et al. *Ann Surg Oncol.* 2015;22:4287–4294;
   b) Gaumann AK, Kiefer F, Alfer J, Lang SA, Geisser EK, Breier G. *Int J Cancer.*

2016;138:540–554;
c) Giuliano S, Cormerais Y, Dufies M, et al. *Autophagy.* 2015;11:1891–1904.
5. a) Dufies M, Grytsai O, Ronco C, et al.*Theranostics.* 2019. https://doi.org/10.7150/thno.35032;
b) Marzag H, Zerhouni M, Tachallait H, et al. *Bioorg Med Chem Lett.* 2018;28:1931–1936;
c) Allaoui S, Dufies M, Driowya M, et al. *Bioorg Med Chem Lett.* 2017;27(9):1989–1992;
d) Ronco C, Martin AR, Demange L, Benhida R. *Med Chem Commun.* 2017;8(2):295–319;
e) Houzé S, Hoang NT, Lozach O, et al. *Molecules.* 2014;19(9):15237–15257.
6. a) Jarray R, Pavoni S, Borriello L, et al. *Biochimie.* 2015;118:151–161;
b) Liu WQ, Borriello L, Allain B, et al. *Int J Pept Res Ther.* 2015;21(1):117–124;
c) Goldwaser E, DeCourcy B, Demange L, et al. *J Mol Model.* 2014;20(11):1–24;
d) Borriello L, Montès M, Lepelletier Y, et al. *Cancer Lett.* 2014;349(2):120–127;
e) Liu WQ, Megale V, Borriello L, et al. *Bioorg Med Chem Lett.* 2014;24(17):4254–4259.
7. Liu WQ, Lepelletier Y, Montes M, et al. *Cancer Lett.* 2018;414:88–98.
8. a) Abbavaram BRA, Reddyvari HRV. *J Kor Chem Soc.* 2013;57:731–737;
b) Kendall JD, Giddens AC, Tsang KY, et al. *Bioorg Med Chem.* 2012;20:58–68;
c) Zhang R, Lei L, Xu YG, Hua WY, Gong GQ. *Bioorg Med Chem.* 2007;17:2430–2433.
9. Singh R, Bordeaux M, Fasan R. *ACS Catal.* 2014;4:546–552.
10. Ashikawa M, Sakagami S. JP 2009167142, 2009.
11. Hadj-Slimane R. WO 2015004212, 2015.
12. Jenkis TJ, Guan B, Dai M, et al. *J Med Chem.* 2007;50:566–584.
13. Sheldrick GM. *SHELXS-97, Program for Crystal Structure Solution.* Göttingen, Germany: University of Göttingen; 1997.
14. Sheldrick GM. *Acta Crystallogr, Sect A: Found Crystallogr.* 2008;64:112–122.
15. Farrugia LJ. *J Appl Cryst.* 1999;32:837.
16. Crystal data and structure refinement for NRPa-308: Orthorhombic crystal, space group P212121 (no. 19), a = 7.8694(2) Å, b = 14.9423(5) Å, c = 17.9015(5) Å, V = 2104.98(11) Å3, Z = 4, T = 100(2) K, μ(CuKα) = 1.597 mm-1, Dcalc = 1.339 g/cm3, 23575 reflections measured (7.706° ≤ 2Θ ≤ 133.216°), 3719 unique (Rint = 0.0396, Rsigma = 0.0264) which were used in all calculations. The final R1 was 0.0252 (I > 2σ(I)) and wR2 was 0.0617 (all data). More details are provided in the Supporting Information section.
17. a) Zanuy D, Kotla R, Nussinov R, et al. *J Struct Biol.* 2013;182:78–86;
b) Teesalu T, Sugahara KN, Kotamraju VR, Ruoslahti E. *Proc Natl Acad Sci USA.* 2009;106:16157–16162.
18. a) Roth L, Agemy L, Kotamraju VR, et al. *Oncogene.* 2012;31:3754–3763;
b) Ye Y, Zhu L, Ma Y, Niu G, Chen X. *Bioorg Med Chem Lett.* 2011;21:1146–1150; c) Fu KF, Zhang WQ, Luo LM, et al. *Int J Nanomed.* 2013;8:2473–2485;
d) Sugahara KN, Teesalu T, Karmali PP, et al. *Cancer Cell.* 2009;16:510–520.
19. a) Liu H, Shi X, Wu D, et al. *ACS Appl Mater Interfaces.* 2019;11:19700–19711;
b) Ding N, Zou Z, Sha H, et al. *Nat Commun.* 2019. https://doi.org/10.1038/s41467-019-09296-6;
c) Barman S, Das G, Gupta V, et al. *Mol Pharm.* 2019;16:2522–2531;
d) Lo JH, Hao L, Muzumdar MD, et al. *Mol Cancer Ther.* 2018;17(11):2377–2388.

Synthesis, 3D-structure and stability analyses of NRPa-308, a new promising anti-cancer agent.

Etienne Brachet,[a]† Aurore Dumond,[b]† Wang-Qing Liu, [c,d]† Marie Fabre,[e]† Mohamed Selkti,[a] Françoise Raynaud,[c] Olivier Hermine, [f,g,h] Rachid Benhida,[e,i] Philippe Belmont,[a] Christiane Garbay,[d] Yves Lepelletier,[f,g,h] Cyril Ronco,[e] Gilles Pagès,[b,j¤] Luc Demange.[a ¤*]

SUPPORTING INFORMATION

a) Université de Paris, CiTCoM, UMR 8038 CNRS, Faculté de Pharmacie, F-75006 Paris, France.
b) Centre Scientifique de Monaco, Biomedical Department, 8 quai Antoine Ier, MC-98000, Monaco.
c) Université de Paris, CiTCoM, UMR 8038 CNRS & U 1268 INSERM, Faculté de Pharmacie, F-75006 Paris, France.
d) Université de Paris, LCBPT, UMR 8601 CNRS, UFR Biomédicale des Saints-Pères, F-75006 Paris, France.
e) Université Côte d'Azur, ICN, UMR 7272 CNRS, F-06108 Nice, France.
f) INSERM UMR 1163, Laboratory of cellular and molecular basis of normal hematopoiesis and hematological disorders: therapeutical implications, 24 boulevard Montparnasse, F-75015 Paris, France.
g) Université de Paris, Imagine Institute, 24 boulevard Montparnasse, F-75015 Paris, France.
h) CNRS ERL 8254, 24 boulevard Montparnasse, F-75015 Paris, France.
i) Mohamed VI Polytechnic University, UM6P, 43150 BenGuerir, Morocco.
j) Université Côte d'Azur, UMR 7284 CNRS and INSERM U 1081, Institute for Research on Cancer and Aging (IRCAN), Centre Antoine Lacassagne, 33 Avenue de Valombrose, F- 06189 Nice, France.

* Correspondence should be addressed to:
Luc Demange, e-mail : luc.demange@parisdescartes.fr; phone : +33 1 53 73 98 05.

† These authors contributed equally to this work.
¤ These authors co-directed the work

Chemistry.

General procedures.

Chemical reagents and solvents were purchased from Sigma-Aldrich, Fluka and Carlo Erba. Reactions were monitored by TLC using Merck silica gel 60F-254 thin layer plates. Column chromatographies were performed on SDS Chromagel 60 ACC 40-63 μM. Melting points were determined on a Köfler hot-stage (Reichert) and are uncorrected. NMR spectra were recorded on a Bruker Avance 250 MHz at 300 K, or on a Bruker Avance 400 MHz (100 MHz for ^{13}C NMR) at 300K. Chemical shifts were reported as □ values (ppm) indirectly referenced to the solvent signal, or to tetramethylsilane (TMS) as internal standard. Data are reported in the conventional form. Mass spectra were recorded on a ZQ 2000 Waters using a Z-spray (ESI-MS). HRMS spectrum was recorded on a ThermoFisher Q Exactive (ESI-MS) at a resolution of 140 000 at m/z 200. HPLC spectra were monitored with analytical reversed-phase HPLC on a Vydac C_{18} column (4.6×250 mm) with acetonitrile/water gradient containing 0.1% trifluoroacetic acid.

Synthetic procedures:

Pathway A (Scheme 1).

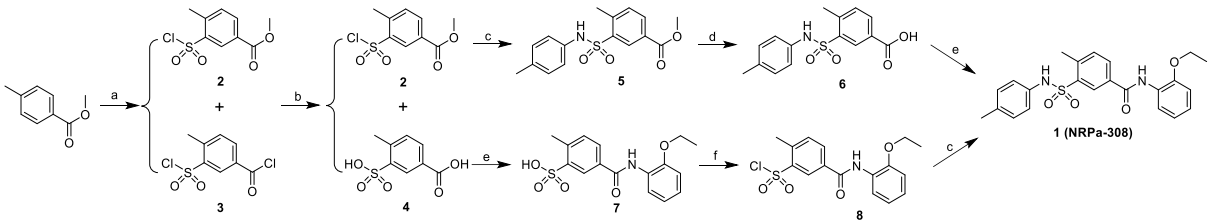

Methyl 3-(chlorosulfonyl)-4-methylbenzoate (2); 3-(chlorosulfonyl)-4-methylbenzoyl chloride (3); 4-methyl-3-sulfobenzoic acid (4).

Methyl *p*-toluate (12.7 g, 84.4 mmoles) was heated at 120°C in absence of solvent. When the solid material melted, the chlorosulfonic acid (6 mL, 90 mmoles) was added dropwise. The mixture was stirred at 120°C for 4 hrs, then cooled to room temperature and hydrolysed with 200 mL of cold water. Crude material was extracted with ethyl acetate (3 x 75 mL). The organic layers were collected and washed with water and brine, dried with Na_2SO_4, and concentrated *in vacuo*. The resulting mixture consisted in a solid in dispersion in oil, containing the unreacted starting material (methyl *p*-toluate), and the compounds **2** and **3**. At this point it was not possible

to isolate separately these products. Therefore, this crude material was solubilized in a mixture of 100 mL of toluene and 20 mL of brine, and treated with 50 mL of aqueous HCl (2N) in presence of a catalytic amount (3%) of tetrabutylammonium bromide. The mixture was refluxed overnight and then cooled to room temperature and the two layers were separated cautiously. The organic layer was washed twice with water and brine, dried with Na_2SO_4, and concentrated *in vacuo*. The crude material consisted in a solid in dispersion in oil. Successive cooling to 0°C and filtration led to compound **2** (4.2 g, about 20% yield, contaminated by starting methyl toluate) isolated as white solid, and compound **3** as an oil (2.1 g, 10% yield). Compound **2** has yet been described in the literature. The ^{1}H NMR spectra and the ESI-MS analysis of the white solid containing compound **2** and unreacted methyl *p*-toluate allowed us to identify unambiguously its presence.

Compound **2**: ^{1}H NMR (250 MHz, $CDCl_3$) □ (ppm): 8.70 (s, 1H), 8.34 (d, *J* = 8.5 Hz, 1H), 7.55 (d, *J* = 8.5 Hz, 1H), 4.10 (s, 3H), 2.90 (s, 3H). ESI-MS: *m/z* calcd for $C_9H_9ClO_4S$ $[M+H]^+$: 248.9 ; found 248.9.

The aqueous layer was precipitated with brine and filtrated, and compound **5** was obtained as a white solid (8.9 g, 49% yield).

Compound **4**: ^{1}H NMR (250 MHz, $CDCl_3$) □ (ppm): 8.49 (s, 1H), 8.34 (d, *J* = 8.5 Hz, 1H), 7.67 (d, *J* = 8.5 Hz, 1H), 2.64 (s, 3H). ESI-MS: *m/z* calcd for $C_8H_8O_5S$ $[M+H]^+$: 216.2 ; found 216.1.

4-Methyl-3-(*N*-(*p*-tolyl)sulfamoyl)benzoate (5).

Impure compound **2** (4 g, about 16 mmol) was dissolved into acetonitrile (20 mL), *p*-toluidine (8.5 g, 89 mmol) and a catalytic amount of DMAP were added. The mixture was stirred overnight at room temperature, then water was added (75 mL) and extracted with ethyl acetate (4 x 45 mL). The organic extract was collected, washed twice with a solution of $KHSO_4$ (1M) and brine, dried with Na_2SO_4, and concentrated to give 4.3 g of compound **5** as crude product. ^{1}H NMR (250 MHz, $CDCl_3$) □ (ppm): 8.6 (s, 1H), 8.1 (d, 1H) 7.3 (d, 1H), 7.0 (dd, 4H), 6.85 (s, 1H), 3.95 (s, 3H), 2.6 (s, 3H), 2.2 (s 3H).

4-Methyl-3-(*N*-(*p*-tolyl)sulfamoyl)benzoic acid (6).

Without purification, the crude compound **5** (4.3 g) was dissolved in methanol (50 mL) and treated with NaOH 2M (50 mL) to hydrolyse the carboxylate ester function. The mixture was stirred at room temperature for 3 hrs, and then methanol was evaporated by concentration. The crude resulting product was diluted in ice-water (50 mL) and the unsoluble impurities were filtered off. The aqueous solution was then acidified by HCl 12 N till pH 1, and extracted with diethyl ether (5 x 45 mL). The organic phases were collected, washed twice with a solution of $KHSO_4$ (1M) and brine, dried with Na_2SO_4, and concentrated *in vacuo*. The crude product was triturated several times with diethyl ether and filtered to give pure compound **6** as a white solid (1.5 g, 31% yield). ^{1}H NMR (250 MHz, DMSO-d6) □ (ppm): 13.30 (s, 1H), 10.41 (s, 1H), 8.40 (d, *J* = 8.3 Hz, 1H), 8.05 (d, *J* = 8.3 Hz, 1H), 7.55 (d, J = 8.3 Hz, 1H), 7.00 (m, 4H), 2.6 (s, 3H), 2.09 (s, 3H). ESI-MS: *m/z* calcd for $C_{15}H_{15}NO_4S$ $[M+H]^+$: 306.4 ; found 306.3.

5-((2-ethoxyphenyl)carbamoyl)-2-methylbenzenesulfonic acid (7). Compound **4** (4.3 g, 20 mmol) was dissolved in DMF (80 mL), then diisopropylethylamine (10 mL, 60 mmol), *o*-ethoxyaniline (3 g, 24 mmol) and BOP as coupling agent (8.8 g, 20 mmol) were successively added. The resulting mixture was stirred at room temperature for 48 hrs, and then the DMF was partly evaporated and the solution adjusted to pH = 2 by a solution of $KHSO_4$ 1M. The solution was then diluted with brine (25 mL) and extracted several time with ethyl acetate. The organic extracts were collected, washed twice with a solution of $KHSO_4$ (1M) and brine, dried with Na_2SO_4, and concentrated *in vacuo*. The crude material was triturated several times with methanol, and the resulting precipitate was filtered. This operation was repeated several times until the pure compound **7** was obtained (4.1 g, 62% yield). ^{1}H NMR (250 MHz, DMSO-d6) □ (ppm): 9.3 (s, 1H), 8.30 (s, 1H), 7.92 (d, *J* = 8.3 Hz, 1H), 7.82 (d, *J* = 8.3 Hz, 1H), 7.15-7.35 (m, 4H), 4.10 8.05 (d, *J* = 8.3 Hz, 1H), 7.55 (d, J = 8.3 Hz, 1H), 7.00 (m, 4H), 2.6 (s, 3H), 2.09 (s, 3 (q, *J* = 7.4 Hz, 2H), 2.60 (s, 3H), 1.31 (t, J = 7.4 Hz, 3H). ESI-MS: *m/z* calcd for $C_{16}H_{17}NO_5S$ $[M+H]^+$: 336.4 ; found 336.1.

***N*-(2-ethoxyphenyl)-4-methyl-3-(*N*-(*p*-tolyl)sulfamoyl)benzamide (1, NRPa-308).**

Compound **6** (1.3 g, 4 mmol) was dissolved in DMF (5 ml), then diisopropylethylamine (2 ml, 12.7 mmol), *o*-ethoxyaniline (0.7 g, 4.8 mmol) and BOP as coupling agent (1.8 g, 4.2 mmol) were successively added. The resulting mixture was stirred overnight at room temperature, and then diluted with ethyl acetate (20 mL), washed twice with a solution of $KHSO_4$ (1M) and brine, dried with Na_2SO_4, and concentrated *in vacuo*. The resulting crude material was purified by flash chromatography (ethyl acetate/hexane 1:3). The solid obtained after evaporation was further recrystallized from ethanol to afford compound **2a** as a pure pale pink powder (1.23 g, 73% yield).

Alternatively, compound **7** (0.5g, 1.49 mmol) was dissolved in DMF (2 mL), thionyl chloride (0.3 mL, 3 mmol) was added and the mixture was stirred at RT overnight. $SOCl_2$ was then evaporated and the residue was added with DIEA (1.6 mL 9 mmol), catalyst DMAP and o-ethoxyaniline (0.2 g, 1.79 mmol). The mixture was stirred at RT overnight, then was diluted with water (75 mL) and the solution was extracted with ethyl acetate several times. The organic phases were combined and washed with 1 M $KHSO_4$, brine, dried with Na_2SO_4 and evaporated, to obtained an impure product as yellow gel with worse quality of crude **2a**. Purification by flash chromatography gave 0.15 g pure compound **2a** (24% yield).

Mp 176°C. ^{1}H NMR (400 MHz, DMSO-d_6) δ 10.57 (s, 1H), 9.80 (s, 1H), 8.65 (s, 1H), 8.28 (d, *J* = 7.9 Hz, 1H), 7.95 (d, *J* = 7.7 Hz, 1H), 7.75 (d, *J* = 7.9 Hz, 1H), 7.40 (t, *J* = 7.8 Hz, 1H), 7.31 (d, *J* = 8.1 Hz, 1H), 7.28 – 7.10 (m, 5H), 4.31 (q, *J* = 6.9 Hz, 2H), 2.86 (s, 3H), 2.38 (s, 3H), 1.56 (t, *J* = 6.9 Hz, 3H). ^{13}C NMR (101 MHz, DMSO) δ 163.95, 151.45, 140.85, 138.55, 135.10, 133.55, 133.31, 133.01, 131.75, 130.10, 129.25, 127.21, 126.49, 125.00, 120.70, 120.20, 113.07, 64.42, 20.70, 20.23, 15.07; ESI-HRMS: *m/z* calcd for $C_{23}H_{24}N_2O_4S$ $[M+H]^+$: 425,15295 ; found 425.15308. HPLC analysis: (Shimadzu CBM-20A, column Phenomenex Luna 5µ, C_{18}, 100 Å, 250×4.6 mm. A: H_2O with 0.1% TFA, B: 70% acetonitrile with 0.09% TFA. Flow 1 mL/min, UV

detection at 214 and 254 nm), gradient: 70% B to 100% B in 30 minutes; Rt: 27.96 min, purity up to 99%.

Pathway B (Scheme 2):

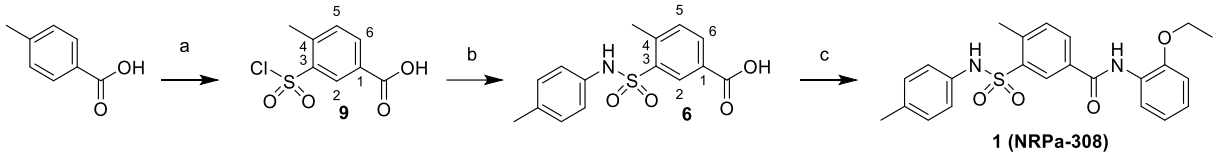

3-(chlorosulfonyl)-4-methylbenzoic acid (9).

A solution of 4-methylbenzoic acid (1.6g, 11.7mmol) in 13mL of chlorosulfonic acid was stirred at 100°C overnight. After cooling to room temperature, mixture was added on ice very slowly occurring precipitation of the desired product. Precipitate was filtered, washed with water and dried under reduced pressure to afford 2.3g of the compound **9** (84% yield) which was not purified for the next step.

4-methyl-3-(*N*-(*p*-tolyl)sulfamoyl)benzoic acid (10).

To a cooled solution (0°C) of compound **9** (1g, 4.3mmol) in 40 mL of DCM was added portion wise p-toluidine (6.9g, 64.5mmol). Reaction is warmed back to room temperature and check by TLC until consumption of the starting material (1 hour). Reaction was then quench by the addition of AcOEt (100mL) and HCl 3M (100mL). Organic layer is separated and successfully washed with 100mL of HCl (3M), 50mL of Brine. Organic layer is then dried on MgSO4 and concentrated under reduced pressure to afford 1.0 g of pure compound **6** (3.3 mmol, 78%). Compound **10**: ^{1}H NMR (400 MHz, DMSO-d_6) δ 13.17 (s, 0H), 10.34 (s, 0H), 8.38 (s, 0H), 7.99 (d, J = 7.9 Hz, 0H), 7.49 (d, J = 8.0 Hz, 0H), 7.02 (d, J = 8.2 Hz, 1H), 6.95 (d, J = 8.3 Hz, 1H), 2.62 (s, 1H), 2.15 (s, 1H).

Compound 1 (NRPa-308)

Compound **10** (0.5 g, 1.54 mmol) was dissolved in 2 mL of DMF at room temperature. To this solution was successfully added o-ethoxyaniline, EDCI (0.31 g, 1.62 mmol) and

diisopropylethylamine (770 µl, 4.88 mmol). The resulting mixture was stirred overnight at room temperature, and then diluted with ethyl acetate (20 mL), washed twice with a solution of saturated NaHCO3 and brine. Organic layer is then dried with Na2SO4, and concentrated in vacuo. The resulting crude material was purified by flash chromatography to afford NRPa-308 as a white powder (0.43 g, 1.0 mmol, yield 65%). Compound was recrystallized from hot toluene.

NMR spectra for compound NRPa-308

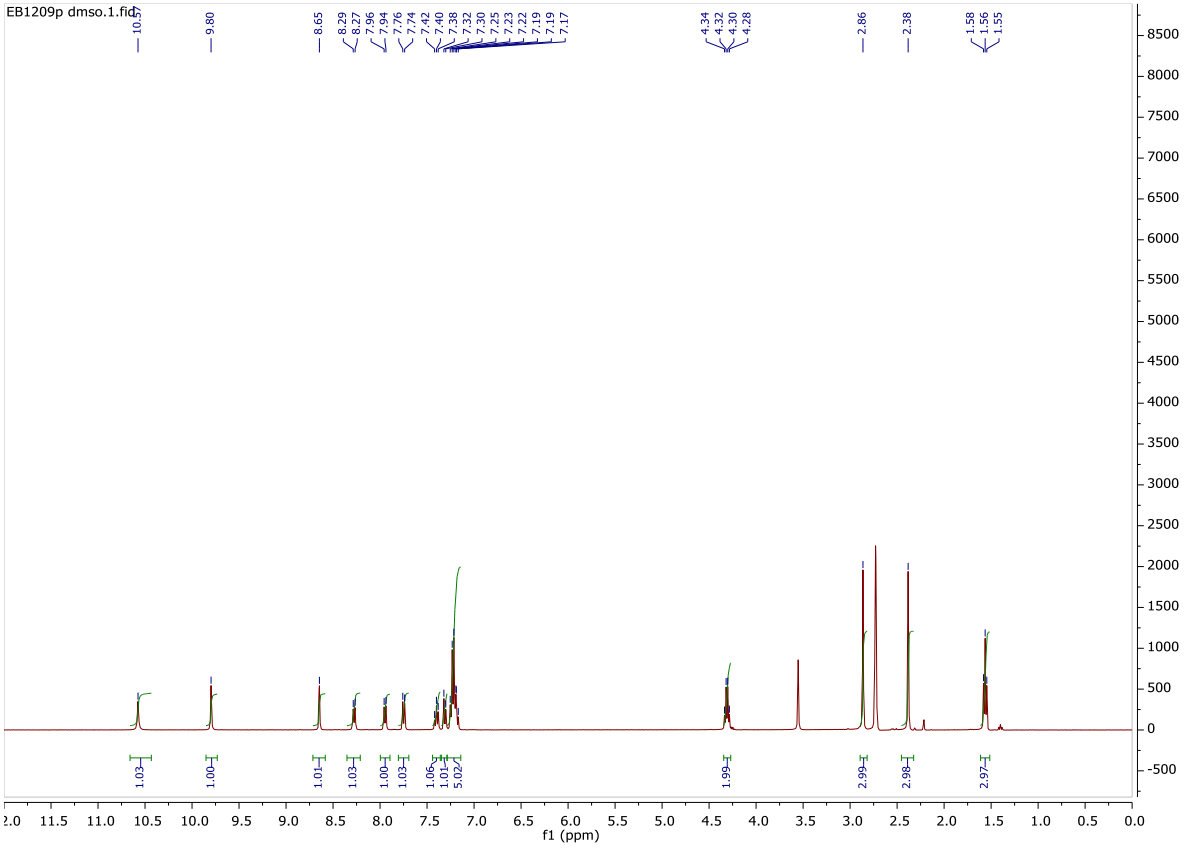

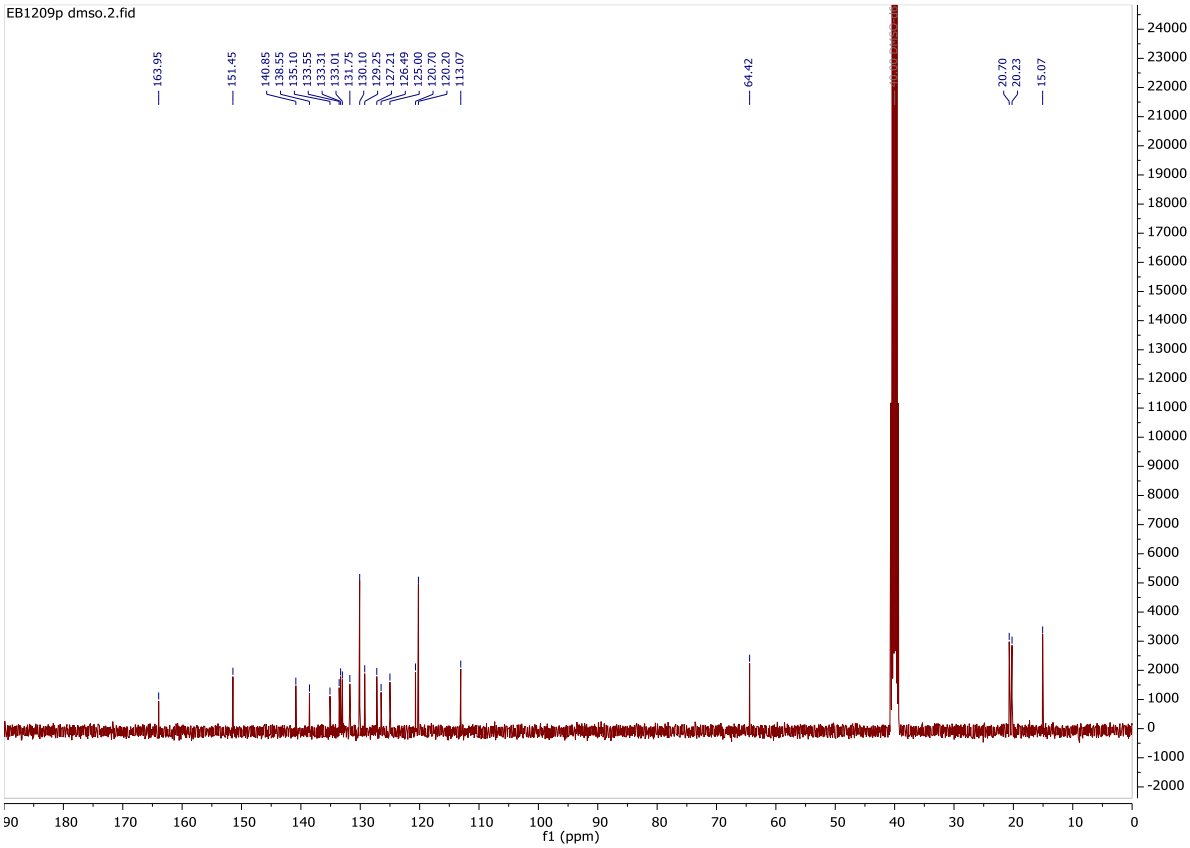

X-Ray analyses of NRPa-308 crystal.

Experimental procedure:

The X-ray diffraction data for the compound was collected by using a VENTURE PHOTON100 CMOS Bruker diffractometer with Micro-focus1□S source Cu K□ radiation. Crystal was mounted on CryoLoop (Hampton Research) with Paratone N (Hampton Research) as cryoprotectant and then flashfrozen in nitrogen gas stream at 100K. The temperature of crystal was maintained by means of 700 series Cryostream cooling device to within accuracy of 1K. The data was corrected for Lorentz polarization, and absorption effects.

Table S1. Crystal data and structure refinement for NRPa-308.

Temperature/K	100(2)
Crystal system	orthorhombic
Space group	$P2_12_12_1$
a/Å	7.8694(2)
b/Å	14.9423(5)
c/Å	17.9015(5)
α/°	90
β/°	90
γ/°	90
Volume/Å^3	2104.98(11)
Z	4
ρ_{calc}g/cm^3	1.339
μ/mm^{-1}	1.597
F(000)	896.0
Crystal size/mm^3	0.200 × 0.090 × 0.030
Radiation	CuKα (λ = 1.54178)
2Θ range for data collection/°	7.706 to 133.216
Index ranges	-9 ≤ h ≤ 8, -16 ≤ k ≤ 17, -21 ≤ l ≤ 21
Reflections collected	23575
Independent reflections	3719 [R_{int} = 0.0396, R_{sigma} = 0.0264]
Data/restraints/parameters	3719/1/271
Goodness-of-fit on F^2	1.042
Final R indexes [I>=2σ (I)]	R_1 = 0.0252, wR_2 = 0.0608
Final R indexes [all data]	R_1 = 0.0272, wR_2 = 0.0617
Largest diff. peak/hole / e Å^{-3}	0.26/-0.28
Flack parameter	0.026(5)

Tables of crystal analyse:

Table S2. Fractional Atomic Coordinates ($\times 10^4$) and Equivalent Isotropic Displacement Parameters ($Å^2 \times 10^3$) for NRPa-308. U_{eq} is defined as 1/3 of of the trace of the orthogonalised U_{IJ} tensor.

Atom	*x*	*y*	*z*	U(eq)
C1	10743(4)	3009.1(18)	6270.1(14)	37.7(7)
C2	11062(3)	3319.3(16)	5479.0(12)	24.1(5)
C3	11819(3)	4147.4(15)	5345.0(12)	22.8(5)
C4	12104(3)	4446.1(15)	4623.7(12)	18.7(5)
C5	11606(2)	3930.1(14)	4016.5(11)	14.5(4)
C6	10886(3)	3092.0(15)	4136.0(12)	19.2(5)
C7	10630(3)	2798.6(16)	4862.6(13)	22.8(5)
C8	9618(2)	3795.1(15)	2199.8(11)	14.5(4)
C9	8938(2)	2939.6(14)	2119.8(11)	13.8(4)
C10	7280(2)	2831.8(14)	1864.3(10)	13.6(4)
C11	6349(3)	3590.7(14)	1667.2(11)	16.6(4)
C12	7046(3)	4434.5(15)	1742.8(12)	19.2(5)
C13	8686(3)	4568.2(15)	2019.4(11)	16.8(4)
C14	9326(3)	5508.8(15)	2115.3(14)	24.6(5)
C15	6612(2)	1901.3(13)	1752.9(10)	13.8(4)
C16	3972(2)	1094.4(15)	1460.4(11)	16.4(4)
C17	4344(3)	219.1(16)	1631.7(14)	24.9(5)
C18	3501(3)	-468.4(17)	1257.8(17)	34.2(6)
C19	2264(3)	-270.1(18)	740.9(15)	33.3(6)
C20	1814(3)	607.9(16)	595.3(13)	25.4(5)
C21	2669(3)	1300.0(15)	953.7(12)	17.3(4)
C22	1058(3)	2453.6(17)	348.7(12)	23.0(5)
C23	1189(3)	3452.2(16)	276.2(13)	26.9(5)
N1	11811(2)	4334.5(11)	3303.6(10)	15.6(4)
N2	4899(2)	1824.6(12)	1763.0(10)	16
O1	12621.5(18)	4482.8(11)	2001.3(8)	18.9(3)
O2	12402.0(16)	2973.0(9)	2559.4(8)	17.4(3)
O3	7589.1(17)	1271.3(10)	1639.5(8)	18.1(3)
O4	2416.3(19)	2188.4(11)	835.0(8)	21.2(3)
S	11773.1(5)	3869.7(3)	2492.0(3)	13.90(12)

Table S3. Anisotropic Displacement Parameters ($Å^2 \times 10^3$) for NRPa-308. The Anisotropic displacement factor exponent takes the form: $-2\pi^2[h^2a^{*2}U_{11}+2hka^*b^*U_{12}+\ldots]$.

Atom	U_{11}	U_{22}	U_{33}	U_{23}	U_{13}	U_{12}
C1	64.5(18)	28.0(16)	20.7(13)	6.4(11)	5.8(13)	5.0(13)
C2	31.6(13)	21.8(13)	18.9(11)	5.1(9)	0.5(9)	8.2(10)
C3	28.6(12)	21.6(13)	18.1(11)	-4.2(9)	-2.8(9)	4.1(9)
C4	20.9(11)	16.5(12)	18.8(10)	-2.0(8)	-0.5(8)	-1.3(8)
C5	12.6(9)	15.1(11)	15.7(9)	-0.7(8)	0.4(7)	2.5(8)
C6	24.1(11)	14.5(12)	19.0(10)	-2.0(9)	-0.6(9)	-0.6(9)
C7	30.1(12)	12.9(12)	25.4(12)	3.6(9)	1.8(10)	2.1(9)
C8	12.4(9)	18.6(12)	12.5(9)	-0.9(8)	1.1(7)	1.4(8)
C9	15.8(10)	14.7(11)	10.8(9)	-0.4(8)	0.8(8)	3.4(8)
C10	15.3(9)	15.5(11)	10.1(9)	-0.8(7)	1.2(7)	1.3(8)
C11	15.4(10)	19.1(12)	15.4(10)	-1.3(8)	-2.3(8)	2.5(8)
C12	18.8(10)	17.3(12)	21.5(11)	0.9(9)	-1.8(9)	5.8(8)
C13	18.0(10)	15.6(12)	16.8(10)	-1.7(8)	2.3(8)	2.0(8)
C14	20.3(10)	16.8(13)	36.8(13)	-1.5(10)	-3.3(10)	0.8(9)
C15	15.5(9)	17.4(11)	8.3(9)	1.1(8)	-1.0(8)	1.9(8)
C16	14.3(9)	15.5(11)	19.3(10)	0.2(9)	5.7(8)	-1.0(8)
C17	17.2(10)	19.7(13)	37.7(14)	5.1(10)	7.8(10)	0.8(9)
C18	22.5(13)	13.6(13)	66.5(18)	-1.1(12)	15.5(12)	-2.2(9)
C19	22.4(12)	23.8(15)	53.6(17)	-13.0(12)	10.4(11)	-10.7(10)
C20	19.6(10)	26.6(14)	29.9(12)	-8.2(10)	0.9(10)	-8.6(10)
C21	16.6(10)	17.1(12)	18.2(10)	-1.8(8)	4.0(8)	-5.2(8)
C22	20.4(11)	32.5(14)	16.3(11)	-1.1(9)	-6.0(9)	0.6(9)
C23	28.2(12)	32.4(15)	20.1(12)	6.6(10)	-5.0(10)	6.6(10)
N1	20.8(8)	11.4(9)	14.7(8)	-0.7(7)	-1.0(7)	-2.6(7)
N2	14	15	18	-2	0	2
O1	16.1(7)	23.8(9)	16.8(7)	1.0(6)	2.1(6)	-1.2(6)
O2	15.5(6)	17.3(8)	19.5(7)	-4.2(6)	-1.8(6)	4.0(6)
O3	16.5(7)	13.2(8)	24.5(8)	-0.5(6)	0.5(6)	2.4(6)
O4	22.4(8)	17.7(9)	23.3(8)	1.9(6)	-10.1(6)	-2.7(6)
S	12.1(2)	16.1(3)	13.4(2)	-2.0(2)	-0.2(2)	0.86(18)

Table S4. Bond Lengths for NRPa-308.

Atom	Atom	Length/Å		Atom	Atom	Length/Å
C1	C2	1.511(3)		C13	C14	1.503(3)
C2	C7	1.392(3)		C15	O3	1.232(2)
C2	C3	1.394(3)		C15	N2	1.353(3)
C3	C4	1.384(3)		C16	C17	1.375(3)
C4	C5	1.389(3)		C16	C21	1.403(3)
C5	C6	1.391(3)		C16	N2	1.420(3)
C5	N1	1.421(3)		C17	C18	1.394(3)
C6	C7	1.387(3)		C18	C19	1.375(4)
C8	C9	1.393(3)		C19	C20	1.384(4)
C8	C13	1.406(3)		C20	C21	1.391(3)
C8	S	1.7781(19)		C21	O4	1.359(3)
C9	C10	1.392(3)		C22	O4	1.434(3)
C10	C11	1.395(3)		C22	C23	1.501(3)
C10	C15	1.500(3)		N1	S	1.6107(17)
C11	C12	1.381(3)		O1	S	1.4341(15)
C12	C13	1.397(3)		O2	S	1.4334(15)

Table S5. Bond Angles for NRPa-308.

Atom	Atom	Atom	Angle/˚		Atom	Atom	Atom	Angle/˚
C7	C2	C3	117.6(2)		O3	C15	C10	120.77(17)
C7	C2	C1	122.1(2)		N2	C15	C10	115.20(17)
C3	C2	C1	120.3(2)		C17	C16	C21	120.5(2)
C4	C3	C2	121.1(2)		C17	C16	N2	122.45(19)
C3	C4	C5	120.3(2)		C21	C16	N2	117.0(2)
C4	C5	C6	119.63(19)		C16	C17	C18	119.5(2)
C4	C5	N1	115.75(19)		C19	C18	C17	120.1(2)
C6	C5	N1	124.55(18)		C18	C19	C20	120.8(2)
C7	C6	C5	119.2(2)		C19	C20	C21	119.6(2)
C6	C7	C2	122.1(2)		O4	C21	C20	125.7(2)
C9	C8	C13	121.99(18)		O4	C21	C16	114.97(18)
C9	C8	S	117.01(16)		C20	C21	C16	119.3(2)
C13	C8	S	120.91(16)		O4	C22	C23	106.01(18)
C10	C9	C8	120.00(19)		C5	N1	S	128.65(14)
C9	C10	C11	118.75(19)		C15	N2	C16	124.87(18)
C9	C10	C15	118.64(18)		C21	O4	C22	118.29(17)
C11	C10	C15	122.42(17)		O2	S	O1	119.20(9)
C12	C11	C10	120.59(19)		O2	S	N1	108.71(9)
C11	C12	C13	122.13(19)		O1	S	N1	105.58(9)
C12	C13	C8	116.49(19)		O2	S	C8	107.19(9)
C12	C13	C14	118.96(19)		O1	S	C8	107.69(9)
C8	C13	C14	124.55(18)		N1	S	C8	108.05(9)
O3	C15	N2	124.00(19)					

Table S6. Hydrogen Atom Coordinates (Å×10^4) and Isotropic Displacement Parameters (Å^2×10^3) for NRPa-308.

Atom	*x*	*y*	*z*	U(eq)
H1A	10587.85	3530.53	6595.08	57
H1B	11717.06	2658.21	6444.74	57
H1C	9717.22	2637.56	6283.42	57
H3	12144.1	4512.58	5755.13	27
H4	12642.91	5006.84	4543.56	22
H6	10573.63	2724.94	3725.01	23
H7	10144.31	2224.3	4942.03	27
H9	9605.88	2429.82	2239.6	17
H11	5226.77	3526.54	1479.39	20
H12	6387.62	4940.18	1602.16	23
H14A	9619.05	5610.53	2640.56	37
H14B	8440.32	5932.19	1963.36	37
H14C	10337.65	5597.09	1804.34	37
H17	5169.23	83.84	2002.24	30
H18	3781.45	-1074.5	1360.07	41
H19	1711.92	-741.72	480.58	40
H20	925.28	737.16	252.63	30
H22A	-53.96	2282.65	564.36	28
H22B	1178.4	2163.84	-145.87	28
H23A	253.05	3673.83	-34.01	40
H23B	2275.38	3608.3	42.48	40
H23C	1123.76	3726.26	772.68	40
H1	11980.5	4916.61	3305.97	19
H2	4320(30)	2294(11)	1856(12)	19

NRPa-308 Stability assays.

HPLC analyses

HPLC analyses were performed on a JASCO PU-2089 apparatus with Supelco analytical column Ascentis Express C18, 100 mm × 46 mm 5 µ. Eluent A: water with 1‰ formic acid. Eluent B: CH_3CN with 1‰ formic acid. Method used: 0%B to 100%B over 4 min, then 100%B for 4 min (8 min in total).

Chemical stability in buffered solutions.

1 mg of NRP-a308 was dissolved in 200 µL DMSO and diluted in the corresponding buffer solution, pH 0.9, 7.4 and 8.4 (1.8 mL). These solutions were stored at 25°C or 37°C and analysed by HPLC at 0, 1, 2, 5, 6, 7, 12 and 16 days. The areas of the compound peak at 280 nm were reported at the different times and pH.

NRPa-308 stability and accumulation in cancer cells.

MDA-MB231 and BT549 cells were purchased from the American Type Culture Collection. Cells were grown in DMEM supplemented with 7 or 10% FCS plus 1% of non-essential amino-acid at 37°C in a humidified atmosphere containing 5% CO_2 in the presence of 2µM of NRPa-308. After three days, the supernatant was discarded, the cells were washed with 10mL of PBS from Dutscher and they were then lysed with 1mL of methanol. The methanolic lysates were extracted with $CHCl_3$/MeOH, 9/1, v/v, dried with $MgSO_4$ and the solvents were evaporated. The residues were dissolved in 1 mL MeOH and quantitatively analysed by HPLC thanks to a calibration curve.

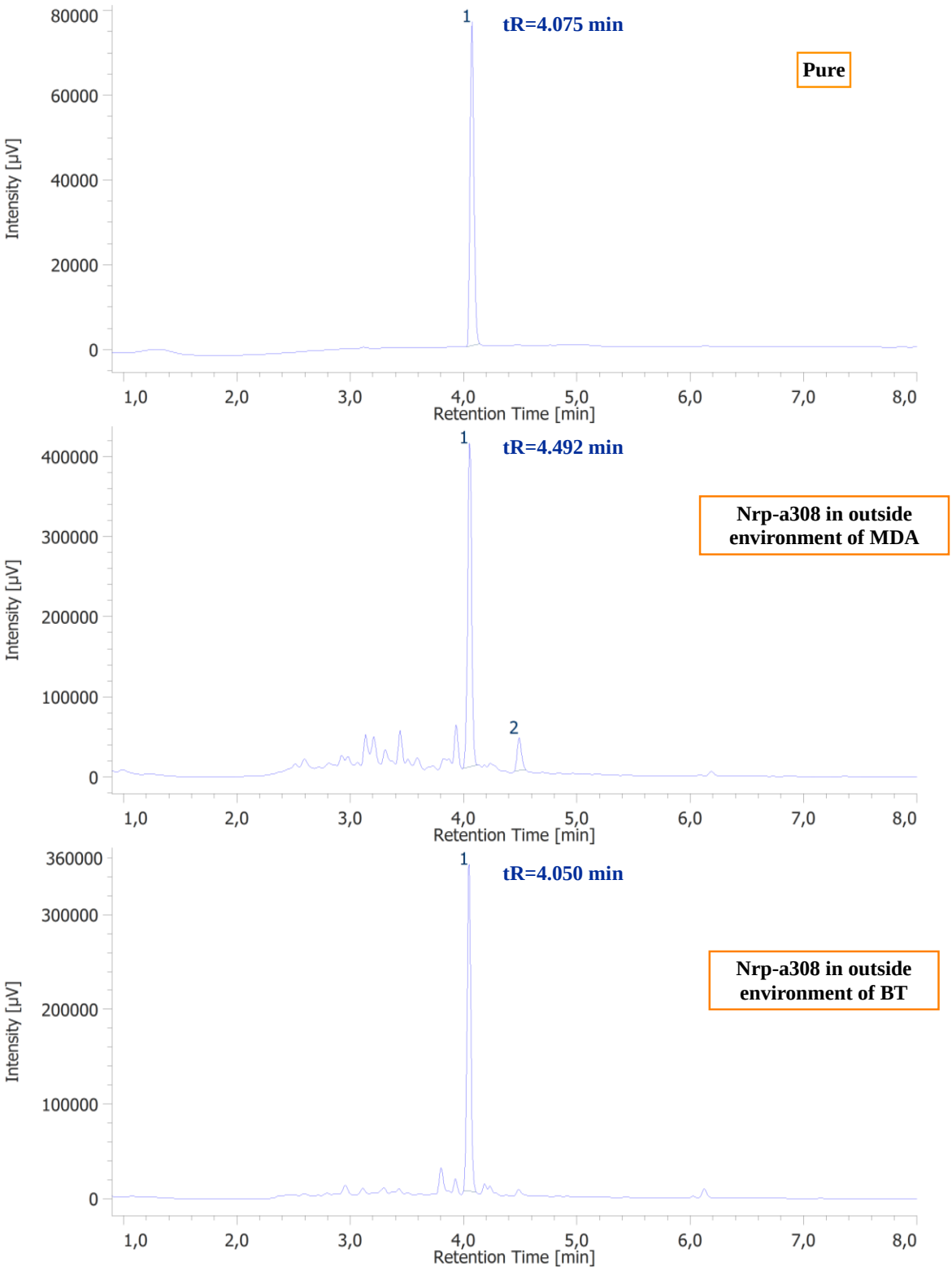

Figure S1. Stability of Nrp-a308 in outside environment of MDA and BT after three days incubation at 37°C.

ARTICLE 2

ARTICLE 2

Neuropilin 1 and Neuropilin 2 gene invalidation or pharmacological inhibition reveals their relevance for the treatment of metastatic renal cell carcinoma.

Aurore Dumond*, Etienne Brachet, Jérôme Durivault, Valérie Vial, Anna K. Puszko, Yves Lepelletier, Christopher Montemagno, Marina Pagnuzzi-Boncompagni, Olivier Hermine, Christiane Garbay, Nathalie Lagarde, Matthieu Montes, Luc Demange, Renaud Grépin and Gilles Pagès.

*First author

Article in revision at Cancer Letters.

I) Scientific context and objectives

The transient efficacy or the refractoriness to the current anti-angiogenic therapies approved for the advanced ccRCC is a major concern. The discovery of new targets involved in different hallmarks of cancer is urgently needed to develop new efficient treatments. During the last years, the role of Neuropilins (NRPs) in driving the aggressiveness of different cancers was described in several publications. In reviews published in Frontiers in Oncology [156] and in Medecine/Sciences [157], we compiled the results of pivotal studies that highlight the role of Neuropilins in tumor cells and in cells from the microenvironment.

Indeed, NRPs expressed by immune cells can either activate or inactivate the immune system. For example, the homophilic interaction between NRP1, expressed on naive T cells, and NRP1, expressed by dendritic cells, prolonged the antigen presentation by dendritic cells to T cells resulting in T cell activation. However, at a later stage, cytotoxic T cells express SEMA3A that inhibits NRP1 homophilic interaction and antigen presentation to T cells. In this case, NRP1 inactivates immune system cells. The expression of NRP1 by Treg is another example: i) its interaction with SEMA4A, expressed by dendritic cells, maintains Treg function and immunosuppression; ii) its interaction with VEGF expressed by tumor cells induces Treg infiltration in the tumor and also immunosuppression.

Many studies have highlighted the role of NRPs expressed on tumor cells and cells of the microenvironment in the induction of angiogenesis [76]. Indeed, exacerbated angiogenesis and poor prognosis are correlated to NRP1 expression in different animal models [158]. The opposite

phenomenon was only observed in pancreatic cancer [110], in which NRP2 expression is correlated to tumor progression. NRPs' expression is also correlated to the stemness of cancer cells mediating their self-renewal, their heterogeneity and their resistance to chemo- and radiotherapies. NRP1 stimulates the proliferation of cancer-associated fibroblasts (CAFs) which favors tumor progression. NRP1 and NRP2 enhance the resistance to chemo-, radio- and targeted therapies.

The long-term disappointing efficacy of current anti-angiogenics for ccRCC treatments, incited us to evaluate the relevance of targeting NRP1 and NRP2. Cao Y *et al.*, by using a genetic approach with shRNA for down-regulating both NRPs, highlighted the role of NRP1 in ccRCC cell migration, invasion and tumor growth and the role of NRP2 in ccRCC tumor cell extravasation and metastasis [91,92]. In my study, I deciphered more precisely the role of each NRP by a genetic approach using the same shRNA as Cao's team but also by knocking-out NRPs' expression by CRISPR/Cas9. We also demonstrated the pivotal role of NRPs by a pharmacological approach with the NRPs' inhibitor NRPa-308.

II) Results

1) NRPs' down-regulation by shRNA

Cao *et al.* did not observe any changes induced by NRP1 or 2 down-regulations on cell proliferation at short term (24h). Our long-term experiments (72 to 96h) showed that NRP1 down-regulation slightly decreased cell proliferation and NRP2 down-regulation stimulated cell proliferation. Cao *et al.* stated that NRP1 or NRP2 down-regulation did not impact cell migration evaluated after 2 hours in Boyden chambers. We carried out migration experiments for 10 hours by measuring wound closure on a cell monolayer every hour to determine a migration velocity. We determined that NRPs' down-regulation decreased ccRCC cell migration but had no impact on the production of their ligands (VEGFA and VEGFC).

shRNA down-regulated NRPs' expression by only 60%. We hypothesized that the remaining proteins give discrepant results. Therefore, we knocked-out NRPs' genes by the CRISPR-Cas9 method to evaluate the effects of a full invalidation of NRPs.

2) NRPs knock-out by CRISPR/Cas9

We compared the effects of a down-regulation by shRNA versus a knock-out (KO) (60% decrease with shRNA *vs*. 100% with CRISPR/Cas9) in ccRCC on cell proliferation, migration and the production of NRPs' ligands. The NRP1 KO slightly reduced ccRCC cell proliferation, a result consistent with those obtained with the down-regulation by shRNA. However, the NRP2 KO decreased cell proliferation more efficiently than NRP1 KO, an opposite effect as compared to its down-regulation. Thus, stronger the inactivation of NRP2 is, better the proliferation of ccRCC cell is reduced. NRPs' down-regulation or KO consistently inhibited cell migration. Whereas NRPs down-regulation did not affect the production of their respective ligands, NRP1 KO increased VEGFA and slightly VEGFC expression, and NRP2 KO increased VEGFC and, inconsistently, VEGFA expression.

. In immunodeficient mice, NRPs' KO delayed tumor growth and the tumor volumes were smaller as compared to tumors generated with control cells. Furthermore, in immunocompetent mice, tumors did not develop after grafting NRPs' KO cells. Thus, NRPs expressed by ccRCC tumor cells stimulate tumor growth and inactivate the anti-tumor immune system.

These results prompted us to test pharmacological inhibitors of NRPs in collaboration with the chemists from University Paris-Descartes. The relevance of the NRPs inhibitor, NRPa-308, was investigated.

3) NRPs inhibition by NRPa-308

NRPa-308 showed a better therapeutic profile as compared to sunitinib, with a better IC_{50} and reduced toxic effects on normal cells.

The wide range of sensitivity of primary RCC cells to NRPa-308 correlated with NRP mRNA levels. This result was confirmed by measuring the effects of NRPa-308 on NRP KO ccRCC cells. NRPa-308 effects on ccRCC cell proliferation mainly depend on NRP2 rather than on NRP1. These experiments highlighted the importance to determine the level of expression of each NRP in the tumor before using NRPs inhibitors in patients.

Finally, *in-vivo* experiments highlighted that NRPa-308 decreased ccRCC tumor growth, weight and tumor's functional blood vessels in a reverse dose-dependent manner. The best effect was obtained at 5 µg/kg corresponding to the *in-vitro* concentration at which NRPa-308 decreased cell proliferation and migration without increasing pro-angio/lymphangiogenic and pro-inflammatory factors (NRPa-308 stimulates VEGFA and -C, CXCL5 and -8 expression at high dose (2µM) but not a low doses (0. 2µM). At this low dose, NRPa-308 decreased most of the

pro-tumoral factors. The same results were obtained in immunocompetent and immunodeficient mice.

These different experiments highlight the major role of the NRP2 pathway in the aggressiveness of ccRCC, confirmed by TCGA patients' study showing the importance of NRP2 pathway's members in mccRCC.

III) Conclusion and perspectives

This study highlighted the importance of NRPs in the aggressiveness of ccRCC. Notably, the experiments on the down-regulation (shRNA) and the KO (CRISPR/Cas9) highlighted that the level of inactivation of NRPs directly correlates with the anti-tumoral effects. This phenomenon is particularly striking for NRP2 for which down-regulation or KO resulted in opposite results. This result was confirmed by using NRPa-308 that inhibits NRP2/VEGFC binding more efficiently as compared to NRP1/VEGFA binding. However, in cells expressing NRP 1 and 2, targeting both NRPs remains the best strategy. Indeed, we tried several times to obtain ccRCC cells with a double NRPs KO without any success. This result strongly suggests that ccRCC cells are addicted to the NRPs' pathways and therefore their inactivation is lethal.

In the context of ccRCC, expressing NRP1 and NRP2, NRPa-308 is a "hit" molecule, reducing, at a low dose (0.2 µM), *in-vitro* ccRCC cell proliferation, migration without enhancing the expression of NRPs' ligands. At this low dose, corresponding to an *in-vivo* concentration of 5 µg/kg in the mice, NRPa-308 decreased tumor growth, the expression of pro-tumoral genes such as VEGFs or VEGFRs and stimulated the expression of genes related to an active immune system, for example CD69 or ARG1.

Thus, in ccRCC expressing NRP1 and NRP2, NRPa-308 is a "hit" molecule. Our results pave the way toward its use in early phase clinical trials.

Neuropilin 1 and Neuropilin 2 gene invalidation or pharmacological inhibition reveals their relevance for the treatment of metastatic renal cell carcinoma

Aurore Dumond[1], Etienne Brachet[2], Jérôme Durivault[1], Valérie Vial[1], Anna K. Puszko[3], Yves Lepelletier[4,5], Christopher Montemagno[1], Marina Pagnuzzi-Boncompagni[1], Olivier Hermine[4,5], Christiane Garbay[6], Nathalie Lagarde[7], Matthieu Montes[7], Luc Demange[2,8], Renaud Grépin[1] and Gilles Pagès,[1,9#].

1. Centre Scientifique de Monaco, Biomedical Department, 8 Quai Antoine Ier, MC- 98000 Monaco, Principality of Monaco.
2. Université de Paris, CiTCoM, UMR 8038 CNRS, F-75006 Paris, France.
3. Faculty of Chemistry, University of Warsaw, Pasteura 1, 02-093 Warsaw, Poland
4. INSERM UMR 1163, Laboratory of Cellular and Molecular Basis of Normal Hematopoiesis and Hematological Disorders: Therapeutical Implications, F-75015 Paris, France
5. Université de Paris, Imagine Institut, F-75015 Paris, France
6. Université de Paris, LCBPT, UMR8601 CNRS, UFR Biomédicale des Saints-Pères, F- 75006 Paris, France
7. Laboratoire GBCM EA7528, Conservatoire National des Arts et Métiers, 2 Rue Conté, 75003 Paris, France.
8. Université Côte d'Azur, ICN, UMR 7272 CNRS, F-06108 Nice, France
9. University Cote d'Azur (UCA), Institute for research on cancer and aging of Nice, CNRS UMR 7284; INSERM U1081, Centre Antoine Lacassagne, France.

Corresponding author
Gilles Pagès: Gilles.Pages@unice.fr
Centre Scientifique de Monaco. 8 quai Antoine 1er. 98000 Monaco.
MONACO 0033492031231 / 0033665367355

Abstract

Despite the improvement of relapse-free survival, metastatic clear cell Renal Cell Carcinoma (mccRCC) remain incurable. Hence, new relevant treatments are urgently needed. The VEGFs coreceptors, Neuropilins 1, 2 (NRP1/2) are expressed on several tumor cells including ccRCC. We analyzed the role of the VEGFs/NRPs signaling in ccRCC aggressiveness and evaluated the relevance to target this pathway with the competitive inhibitor of NRPs, NRPa-308. Invalidation of the *NRP1* and *NRP2* genes inhibited cell proliferation and migration and stimulated the expression of VEGFA or VEGFC, the natural ligands of NRP1/2 respectively. NRPa-308 decreased the proliferation and migration of ccRCC cells more efficiently than sunitinib, the reference treatment of ccRCC and, than the commercially available NRP inhibitor EG00229. NRPa-308 inhibited the growth of experimental ccRCC in immunocompetent and immunodeficient mice. Such inhibition was associated with a decreased expression of several pro-tumoral factors. Analysis of the TCGA database showed that in metastatic patients, the NRP2, more than the NRP1 pathway correlates with tumor aggressiveness. Our study suggests that inhibiting NRPs is a relevant therapeutic strategy for mccRCC patients in therapeutic impasses and NRPa-308 represents a relevant hit.

Keywords ccRCC, Neuropilins, oncology, immunology, cancer

Abbreviations

ATCC: American type culture collection;
BSA: bovine serum albumin;
ccRCC: clear cell Renal Cell Carcinoma;
CXCL: C-X-C motif chemokine;
DNA: deoxyribonucleic acid;
EMT: epithelial/mesenchymal transition;
GFP: green fluorescent protein;
HDF: normal dermal fibroblast;
HGF: hepatocyte growth factor;
HIF: hypoxia inducible factor;
HRP: horseradish peroxidase;
IC_{50}: half maximal inhibitory concentration;
KO: knock-out;
Luc: luciferase;
mccRCC: metastatic clear cell Renal Cell Carcinoma;
MET: c-MET tyrosine-kinase receptor;
mRNA: messenger ribonucleic acid;
NRP: Neuropilin;
PBS: phosphate buffered saline;
PEI: polyethylenimine;
qPCR: quantitative polymerase chain reaction;
sgRNA: single guide ribonucleic acid;
shRNA: short-hairpin ribonucleic acid;
SI: selectivity index;
TBS: tris-buffered saline;
TCGA: the cancer genome atlas;
TKi: tyrosine-kinase inhibitor;
VEGF: vascular endothelial growth factor;
VEGFR: vascular endothelial growth factor receptor;
VHL: Von-Hippel Lindau;
α SMA: α smooth muscle actin;

Highlights

1- NRP2 knock-out impacts more importantly RCC cell proliferation as compared to NRP1 knock-out.

2- The competitive NRPs inhibitor, NRPa-308, efficiently inhibits the growth of experimental RCC

3- The presence of both NRPs is necessary for the efficacy of NRPa-308 at a low dose.

4- Genes related to the NRP2 pathways are of good prognosis in low grade, but of poor prognosis in high grade RCC

1. Introduction

Clear cell Renal Cell Carcinoma (ccRCC), the most frequent form of RCC, are inactivated for the *von Hippel-Lindau* gene (*VHL*), leading to Hypoxia Inducible Factor-1 and 2 alpha (HIF-1, 2α) stability [1]. HIFs participate in tumor aggressiveness through Vascular Endothelial Growth Factor-A (VEGFA)-dependent angiogenesis and VEGFC-dependent lymphangiogenesis [1]. VEGFA exerts its activity through its receptors VEGFR1/2 and its coreceptor Neuropilin 1 (NRP1) and VEGFC through VEGFR2/3 and Neuropilin 2 (NRP2) [2]. Tyrosine-kinase inhibitors (TKi) targeting the kinase domain of VEGF receptors such as sunitinib (Sutent ®) are reference treatments [3]. Immunotherapies, alone or combined with TKi [4, 5] were approved more recently. Sunitinib increases median survival length from few months to few years [6]. This transient effect is related at least to a VEGFC-dependent development of a lymphatic network favoring metastasis [7]. Despite the improvement obtained with the current treatments, mccRCC remains incurable. Therefore, alternative therapies are needed. NRPs were described as mediators of neuronal guidance. NRP1 and NRP2 share 44 % amino acid sequence and close domain structures. They form ternary complexes with VEGFR tyrosine kinase domains. They represent key actors of the pro-angiogenic and pro- lymphangiogenic signaling pathways and they play a key role in the immune response [8]. NRPs overexpression in cancer cells correlates to a poor prognosis [9]. Down-regulation of *NRP1* by shRNA in ccRCC cells decreases experimental tumor growth [10], while *NRP2* down- regulation results in reduced metastasis [11]. Thus, targeting NRPs in ccRCC appears as a relevant therapeutic strategy. Therefore, we developed a NRPs inhibitor, NRPa-308, which exerts anti-angiogenic and anti-proliferative effects, and prevents the growth of experimental triple negative breast cancers [12, 13]. The aim of this study was to validate the relevance of NRPs targeting in experimental ccRCC generated in immunodeficient and immunocompetent mice. Genetic and pharmacological approaches were used to this end.

2. Materials and methods

2.1 Genomic disruption of Neuropilins using CRISPR-CAS9

It was performed as described [14]. The sgRNA sequence used to target the NRP1 gene was: 5'-CGGGTACCTTACATCTCCTG-3'; the sgRNA sequence targeting the NRP2 gene was: 5'-TTCAAACGACCTCCGCACGG-3'. Sequencing of human genomic DNA to confirm the mutations leading to NRP1 or NRP2 invalidation was performed using the following primers: Forward NRP1 5'- CACGAAGGACTTACGGGG-3' and Reverse NRP1 5'-AGACAGGCGTGACCAGTAG-3', and Forward NRP2 5'-TGAGCCGGAATAATCTCTTCCAC-3' and Reverse NRP2 5'-GGTGCTTACTTGCAGTCGTG-3'.

2.2 Protein level measurement by flow cytometry analysis (FACS)

Knock-out (KO) cells were incubated for one hour with: i) polyclonal anti-human NRP1 antibody (sheep IgG; AF3870; R&D systems); ii) polyclonal anti-human/Mouse/Rat NRP2 antibody (goat IgG; AF2215; R&D systems). After washing with PBS, the cells were incubated for 30min with secondary antibodies: i) Donkey Anti-Sheep IgG H&L, Alexa Fluor 594 (Abcam); ii) Goat anti-Human IgG (H+L) Cross-Adsorbed Secondary Antibody, Alexa Fluor 488 (Thermo Fisher). Cells were washed with PBS and resuspended in the FACS medium (PBS + 2.5mM EDTA). NRP1 and NRP2 levels were determined using a fluorescence-activated cell sorter (FACS Melody BD Biosciences) with a 488nm and a 594nm laser beam.

3. Results

3.1 *NRP1* or *NRP2* gene invalidation inhibited cell proliferation and migration

Our team [15] and Cao Y et al [10, 11] reported that ccRCC cells did not express VEGFR 1, 2 and 3. Moreover, VEGFA and VEGFC exert autocrine proliferation loops via NRPs. Cao Y et al showed that neither NRP1 or NRP2 knock-down by shRNA impacted ccRCC cell proliferation and migration [10, 11]. These results were surprising since the NRPs-mediated signaling pathways were associated with cell proliferation and migration in several cancers [16]. By using

the same shRNA, we obtained comparable knock-down levels (Fig. S1A and B) and we showed that NRP1 knock-down decreased NRP2 expression suggesting a crosstalk between the NRP1 and NRP2 signaling pathways (Fig. S1A and B). A small but significant inhibition of cell proliferation for the shNRP1 cells and an increased cell proliferation for the shNRP2 cells were obtained (Fig. S1C). Migration was also inhibited for shNRP1 and shNRP2 cells (Fig. S1D). VEGFA and VEGFC were not affected by the knockdowns (Fig. S1E). These discrepancies with the results of Cao Y et al incited us to decipher the role of NRP1 and NRP2 by knocking-out (KO) their genes in human (786-O) and mouse (RENCA) ccRCC cells. Two independent KO clones for NRP1 and NRP2 genes were obtained for 786-O (Fig. 1A and B), and one KO clone for NRP1 and NRP2 genes for RENCA (Fig. S2A) cells. NRP1 and NRP2 protein levels were undetectable in the KO clones (Fig. 1C and Fig. S2B). However, NRP1 KO tends to increase NRP2 levels whereas NRP2 KO decreased NRP1 levels in 786-O cells (Fig. 1C). Although the trend in decreased NRP1 levels were observed in NRP2 KO cells, the NRP1 KO resulted in decreased expression of NRP2 in RENCA cells (Fig. S2B). We obtained opposite results between KO and down-regulation of NRP1 by shRNA for NRP2 expression in 786-O cells. These results (Table S2) suggest a fine-tuned crosstalk between NRP1 and NRP2 signaling, which mediates an equilibrated expression of each protein compatible with proliferation/survival. In 786-O cells, NRP1 KO moderately impacted cell proliferation while NRP2 KO decreased cell proliferation more importantly (Fig. 1D). These results were consistent between NRP1 down-regulation and KO. However, NRP2 KO inhibited whereas NRP2 down-regulation stimulated cell proliferation (Fig. 1D and Fig. S1C). A moderate but non-significant inhibition of cell proliferation was observed in NRP1 KO but NRP2 KO resulted in inhibition of RENCA cell proliferation (Fig. S2C). Except for one NRP1 KO clone, NRPs KO decreased the migration of 786-O cells which is consistent with the results obtained by down-regulating NRP1 and NRP2 (Fig. 1E and Fig. S1D). Since the NRPs signaling depends on the stimulation by VEGFA and VEGFC, we tested their expression in KO cells. NRP1 KO increased VEGFA levels without consistently affecting VEGFC expression in 786-O cells. NRP2 KO induced VEGFC expression with inconsistent effects on VEGFA (Fig. 1F). VEGFA levels decreased in NRP1 and NRP2 KO

RENCA cells and VEGFC was down-regulated only in NRP2 KO cells (Fig. S2D). Table S3 recapitulates the impact of the KO or the knock-down on VEGFA and VEGFC levels in the different cells. These results suggest a steady state level of autocrine loops involving the NRP1/VEGFA and NRP2/VEGFC signaling pathways.

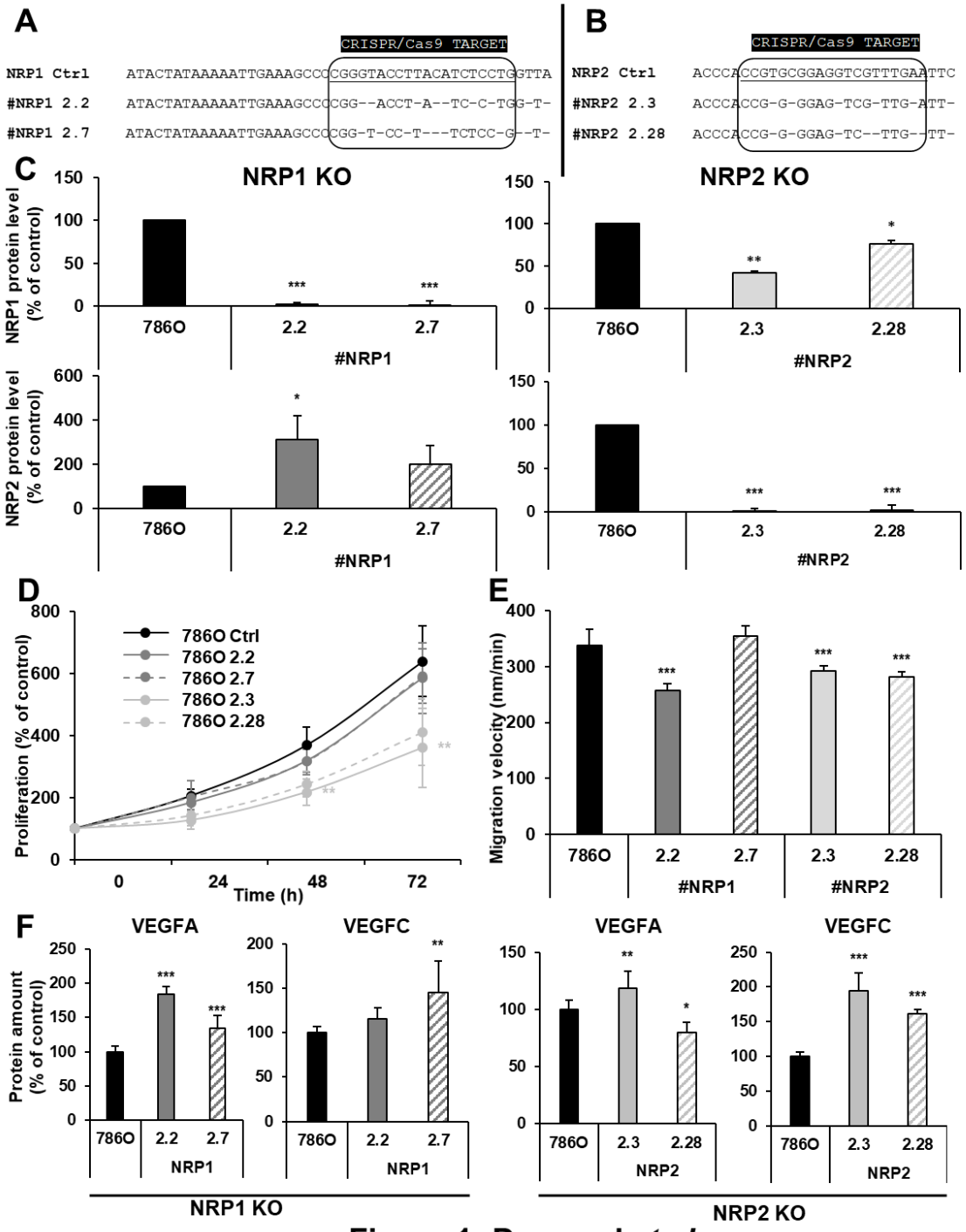

Figure 1: Dumond *et al*

Fig. 1. *NRP1* or *NRP2* gene invalidation results in inhibition of cell proliferation and migration. (A) The locus of the *NRP1* gene was sequenced in control (NRP1 Ctrl) and in two independent clones (#NRP1 2.2 and #NRP1 2.7) KO for *NRP1*. **(B**) The locus of *NRP2* was sequenced in control (NRP2 Ctrl) and in two independent clones (#NRP2 2.3 and #NRP1 2.28) KO for *NRP2*. **(C)** NRP1 and NRP2 protein levels were evaluated by flow cytometry in control (786O), in two independent clones (#NRP1 2.2 and 2.7) KO for *NRP1*, and in two independent clones (#NRP2 2.3 and 2.28) KO for *NRP2.* **(D)** The proliferation of *NRP1* and *NRP2* KO cells were tested by counting the cells at the indicated time points. **(E)** The migration of *NRPs* KO cells was determined in scratch assays by measuring the time of wound closure. **(F)** VEGFA and VEGFC expression was tested in control (Ctrl) and KO clones by ELISA. *p < 0.05; **p<0.01; *** p<0.001.

3.2 NRPs KO inhibited ccRCC growth in immunocompetent and immunodeficient mice

Considering the importance of the immune system for the development of mccRCC, we tested the impact of NRPs on tumor growth in immunocompetent and immunodeficient mice. The *NRP1* and *NRP2* 786-O KO clones generated smaller tumors in nude mice as compared to the controls (Fig. S3). *NRP1* or *NRP2* KO in RENCA cells delayed tumor development in nude mice (Fig. 2A). The same cells in immunocompetent mice did not generate tumors (Fig. 2B). These results suggest that NRPs expression by tumor cells prevents the efficacy of immune cells to inhibit tumor development.

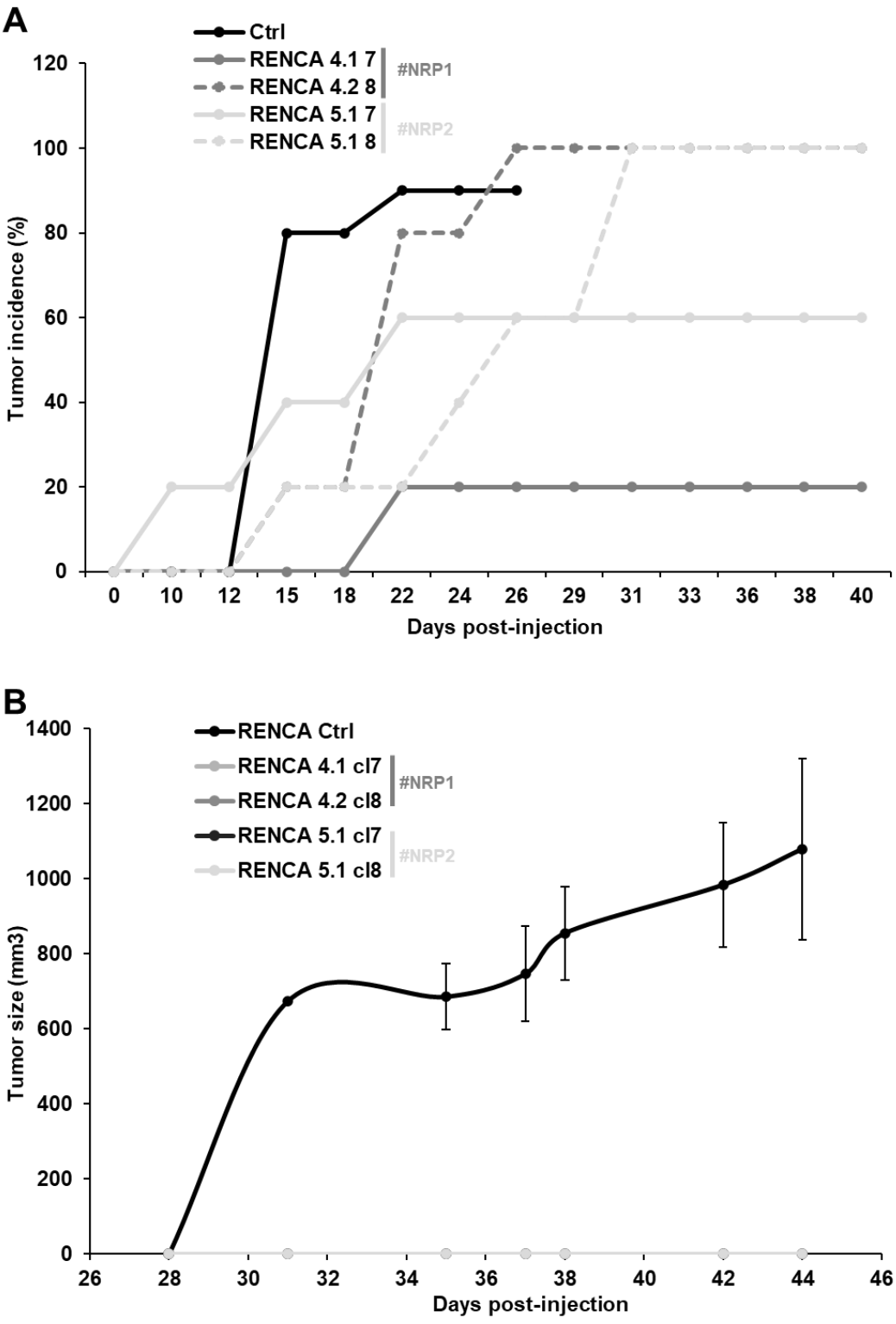

Figure 2: Dumond *et al.*

Fig. 2. NRPs KO inhibits experimental RCC growth in immunocompetent and immunodeficient mice. (A) Experimental tumors in nude mice (5 mice per condition) were obtained after injection of $3x10^5$ control (Ctrl) or NRPs KO RENCA cells. Two independent *NRP1* (4.1 7 and 4.2 8) and two independent NRP2 (5.1 7 and 5.1 8) clones were injected. Tumor incidence (percentage of mice with tumors) at the indicated times is presented. **(B)** Experimental tumors in immuno-competent Balb-C mice (5 mice per condition) were obtained after subcutaneous injection of $3x10^5$ control (Ctrl) or the above-mentioned NRPs KO RENCA cells. The tumor volume is represented for the indicated time.

3.3 NRPa-308 inhibited ccRCC cell proliferation more efficiently than sunitinib and EG00229

The therapeutic impact of NRPa-308 on different parameters of ccRCC cells aggressiveness was compared to sunitinib and to the NRPs inhibitor EG00229. EG00229 modestly inhibited the proliferation of ccRCC cells (Fig. 3A and B). Sunitinib inhibited ccRCC cell proliferation more efficiently in 786-O as compared to A498 cells. NRPa-308 inhibited cell proliferation to a better extent as compared to sunitinib. Moreover, the IC_{50} of NRPa-308 was superior for normal cells (HDF) (Fig. 3C). The selectivity index (SI) for which normal cells (HDF) served as the reference, was inferior to 1 which indicates that NRPa-308 is more efficient on tumor cells and that its toxicity is low. he lower SI of NRPa-308 as compared to sunitinib suggested higher anti-proliferative and less toxic effects (Fig. 3D). Hence, NRPa-308 presents, at least in vitro, a better therapeutic profile than sunitinib.

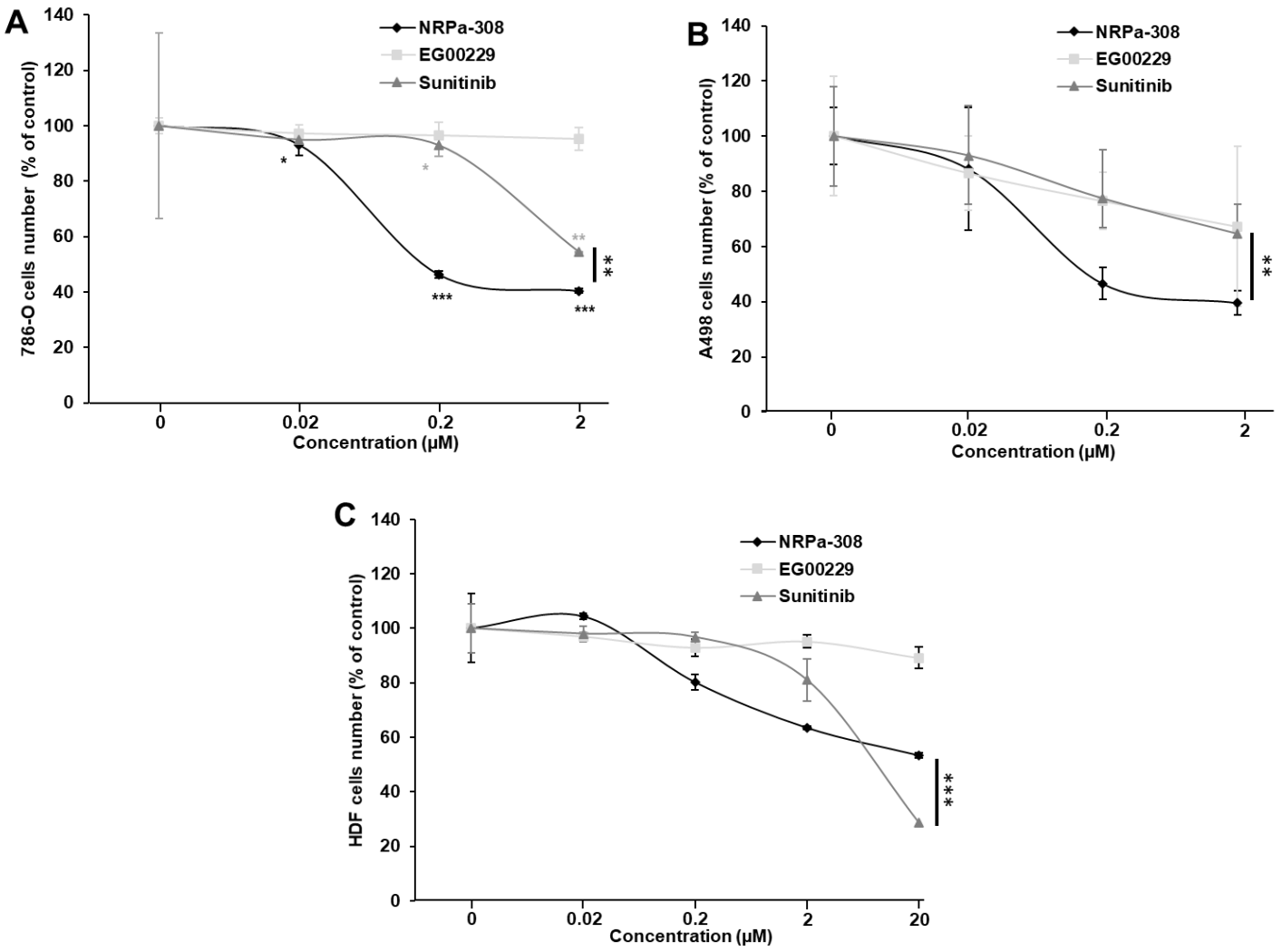

D

IC_{50} after 48h of treatment (µM)	NRPa-308	Sunitinib	EG00229
786-O	0.17	3.22	> 20µM
A498	0.18	9.07	> 20µM
HDF	> 20µM	13.25	> 20µM
Selectivity 786-O/HDF	< 0.009	0.24	
Selectivity A498/HDF	< 0.009	0.68	

Figure 3: Dumond *et al.*

Fig. 3. The NRP inhibitor NRPa-308 inhibits ccRCC cell proliferation more efficiently than sunitinib and EG00229. The effects of NRPa-308, sunitinib and the commercially NRP inhibitor (EG00229) measured by XTT assays, were tested in **(A)** 786-O cells, **(B)** on A498 cells and **(C)** on HDF cells. **(D)** Determination of the IC_{50} for each treatment in the different cell lines and their selectivity index. *p < 0.05; **p<0.01; *** p<0.001.

3.4 NRPa-308 exerted a wide range of anti-proliferative effect on primary ccRCC cells

Resistance to treatments especially to sunitinib is a critical concern for mccRCC patients [7]. NRPa-308 was ineffective on sunitinib-resistant 786-O cells (786R) [17] (IC_{50} > 2 □M), which is consistent with reduced NRP1 and NRP2 mRNA levels (Fig. 4A and B). Primary RCC cells presented a wide range of sensitivity to NRPa-308 as compared to 786-O cells (Fig. 4C) [18] which was consistent with variable mRNA levels (Fig. 4D)**.** The influence of NRPs expression on NRPa-308 efficacy suggests that the determination of NRPs levels is a prerequisite for the utilization of NRPs inhibitors in the clinic.

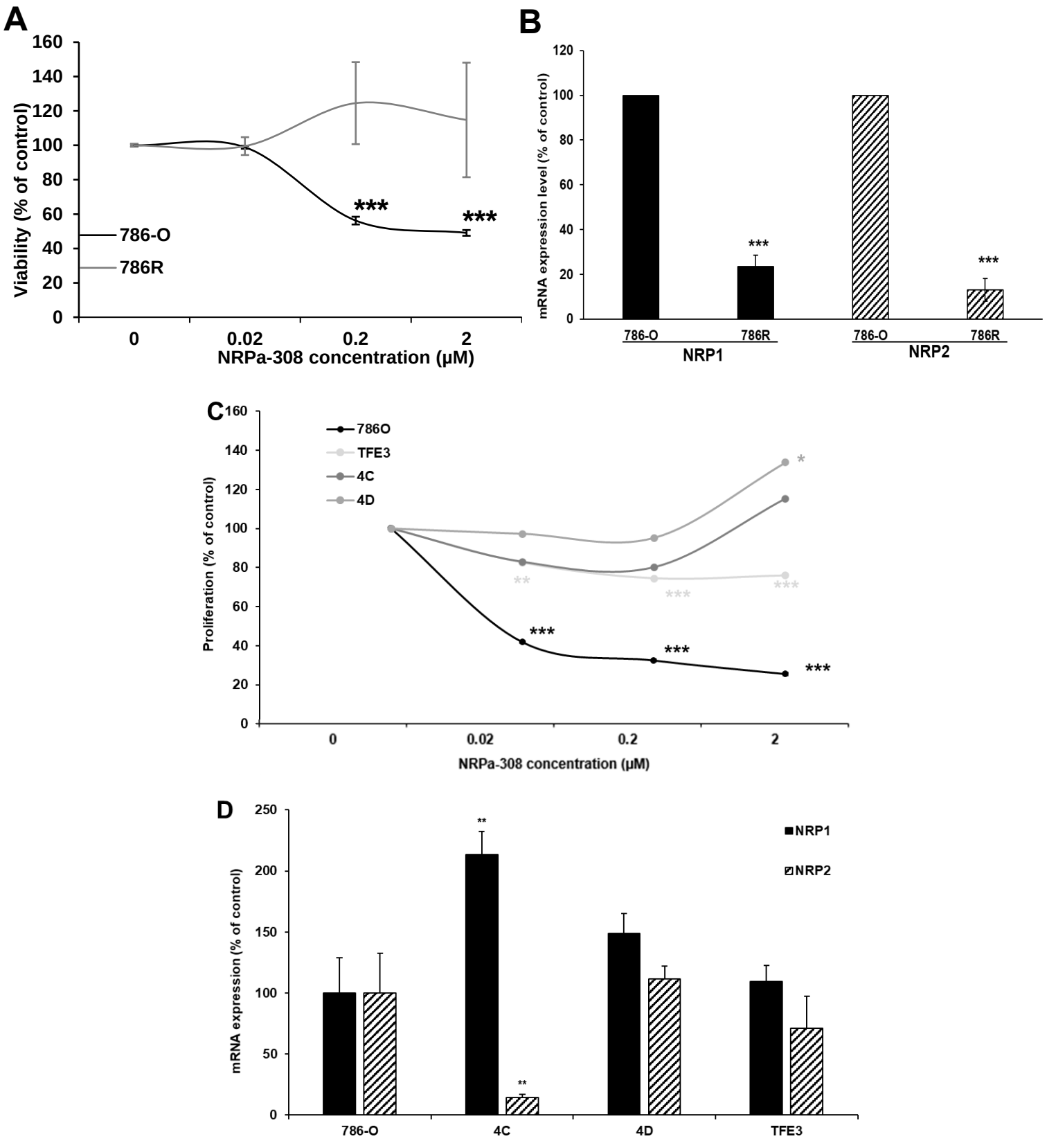

Figure 4: Dumond *et al.*

Fig. 4. NRPa-308 exerts a wide range of anti-proliferative effect on primary ccRCC cells. (**A**) The effects of NRPa-308 on cell viability were tested on 786-O (786O) and 786-O cells resistant to sunitinib (786R). **(B)** The relative expression of NRP1 and NRP2 mRNA in 786O and 786R cells were evaluated in a RNA seq analyzis and confirmed by RT qPCR. (**C**) The sensitivity of NRPa-308 were tested on already described primary cells by XTT assays. (**D**) The relative mRNA levels were evaluated in the reference 786 cells which served as reference values (100%) and in the different primary cells.

3.5 NRPa-308-dependent inhibition of cell proliferation relied on NRP2 in 786-O cells

NRP1 and NRP2 KO cells constitute valuable tools to test the specificity of NRPa-308. Although increased in *NRP1* and *NRP2* KO clones, the IC_{50} of NRPa-308 was superior for the NRP2 KO clones. These results suggest that NRPa-308 exerts its anti-proliferative effects mainly *via* NRP2 (Fig. 5A). Moreover, NRPa-308 inhibited VEGFA/NRP1 binding in a dose-dependent manner but inhibited VEGFC/NRP2 binding in a reverse dose-dependent manner. Hence, low doses of NRPa-308 were sufficient to prevent VEGFC binding to NRP2 which also suggests a stronger affinity for NRP2 (Fig. 5B).

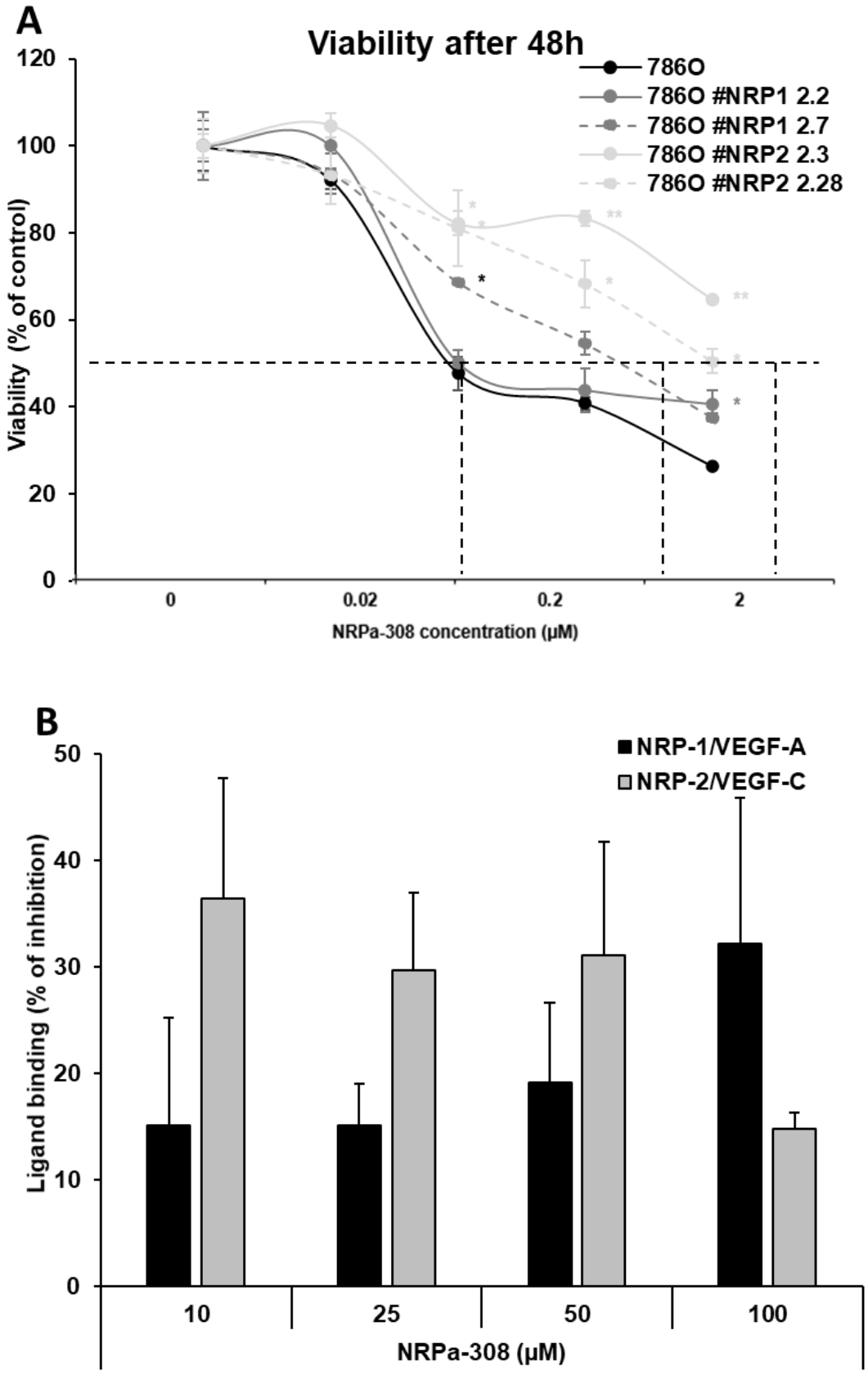

Figure 5: Dumond *et al.*

Fig. 5. NRPa-308-dependent inhibition of cell proliferation relies mainly on NRP2 in 786-O cells. (A) Effects of NRPa-308 on cell viability of 786-O cells, of two independent *NRP1* (#NRP1 2.2 and #NRP1 2.7) KO clones and of two independent NRP2 (#NRP2 2.3 and #NRP2 2.28) KO clones, measured by XTT assays, are represented to determine NRPa-308 specificity to NRP1 and/or to NRP2. **(B)** The percentage of inhibition by NRPa308 of VEGFA binding to NRP1 and of VEGFC binding to NRP2 at different concentration is presented. *$p < 0.05$; **$p<0.01$.

3.6 NRPa-308 binding mode was different between NRP1 and NRP2

The selectivity of NRPa-308 for NRPs was assessed by docking studies (Fig. 6A). The orientation of NRPa-308 into NRP1 binding site is flipped relatively to those obtained into the NRP2 binding site. NRPa-308 is stabilized in the binding site through hydrogen bonds, π-stacking and hydrophobic interactions (Fig. 6B), but the main interacting residues are distinct for NRP1 and NRP2. Few residues involved in these interactions are conserved in NRP1 and NRP2 (W301/304, S346/349, E348/351, Y353/356) but they establish interactions with different part of NRPa-308. Comparison of NRP1 and NRP2 structures revealed that the residues forming each binding site and the NRP1 and NRP2 binding sites properties differ (Table S4). This result explains the docking studies and the difference of affinity experimentally obtained (Fig. 5B).

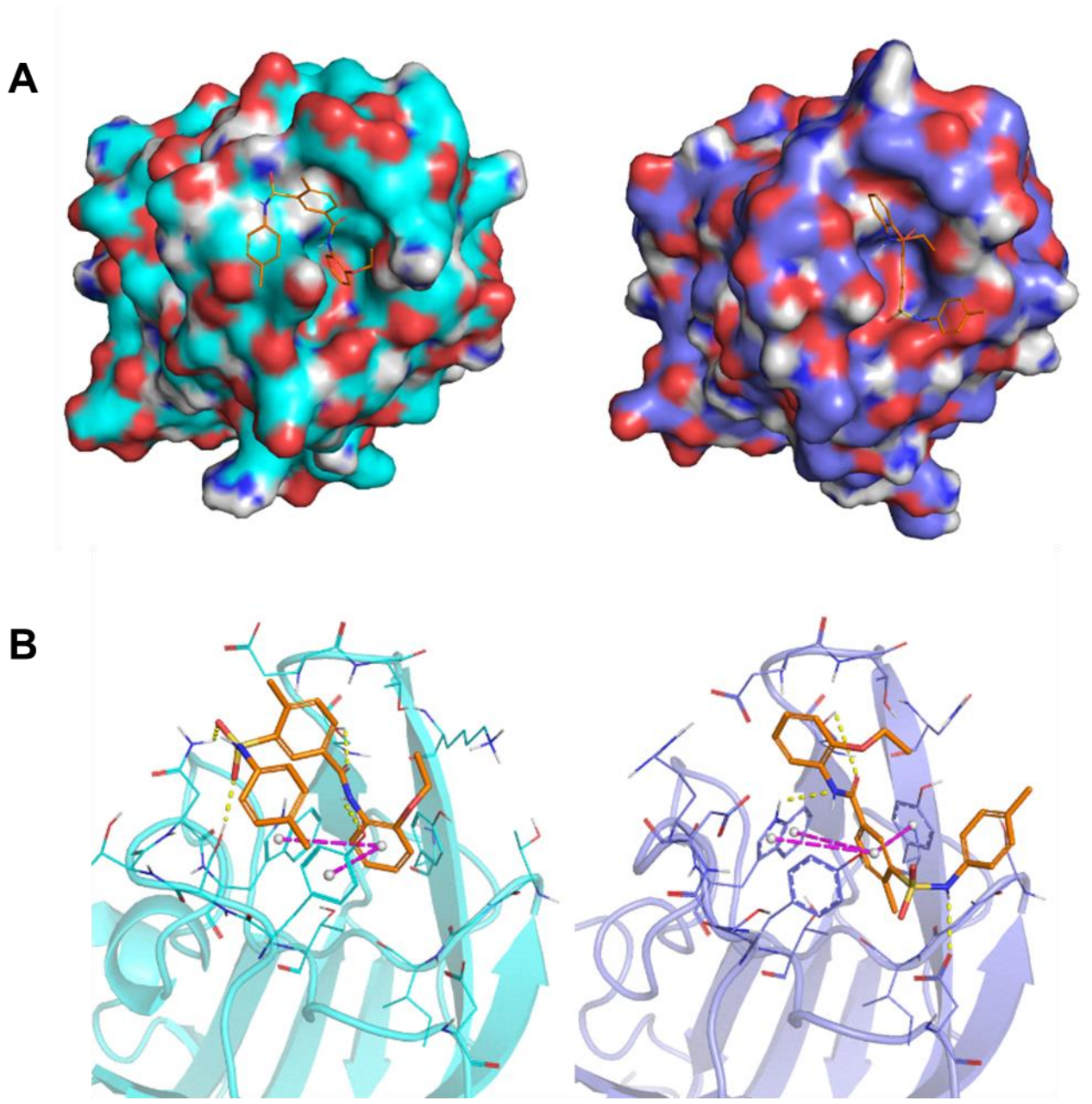

Figure 6: Dumond *et al.*

Fig. 6. NRPa-308 binding mode is different between NRP1 and NRP2

NRPa-308 (colored in orange) predicted binding mode into the NRP1 (A and B in cyan, left panels) and NRP2 (A and B in blue, right panels) binding sites. Hydrogen bonds are depicted as yellow dashed lines and π-stacking are depicted as magenta dashed lines.

3.7 NRPa-308 inhibited 786-O cell migration more efficiently than sunitinib

NRPs down-regulation and KO inhibited cell migration. NRPa-308 reduced 786-O cell migration more efficiently than sunitinib at a very low concentration (0.02µM compared to 2µM for sunitinib, Fig. 7A and B). This result suggests an anti-metastatic effect of NRPa-308 in ccRCC equivalently to those described for breast cancers [13].

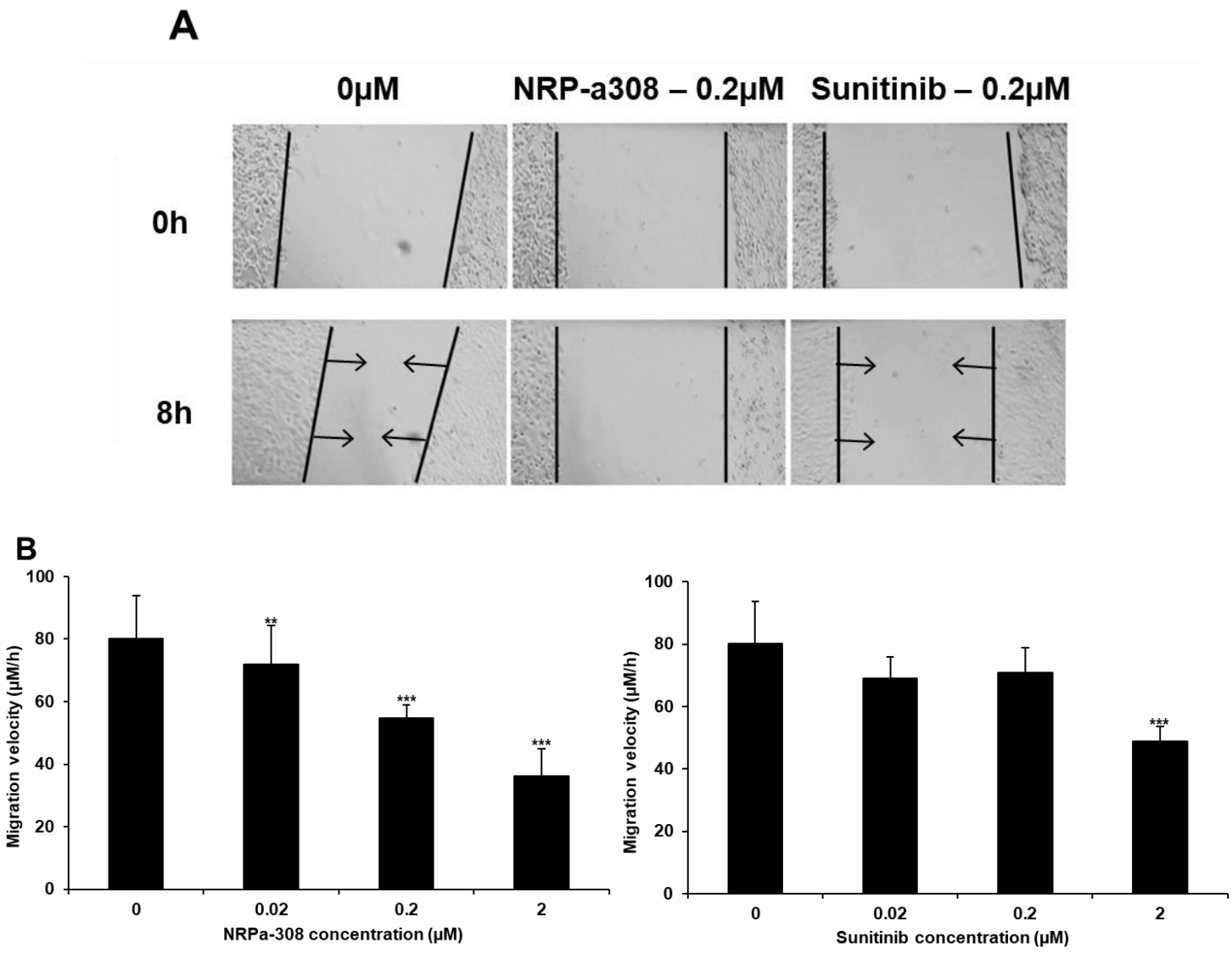

Figure 7: Dumond *et al.*

Fig. 7. NRPa-308 inhibits 786-O cell migration velocity more efficiently than sunitinib. (A) Photographs of scratch assay on cell monolayers in different experimental conditions; untreated, treated by NRPa-308 and by sunitinib. **(B)** The effects of NRPa-308 and sunitinib on 786-O cell migration at different concentrations by quantifying the above-mentioned experiments. **p<0.01; *** p<0.001.

3.8 High doses of NRPa-308 stimulated the production of NRPs ligands and of pro-angiogenic/pro-inflammatory cytokines

NRPs KO increased the production of VEGFA/VEGFC (Fig. 1) that can stimulate angio/lymphangiogenesis and immunotolerance. Hence, we evaluated the impact of NRPa-308 on the cell secretome. We also tested the effects of equivalent concentrations of sunitinib that have no impact on cell proliferation. NRPa-308 increased the expression of VEGFA and VEGFC at the highest concentration (2 µM). The lowest concentration (0.2 µM) stimulated modestly the expression of VEGFC (Fig. 8A and B). The expression of CXCL5 and CXCL8 was also evaluated since they participate in resistance to bevacizumab and sunitinib [19, 20]. A high dose of NRPa-308 increased CXCL5 and CXCL8 while a low dose modestly induced CXCL8. Sunitinib low concentrations (below the IC_{50} [17]), had no influence on VEGFA and VEGFC (Fig. 8A and B) but increased CXCL5 and CXCL8 expression (Fig. 8C and D) [19]. Hence, a low dose of NRPa-308 induced the best beneficial/detrimental ratio for ccRCC.

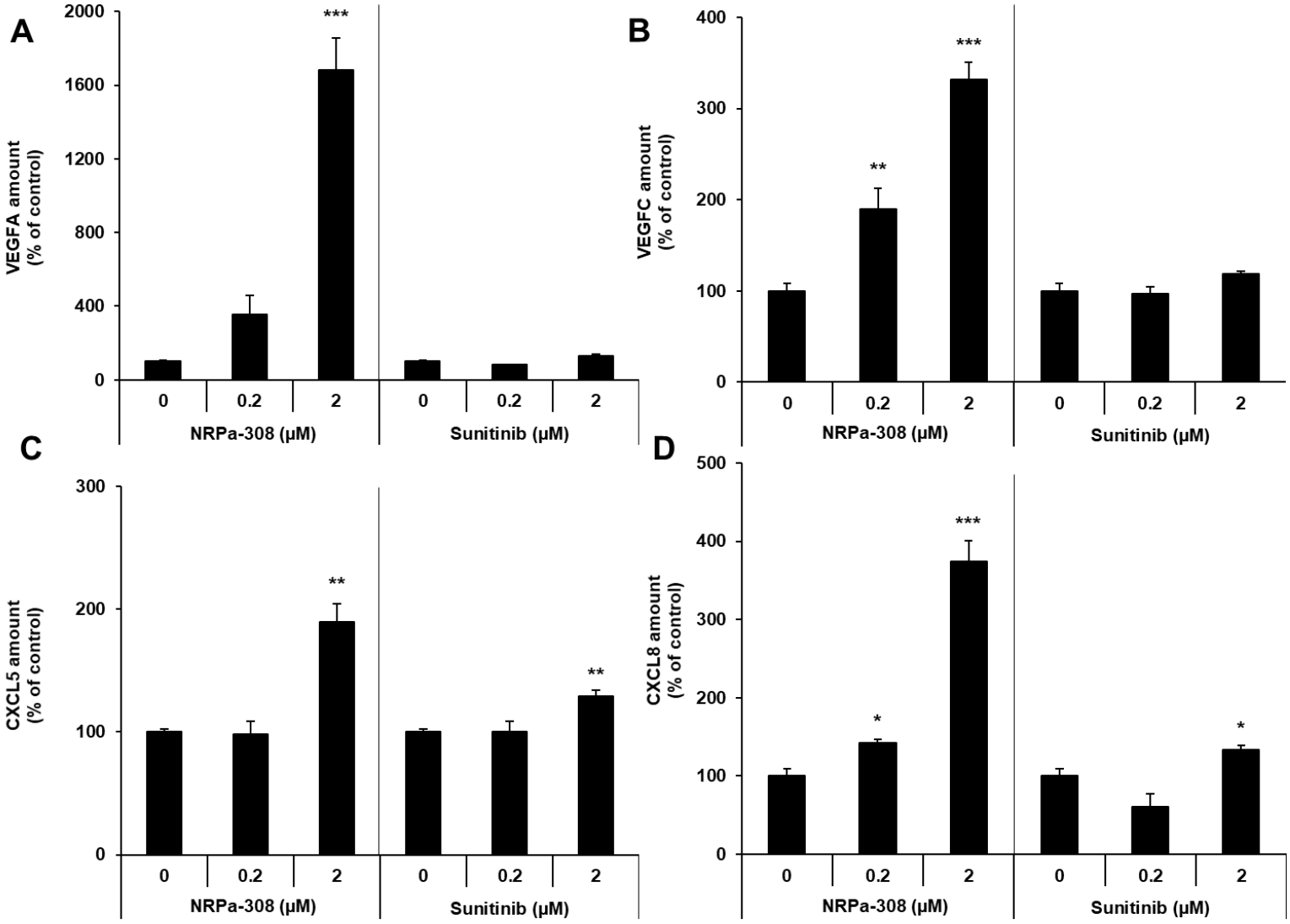

Figure 8: Dumond *et al.*

Fig. 8. High NRPa-308 concentration stimulates the production of NRPs ligands and of pro-angiogenic/pro-inflammatory cytokines. The effects of NRPa-308 and sunitinib on the production of different cytokines were evaluated by ELISA; **(A)** VEGFA, **(B)** VEGFC, production **(C)** CXCL8, **(D)** CXCL5. *p < 0.05; **p<0.01; *** p<0.001.

3.9 NRPa-308 decreased ccRCC growth in a reverse dose-dependent manner

Possible paracrine effects of high concentrations of NRPa-308 incited us to perform a dose response (5 µg/kg, 500 µg/kg and 50 mg/kg) on the growth of experimental ccRCC in immunodeficient and immunocompetent mice. Considering a full distribution in the blood and a 1.5 ml of blood in a mouse of 25 grams, a rough estimation of NRPa-308 blood concentration at 5 µg/kg, 500 µg/kg and 50 mg/kg should be around 0.2, 20 and 2000 □mol/L. The lowest concentration was in the range of concentration inhibiting cell proliferation and migration without affecting the production of pro-angio/lymphangiogenic and pro-inflammatory cytokines. No effect of the highest NRPa-308 dose was observed. However, tumor growth was inhibited by the lower amounts in both mouse models (Fig. 9A and B). The number of blood vessels (CD31 labelling) and of pericytes (αSMA labelling) per cm^2 was high in the control group and increased in a dose-dependent manner (Fig. 9C and D). However, functional blood vessels (CD31/αSMA co-labelling) decreased with high NRPa-308 concentrations (Fig. 9E and F). Hence, a low dose of NRPa-308 represents a relevant therapeutic strategy for ccRCC associating efficacy and low toxicity (no modification of mouse weight) (Fig. S4).

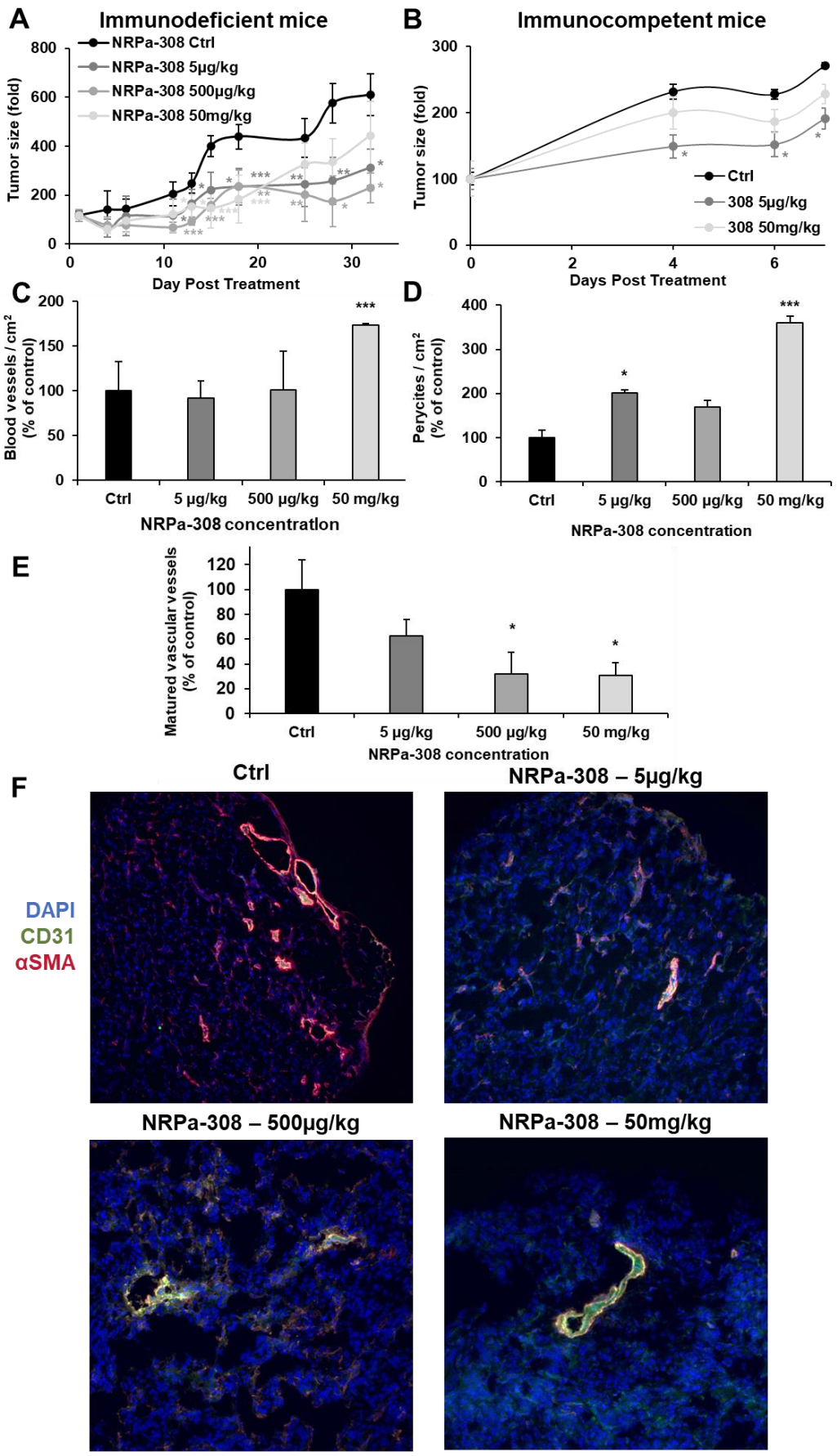

Figure 9: Dumond *et al.*

Fig. 9. NRPa-308 decreases experimental ccRCC growth in a reverse dose-dependent manner. (A) Experimental tumors in nude mice (5 mice per condition) were obtained after injection of $3x10^6$ 786-O cells. Treatment (NRPa-308) was given trice a week by oral gavage. Three concentrations of NRPa-308 were tested (5µg/kg, 500µg/kg and 50mg/kg) and was diluted in carboxymethyl cellulose, the control group (Ctrl) received carboxymethyl cellulose. Tumor volume fold increase from the beginning of the treatment is presented. **(B)** Experimental tumors in immunocompetent mice Balb-C (5 mice per condition) were obtained after injection of $3x10^5$ RENCA cells. Treatment (NRPa-308) was given trice a week by oral gavage. Two concentrations of NRPa-308 were tested (5µg/kg and 50mg/kg) and was diluted in carboxymethyl cellulose, the control group (Ctrl) received carboxymethyl cellulose. Tumor volume fold increase from the beginning of the treatment. The tumor vasculature in each experimental group was detected by immuno-staining for CD31 (endothelial cells, green) and α-SMA (pericytes, red). Tumor sections were counterstained with 40,6-diamidino-2- phenylindole (DAPI) (nucleus, blue). **(C)** Quantification of the blood vessels. **(D)** Quantification of pericytes and smooth muscle cells. **(E)** Quantification of mature blood vessels (blood vessels covered with pericytes, yellow labeling). **(F)** Representative images of the dose-dependent decrease in mature blood vessels. *p < 0.05; **p<0.01; *** p<0.001.

3.10 Efficient NRPa-308 doses decreased the expression of pro-tumoral factors

To decipher the molecular mechanism associated with NRPa-308 efficacy, we evaluated the expression of genes involved in proliferation, angio/lymphangiogenesis, epithelial/mesenchymal transition (EMT) and immune tolerance. The small size of the tumors obtained with the lowest dose of NRPa-308 forced us to assess the expression of the above- mentioned genes by qPCR (Fig. 10). Genes associated with lymphangiogenesis including human (h) NRP2, Prox1 and VEGFC and murine (m) Prox1 and VEGFC in the immunodeficient model (Fig. 10A) and NRP2, Prox1 and VEGFC in the immunocompetent model were the most downregulated (Fig. 10B). Only mProx1 and mVEGFC were downregulated by the intermediate dose in the immunodeficient model (Fig. 10A). hNRP2, hProx1, hVEGFC and mNRP2 were upregulated by the highest dose in the immunodeficient model (Fig. 10A). hNRP1, hVEGFA and mNRP1, mVEGFA, mVEGFR1 and mVEGFR2 were downregulated by the highest dose in immunodeficient mice (Fig. 10A). Some of them (hVEGFA and hVEGFR1 and mNRP1, mVEGFR1 and mVEGFR2) were downregulated by the lowest/intermediate dose (Fig. 10A). hNRP1 and hVEGFR1, and mVEGFA and mVEGFR2 were upregulated by using the lowest or the highest dose (Fig. 10A). In the immunocompetent model, mNRP1 and mVEGFR1 were downregulated for the two doses (Fig. 10B). mPDL1 was downregulated by the lowest and intermediate doses, it was unchanged for the highest dose in immunodeficient mice (Fig. 10A) and it was downregulated by the two doses in immunocompetent mice. hMET and hHGF and mMET and mHGF were downregulated by the lowest and the intermediate doses in immunodeficient mice (Fig. 10A). mMET was downregulated by the highest dose, hMET and hHGF and mHGF were upregulated by the intermediate and the highest doses (Fig. 10A). In the immunocompetent model mMET and mHGF were downregulated by the two doses (Fig. 10B). In the immunodeficient model, mCD69, a marker of the lymphocytes' activation, was upregulated (Fig. 10A). The M2 macrophages marker mARG1 was decreased (Fig. 10A). We gave an arbitrary value of +2 when a gene of poor prognosis decreased and a value of -2 when it increased and vice versa for a gene of good prognosis. The score for the lowest concentration of NRPa-308 was of 18 in the immunodeficient (Fig. 10A) and of 12 in the immunocompetent models (Fig.

10B). It was of 20 for the intermediate dose in the immunodeficient model (Fig. 10A) and of 2 and 6 respectively for the highest dose in the immunodeficient (Fig. 10A) and the immunocompetent models (Fig. 10B). This evaluation, in addition to the reduced tumor growth favored the notion that a low dose of NRPa-308 had the best therapeutic efficacy.

A

Immunodeficient mice				
NRPa-308 Concentration	Control	5µg/kg	500µg/kg	50mg/kg
Angiogenesis genes				
h-NRP1	100	129 (*)	103	77 (*)
m-NRP1	100	87	64 (*)	87
h-VEGFA	100	91	115	60 (**)
m-VEGFA	100	133 (*)	105	31 (***)
h-VEGFR1	100	14 (***)	76 (**)	202 (**)
m-VEGFR1	100	140	53 (**)	42 (**)
h-VEGFR2	x	x	x	x
m-VEGFR2	100	152 (*)	63 (**)	50 (***)
Lymphangiogenesis genes				
h-NRP2	100	49 (***)	93	117 (*)
m-NRP2	100	94	86	85 (*)
h-Prox	100	18 (***)	113	243 (**)
m-Prox	100	26 (***)	67 (***)	119
h-VEGFC	100	48 (**)	102	173 (**)
m-VEGFC	100	60	71	118
h-VEGFR3	x	x	x	x
m-VEGFR3	100	43 (**)	64 (*)	113
Immune tolerance genes				
m-PDL1	100	26 (***)	79 (**)	114
h-MET	100	78 (***)	94 (**)	108 (**)
m-MET	100	91 (*)	54 (***)	67 (***)
h-HGF	100	18 (***)	103 (*)	222 (***)
m-HGF	100	23 (***)	53 (***)	142 (**)
Lymphocytes activation				
m-CD69	100	320 (**)	296 (**)	187 (***)
Macrophage M1 genes				
m-iNOS	100	46 (***)	60 (**)	170
m-TNF	100	152	170	43 (**)
Macrophage M2 genes				
m-ARG1	100	84 (*)	25 (***)	60 (**)
Score		**18**	**20**	**2**

B

Immunocompetent mice			
NRPa-308 Concentration	Control	5µg/kg	50mg/kg
Angiogenesis genes			
m-NRP1	100	9 (***)	52 (***)
m-VEGFR1	100	1 (***)	1 (***)
Lymphangiogenesis genes			
m-NRP2	100	28 (***)	103
m-Prox	100	26 (***)	150
m-VEGFC	100	22 (***)	139
m-VEGFR3	100	173 (*)	626 (***)
Immune tolerance genes			
m-PDL1	100	26 (***)	51 (**)
CTLA4	x	x	x
m-MET	100	0.2 (***)	4 (***)
m-HGF	100	3 (***)	26 (***)
Macrophage M1 genes			
m-iNOS	100	73 (***)	16 (***)
Score		**12**	**6**

Figure 10: Dumond *et al.*

Fig. 10. Efficient NRPa-308 dose decreases the expression of pro-tumoral factors. Detection by qPCR of pro-tumoral genes in tumors generated in **(A)** immunodeficient and **(B)** immunocompetent mice with wild-type and with NRPs knock-out cells. *p < 0.05; **p<0.01; *** p<0.001.

3.11 The NRP2 associated pathway was determinant for the aggressiveness of mccRCC

The results showing that a high dose of NRPa-308 was the most efficient on experimental breast cancers [13] whereas it has no effect on ccRCC were puzzling. Analysis of the TCGA data base showed that VEGFA and NRP1 were expressed at high levels in most of the ccRCC and and breast cancer cell lines, especially in 786-O and MDA-MB-231 (Fig. 11A and C). VEGFC and NRP2 were expressed by all the ccRCC cells. However, VEGFC levels were very low in three out of five breast cancer cell lines and NRP2 levels were very low in all the breast cancer cell lines including MDA-MB-231 (Fig. 11B and D). The very low levels in MDA-MB-231 and the more specific effects of NRPa-308 on NRP2, partly explained the difference in the efficient concentrations for experimental ccRCC and TNBC. The prognostic role of NRP1 and NRP2 and of their known partners VEGFA, VEGFR1, VEGFR2, Semaphorin 3A (Sema3A) and plexin A1 (PLXNA1) (NRP1 partners) and VEGFC, VEGFR3, Semaphorin 3F (Sema3F), plexin A2 (PLXNA1) and Prospero homeobox protein 1 (Prox1), a master transcription factor of lymphangiogenesis (NRP2 partners) was analyzed. For each gene, we defined the best cut off that determines a survival difference. 425 samples were from M0 and 103 from M1 ccRCC patients. 115 samples were from TNBC patients. **For M0 ccRCC patients**, expression of VEGFR2, NRP2, VEGFC, VEGFR3, PLXA2 above their best cut off was of good prognosis for disease-free survival ((DFS) trend (T, p between 0.08 and 0.06) for NRP2, VEGFC) and significant (S) for VEGFR2, VEGFR3, PLXA2). Expression above the best cut off for Sema3A (S), PLXNA1 (T) and Prox1 (S) was of poor prognosis for DFS. Expression above the best cut off for NRP1 (T), VEGFR1 (S), VEGFR2 (S), NRP2 (S), VEGFC (T), VEGFR3 (T), Sema3F (S) and PLXA2 (S) was beneficial for overall survival (OS), whereas it was detrimental for Sema3A (S), PLXNA1 (S) and Prox1 (S). For M1 patients: Only Sema3F (T) was correlated with a longer progression-free survival (PFS). NRP1 (S), VEGFR2 (S), Sema3A (S), NRP2 (S), VEGFC (S), VEGFR (S)3, PLXA2 (T) and Prox1 (S)) were correlated to a shorter PFS. NRP1 (S), VEGFR1 (S), VEGFR2 (S), Sema3F (S) and PLXA2 (S) were correlated with a longer OS while Sema3A (S), PLXA1 (S), NRP2 (S), VEGFC (S) and Prox1 (S) were correlated to a shorter one.

For TNBC, VEGFA was correlated with a longer PFS (T) but NRP1 (S), VEGFR1 (S), PLXNA1

(S), NRP2 (T), VEGFC (T), Sema3F (S) and PLXNA2 (T) were correlated with a shorter one. NRP1 (S), VEGFR1 (S), VEGFR2 (T), PLXNA1 (S), VEGFC (T), Sema3F (S)
and PLXNA2 (T) were correlated with a shorter OS. NRP2 was not correlated to survival in that case. A relative weight of -2 was given for a gene associated with a significant poor prognosis and a relative weight of -1 for a trend. A relative weight of +2 was given for a gene associated with a significant good prognosis and +1 for a trend. NRP1 and NRP2 pathways were considered separately. For the NRP1 pathway, a -1 score was obtained for DFS and OS of M0 ccRCC patients, -6 and +2 scores for PFS and OS of M1 ccRCC patients, and -5 and -7 scores for the PFS and OS of TNBC patients. For the NRP2 pathway, a score of +4 and +6 were obtained for the DFS and OS of ccRCC patients, -8 and -2 scores for M1 ccRCC patients and -5 and -7 scores for the PFS and OS of TNBC patients. These results suggest that NRP1 targeting is more adapted for TNBC while NRP2 targeting is better for ccRCC.

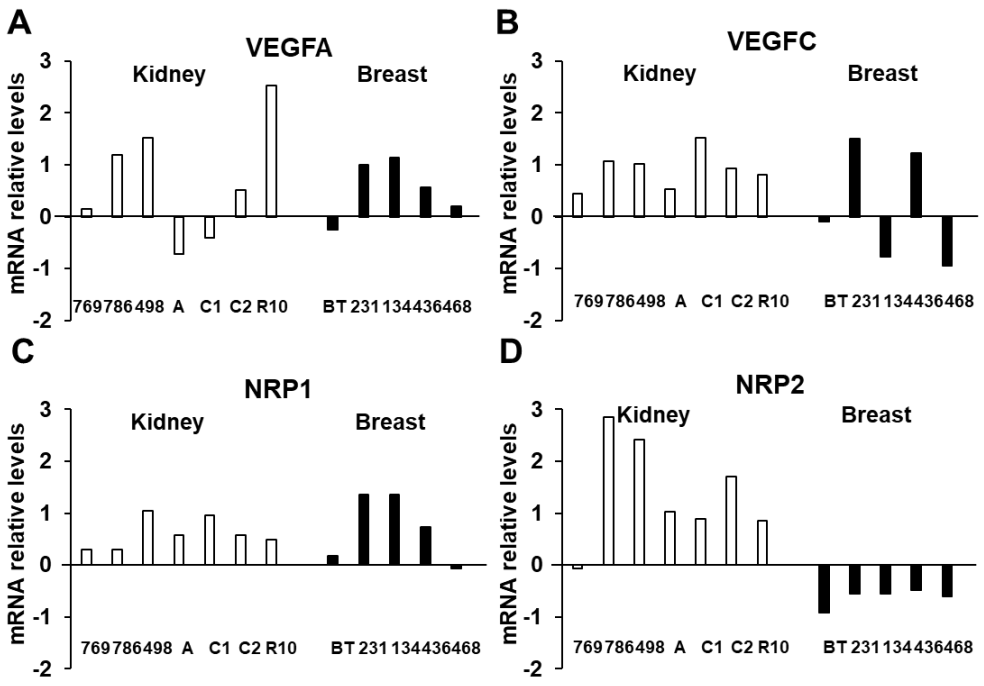

E

Survival	N1	VEGFA	R1	R2	Sema3A	PLXNA1	SCORE NRP1	N2	VEGFC	R3	Sema3F	PLXNA2	PROX1	SCORE NRP2
M0 ccRCC														
DFS	NS	NS	NS	0.014 (3° Q)	9e-3 (3° Q)	T (2° Q)	-1	T (sup 3° Q)	T (sup 3° Q)	0.015 (3° Q)	NS	0.01 (3° Q)	1.6e-3 (sup 3° Q)	4
OS	T (1° & 3° Q)	0.02 (3° Q)	1.5e-3 (1° Q)	9e-3 (3° Q)	5e-4 (3° Q)	4.2 e-3 (2° Q)	-1	0.04 (bet. 2°&3° Q)	T (sup 3° Q)	T (3° Q)	0.03 (1° Q)	2.6e-3 (3° Q)	0.01 (sup 3° Q)	6
M1 ccRCC														
PFS	0.03 (sup3 ° Q)	NS	NS	0.01 (sup3° Q)	0.04 (2° Q)	NS	-6	0.05 (2° Q)	0.01 (sup3° Q)	0.03 (sup3° Q)	T (2° Q)	T (2° Q)	0.026 (2° Q)	-8
OS	6.3e-4 (1°Q)	NS	4.3e-3 (1°Q)	4e-3 (1°Q)	0.05 (2° Q)	9.3e-4 (3° Q)	2	0.04 (sup 3° Q)	0.004 (sup 3° Q)	NS	0.015 (2° Q)	0.01 (1° Q)	0.027 (2° Q)	-2

F

Survival	N1	VEGFA	R1	R2	Sema3A	PLXNA1	SCORE NRP1	N2	VEGFC	R3	Sema3F	PLXNA2	PROX1	SCORE NRP2
TNBC														
PFS	0.02 (2° Q)	T (1° Q)	0.05 (2° Q)	NS	NS	0.02 (2° Q)	-5	T (2° Q)	T (2° Q)	NS	0.025 (2° Q)	T (1° Q)	NS	-5
OS	0.02 (2° Q)	NS	0.02 (2° Q)	T (2° Q)	NS	0.016 (2° Q)	-7	NS	T (2° Q)	NS	0.05 (2° Q)	T (1° Q)	NS	-7

Figure 11: Dumond *et al.*

Fig. 11. The NRP2 associated pathway is more determinant for the aggressiveness of mccRCC but not for triple negative breast cancers.

Analysis of cbioportal database highlighted the relative levels of VEGFA (**A**), VEGFC (**B**), NRP1 (**C**) and NRP2 (**D**) mRNA in a panel of RCC (769 (769P), 786-O (786), ACHN (A), Caki1 (C1), Caki2 (C2), RCC10 (R10)) and TNBC (BT474 (BT), MDAMB231 (231), MDAMB134 (134), MDAMB436 (436), MDAMB468 (468)). Correlation between genes of the NRP1 and NRP2 pathways and survival (DFS/PFS/OS) in M0 and M1 RCC patients (**E**) and TNBC (**F**) patients. The tested genes of the NRP1 pathway were the following: *NRP1* (N1), *VEGFA*, *VEGFR1* (R1), *VEGFR2* (R2), *Semaphorin 3A* (Sema3A), *Plexin A1* (PLXNA1). The tested genes of the NRP2 pathway were the following: *NRP2* (N1), *VEGFC*, *VEGFR3* (R3), *Semaphorin 3F* (Sema3F), *Plexin A2* (PLXNA1) and *PROX1*. The p- values of genes associated with shorter DFS/PFS/OS appear white on a black background; the p-values of genes associated with a longer DFS/PFS/OS appear black on a gray background. Significant p-values are given; a trend to significance is indicated by a “T”. Specific cut-off are indicated (First, second or third quartile (1°, 2°, 3° Q). A score was established as follows: a positive point was given for a gene with a trend to good prognosis; two positive points for a gene associated with good prognosis and with a significant p-value; a negative point was given for a gene with a trend to poor prognosis; two negative points were given for a gene associated with poor prognosis and with a significant p-value. Positive scores were obtained for DFS and OS of M0 RCC patients and the NRP2 pathway (respectively 4 and 6) and for the OS of M1 RCC patients and the NRP1 pathway (2). Negative scores were obtained for obtained for the DFS and OS of M0 and PFS of M1 RCC patients and the NRP1 pathway (respectively (-1), (-1) (-6), for the PFS and OS of M1 RCC patients and the NRP2 pathway. Negative scores were obtained for the NRP1 and NRP2 pathways for PFS and OS.

4 Discussion

NRPs, through their effects on tumor cells and on cells of the microenvironment are key signaling molecules stimulating ccRCC growth and metastasis. However, the multi partnerships of NRPs render difficult the determination of the relative importance of each pathway. Moreover, NRP1 and NRP2 signaling cross-talked to establish a steady state. Depending on the level of inhibition, compensatory mechanisms mediated by the production of VEGFA and VEGFC occur and inflammatory cytokines compensate for the inhibition of NRPs pathways. These mechanisms are key for an optimized targeting of NRPs in the context of ccRCC treatment. Our results had to be compared to those of Cao Y *et al* who showed that inhibition of experimental tumor growth generated with cells down-regulated for NRPs only relies on microenvironment shaping [10, 21]. Modifications of the secretomes depend on a partial or complete inhibition by KO of the NRPs' signaling, an important concern if NRPs' inhibition enters in a therapeutic strategy. The importance of NRP1 or NRP2 signaling depends also on the cancer type. NRP1 is a better therapeutic target for TNBC and NRP2 is a better one for ccRCC. This result suggests that specific NRP1 or NRP2 inhibitors are more relevant for a specific cancer. The relevance of the double targeting was investigated by invalidating both genes in 786-O cells. Several attempts were unsuccessful suggesting that the double KO is lethal. Hence, an inhibitor of NRP1 and of NRP2 should present a maximal therapeutic efficacy. Our results suggest that resistance to anti-angiogenics especially sunitinib, involved a down-regulation of NRPs. Therefore, NRPs inhibitors do not represent a second line treatment at relapse on sunitinib. However, NRP inhibitors represent an alternative following relapse on immunotherapies [4]. Adjuvant treatment for M0 ccRCC patients is a debated issue. While some trials showed that an adjuvant treatment by anti-angiogenics is not relevant, another trial demonstrated its importance for advanced M0 patients [22, 23]. Our results showed that the NRP2 pathway is correlated with a good prognosis for M0 patients and NRP1 did not correlate with shorter survival rates. Our results emphasized the relevance of NRPs targeting in M1 ccRCC patients and administration of anti NRPs in an adjuvant setting is probably not a good

strategy. Specific drugs and evaluation of NRPs expression is determinant to validate NRPs targeting to reach the “golden age” of the therapeutic arsenal of ccRCC [24].

5 Acknowledgements

The authors acknowledge funding from Helsinn Company. This work was supported by The Centre Scientifique de Monaco, the Fondation de France, the French National Institute for Cancer Research (INCA, SUNITRES contract), the Agence Nationale de la Recherche (ANR), the Ligue Nationale contre le Cancer (Equipe labellisée 2019), the “Conseil Général des Alpes Maritimes”, the association “Cordon de Vie” directed by Mrs Fabienne Mourou, the Fondation François Xavier Mora and the Fondation Flavien.

6 Competing Interests

The authors have declared that no competing interest exists.

7 Authors’ contributions

Conception and design : Luc Demange, Renaud Grépin, Gilles Pagès.

Development of methodology: Aurore Dumond, Etienne Brachet, Jérôme Durivault, Valérie Vial, Anna K. Pusko, Yves Lepelletier, Christopher Montemagno, Marina Pagnuzzi.

Acquisition of data: Aurore Dumond, Etienne Brachet, Jérôme Durivault, Valérie Vial, Anna K. Pusko, Yves Lepelletier, Nathalie Lagarde, Matthieu Montes, Christopher Montemagno, Marina Pagnuzzi,

Analysis and interpretation of data: Aurore Dumond, Luc Demange, Renaud Grépin and Gilles Pagès.

Writing, review: Aurore Dumond, Olivier Hermine, Christiane Garbay, Luc Demange, Renaud Grépin and Gilles Pagès.

Administrative, technical, or material support: Gilles Pagès

Study supervision: Renaud Grépin, Gilles Pagès.

8 References

[1] J. Schodel, S. Grampp, E.R. Maher, H. Moch, P.J. Ratcliffe, P. Russo, D.R. Mole, Hypoxia, Hypoxia-inducible Transcription Factors, and Renal Cancer, Eur Urol, 69 (2016) 646-657.

[2] S. Niland, J.A. Eble, Neuropilins in the Context of Tumor Vasculature, Int J Mol Sci, 20 (2019).

[3] R.J. Motzer, A. Ravaud, J.J. Patard, H.S. Pandha, D.J. George, A. Patel, Y.H. Chang, B. Escudier, F. Donskov, A. Magheli, G. Carteni, B. Laguerre, P. Tomczak, J. Breza, P. Gerletti, M. Lechuga, X. Lin, M. Casey, L. Serfass, A.J. Pantuck, M. Staehler, Adjuvant Sunitinib for High-risk Renal Cell Carcinoma After Nephrectomy: Subgroup Analyses and Updated Overall Survival Results, Eur Urol, 73 (2018) 62-68.

[4] R.J. Motzer, N.M. Tannir, D.F. McDermott, O. Aren Frontera, B. Melichar, T.K. Choueiri, E.R. Plimack, P. Barthelemy, C. Porta, S. George, T. Powles, F. Donskov, V. Neiman, C.K. Kollmannsberger, P. Salman, H. Gurney, R. Hawkins, A. Ravaud, M.O. Grimm, S. Bracarda, C.H. Barrios, Y. Tomita, D. Castellano, B.I. Rini, A.C. Chen, S. Mekan, M.B. McHenry, M. Wind-Rotolo, J. Doan, P. Sharma, H.J. Hammers, B. Escudier, I. CheckMate, Nivolumab plus Ipilimumab versus Sunitinib in Advanced Renal-Cell Carcinoma, N Engl J Med, 378 (2018) 1277-1290.

[5] B.I. Rini, E.R. Plimack, V. Stus, R. Gafanov, R. Hawkins, D. Nosov, F. Pouliot, B. Alekseev, D. Soulieres, B. Melichar, I. Vynnychenko, A. Kryzhanivska, I. Bondarenko, S.J. Azevedo, D. Borchiellini, C. Szczylik, M. Markus, R.S. McDermott, J. Bedke, S. Tartas, Y.H. Chang, S. Tamada, Q. Shou, R.F. Perini, M. Chen, M.B. Atkins, T. Powles, K.-. Investigators, Pembrolizumab plus Axitinib versus Sunitinib for Advanced Renal- Cell Carcinoma, N Engl J Med, 380 (2019) 1116-1127.

[6] M.E. Gore, C. Szczylik, C. Porta, S. Bracarda, G.A. Bjarnason, S. Oudard, S.H. Lee, J. Haanen, D. Castellano, E. Vrdoljak, P. Schoffski, P. Mainwaring, R.E. Hawkins, L. Crino, T.M. Kim, G. Carteni, W.E. Eberhardt, K. Zhang, K. Fly, E. Matczak, M.J. Lechuga, S. Hariharan, R. Bukowski, Final results from the large sunitinib global expanded-access trial in metastatic renal cell carcinoma, Br J Cancer, 113 (2015) 12-19.

[7] M. Dufies, S. Giuliano, D. Ambrosetti, A. Claren, P.D. Ndiaye, M. Mastri, W. Moghrabi, L.S. Cooley, M. Ettaiche, E. Chamorey, J. Parola, V. Vial, M. Lupu-Plesu, J.C. Bernhard, A. Ravaud, D. Borchiellini, J.M. Ferrero, A. Bikfalvi, J.M. Ebos, K.S. Khabar, R. Grepin, G. Pages, Sunitinib Stimulates Expression of VEGFC by Tumor Cells and Promotes Lymphangiogenesis in Clear Cell Renal Cell Carcinomas, Cancer Res, 77 (2017) 1212- 1226.

[8] A. Dumond, L. Demange, G. Pages, [Neuropilins: relevant therapeutic targets to improve the treatment of cancers], Med Sci (Paris), 36 (2020) 487-496.

[9] J.R. Wild, C.A. Staton, K. Chapple, B.M. Corfe, Neuropilins: expression and roles in the epithelium, Int J Exp Pathol, 93 (2012) 81-103.

[10] Y. Cao, L. Wang, D. Nandy, Y. Zhang, A. Basu, D. Radisky, D. Mukhopadhyay, Neuropilin-1 upholds dedifferentiation and propagation phenotypes of renal cell carcinoma cells by activating Akt and sonic hedgehog axes, Cancer Res, 68 (2008) 8667- 8672.

[11] Y. Cao, L.H. Hoeppner, S. Bach, G. E, Y. Guo, E. Wang, J. Wu, M.J. Cowley, D.K. Chang, N. Waddell, S.M. Grimmond, A.V. Biankin, R.J. Daly, X. Zhang, D. Mukhopadhyay, Neuropilin-2 promotes extravasation and metastasis by interacting with endothelial alpha5 integrin, Cancer Res, 73 (2013) 4579-4590.

[12] E. Brachet, A. Dumond, W.Q. Liu, M. Fabre, M. Selkti, F. Raynaud, O. Hermine, R. Benhida, P. Belmont, C. Garbay, Y. Lepelletier, C. Ronco, G. Pages, L. Demange, Synthesis, 3D-structure and stability analyses of NRPa-308, a new promising anti-cancer agent, Bioorg Med Chem Lett, 29 (2019) 126710.

[13] W.Q. Liu, Y. Lepelletier, M. Montes, L. Borriello, R. Jarray, R. Grepin, B. Leforban, A. Loukaci, R. Benhida, O. Hermine, S. Dufour, G. Pages, C. Garbay, F. Raynaud, R. Hadj-Slimane, L. Demange, NRPa-308, a new neuropilin-1 antagonist, exerts in vitro anti- angiogenic and anti-proliferative effects and in vivo anti-cancer effects in a mouse xenograft model, Cancer Lett, 414 (2018) 88-98.

[14] P.D. Ndiaye, M. Dufies, S. Giuliano, L. Douguet, R. Grepin, J. Durivault, P. Lenormand, N. Glisse, J. Mintcheva, V. Vouret-Craviari, B. Mograbi, M. Wurmser, D. Ambrosetti, N. Rioux-Leclercq, P. Maire, G. Pages, VEGFC acts as a double-edged sword in renal cell carcinoma aggressiveness, Theranostics, 9 (2019) 661-675.

[15] R. Grepin, M. Guyot, A. Dumond, J. Durivault, D. Ambrosetti, J.F. Roussel, F. Dupre, H. Quintens, G. Pages, The combination of bevacizumab/Avastin and erlotinib/Tarceva is relevant for the treatment of metastatic renal cell carcinoma: the role of a synonymous mutation of the EGFR receptor, Theranostics, 10 (2020) 1107-1121.

[16] V. Napolitano, L. Tamagnone, Neuropilins Controlling Cancer Therapy Responsiveness, Int J Mol Sci, 20 (2019).

[17] S. Giuliano, Y. Cormerais, M. Dufies, R. Grepin, P. Colosetti, A. Belaid, J. Parola, A. Martin, S. Lacas-Gervais, N.M. Mazure, R. Benhida, P. Auberger, B. Mograbi, G. Pages, Resistance to sunitinib in renal clear cell carcinoma results from sequestration in lysosomes and inhibition of the autophagic flux, Autophagy, 11 (2015) 1891-1904.

[18] R. Grepin, D. Ambrosetti, A. Marsaud, L. Gastaud, J. Amiel, F. Pedeutour, G. Pages, The relevance of testing the efficacy of anti-angiogenesis treatments on cells derived from primary tumors: a new method for the personalized treatment of renal cell carcinoma, PLoS ONE, 9 (2014) e89449.

[19] S. Giuliano, M. Dufies, P.D. Ndiaye, J. Viotti, D. Borchiellini, J. Parola, V. Vial, Y. Cormerais, M. Ohanna, V. Imbert, E. Chamorey, N. Rioux-Leclercq, A. Savina, J.M. Ferrero, B. Mograbi, G. Pages, Resistance to lysosomotropic drugs used to treat kidney and breast cancers involves autophagy and inflammation and converges in inducing CXCL5, Theranostics, 9 (2019) 1181-1199.

[20] R. Grepin, M. Guyot, M. Jacquin, J. Durivault, E. Chamorey, A. Sudaka, C. Serdjebi, B. Lacarelle, J.Y. Scoazec, S. Negrier, H. Simonnet, G. Pages, Acceleration of clear cell renal cell carcinoma growth in mice following bevacizumab/Avastin treatment: the role of CXCL cytokines, Oncogene, 31 (2012) 1683-1694.

[21] Y. Cao, G. E, E. Wang, K. Pal, S.K. Dutta, D. Bar-Sagi, D. Mukhopadhyay, VEGF exerts an angiogenesis-independent function in cancer cells to promote their malignant progression, Cancer Res, 72 (2012) 3912-3918.

[22] A. Ravaud, R.J. Motzer, H.S. Pandha, D.J. George, A.J. Pantuck, A. Patel, Y.H. Chang, B. Escudier, F. Donskov, A. Magheli, G. Carteni, B. Laguerre, P. Tomczak, J. Breza, P. Gerletti, M. Lechuga, X. Lin, J.F. Martini, K. Ramaswamy, M. Casey, M. Staehler, J.J. Patard, S.T. Investigators, Adjuvant Sunitinib in High-Risk Renal-Cell Carcinoma after Nephrectomy, N Engl J Med, 375 (2016) 2246-2254.

[23] N.B. Haas, J. Manola, R.G. Uzzo, K.T. Flaherty, C.G. Wood, C. Kane, M. Jewett, J.P. Dutcher, M.B. Atkins, M. Pins, G. Wilding, D. Cella, L. Wagner, S. Matin, T.M. Kuzel, W.J. Sexton, Y.N. Wong, T.K. Choueiri, R. Pili, I. Puzanov, M. Kohli, W. Stadler, M. Carducci, R. Coomes, R.S. DiPaola, Adjuvant sunitinib or sorafenib for high-risk, non- metastatic renal-cell carcinoma (ECOG-ACRIN E2805): a double-blind, placebo- controlled, randomised, phase 3 trial, Lancet, 387 (2016) 2008-2016.

[24] J.J. Hsieh, M.P. Purdue, S. Signoretti, C. Swanton, L. Albiges, M. Schmidinger, D.Y. Heng, J. Larkin, V. Ficarra, Renal cell carcinoma, Nat Rev Dis Primers, 3 (2017) 17009.

Supplementary information

1. Supplementary methods

1.1 Cell lines

786-O, A498 and RENCA cell lines were purchased from the American Tissue Culture Collection (ATCC). They were cultured as indicated by ATCC and as already described [1].

1.2 Reagents

NRPa-308 has been synthesized at Université de Paris. Sunitinib was purchased from Selleckem and prepared as a 2.5 mmol/L stock solution in dimethyl sulfoxide (Sigma, 472301) and stored at -20°C. EG00229 was purchased from Tocris.

1.3 Quantitative Real-Time PCR (qPCR) experiments

It was performed as already described [2]. For oligo sequences, see Table S1.

1.4 Competitive NRP1/2 VEGFA/VEGFC binding assay

The flat bottom surface of a 96-well plate was coated with 100 µL (200 ng/well) recombinant human NRP1 or NRP2 and incubated overnight at 4°C. Non-specific binding was blocked by the incubation with 0.5% BSA in PBS. 50 µL of NRPa-308 dissolved in range concentrations and 50 µL (400 ng/mL) of human (bt)-VEGFA or VEGFC in PBS containing 4 µg/mL of heparin were mixed. After two hours incubation at room temperature, the (bt)-VEGFA plate was washed and treated with streptavidin-horseradish peroxidase (HRP) conjugate in PBS (1:8000). The VEGFC plate was incubated with (bt)-anti-VEGFC for one hour and then revealed using HRP conjugate. Luminescence was quantified immediately after addition of 100µL chemiluminescent substrate. In a positive control, only (bt)-VEGFA was present in wells, while, in negative control (NS), wells were not coated with NRP1. Percentages of inhibition were calculated by the following formula: $100\% - [[(S - NS)/(P - NS)] \cdot 100\%]$, where S is the signal intensity measured, NS is the signal measured in negative control, and P is the signal measured in positive control. Presented data are the mean ± SEM of two or three independent experiments, each performed in triplicate.

1.5 Measurement of cytokines

CXCL8 cytokines and VEGFA were detected by using PeproTech ELISA kits according to the manufacturer's indication as already described [3]. VEGFC and CXCL5 were measured using R&D systems ELISA kits according to the manufacturer recommendations.

1.6 Docking study

NRP1 (PDB ID : 6FMF) and NRP2 (PDB ID : 5DN2) structures were retrieved from the Protein Data Bank (PDB) [4]. The NRP2 structure was aligned with the NRP1 structure and both structures were prepared using MGL tools (https://www.ncbi.nlm.nih.gov/pubmed/19399780. (Accessed: 1st February 2019). Three-dimensional conformations of NRPa-308 were generated using iCon, the LigandScout v.4.3 conformer generator [5] (defaults settings of the BEST option were used, except for the maximum number of conformations generated that was set to 50 instead of 25). Protein – ligand docking of compound NRPa-308 into the NRP1 and NRP2 structures was performed using AutoDock Vina v.1.1.2 [6]. The x, y, z grid centre coordinates used are 12.045, 21.518, 15.783 and the size of the search space was set to 20 Å x 20 Å x 20 Å. Only the pose associated with the best score was considered for each run.

1.7 Measurement of cell migration velocity

At confluency, a wound was created on the cell monolayer and its width was measured every hour for 10 hours to determine the migration velocity. At the end of the experiment, the cells were counted to verify if cell death or proliferation had not influenced the wound closure.

1.8 Tumor xenograft formation, size evaluation and treatment

786-O cells expressing luciferase (Luc 1) or RENCA cells expressing luciferase (Luc 2) were injected subcutaneously into the flanks of 5 weeks old nude female mice or Balb-C mice. Treatment by NRPa-308 in carboxymethyl cellulose was carried out by oral gavage trice a week; the control group was treated with carboxymethyl cellulose. Tumors measurements were carried out once a week with a caliper and by luciferase measurements with IVIS chamber as previously described [7]. This study was carried out in strict accordance with the recommendations in the Guide for the Care and Use of Laboratory Animals. Our experiments were approved by our internal ethic committee.

1.9 Immuno-fluorescence

Tumor sections (5µm cryostat sections) were incubated with anti-rabbit LYVE-1 polyclonal (Ab14917, 1:200; Abcam) or rat monoclonal anti-mouse CD31 (clone MEC 13.3, 1:1000; BD Pharmingen) and monoclonal anti- mouse α-smooth muscle actin (αSMA A2547, 1:1000; Sigma) antibodies. Preparations were mounted and analyzed with a Leica microscope, and counted at a 10x magnification.

1.10 Statistical analysis

Statistical significance and P values were determined with the two-tailed t-test. The Kaplan–Meier method was used to produce survival curves and analyses of censored data were performed using the log-rank test.

1.11 Patients online data

Normalized RNA sequencing (RNA-Seq) data of The Cancer Genome Atlas (TCGA) were downloaded from cBioportal (www.cbioportal.org, TCGA Provisional; RNA-Seq V2). Data were available for 534 RCC tumor samples or from 1020 different cell lines. The results published here are in whole or in part based upon data generated by the TCGA Research Network: http://cancergenome.nih.gov/ [8, 9].

2. References for supplementary methods

[1] R. Grepin, D. Ambrosetti, A. Marsaud, L. Gastaud, J. Amiel, F. Pedeutour, G. Pages, The relevance of testing the efficacy of anti-angiogenesis treatments on cells derived from primary tumors: a new method for the personalized treatment of renal cell carcinoma, PLoS ONE, 9 (2014) e89449.

[2] P.D. Ndiaye, M. Dufies, S. Giuliano, L. Douguet, R. Grepin, J. Durivault, P. Lenormand, N. Glisse, J. Mintcheva, V. Vouret-Craviari, B. Mograbi, M. Wurmser, D. Ambrosetti, N. Rioux-Leclercq, P. Maire, G. Pages, VEGFC acts as a double-edged sword in renal cell carcinoma aggressiveness, Theranostics, 9 (2019) 661-675.

[3] R. Grepin, M. Guyot, M. Jacquin, J. Durivault, E. Chamorey, A. Sudaka, C. Serdjebi, B. Lacarelle, J.Y. Scoazec, S. Negrier, H. Simonnet, G. Pages, Acceleration of clear cell renal cell carcinoma growth in mice following bevacizumab/Avastin treatment: the role of CXCL cytokines, Oncogene, 31 (2012) 1683-1694.

[4] H.M. Berman, J. Westbrook, Z. Feng, G. Gilliland, T.N. Bhat, H. Weissig, I.N. Shindyalov, P.E. Bourne, The Protein Data Bank, Nucleic Acids Res, 28 (2000) 235-242.

[5] G. Wolber, T. Langer, LigandScout: 3-D pharmacophores derived from protein-bound ligands and their use as virtual screening filters, J Chem Inf Model, 45 (2005) 160-169.

[6] O. Trott, A.J. Olson, AutoDock Vina: improving the speed and accuracy of docking with a new scoring function, efficient optimization, and multithreading, J Comput Chem, 31 (2010) 455-461.

[7] R. Grepin, M. Guyot, S. Giuliano, M. Boncompagni, D. Ambrosetti, E. Chamorey, J.Y. Scoazec, S. Negrier, H. Simonnet, G. Pages, The CXCL7/CXCR1/2 axis is a key driver in the growth of clear cell renal cell carcinoma, Cancer Res, 74 (2014) 873-883.

[8] J. Gao, B.A. Aksoy, U. Dogrusoz, G. Dresdner, B. Gross, S.O. Sumer, Y. Sun, A. Jacobsen, R. Sinha, E. Larsson, E. Cerami, C. Sander, N. Schultz, Integrative analysis of complex cancer genomics and clinical profiles using the cBioPortal, Sci Signal, 6 (2013) pl1.

[9] E. Cerami, J. Gao, U. Dogrusoz, B.E. Gross, S.O. Sumer, B.A. Aksoy, A. Jacobsen, C.J. Byrne, M.L. Heuer, E. Larsson, Y. Antipin, B. Reva, A.P. Goldberg, C. Sander, N. Schultz, The cBio cancer genomics portal: an open platform for exploring multidimensional cancer genomics data, Cancer Discov, 2 (2012) 401-404.

3. Supplementary figures and tables

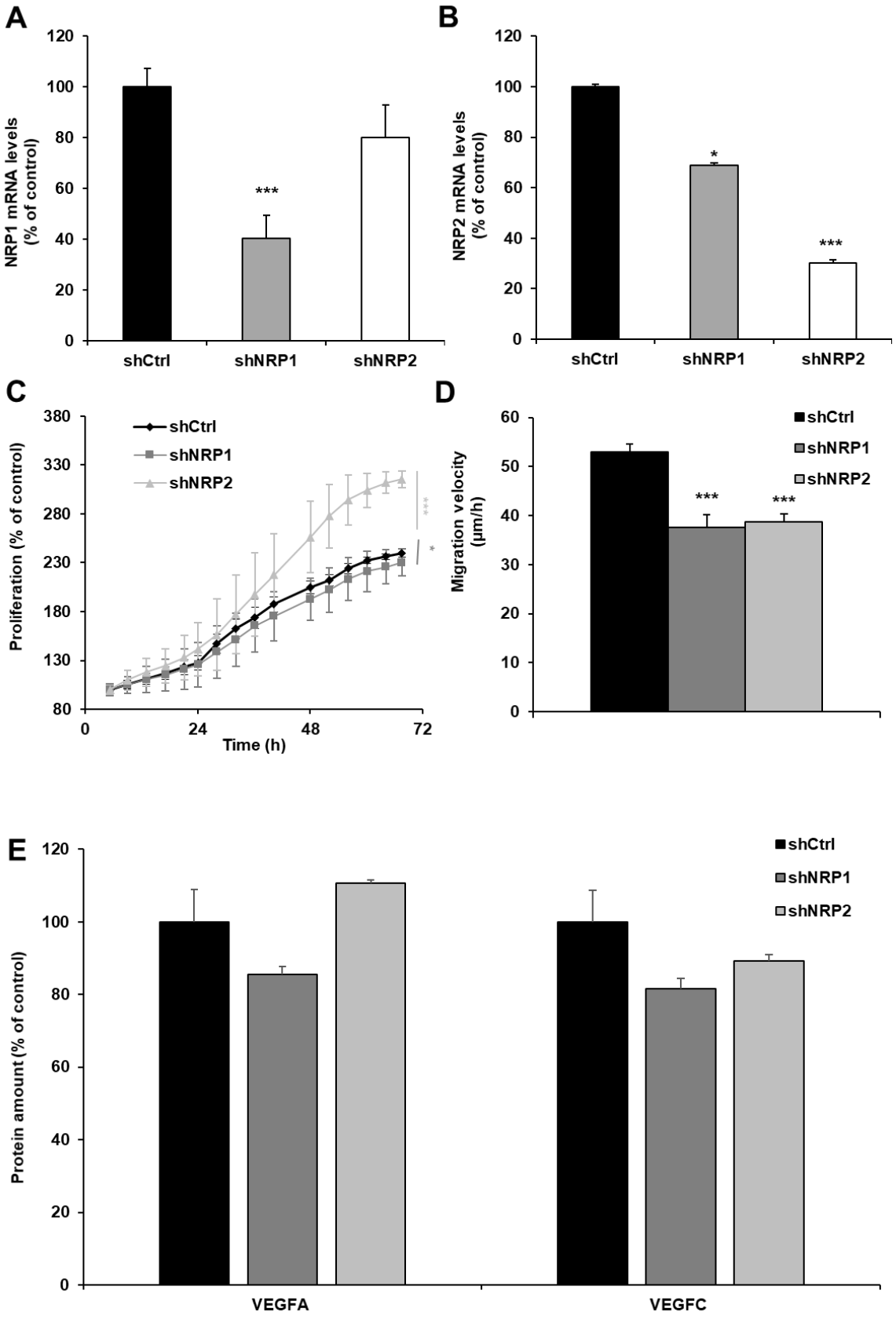

Fig, S1: Dumond *et al*

Fig. S1. Study of down-regulation of NRPs by shRNA in 786-O cells. (A-B) Effects of the downregulation of NRP by shRNA on NRP1 and NRP2 mRNA expression measured by qPCR. **(C)** Effects on cell proliferation measured by MTT assays. **(D)** Down-regulation of NRPs decreased cell migration. Bevacizumab increased this effect for NRP1 down-regulation. **(E)** Down-regulation of NRPs had no effect on VEGFA and VEGFC production measured by ELISA. *p < 0.05; **p<0.01; *** p<0.001.

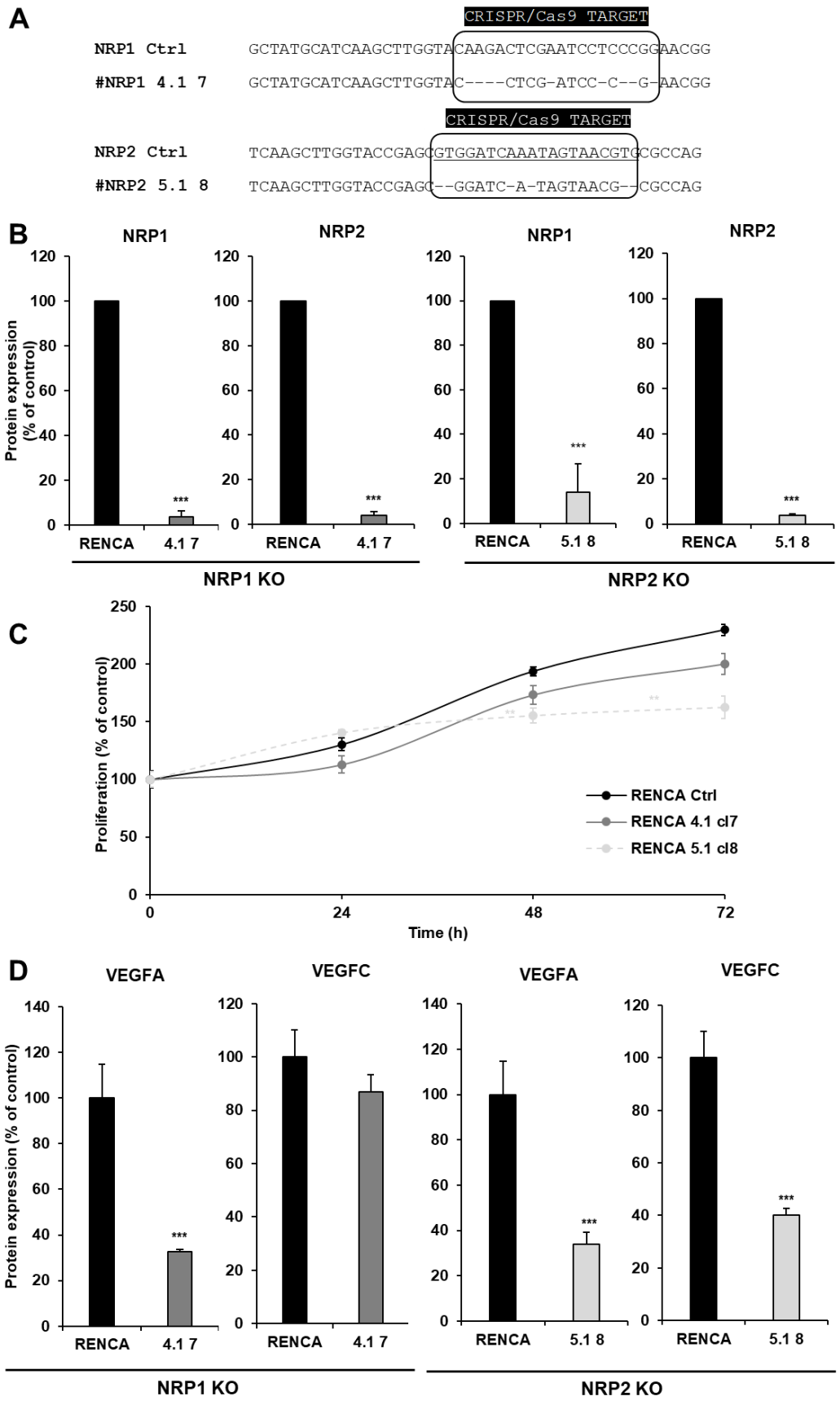

Fig. S2: Dumond *et al*

Fig. S2. Effects of NRP1 or NRP2 gene invalidation in RENCA cells. (B) NRP1 and NRP2 protein levels were evaluated by flow cytometry in control (RENCA), in two independent clones (#NRP1 4.1 7 and 4.2 8) KO for NRP1, and in two independent clones (#NRP2 5.1 7 and 5.1 8) KO for NRP2. **(C)** Effects of NRPs KO on RENCA cell proliferation measured by MTT assays. **(D)** Effects of NRPs KO in RENCA cells on the VEGF-A and VEGF-C protein levels measured by ELISA. *p < 0.05; **p<0.001.

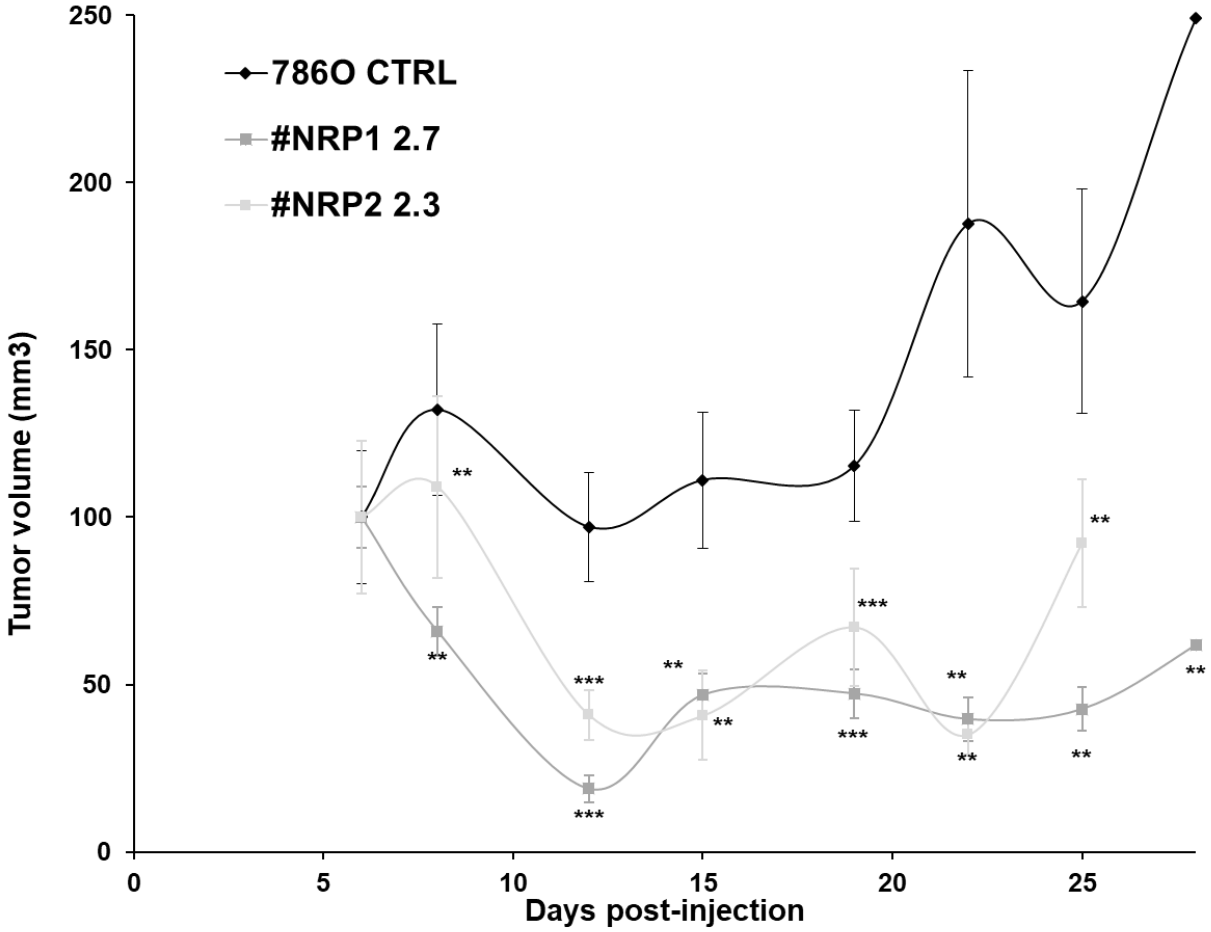

Fig. S3: Dumond *et al*.

Fig. S3. NRPs KO in 786-O tumor cells inhibited experimental RCC growth in immunodeficient mice. Experimental tumors in nude mice (5 mice per condition) were obtained after injection of 3x106 wildtype (Ctrl) or NRPs KO 786-O cells. One NRP1 (#NRP1 2.7) clone and one NRP2 (#NRP2 2.3) clone were injected. Tumor volume is presented. *p < 0.05; **p<0.001.

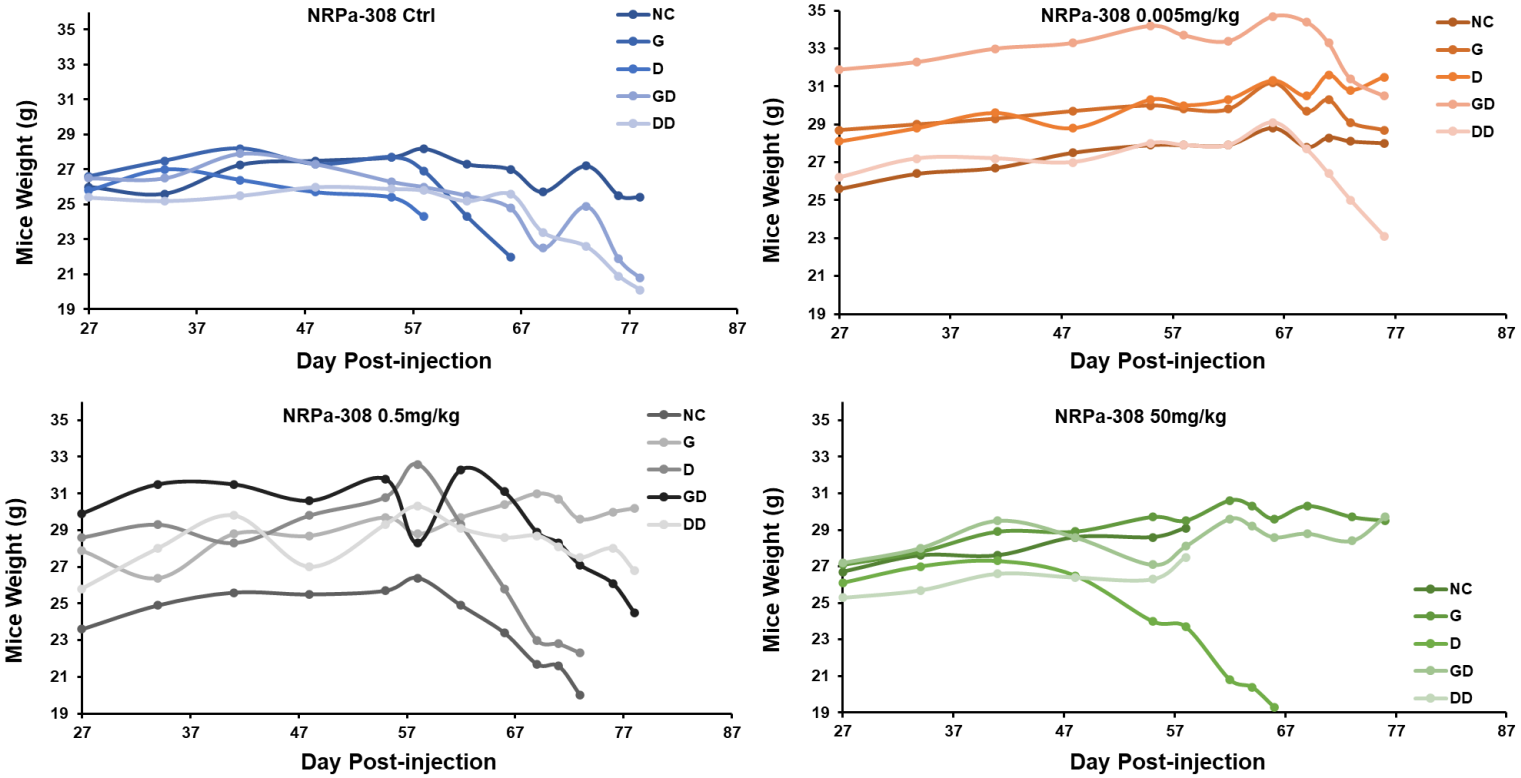

Fig. S4: Dumond *et al.*

Fig. S4. In-vivo effects of NRPa-308 on mice weight. Mice weight was evaluated once a week.

	Forward (5' to 3')	Reverse (5' to 3')
36B4	CAGATTGGCTACCCAACTGTT	GGCCAGGACTCGTTTGTACC
m-RPLP0	AGATTCGGGATATGCTGTTGGC	TCGGGTCCTAGACCAGTGTTC
GAPDH	TGCACCACCAACTGCTTAGC	GGCATGGACTGTGGTCATGAG
Angiogenesis genes		
h-NRP1	GGCGCTTTTCGCAACGATAA	TCGCATTTTTTCACTTGGGTGAT
m-NRP1	GACAAATGTGGCGGGACCATA	TGGATTAGCCATTCACACTTCTC
h-VEGF-A	TTTCTGCTGTCTTGGGTGCATTGG	ACCACTTCGTGATGATTCTGCCCT
m-VEGFA	GCACATAGAGAGAATGAGCTTCC	CTCCGCTCTGAACAAGGCT
h-VEGFR1	ATGGAAAACGCATAATCTGCA	AAATGCCCATTGACTGTTGCT
m-VEGFR1	TGGCTCTAC GACCTTAGACTG	CAGGTTTGACTTGTCTGAGGTT
h-VEGFR2	CATGTTGGTCACTAACAGAAG	GTGATCGGAAATGACACTGGA
m-VEGFR2	TTTGGCAAATACAACCCTTCAGA	GCAGAAGATACTGTCACCACC
Lymphangiogenesis genes		
h-NRP-2	GCTGGCTATATCACCTCTCCC	TCTCGATTTCAAAGTGAGGGTTG
m-NRP-2	GCTGGCTACATCACTTCCCC	CAATCCACTCACAGTTCTGGTG
h-Prox	AGTTCAACAGATGCATTACC	TCTCTGGTTATAGACAGCTC
m-Prox	AGAAGGGTTGACATTGGAGTGA	TGCGTGTTGCACCACAGAATA
h-VEGFC	TTACGGTCTGTGTCCAGTGTA	TTCTCTGTTATGTTGCCAGCC
m-VEGF-C	CTCTGTGGGACCACATGGTAA	TCCTCTCCCGCAGTAATCCA
h-VEGFR3	TGCACGAGGTACATGCCAAC	GCTGCTCAAAGTCTCTCACGAA
m-VEGFR3	CGAGTCGGAGCCTTCTGAGG	GCAGTCCAGCAATAGGGGGT
Immune tolerance genes		
m-PDL1	CCAGGATGGTTCTTAGACTCCC	TTTAGCACGAAGCTCTCCGAT
h-MET	AGCGTCAACAGAGGGACCT	GCAGTGAACCTCCGACTGTATG
m-MET	AGCGTCAACAGAGGGACCT	GCAGTGAACCTCCGACTGTATG
h-HGF	GCTATCGGGGTAAAGACCTACA	CGTAGCGTACCTCTGGATTGC
m-HGF	ATGTGGGGGACCAAACTTCTG	GGATGGCGACATGAAGCAG
Lymphocyte activation		
m-CD69	AAAAGGACATGACGTTTCTG	CAGCTGTTAAATTCTTTGCC
Macrophage M1 genes		
m-iNOS	TCACCTTCGAGGGCAGCCGA	TCCGTGGCAAAGCGAGCCAG
m-TNF	CTATGTCAGCCTCTTCTC	CATTTGGGAACTTCTCATCC
Macrophages M2 genes		
m-ARG1	GATTATCGGAGCGCCTTTCT	CCACACTGACTCTTCCATTCTT

Table S1. List of oligonucleotides used in qPCR experiments

		NRP1	NRP2
786-O	KO NRP1	---	+++
	KO NRP2	-	---
RENCA	KO NRP1	---	---
	KO NRP2	-	---
786-O	SH NRP1	--	-
	SH NRP2	-	--

Table S2. Recapitulative table of the expression of NRP1 and NRP2 in KO and knock-down cells. Three (-) mean a statistically significant decrease, three (+) mean a statistically significant increase. A (-) appearing on a grey background means a trend toward a decreased expression of the examined gene.

		VEGFA	VEGFC
786-O	KO NRP1	+++	+
	KO NRP2	-	+++
RENCA	KO NRP1	---	-
	KO NRP2	---	---
786-O	SH NRP1	-	-
	SH NRP2	+	-

Table S3. Recapitulative table of the expression of VEGFA and VEGFC in KO and knock-down cells. Three (-) mean a statistically significant decrease, three (+) mean a statistically significant increase. A (-) appearing on a grey background means a trend toward a decreased expression of the examined gene. A (+) appearing on a grey background means a trend toward an increased expression of the examined gene.

	NRP1 (6FMF)	NRP2 (5DN2)
Volume (Å^3)	317.632	284.096
Surface (Å^2)	319.52	302.24
Depth (Å)	14.1421	14.1365
Nb of HBA	16	15
Nb of HBD	15	12
Hydrophobicity	0.707317	0.706667
Nb of negative AA	3	3
Nb of positive AA	1	1
Nb of polar AA	12	8
Nb of apolar AA	3	5
Total nb of AA	19	17

Table S4. NRP1 and NRP2 binding site descriptors computed with DogSite Scorer (Nb: number, HBA: Hydrogen Bond Acceptor, HBD: Hydrogen Bond Donor, AA: amino acids)

PART IV: DISCUSSION

Discussion

I) Current ccRCC treatments

ccRCC is one of the most vascularized tumors. Thus, reference treatments are anti-angiogenics targeting the VEGF/VEGFR pathways, but today immune checkpoints inhibitors are also used more often as first lines treatments. However, these treatments have either transient effects or are even ineffective in some patients. These transient effects are mainly explained by the fact that tumor cells adapt by activating other proliferation or angiogenic pathways or by sequestrating weak base drugs. Thus, our objective was to find new targets involved in other tumoral pathways and targeting other hallmarks of cancer.

II) Hallmarks of Cancer

Cancer's hallmarks are characteristics acquired during tumor development that give the tumor survival, resistance and aggressiveness capacities. The hallmarks comprise six characteristics [159]:

- Sustaining proliferative signaling: in normal conditions, normal cells control the production of growth factors to ensure a homeostatic cell number. However, cancer cells have the capacity to deregulate this homeostasis enabling them to survive and proliferate sustainably.

- Evading growth suppressors: cell proliferation is also negatively controlled by different growth suppressor factors, such as the RB or TP53 proteins and TGFβ, thus, cancer cells must evade these factors by defecting their signals.

- Resisting cell death: cancer cells are bypassing apoptosis by losing the TP53 tumor suppressor factor function and by increasing anti-apoptotic factors of the Bcl family or decreasing the pro-apoptotic ones such as Bax or Bim. Autophagy mediates tumor cell death, but also in some conditions, autophagy can be beneficial for tumor survival. Finally, necrosis, compared to the two other cell death, produces pro-inflammatory factors, enabling the recruitment of inflammatory cells from the immune system. In this case, the immune system plays a tumor-promoting role.

- Enabling replicative immortality: senescence and apoptosis are two anti-proliferative defences. Cancer cells manage to bypass these two phenomena by upregulating telomerase, which prevents telomeric shortening responsible of the limited replicative potential of cells and consequently apoptosis and senescence.

- Inducing angiogenesis: tumor angiogenesis is sustained by the production of pro-angiogenic factors such as VEGFA or FGF. This part was more precisely described previously (1.3 Principal mechanisms of angiogenesis).

- Activating invasion and metastasis: expression of EMT factors, such as Snail or Slug, the loss of E-cadherin, decreasing cell adhesion, and the up-regulation of N-cadherin, increasing migration, in many carcinomas, induce invasion and metastasis.

More recently, four other characteristics involved in cancer survival and resistance, have been added [160]:

- Genome instability and mutation: in normal conditions, genome's ability to detect and repair DNA defects enables to maintain spontaneous mutations at a very low number. However, cancer cells acquire the capacity to increase the rate of mutations by defecting and being insensitive to different genomic maintenance components such as detecting or repairing DNA damage. These high rates of DNA mutations in cancer cells induce the acquisition of the different hallmarks responsible of cancer survival and proliferation.

- Tumor-promoting inflammation: many tumors are densely infiltrated by immune cells. However, these immune cells do not induce anti-tumoral response but their tumor-associated inflammatory response is involved in tumorigenesis and progression by supplying the tumor with proliferative, survival and proangiogenic growth factors.

- Reprogramming energy metabolism: cancer cells reprogram their energy metabolism by up-regulating glucose transporters, such as GLUT1, to focus on glycolysis resulting in increased cell proliferation.

- Avoiding immune destruction: tumors have the capacity to avoid immune system anti-tumoral effects by, for example, secreting TGF-β and other immune-suppressive factors to reduce cytotoxic T cells and natural killer cells effects.

Thus, cancer's hallmarks are not only due to cancer cells, but also to the contribution of cell from the tumor microenvironment. Hence, our work on NRPs is relvant as they are expressed on many cells from the microenvironment and involved in many cancer's hallmarks.

III) Neuropilins: new target involved in many cancer hallmarks

Our focus was on NRPs, the VEGF co-receptors already known to be involved in stimulating the VEGF/VEGFR signaling pathway resulting in exacerbated angiogenesis and lymphangiogenesis. Cao *et al.* already highlighted the role of NRPs in ccRCC proliferation, migration and invasion [91,92]. NRPs are not only expressed on endothelial cells but also on cancer and immune cells. Hence, they play a key role not only in angiogenesis and lymphangiogenesis but also in tumor growth and immune system (in)activation. Indeed, Cao *et al.* showed that NRPs are expressed on ccRCC cancer cells compared to the VEGFs receptors [92]. This highlights why NRPs might be relevant targets for ccRCC.

Our first objective was to determine the effect of NRPs' inactivation on ccRCC by genetic disruption (by shRNA and by CRISPR/Cas9).

IV) Genetic modulation by shRNA and CRISPR/Cas9

1) NRPs genetic down-regulation by shRNA

Though shRNA only partially decreases gene expression, we still wanted to use the same shRNA sequences as Cao's team to decipher NRPs' role in ccRCC at longer time points. Indeed, after 48 hours, we showed that the partial disruption of NRP1 slightly decreased cell proliferation and the partial disruption of NRP2 increased cell proliferation (Cao's team obtained no effect at 48h). Furthermore, though Cao's team obtained no effect on ccRCC migration after 24 hours [92], we decided to measure NRPs' partial disruption effects during 10 hours to avoid cell proliferation and death's impact on their migration. At 10 hours post seeding, NRPs' partial disruption decreases cell migration velocity, which was not observed after 24 hours.

Thus, though shRNA only disrupts NRP expression by 60%, these different experiments enabled us to decipher more precisely the role of NRPs in ccRCC as compared to Cao's team [91,92]. An interesting observation is that targeting NRP1 decreases cell migration and slightly

cell proliferation. However, targeting NRP2 decreases cell migration but increases cell proliferation. Thus, according to these results, NRP1 should be targeted but not NRP2.

However, we still wanted to confirm these results with CRISPR/Cas9 technology, which totally invalidated the *NRPs* genes.

2) NRP genetic invalidation by CRISPR/Cas9

With CRISPR/Cas9, we managed to obtain a total disruption of NRPs. In our mind, by carrying the same experiments as the ones carried out for the shRNA down-regulation, we should obtain consistent results, but the effects should have been exacerbated. Surprisingly, a total disruption of NRP1 did not decrease further cell proliferation as compared to its down-regulation. Moreover, NRP2 total disruption decreased instead of further increased cell proliferation. Thus, the level of down-regulation (partial versus complete) of NRP2 had opposite effects on cell proliferation: 60% down-regulation increased ccRCC cell proliferation, whereas a complete invalidation inhibited ccRCC cell proliferation more efficiently than NRP1 invalidation. This important difference between NRP2 partial and total disruption might be explained by the overexpression of VEGFC induced by NRP2 total disruption. Indeed, we previously, showed in the laboratory that VEGFC expression in ccRCC decreases cell proliferation [69].

As NRPs have an impact on the (in)activation of the immune system [156,157], we decided to determine NRPs' role in tumor growth on two mice models: immunodeficient (nude mice) and immunocompetent (Balb/C). First, in immunodeficient mice NRPs' disruption on ccRCC delayed the initiation of tumor growth and decreased tumor volume and weight as compared to tumors generated with control cells. The same experiment was carried out on immunocompetent mice to highlight the role of the immune system on tumor growth. NRPs' disruption in ccRCC cells totally inhibited tumor growth compared to tumors generated with control cells. The use of immunodeficient and immunocompetent mice will be discussed later (Paragraph VI)

3) Conclusion

First of all, shRNA gave conflicting results as compared to CRISPR/Cas9. These results highlighted the necessity to completely inhibit NRPs' expression for a maximal therapeutic effect. In my opinion, in addition to CRISRP/Cas9 technology, the partial disruption experiments are relevant:

- to assess the role of the NRPS. Indeed, as NRPs are expressed by different cells, our first objective was to determine if disrupting NRPs could enable to target different cancer

hallmarks and if NRPs could be a relevant target to treat ccRCC. We deciphered their implication in cell migration, proliferation, tumor growth and in the immune system response.

- to determine the best inhibition strategy. Indeed, the use of these two disruption techniques enabled us to highlight the difference between a partial and a total inhibition. Of course, we could only have carried out CRIPSR/Cas9 disruption and observed the effect of a 100% NRPs' disruption on ccRCC cells. However, as we know, chemical inhibitors do not inhibit their target at 100%. Thus, the two techniques highlighted the specific impact of the level of NRPs' inhibition. A partial or total inhibition of NRP1 resulted in the same effects. For NRP2, gene invalidation resulted in decreased ccRCC cell proliferation, but down-regulation (60%) had the opposite effect.

These two disruption techniques (partial/complete) allowed to reach to the conclusion that complete inhibition of NRP2 represents the best therapeutic strategy for the treatment of ccRCC by inhibiting different cancer hallmarks: proliferation, migration, tumor growth, immune tolerance. Genetic invalidation cannot be implemented for patient's treatment. Therefore, our objective was to mimic this invalidation with pharmacological inhibitors. NRPa-308 was developed as a NRP1 inhibitor by the chemists from University Paris-Descartes and was already tested on breast cancers. As for the breast cancers, NRPs' expression was correlated to ccRCC aggressiveness. Hence, we tested the relevance of NRPa-308 on experimental models of ccRCC.

V) Inhibition by NRPa-308 compound

1) NRPa-308 *in-vitro* efficacy on ccRCC cells

One of the objectives was to compare its efficacy to those of sunitinib, one of the current reference treatments. We highlighted that NRPa-308 inhibited cell proliferation and migration more efficiently than sunitinib and was less toxic on normal cells. As presented before (2.3 EG3287 and its derivates), a NRP1 inhibitor, EG00229, already exists but its anti-proliferative effects are less important than those of NRPa-308. The availability of ccRCC cell lines knock-out by CRISPR/Cas9 for each NRP, allowed determining the specificity of NRPa-308 for each NRP. Thus, we highlighted that NRPa-308 acts preferentially through NRP2 and inhibited NRP2/VEGFC binding in a reverse dose-dependent effect compared to NRP1/VEGFA binding that is inhibited at higher dose. Furthermore, we highlighted the anti-tumoral effects of NRPa-308 at low dose with *in-vivo* studies on immunodeficient and immunocompetent mice.

2) NRPa-308 *in-vivo* effects on breast cancer cells

The first studies with NRPa-308 were conducted on breast cancers [154]. Xenografts of triple negative breast cancer cells (MDA-MB231) were carried out on immunodeficient mice treated trice a week with NRPa-308 at 50mg/kg. NRPa-308 at 50mg/kg (corresponding approximately to a concentration of 2000µmol/L) reduced tumor growth and weight. Thus, we decided to conduct the same *in-vivo* experiments with ccRCC cells.

3) NRPa-308 *in-vivo* effects on ccRCC cancer cells

Based on the *in-vivo* results obtained with breast cancer cells and the *in-vitro* efficacy of NRPa-308 on ccRCC cells, our first idea was to carry out the same *in-vivo* experiment as for breast cancer, on immunodeficient mice, treated trice a week with 50mg/kg of NRPa-308. However, the 50mg/kg dose had no effect on experimental ccRCC. The *in-vitro* experiments showed that NRPa-308 more efficiently inhibited NRP2 at low doses. Therefore, we decided to perform an escalation dose *in-vivo* with the following concentrations: 5µg/kg, 500µg/kg and 50mg/kg. At 5µg/kg (corresponding approximately to a dose of 0.2µmol/L), NRPa-308 decreased tumor growth, weight and the expression of different pro-tumoral, pro-angiogenic, pro-lymphangiogenic and immunosuppressing factors. The same experiment was carried out in immunocompetent mice to decipher the effects of NRPa-308 in presence of the immune system. We will talk about this experiment later (Paragraph VI).

Thus, NRPa-308 is more efficient in reducing ccRCC growth as compare to breast cancers. This result was exciting since it combined high efficacy with a low (less toxic) concentration. However, our goal was to understand the discrepancy related to the efficient concentrations.

4) On what depends NRPa-308 efficacy?

To understand why NRPa-308 was less efficient in breast cancers, we focussed on the expression of the two NRPs and their principal ligand VEGFA and -C in breast and ccRCC cell lines. VEGFA **(*Figure 16A*)**, -C ***(Figure 16B)*** and NRP1 ***(Figure 16C)***, are mainly expressed in all the breast and ccRCC cell lines. However, we highlighted that in all breast cancers, NRP2 ***(Figure 16D)*** was not expressed as compared to ccRCC.

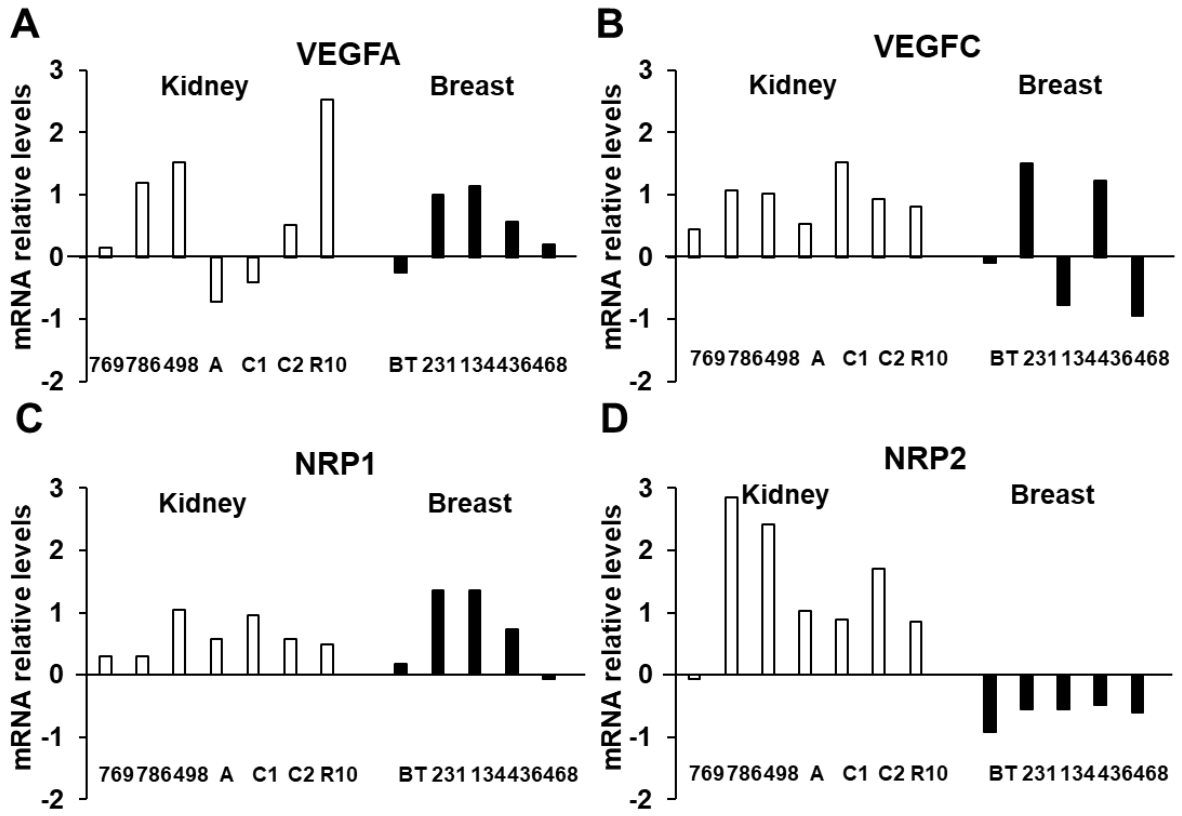

Figure 16. mRNA levels of VEGFA, VEGFC, NRP1 and NRP2 in kidney and breast cancer cell lines. Analysis of cbioportal database highlighted the relative levels of VEGFA (A), VEGFC (B), NRP1 (C) and NRP2 (D) mRNA in a panel of RCC (769 (769P), 786-O (786), ACHN (A), Caki1 (C1), Caki2 (C2), RCC10 (R10)) and TNBC (BT474 (BT), MDAMB231 (231), MDAMB134 (134), MDAMB436 (436), MDAMB468 (468)).

Furthermore, recent clonogenicity studies showed that NRPa-308 exerts its cytotoxic effects through NRP2. Indeed, after one week of treatment at 0.2µmol/L of NRPa-308, cells with NRPs' disruption and control cells seemed to die ***(Figure 17A and B)***. After removing the treatment for one week, cells with NRP2 disruption proliferated again as compared to cells that are still expressing NRP2 (Control and NRP1 disrupted cells) ***(Figure 17C)***. Furthermore, the proliferation properties after NRPa-308 treatment were correlated in a reverse dose dependent manner to the expression of NRP2 ***(Figure 17C)***. Thus, NRPa-308 exert cytotoxic effects mainly through NRP2 and was less efficient when NRP1 is present.

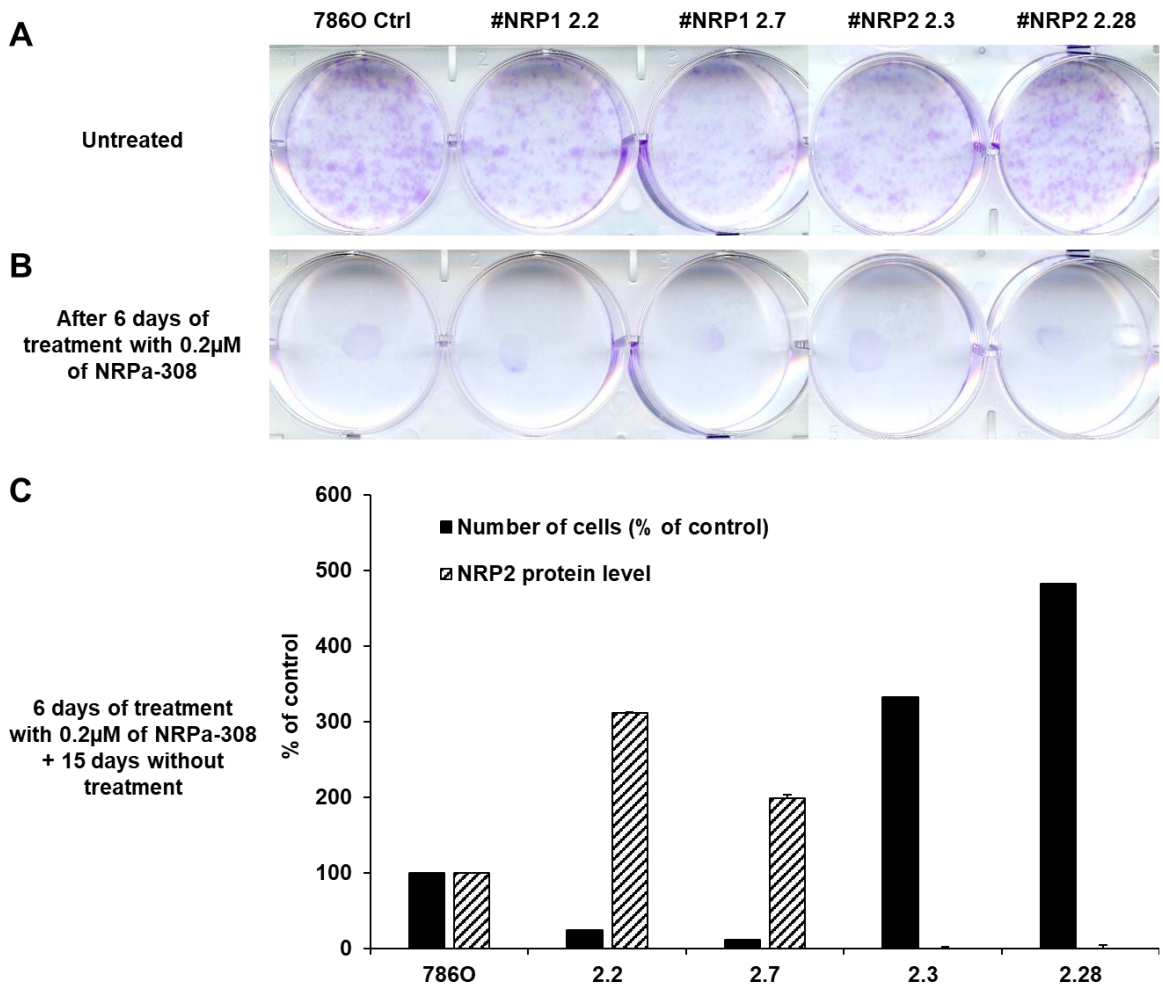

Figure 17. Influence of NRP2 protein level on NRPa-308 effects. *(A)* Clonogenicity assays on untreated 786-O control or with NRPs disruption cells after 6 days. *(B)* Clonogenicity assays on 786-O control or with NRPs disruption cells after 6 days of NRPa-308 treatment at 0.2µM. *(C)* 786-O control or with NRPs disruption cells were treated for 6 days with 0.2µM and then left 15 days without treatment. Cells number were then determined and compared to the level of NRP2 protein in each type of cells.

This result could explain the better efficiency of NRPa-308 in ccRCC as compared to breast cancers that do not express NRP2. Indeed, we showed *in-vitro* that NRPa-308 exerted its anti-proliferative effects through NRP2 and at low doses.

Thus:

- Cancer cell expressing NRP2, such as ccRCC: NRPa-308 acts through NRP2 and is efficient at a low dose, as shown *in-vivo*.
- Cancer cells that are not expressing NRP2, but NRP1, such as breast cancers: NRPa-308 can act only through NRP1 and, as shown previously when cells are expressing only NRP1, NRPa-308 is less efficient. Hence, we observed *in-vivo* in breast cancers that NRPa-308 is efficient at higher doses.

5) Conclusion

Through these *in-vitro* and *in-vivo* studies on ccRCC, we highlighted that NRPa-308 is a “hit” molecule with an anti-tumoral role at low dose for cancers expressing only NRP2 or NRP2 and NRP1. However, for cancers expressing only NRP1, NRPa-308 is poorly efficient at low doses. Higher antitumor efficient doses that could present toxicity. Hence, more specific NRP1 inhibitors must be developed.

As described before, NRPs are involved in the (in)activation of immune response, thus, our next objective was to determine the effects of NRPa-308 on the immune system response.

VI) Effects of NRPa-308 on the immune system response

1) *In-vivo* tests with NRPa-308

As explained before, cancer cells can inactivate the immune cell response to survive and invade. Thus, our objective was to determine the effects of NRPs on the immune system. We are the first to have carried out *in-vivo* experiments using the ccRCC cells with disruption of NRPs in immunodeficient but also in immunocompetent mice. Indeed, immunodeficient mice enable to highlight the direct anti-tumoral effects of NRPs alone without considering the effect of the immune system. However, as NRP are involved in the activation and inactivation of the immune system, it was important to determine the NRPa-308’s effects in the presence of the immune system. Thus, we carried out the same *in-vivo* experiments performed in immunodeficient and in immunocompetent mice. As soon as one NRP is invalidated by CRISPR/Cas9, the tumors did not developed as compared to control cells. This result highlighted that NRP expressed on tumor cells might be involved in the inactivation of the immune system.

The CRISPR/Cas9 clearly showed NRPs-dependent involvement of the immune response and the subsequent inhibition of tumor development. Hence, our next objective was to determine if NRPa-308 re-activate the immune system response. Indeed, NRPa-308 is targeting the NRPs present in tumor cells but also in all the mouse cells. Of course, the invalidation of tumor cells’ NRPs influenced the (in)activation of the mice immune response, as shown in the experiments performed in immunocompetent mice resulting in the total inhibition of tumor growth. Thus, *in-vivo* experiments in immunodeficient and immunocompetent mice were carried out with NRPa-308. We observed in both cases a decreased tumor growth. Further experiments are required to demonstrate that it re-activates the immune response and to determine if a combination of NRPa-308 with an immune checkpoint inhibitor might increase NRPa-308 anti-tumoral effects

(VII) Combination of NRPa-308 with immune checkpoints inhibitors). Experiments should also be performed to identify the main anti-tumoral target of NRPa-308; the NRPs expressed by tumor cells or by immune cells. Conditional NRPs' KO mice will be an asset to answer this question.

2) Conclusion

In-vivo studies in immunodeficient and immunocompetent mice showed that NRPs expressed on tumor cells are responsible of tumor growth but also of the inactivation of immune system response. We also highlighted, with both *in-vivo* experiments, that NRPs inhibition by NRPa-308 is efficient to disrupt tumor growth and the pro-tumoral effects of the immune system.

Thus, these experiences with NRPs inhibited by CRISPR/Cas9 and by the NRPa-308 inhibitor highlight that targeting NRPs is a relevant strategy to treat ccRCC as it enables to target different cancer hallmarks: tumor growth, migration and immune system.

VII) Combination of NRPa-308 with immune checkpoints inhibitors

As stated before, NRPs are involved in the regulation of immune checkpoints such as PD-L1 through HGF/c-MET *(3.4 HGF/cMET).* Thus, after *in-vivo* experiments we decided to measure the mRNA expression of different immune checkpoints in the tumors gathered from the mice (immunodeficient and immunocompetent) after the treatment by NRPa-308. All the pro-tumoral immune factors are decreased after NRPa-308 treatment. However, analysis of the tumors' infiltrated cells by flow cytometry must be performed to deep insight in the global mechanism of action of the drug, which can put forward the relevance of a combination between NRPa-308 and an immune checkpoints inhibitor.

Several immunotherapies alone or combined with anti-angiogenics showed promising results *(4.6 Anti-angiogenics and immunotherapies combinations)*. With most of these combinations, PFS and OS are increased compared to the current reference treatment, sunitinib.

Thus, combining NRPa-308 with either nivolumab (anti PD-1), ipilimumab (anti CTLA-4) or atezolizumab (anti PD-L1) would be interesting. However, the availability of syngeneic models is limited (only RENCA cells can be used). Hence, *in-vivo* experiments are poorly demonstrative. Moreover, the "mice" antibodies to perform these combinations in immunocompetent mice are very expensive. An alternative is to inactivate these immune checkpoints by siRNA in RENCA

cells before injecting them to immunocompetent mice and then treat mice with NRPa-308 treatment.

VIII) *In-vivo* ccRCC metastatic models

In-vivo studies are an important step to assess the efficiency of a drug in a complete organism including tumor microenvironment effects, and so to mimic in the best way the effects that will be obtained in the clinic. Furthermore, advanced ccRCC is mainly metastatic and metastasis are the main causes of death linked to ccRCC. Thus, it would be important to assess the effects of NRPa-308 on the formation and on the growth of metastases. Different *in-vivo* models of metastasis are the following:

Cell line xenografts injections enable to test rapidly drug's effects on the primary tumor. This technic enables to study the early stages of tumor development and the effects of a drug on these early stages of tumor development. However, its effects on metastasis cannot be determined this way. Different technics exist with cell lines to evaluate metestatic dissemination: i) injection of tumor cells in the blood stream to observe lung metastasis; ii) orthotopic injection in the kidney or tumor cell xenografts. When the limit point is reached, the kidney or tumor xenograft is removed and measured. Mice are still monitored for several days before observing lung metastases. Another option is to reiterated injections of cell from primary tumor in the kidney or the lung to generate more aggressive cells as suggested by Cooley's team [161]. For my *in-vivo* experiments, (xeno)grafts were preferred since we considered it mimics a metastatic situation. However, in immunodeficient and in immunocompetent experiment, most of the mice in the control and in the high doses (500µg/kg and 50mg/kg) were sacrificed because of their weight loss, sometimes even before reaching the tumor volume limit point. Thus, we could not pursue the experiment up to observe metastatic site. Cao's team [92] carried out these experiments in immunodeficient mice with the injection of $2x10^6$ 786-O cells (control and NRP disrupted cells by shRNA) and observed pulmonary metastasis 4 months after the removal of the xenografts. We carried out the experiment with $3x10^6$ 786-O cells treated with NRPa-308, maybe by injecting less cells we would have been able to maintain acceptable mice weight longer and carried out the experiment until the end. Furthermore, according to the implication of NRPs on the immune system, these experiments should have been carried out in immunocompetent mice. However, establishing this type of experiment with RENCA cells is challenging as a few hundred of RENCA cells (about 300000 cells) are sufficient to induce rapidly a high tumor volume. Thus, to set up this experiment, it is necessary to inject different cell number to determine the best dose consistent with the observation of metastases. In

addition to the difficulty to establish metastatic models, experimental tumors generated with primary cells are long to develop in nude mice (more than 4 months) and the cells lose the original tumor heterogeneous characteristics after several passages and the time period of culture in culture media [162]. Thus, cell line xenograft is a good technic to determine the effect of a drug rapidly and in the early stages of the tumor development. However, it does not reflect exactly the clinical reality, particularly the metastatic development.

Genetically engineered mouse models are obtained either by the introduction of the DNA of an oncogene of interest in fertilized egg, or the knockout of a tumor suppressor gene in embryonic stem cells [162]. These models enable the understanding of tumor initiation, the relapse on therapies in the appropriate tumor microenvironment. However, these spontaneous initiated tumors are generated from mouse cells and do not reflect human tumors characteristics and responses to drugs. Moreover, the time to obtain these kind of tumors is very long (around 1 year) [162].

The model that reflects the most clinical human tumors are the PDX (Patient-Derived Xenografts). They are piece of human tumors directly injected subcutaneous or orthotopically to highly immunodeficient mice (non-obese diabetic (NOD) mice), preventing any *in-vitro* genetic modifications of the tumor cells as it is observed in cell lines after many passages. Orthotopic injection have an advantage as it enables to mimic more precisely the microenvironment around the tumor and it induces more spontaneously metastasis, as compared to subcutaneous injection [162]. Compared to the two other technics, PDX are the best models to study metastasis, but PDX are injected in immunodeficient mice. Hence, the tumor microenvironment does not reflect perfectly clinical reality. Thus, PDX models are the best technics to mimic clinical drugs' effects and to improve drug development. However, this technic's disadvantages are its high costs, the difficulty to establish metastasis and the absence of the immune system in the microenvironment [162]. To overcome this last disadvantage, humanized mice, injected with human immune cells are developed, which by interacting with PDX, can mimic precisely clinical reality [162]. In the case of ccRCC, PDX models have widely been used to test sunitinib, everolimus or cabozantinib treatment for example, but also to study sunitinib-resistant tumors from patients [163].

Another metastatic model is the zebrafish embryo. Indeed because of its transparency, tumor growth, invasion and metastasis are easy to evaluate with high resolution *in-vivo* imaging technics [164]. Fluorescently labelled human tumor xenotransplantation, generally in the yolk sac because of its acellular characteristic, can be carried out on zebrafish embryos. The xenotransplantation is done on 2 days post-fertilization embryos to have a large transplant site and before the adaptative immune response establishment [164]. Zebrafish are a rapid technic

to obtain and measure the effects on metastasis, generally observed in the tail. Furthermore, interactions with cells from the tumor microenvironment can also be observed by co-injecting these cells, labelled with another fluorochrome, at the same time as the tumor cells. The biggest advantages of this technic are: i) a large number of zebrafish embryos can be produced and hosted simultaneously for one experiment; ii) tumor engraftment take only 2 to 3 days (compared to weeks/months for mice) and metastasis are also observed maximum a week after tumor injection [164]. However, the main disadvantage is the conserved genome of 70% between human and zebrafish and the absence of important genes involved in the tumor development, such as BRCA1 (tumor-suppressor gene), which could influence tumor growth and invasion but also suppress some interactions between the tumor cells and the host cells that are necessary like for hematopoiesis [164]. Thus, comparing to the previous technics described, zebrafish enable to study drug effects on metastasis rapidly and to study many different conditions (drug dose-dependent effects for example).

The chick chorioallantoic membrane (CAM) is present in fertilized eggs and contains numerous blood vessels, that are easy to observe with a microscope [165]. Furthermore the CAM is composed of three epithelium layers: the ectoderm (at the air interface), the mesoderm and the endoderm (at the allantoic sac interface), and contains extracellular matrix proteins, which imitates well the tumor environment [166]. It can be used as a low-cost metastatic model but CAM assay is less used for metastatic than for angiogenic measures [166]. Human cancer cells are mixed with Matrigel and graft to the CAM at day 11 until day 14. At day 14, the invasion of cancer cells from the ectoderm to the mesoderm is visible [166]. After collecting the membrane, qPCR or immunohistochemistry can be carried out to determine the presence of metastatic human cancer cells in the inferior membrane and in the organs [166].

I consider that all these different metastatic models have their advantages and disadvantages. In the laboratory, the easiest model to use is cell lines xenografts but the other models described are, for me, more complete in terms of tumor/microenvironment interactions. Considering time saving, zebrafish is, for my point of view, the best choice to decipher drug's role on metastasis. However, the human/zebrafish genome differences and the absence of some organs in the fish may influence the tumor behaviour. Thus, the model, which mimics the clinic reality is the PDX model with humanised mice. However, such experiments need a longer time frame and their costs are more important. In any case, all these *in-vivo* metastatic models must be developed continuously to get closer to clinic responses as they are a key step before early phase studies.

IX) *In-vivo* ccRCC angiogenic models

ccRCC being one of the most vascularized tumors, determining the effects of NRPs chemical inhibition is an important step. *In-vitro* assays enable early and quick studies of angiogenesis. These assays consist in proliferation, migration or tube formation measurements, and each assay focusses only on one characteristic of angiogenesis. Thus, they do not mimic the reality [165].

In-vivo assays allow to test the effects of a drug on angiogenesis in a complete organism [165].

As described in the previous paragraph, zebrafish experiments represent interesting *in-vivo* models due to the number of embryos available for one experiment and to its transparency to observe vascularization processes. Furthermore, transgenic zebrafishes have been developed to exhibit blood vessels expressing green fluorescent protein and blood cells another fluorescent protein to observe the formation of new vessels and the impact of the treatments [165]. However, the main disadvantage of working on embryo is to determine if the newly formed vessels originate from vasculogenesis or angiogenesis processes [165].

The chick chorioallantoic membrane (CAM) can also be used for angiogenic assays [165]. We tested this technic by transferring the entire membrane from the egg to a petri dish, which favors the observation of the CAM. However, the reproducibility from an embryo to another is a real concern [165]. Furthermore, even though one of its advantage is its low cost, the transfer from the egg to the petri dish is technically difficult to avoid sample loss. To conclude, for me, this technic, if well-controlled, allows a great visualization of blood vessels and of the effects of a drug on angiogenesis.

Angiogenesis assay can be carried out in the cornea; indeed, cornea is transparent and does not contain vasculature. Thus, any newly blood vessels are the result of angiogenesis and this technic has been widely used to test pro-angiogenic factors [165]. However, the ethic problem and the technical problems are important issues. [165].

Matrigel plugs saturated with pro/anti-angiogenics or drugs and implanted subcutaneously in mice have been used several times. After a few days, Matrigel plugs are immunohistology stained with CD31 to count the number of vessels [165]. As for the cornea, this technic allows the evaluation of the effect of pro-angiogenic factors on the formation of blood vessels but not for anti-angiogenics.

Angiogenesis can also be measured directly on xenografts by immunohistology staining of the blood vessels in the tumors. For us, this was the most suitable technic to implement.

To conclude, our objective being to investigate the anti-angiogenic effect of NRPs inhibition, cornea and Matrigel plug assays are not suitable. Thus, zebrafish, CAM and xenograft immunohistology staining were the most useful technics in our case. In the laboratory, the two technics that could be carried out are CAM and xenografts on mice. As said before, we tested CAM assays, but we were still not enough experienced to obtain reproducible results, but for me this technic is interesting since the visual assessment is direct. Thus, we carried out xenografts and stained them with CD31 to measure the number of blood vessels in control mice and mice treated by NRPa-308. For me, CAM and zebrafish are the best "visual" technics to evaluate the effects of a treatment on angiogenesis. However, the zebrafish model is more relevant for a statistical point of view since the number of available samples for one experiment is important.

X) NRPa-308 *in-vivo* bioavailability at the tumor

The efficacy of NRPa-308 was observed at a low dose of 5µg/kg, corresponding to 0.2 µmol/L. However, the first question to assess after animal experimentations is the real dose of NRPa-308 available at the tumor site. This experiment requires mice plasma or the tumors for NRPa-308 measurement by HPLC. For me, this is a very interesting experiment for the development of a drug, indeed the determination of the ADMET (Absorption, Distribution, Metabolism, Excretion and Toxicity) properties of a drug are the main steps of preclinical studies. Thus, the determination of drug bioavailability in the tumor should be performed as a routine for each animal experiments, which is not yet the case in the laboratory.

XI) Targeting specifically NRP1

All our *in-vitro* and *in-vivo* experiments highlighted that:

i) The total inhibition of NRP2 is the best therapeutic strategy for ccRCC
ii) NRPa-308 is a "hit" molecule to treat ccRCC since it is efficient at low doses
iii) For cancers that are not expressing NRP2 but only NRP1, NRPa-308 is efficient at high doses.

Thus, one of our perspectives is to develop NRP1 specific inhibitors to treat this last type of cancers. Docking studies deciphered the binding mode of NRPa-308 on each NRP and the composition of NRP1 and NRP2 binding pockets. NRPa-308 binding mode differs between NRP1 and NRP2: NRPa-308 binding into NRP1 is more flipped than its binding into NRP2. In both cases, NRPa-308 binding is stabilized by hydrogen bonds, π-stacking and hydrophobic interactions. However, the comparison of NRP1 and NRP2 structures highlighted that the residues forming each binding site differ and that the NRP2 binding site is larger and more open than the NRP1 binding site. These results could explain the better affinity of NRPa-308 to NRP2 than to NRP1.

However, these differing residues between NRP1 and NRP2 are also an advantage to obtain a specific NRP1 inhibitor for the treatment of cancers expressing only NRP1 such as breast cancers. Thus, our current strategy is to optimize NRPa-308 structure based on the specific residue of NRP1 binding pocket to obtain a molecule more specific to NRP1 than to NRP2.

XII) Parallel studies on NRPa-47

As stated before *(1)Screening of NRPa-47 and NRPa-308)*, NRPa-47 was selected as a NRP1 inhibitor through the same screening as NRPa-308. Thus, it gives us another opportunity to obtain specific NRP1 inhibitors. Indeed, parallel studies on NRPa-47 highlights its anti-proliferative and anti-migrative effects on 786-O cells with an IC_{50} around 0.34µM (unpublished data). Furthermore, its structure is easier to optimize as compared to NRPa-308 ***(Figure 18A)***. The docking of its binding on NRP1 showed that its benzimidazole and its benzodioxane cores are oriented into NRP1 binding pocket and forms different hydrogen bonds with the residues from this pocket. It also highlighted that the methyl points out of the binding pocket ***(Figure 18B)***.

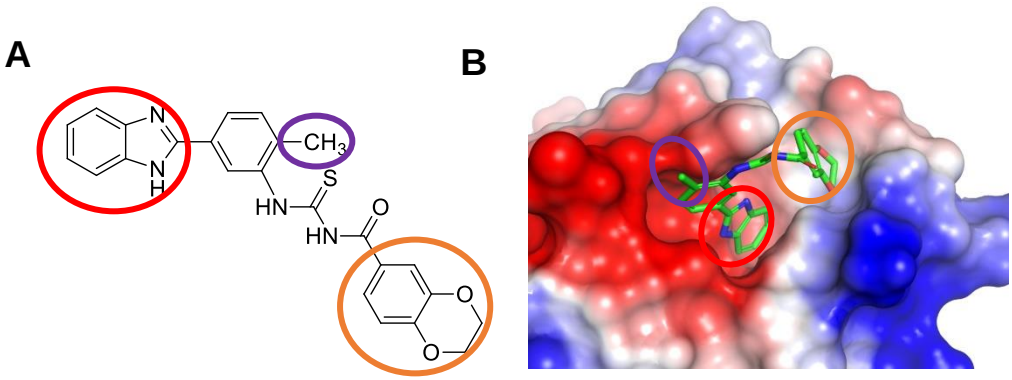

Figure 18. NRPa-47 inhibitor. **A.** NRPa-47 structure. **B.** NRPa-47 binding docking on NRP1.

As the methyl group (in purple) of NRPa-47 is pointing out of the binding pocket, we decided to optimize NRPa-47 by integrating new groups at this position to improve its solubility ***(Figure 19)***. If modifying this position does not alter its binding to NRP1, further studies are planned. Indeed, NRPs have the capacity to enter in the cells after ligand's binding. Thus, the integration of fluorescent probes at the methyl position could enable to determine the traffic of NRPa-47 into the cells. Ultimately, according to this result:

i) NRPa-47 could be used as a transporter of more cytotoxic drugs to the targeted cells: these drugs would be linked by a spacer arm to NRPa-47 at this methyl position. NRPa-47 by binding to NRP1 would enter (if proved with the fluorescent probe) into the cells and would free the cytotoxic drug.

ii) NRPa-47, or NRPa-308, with the fluorescent probes could be used in *in-vivo* studies to observe where the NRPs inhibitor goes and, for example, if it accumulates more in the tumor microenvironment or not.

Optimizations on the benzimidazole (in red) and on the benzodioxane (in orange) cores could improve the specificity of NRPa-47 to NRP1 and its efficacy ***(Figure 19).***

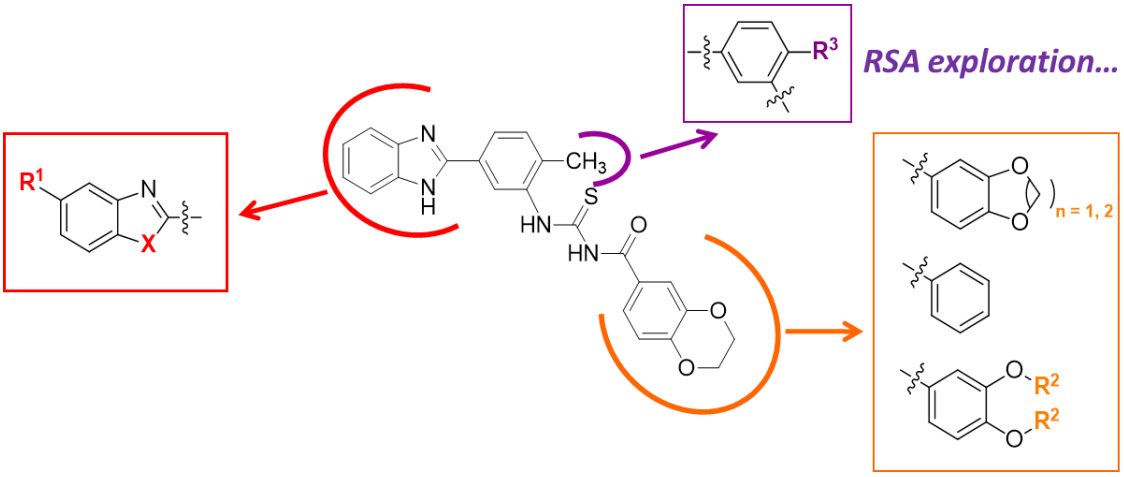

Figure 19. **NRPa-47 structure optimization**s. In purple, optimization to improve NRPa-47 solubility. In red and orange, NRPa-47 optimizations to improve its specificity to NRP1.

I performed the optimizations of the methyl positions at Institute of Chemistry of Nice (ICN). They are pursued, in parallel with the optimizations of the two cores, at the University Paris-Descartes.

Thus, working in parallel on NRPa-308 and NRPa-47 optimizations gives us many opportunities to obtain specific NRP1 inhibitors to target cancers expressing only NRP1 such as breast cancers.

PART V: CONCLUSION

Conclusion

These studies pointed out the relevance of Neuropilins' targeting to overcome resistance to anti-angiogenics. Indeed, NRPs are expressed on different cells from the tumor microenvironment: tumor, endothelial and immune cells. Their knockout highlighted their involvement in many cancer's hallmarks: proliferation, migration, tumor growth and immune suppression. NRP2 knockout is more efficient than NRP1 knockout in decreasing pro-tumoral characteristics: proliferation, migration or tumor growth for example.

Despite the number of NRPs inhibitors currently developed by different teams, the majority have not yet shown anti-tumoral effects or did not enter in clinical trials. The collaboration with the chemists from University Paris-Descartes as allowed the discovery of NRPa-308 thanks to a screening based on the virtual binding to NRPs.

In ccRCC, NRPa-308 exerts greater *in-vitro* and *in-vivo* effects through NRP2 and at low dose (0.2µmol/L) confirming the crucial role of NRP2 in the aggressiveness of ccRCC. Thus, NRPa-308 is an inhibitor that enable to inhibit different cancer's hallmarks in the ccRCC: proliferation, migration, tumor growth and the formation of functional blood vessels. The previous studies carried out on breast cancers highlighted an anti-tumoral efficacy of NRPa-308 at higher doses (2000µmol/L), explained by the absence of NRP2 in these cancers and the lesser affinity of NRPa-308 to NRP1. Thus, NRPa-308 is a "hit" molecule for the treatment of ccRCC, that are expressing NRP2. However, for cancers that do not express NRP2 but only NRP1, NRP1 specific inhibitor have to be developed. For this, our collaboration with the chemists continues and the strategy is to optimize NRPa-308 according to the residues from NRP1 binding pocket that differs from the ones of NRP2 binding pocket. We also started to optimize NRPa-47, the second inhibitor of NRP1 obtained through the screening, which can give us more opportunities to obtain specific NRP1 inhibitors according to its structure and its docking.

All these studies were compared to sunitinib, which was the reference treatment for ccRCC until recently. Indeed, since 2020, immune checkpoints inhibitors and their combination with anti-angiogenics, notably with axitinib, have become the new first line reference treatments. However, the main disadvantages of these new reference treatments are:

i) their formulation: injections at the hospital versus a tablet for sunitinib, which is for the patient's quality of life important to be considered;
ii) their cost, which is a very important concern for the vast majority of patients to have access to healthcare.

Thus, the next tests on NRPa-308 or the NRP1 specific inhibitors should be compared to these combination of immune checkpoints inhibitors/anti-angiogenics and still to sunitinib as many patients will still have only access to this treatment.

Our objective was to define an alternative therapeutic strategy if the reference failed. NRPa-308 showed promising result for the treatment of ccRCC. However, further studies on NRPa-308 are still needed to confirm its relevance for ccRCC treatment, such as its *in-vivo* bioavailability and its efficacy on metastatic models. After that, further studies should be carried out by specialized laboratories or societies to determine if NRPa-308 is a “lead” molecule for the treatment of ccRCC.

REFERENCES

REFERENCES

[1] Fondation ARC pour la recherche sur le cancer, B. Escudier, et J.-J. Patard, *Les Cancers du Rein*. .

[2] « Which microscopic pathologic findings are characteristic of clear cell renal cell carcinoma (CCRCC)? » https://www.medscape.com/answers/1612043-178267/which-microscopic-pathologic-findings-are-characteristic-of-clear-cell-renal-cell-carcinoma-ccrcc (consulté le oct. 07, 2020).

[3] S. Chen *et al.*, « GYS1 induces glycogen accumulation and promotes tumor progression via the NF-κB pathway in Clear Cell Renal Carcinoma », *Theranostics*, vol. 10, n° 20, p. 9186-9199, 2020, doi: 10.7150/thno.46825.

[4] A. M. Roberts, I. R. Watson, A. J. Evans, D. A. Foster, M. S. Irwin, et M. Ohh, « SUPPRESSION OF HIF2α RESTORES p53 ACTIVITY VIA HDM2 AND REVERSES CHEMORESISTANCE OF RENAL CARCINOMA CELLS », *Cancer Res.*, vol. 69, n° 23, p. 9056-9064, déc. 2009, doi: 10.1158/0008-5472.CAN-09-1770.

[5] A. Larcher *et al.*, « Individualised Indications for Cytoreductive Nephrectomy: Which Criteria Define the Optimal Candidates? », *Eur. Urol. Oncol.*, vol. 2, n° 4, p. 365-378, 2019, doi: 10.1016/j.euo.2019.04.007.

[6] A. F. Karamysheva, « Mechanisms of angiogenesis », *Biochem. Mosc.*, vol. 73, n° 7, p. 751-762, juill. 2008, doi: 10.1134/S0006297908070031.

[7] C. Viallard et B. Larrivée, « Tumor angiogenesis and vascular normalization: alternative therapeutic targets », *Angiogenesis*, vol. 20, n° 4, p. 409-426, nov. 2017, doi: 10.1007/s10456-017-9562-9.

[8] B. A. Bryan et P. A. D'Amore, « What tangled webs they weave: Rho-GTPase control of angiogenesis », *Cell. Mol. Life Sci.*, vol. 64, n° 16, p. 2053-2065, août 2007, doi: 10.1007/s00018-007-7008-z.

[9] P. Carmeliet et R. K. Jain, « Angiogenesis in cancer and other diseases », *Nature*, vol. 407, n° 6801, p. 249-257, sept. 2000, doi: 10.1038/35025220.

[10] J. Folkman, « Angiogenesis in cancer, vascular, rheumatoid and other disease », *Nat. Med.*, vol. 1, n° 1, p. 27-30, janv. 1995, doi: 10.1038/nm0195-27.

[11] J. Ma, L. Zhang, G.-Q. Ru, Z.-S. Zhao, et W.-J. Xu, « Upregulation of hypoxia inducible factor 1alpha mRNA is associated with elevated vascular endothelial growth factor expression and excessive angiogenesis and predicts a poor prognosis in gastric carcinoma », *World J. Gastroenterol.*, vol. 13, n° 11, p. 1680-1686, mars 2007, doi: 10.3748/wjg.v13.i11.1680.

[12] S. J. Harper et D. O. Bates, « VEGF-A splicing: the key to anti-angiogenic therapeutics? », *Nat. Rev. Cancer*, vol. 8, n° 11, p. 880-887, nov. 2008, doi: 10.1038/nrc2505.

[13] I. Nilsson *et al.*, « VEGF receptor 2/-3 heterodimers detected in situ by proximity ligation on angiogenic sprouts », *EMBO J.*, vol. 29, n° 8, p. 1377-1388, avr. 2010, doi: 10.1038/emboj.2010.30.

[14] S. Zhang, X. Gao, W. Fu, S. Li, et L. Yue, « Immunoglobulin-like domain 4-mediated ligand-independent dimerization triggers VEGFR-2 activation in HUVECs and VEGFR2-positive breast cancer cells », *Breast Cancer Res. Treat.*, vol. 163, n° 3, p. 423-434, juin 2017, doi: 10.1007/s10549-017-4189-5.

[15] R. Roskoski, « Vascular endothelial growth factor (VEGF) and VEGF receptor inhibitors in the treatment of renal cell carcinomas », *Pharmacol. Res.*, vol. 120, p. 116-132, juin 2017, doi: 10.1016/j.phrs.2017.03.010.

[16] A. Shinkai, M. Ito, H. Anazawa, S. Yamaguchi, K. Shitara, et M. Shibuya, « Mapping of the Sites Involved in Ligand Association and Dissociation at the Extracellular Domain of the Kinase Insert Domain-containing Receptor for Vascular Endothelial Growth Factor », *J. Biol. Chem.*, vol. 273, n° 47, p. 31283-31288, nov. 1998, doi: 10.1074/jbc.273.47.31283.

[17] P. S. Sharma et R. S. and T. Tyagi, « VEGF/VEGFR Pathway Inhibitors as Anti-Angiogenic Agents: Present and Future », *Current Cancer Drug Targets*, mai 31, 2011. https://www.eurekaselect.com/74065/article (consulté le août 03, 2020).

[18] M. J. Karkkainen et T. V. Petrova, « Vascular endothelial growth factor receptors in the regulation of angiogenesis and lymphangiogenesis », *Oncogene*, vol. 19, n° 49, p. 5598-5605, nov. 2000, doi: 10.1038/sj.onc.1203855.
[19] K. H. Plate, G. Breier, H. A. Weich, H. D. Mennel, et W. Risau, « Vascular endothelial growth factor and glioma angiogenesis: Coordinate induction of VEGF receptors, distribution of VEGF protein and possible In vivo regulatory mechanisms », *Int. J. Cancer*, vol. 59, n° 4, p. 520-529, 1994, doi: 10.1002/ijc.2910590415.
[20] N. Ferrara, « Vascular endothelial growth factor: basic science and clinical progress », *Endocr. Rev.*, vol. 25, n° 4, p. 581-611, août 2004, doi: 10.1210/er.2003-0027.
[21] R. J. C. Albuquerque *et al.*, « Alternatively spliced VEGF receptor-2 is an essential endogenous inhibitor of lymphatic vessels », *Nat. Med.*, vol. 15, n° 9, p. 1023-1030, sept. 2009, doi: 10.1038/nm.2018.
[22] S. E. DePrimo *et al.*, « Circulating protein biomarkers of pharmacodynamic activity of sunitinib in patients with metastatic renal cell carcinoma: modulation of VEGF and VEGF-related proteins », *J. Transl. Med.*, vol. 5, n° 1, p. 32, déc. 2007, doi: 10.1186/1479-5876-5-32.
[23] D. F. McDermott *et al.*, « Randomized phase III trial of high-dose interleukin-2 versus subcutaneous interleukin-2 and interferon in patients with metastatic renal cell carcinoma », *J. Clin. Oncol. Off. J. Am. Soc. Clin. Oncol.*, vol. 23, n° 1, p. 133-141, janv. 2005, doi: 10.1200/JCO.2005.03.206.
[24] « Drugs@FDA: FDA-Approved Drugs ». https://www.accessdata.fda.gov/scripts/cder/daf/index.cfm (consulté le sept. 22, 2020).
[25] « Medicines », *European Medicines Agency*. https://www.ema.europa.eu/en/medicines (consulté le sept. 22, 2020).
[26] R. J. Motzer *et al.*, « Kidney Cancer, Version 2.2017, NCCN Clinical Practice Guidelines in Oncology », *J. Natl. Compr. Canc. Netw.*, vol. 15, n° 6, p. 804-834, juin 2017, doi: 10.6004/jnccn.2017.0100.
[27] R. J. Motzer *et al.*, « Overall Survival and Updated Results for Sunitinib Compared With Interferon Alfa in Patients With Metastatic Renal Cell Carcinoma », *J. Clin. Oncol.*, vol. 27, n° 22, p. 3584-3590, août 2009, doi: 10.1200/JCO.2008.20.1293.
[28] R. J. Motzer *et al.*, « Pazopanib versus Sunitinib in Metastatic Renal-Cell Carcinoma », *http://dx.doi.org/10.1056/NEJMoa1303989*, août 21, 2013. https://www.nejm.org/doi/10.1056/NEJMoa1303989?url_ver=Z39.88-2003&rfr_id=ori%3Arid%3Acrossref.org&rfr_dat=cr_pub++0pubmed (consulté le août 03, 2020).
[29] B. Escudier *et al.*, « Randomized phase II trial of first-line treatment with sorafenib versus interferon Alfa-2a in patients with metastatic renal cell carcinoma », *J. Clin. Oncol. Off. J. Am. Soc. Clin. Oncol.*, vol. 27, n° 8, p. 1280-1289, mars 2009, doi: 10.1200/JCO.2008.19.3342.
[30] R. J. Motzer *et al.*, « Tivozanib versus sorafenib as initial targeted therapy for patients with metastatic renal cell carcinoma: results from a phase III trial », *J. Clin. Oncol. Off. J. Am. Soc. Clin. Oncol.*, vol. 31, n° 30, p. 3791-3799, oct. 2013, doi: 10.1200/JCO.2012.47.4940.
[31] B. Escudier *et al.*, « Renal cell carcinoma: ESMO Clinical Practice Guidelines for diagnosis, treatment and follow-up† », *Ann. Oncol. Off. J. Eur. Soc. Med. Oncol.*, vol. 30, n° 5, p. 706-720, 01 2019, doi: 10.1093/annonc/mdz056.
[32] G. Hudes *et al.*, « Temsirolimus, interferon alfa, or both for advanced renal-cell carcinoma », *N. Engl. J. Med.*, vol. 356, n° 22, p. 2271-2281, mai 2007, doi: 10.1056/NEJMoa066838.
[33] R. J. Motzer *et al.*, « Nivolumab plus Ipilimumab versus Sunitinib in Advanced Renal-Cell Carcinoma », *N. Engl. J. Med.*, vol. 378, n° 14, p. 1277-1290, avr. 2018, doi: 10.1056/NEJMoa1712126.
[34] B. I. Rini *et al.*, « Pembrolizumab plus Axitinib versus Sunitinib for Advanced Renal-Cell Carcinoma », *N. Engl. J. Med.*, vol. 380, n° 12, p. 1116-1127, 21 2019, doi: 10.1056/NEJMoa1816714.
[35] R. J. Motzer *et al.*, « Avelumab plus Axitinib versus Sunitinib for Advanced Renal-Cell Carcinoma », *N. Engl. J. Med.*, vol. 380, n° 12, p. 1103-1115, 21 2019, doi: 10.1056/NEJMoa1816047.

[36] R. J. Motzer *et al.*, « Axitinib versus sorafenib as second-line treatment for advanced renal cell carcinoma: overall survival analysis and updated results from a randomised phase 3 trial », *Lancet Oncol.*, vol. 14, nº 6, p. 552-562, mai 2013, doi: 10.1016/S1470-2045(13)70093-7.
[37] T. K. Choueiri *et al.*, « Cabozantinib versus everolimus in advanced renal cell carcinoma (METEOR): final results from a randomised, open-label, phase 3 trial », *Lancet Oncol.*, vol. 17, nº 7, p. 917-927, juill. 2016, doi: 10.1016/S1470-2045(16)30107-3.
[38] R. J. Motzer *et al.*, « Efficacy of everolimus in advanced renal cell carcinoma: a double-blind, randomised, placebo-controlled phase III trial », *Lancet Lond. Engl.*, vol. 372, nº 9637, p. 449-456, août 2008, doi: 10.1016/S0140-6736(08)61039-9.
[39] R. J. Motzer *et al.*, « Nivolumab versus Everolimus in Advanced Renal-Cell Carcinoma », *N. Engl. J. Med.*, vol. 373, nº 19, p. 1803-1813, nov. 2015, doi: 10.1056/NEJMoa1510665.
[40] J. C. Wells *et al.*, « Third-line Targeted Therapy in Metastatic Renal Cell Carcinoma: Results from the International Metastatic Renal Cell Carcinoma Database Consortium », *Eur. Urol.*, vol. 71, nº 2, p. 204-209, 2017, doi: 10.1016/j.eururo.2016.05.049.
[41] J. J. Ko *et al.*, « First-, second-, third-line therapy for mRCC: benchmarks for trial design from the IMDC », *Br. J. Cancer*, vol. 110, nº 8, p. 1917-1922, avr. 2014, doi: 10.1038/bjc.2014.25.
[42] B. Escudier, F. Worden, et M. Kudo, « Sorafenib: key lessons from over 10 years of experience », *Expert Rev. Anticancer Ther.*, vol. 19, nº 2, p. 177-189, 2019, doi: 10.1080/14737140.2019.1559058.
[43] M. Retz *et al.*, « SWITCH II: Phase III randomized, sequential, open-label study to evaluate the efficacy and safety of sorafenib-pazopanib versus pazopanib-sorafenib in the treatment of advanced or metastatic renal cell carcinoma (AUO AN 33/11) », *Eur. J. Cancer Oxf. Engl. 1990*, vol. 107, p. 37-45, 2019, doi: 10.1016/j.ejca.2018.11.001.
[44] E. Calvo, C. Porta, V. Grünwald, et B. Escudier, « The Current and Evolving Landscape of First-Line Treatments for Advanced Renal Cell Carcinoma », *The Oncologist*, vol. 24, nº 3, p. 338-348, 2019, doi: 10.1634/theoncologist.2018-0267.
[45] M. E. Gore *et al.*, « Final results from the large sunitinib global expanded-access trial in metastatic renal cell carcinoma », *Br. J. Cancer*, vol. 113, nº 1, p. 12-19, juin 2015, doi: 10.1038/bjc.2015.196.
[46] S. Buti, A. Leonetti, A. Dallatomasina, et M. Bersanelli, « Everolimus in the management of metastatic renal cell carcinoma: an evidence-based review of its place in therapy », *Core Evid.*, vol. 11, p. 23-36, sept. 2016, doi: 10.2147/CE.S98687.
[47] B. I. Rini *et al.*, « Atezolizumab plus bevacizumab versus sunitinib in patients with previously untreated metastatic renal cell carcinoma (IMmotion151): a multicentre, open-label, phase 3, randomised controlled trial », *Lancet Lond. Engl.*, vol. 393, nº 10189, p. 2404-2415, 15 2019, doi: 10.1016/S0140-6736(19)30723-8.
[48] J. C. Angulo et O. Shapiro, « The Changing Therapeutic Landscape of Metastatic Renal Cancer », *Cancers*, vol. 11, nº 9, août 2019, doi: 10.3390/cancers11091227.
[49] J. J. Schoon, S. L. Wood, et J. E. Brown, « Chapter 39 - TKIs in Renal Cell Carcinoma: What Can We Expect in the Future? », in *Oncogenomics*, F. Dammacco et F. Silvestris, Éd. Academic Press, 2019, p. 551-563.
[50] R. J. Motzer *et al.*, « Lenvatinib, everolimus, and the combination in patients with metastatic renal cell carcinoma: a randomised, phase 2, open-label, multicentre trial », *Lancet Oncol.*, vol. 16, nº 15, p. 1473-1482, nov. 2015, doi: 10.1016/S1470-2045(15)00290-9.
[51] T. K. Choueiri *et al.*, « Cabozantinib Versus Sunitinib As Initial Targeted Therapy for Patients With Metastatic Renal Cell Carcinoma of Poor or Intermediate Risk: The Alliance A031203 CABOSUN Trial », *J. Clin. Oncol. Off. J. Am. Soc. Clin. Oncol.*, vol. 35, nº 6, p. 591-597, 20 2017, doi: 10.1200/JCO.2016.70.7398.
[52] L. Chen *et al.*, « Overexpression of HHLA2 in human clear cell renal cell carcinoma is significantly associated with poor survival of the patients », *Cancer Cell Int.*, vol. 19, avr. 2019, doi: 10.1186/s12935-019-0813-2.

[53] V. Grünwald *et al.*, « Lenvatinib plus everolimus or pembrolizumab versus sunitinib in advanced renal cell carcinoma: study design and rationale », *Future Oncol. Lond. Engl.*, vol. 15, n° 9, p. 929-941, mars 2019, doi: 10.2217/fon-2018-0745.
[54] S. Giuliano et G. Pagès, « Mechanisms of resistance to anti-angiogenesis therapies », *Biochimie*, vol. 95, n° 6, p. 1110-1119, juin 2013, doi: 10.1016/j.biochi.2013.03.002.
[55] C. Montemagno et G. Pagès, « Resistance to Anti-angiogenic Therapies: A Mechanism Depending on the Time of Exposure to the Drugs », *Front. Cell Dev. Biol.*, vol. 8, juill. 2020, doi: 10.3389/fcell.2020.00584.
[56] M. Guyot *et al.*, « Targeting the pro-angiogenic forms of VEGF or inhibiting their expression as anti-cancer strategies », *Oncotarget*, vol. 8, n° 6, p. 9174-9188, févr. 2017, doi: 10.18632/oncotarget.13942.
[57] D. O. Bates *et al.*, « Association between VEGF splice isoforms and progression free survival in metastatic colorectal cancer patients treated with bevacizumab », *Clin. Cancer Res. Off. J. Am. Assoc. Cancer Res.*, vol. 18, n° 22, p. 6384-6391, nov. 2012, doi: 10.1158/1078-0432.CCR-12-2223.
[58] P. Makhov, S. Joshi, P. Ghatalia, A. Kutikov, R. G. Uzzo, et V. M. Kolenko, « Resistance to Systemic Therapies in Clear Cell Renal Cell Carcinoma: Mechanisms and Management Strategies », *Mol. Cancer Ther.*, vol. 17, n° 7, p. 1355-1364, 2018, doi: 10.1158/1535-7163.MCT-17-1299.
[59] D. Huang *et al.*, « Interleukin-8 Mediates Resistance to Antiangiogenic Agent Sunitinib in Renal Cell Carcinoma », *Cancer Res.*, vol. 70, n° 3, p. 1063-1071, févr. 2010, doi: 10.1158/0008-5472.CAN-09-3965.
[60] O. Cuvillier, « The therapeutic potential of HIF-2 antagonism in renal cell carcinoma », *Transl. Androl. Urol.*, vol. 6, n° 1, p. 131-133, févr. 2017, doi: 10.21037/tau.2017.01.12.
[61] W. Chen *et al.*, « Targeting renal cell carcinoma with a HIF-2 antagonist », *Nature*, vol. 539, n° 7627, p. 112-117, 03 2016, doi: 10.1038/nature19796.
[62] A. Kuşoğlu et Ç. Biray Avcı, « Cancer stem cells: A brief review of the current status », *Gene*, vol. 681, p. 80-85, janv. 2019, doi: 10.1016/j.gene.2018.09.052.
[63] C. Saygin, D. Matei, R. Majeti, O. Reizes, et J. D. Lathia, « Targeting Cancer Stemness in the Clinic: From Hype to Hope », *Cell Stem Cell*, vol. 24, n° 1, p. 25-40, 03 2019, doi: 10.1016/j.stem.2018.11.017.
[64] S. Giuliano *et al.*, « Resistance to sunitinib in renal clear cell carcinoma results from sequestration in lysosomes and inhibition of the autophagic flux », *Autophagy*, vol. 11, n° 10, p. 1891-1904, 2015, doi: 10.1080/15548627.2015.1085742.
[65] S. Giuliano *et al.*, « Resistance to lysosomotropic drugs used to treat kidney and breast cancers involves autophagy and inflammation and converges in inducing CXCL5 », *Theranostics*, vol. 9, n° 4, p. 1181-1199, 2019, doi: 10.7150/thno.29093.
[66] M. Dufies *et al.*, « Sunitinib Stimulates Expression of VEGFC by Tumor Cells and Promotes Lymphangiogenesis in Clear Cell Renal Cell Carcinomas », *Cancer Res.*, vol. 77, n° 5, p. 1212-1226, 01 2017, doi: 10.1158/0008-5472.CAN-16-3088.
[67] B. Lévy, « Lymphangiogenesis. Physiological bases and physiopathological approaches », *Innov. Thérapeutiques En Oncol.*, vol. 2, n° 5, p. 245-250, sept. 2016, doi: 10.1684/ito.2016.0061.
[68] A. Alitalo et M. Detmar, « Interaction of tumor cells and lymphatic vessels in cancer progression », *Oncogene*, vol. 31, n° 42, p. 4499-4508, oct. 2012, doi: 10.1038/onc.2011.602.
[69] P. D. Ndiaye *et al.*, « VEGFC acts as a double-edged sword in renal cell carcinoma aggressiveness », *Theranostics*, vol. 9, n° 3, p. 661-675, 2019, doi: 10.7150/thno.27794.
[70] S. Karaman et M. Detmar, « Mechanisms of lymphatic metastasis », *J. Clin. Invest.*, vol. 124, n° 3, p. 922-928, mars 2014, doi: 10.1172/JCI71606.
[71] A. Álvarez-Aznar, L. Muhl, et K. Gaengel, « VEGF Receptor Tyrosine Kinases: Key Regulators of Vascular Function », *Curr. Top. Dev. Biol.*, vol. 123, p. 433-482, 2017, doi: 10.1016/bs.ctdb.2016.10.001.
[72] T. Kawasaki *et al.*, « A requirement for neuropilin-1 in embryonic vessel formation », *Dev. Camb. Engl.*, vol. 126, n° 21, p. 4895-4902, nov. 1999.

[73] T. Kitsukawa, A. Shimono, A. Kawakami, H. Kondoh, et H. Fujisawa, « Overexpression of a membrane protein, neuropilin, in chimeric mice causes anomalies in the cardiovascular system, nervous system and limbs », *Dev. Camb. Engl.*, vol. 121, nº 12, p. 4309-4318, déc. 1995.
[74] L. Yuan *et al.*, « Abnormal lymphatic vessel development in neuropilin 2 mutant mice », *Dev. Camb. Engl.*, vol. 129, nº 20, p. 4797-4806, oct. 2002.
[75] S. Takashima *et al.*, « Targeting of both mouse neuropilin-1 and neuropilin-2 genes severely impairs developmental yolk sac and embryonic angiogenesis », *Proc. Natl. Acad. Sci. U. S. A.*, vol. 99, nº 6, p. 3657-3662, mars 2002, doi: 10.1073/pnas.022017899.
[76] S. Niland et J. A. Eble, « Neuropilins in the Context of Tumor Vasculature », *Int. J. Mol. Sci.*, vol. 20, nº 3, févr. 2019, doi: 10.3390/ijms20030639.
[77] S. Roy, A. K. Bag, R. K. Singh, J. E. Talmadge, S. K. Batra, et K. Datta, « Multifaceted Role of Neuropilins in the Immune System: Potential Targets for Immunotherapy », *Front. Immunol.*, vol. 8, p. 1228, 2017, doi: 10.3389/fimmu.2017.01228.
[78] S. Chauvet *et al.*, « Gating of Sema3E/PlexinD1 signaling by neuropilin-1 switches axonal repulsion to attraction during brain development », *Neuron*, vol. 56, nº 5, p. 807-822, déc. 2007, doi: 10.1016/j.neuron.2007.10.019.
[79] A. Daoust *et al.*, « Neuronal transport defects of the MAP6 KO mouse - a model of schizophrenia - and alleviation by Epothilone D treatment, as observed using MEMRI », *NeuroImage*, vol. 96, p. 133-142, août 2014, doi: 10.1016/j.neuroimage.2014.03.071.
[80] M. Migdal *et al.*, « Neuropilin-1 is a placenta growth factor-2 receptor », *J. Biol. Chem.*, vol. 273, nº 35, p. 22272-22278, août 1998, doi: 10.1074/jbc.273.35.22272.
[81] A. Escudero-Esparza, T. A. Martin, A. Douglas-Jones, R. E. Mansel, et W. G. Jiang, « PGF isoforms, PLGF-1 and PGF-2 and the PGF receptor, neuropilin, in human breast cancer: prognostic significance », *Oncol. Rep.*, vol. 23, nº 2, p. 537-544, févr. 2010.
[82] E. Pagani *et al.*, « Placenta growth factor and neuropilin-1 collaborate in promoting melanoma aggressiveness », *Int. J. Oncol.*, vol. 48, nº 4, p. 1581-1589, avr. 2016, doi: 10.3892/ijo.2016.3362.
[83] T. Van Bergen *et al.*, « The role of placental growth factor (PlGF) and its receptor system in retinal vascular diseases », *Prog. Retin. Eye Res.*, vol. 69, p. 116-136, 2019, doi: 10.1016/j.preteyeres.2018.10.006.
[84] M. Snuderl *et al.*, « Targeting placental growth factor/neuropilin 1 pathway inhibits growth and spread of medulloblastoma », *Cell*, vol. 152, nº 5, p. 1065-1076, févr. 2013, doi: 10.1016/j.cell.2013.01.036.
[85] M. Balan *et al.*, « Novel roles of c-Met in the survival of renal cancer cells through the regulation of HO-1 and PD-L1 expression », *J. Biol. Chem.*, vol. 290, nº 13, p. 8110-8120, mars 2015, doi: 10.1074/jbc.M114.612689.
[86] B. Chaudhary, Y. S. Khaled, B. J. Ammori, et E. Elkord, « Neuropilin 1: function and therapeutic potential in cancer », *Cancer Immunol. Immunother. CII*, vol. 63, nº 2, p. 81-99, févr. 2014, doi: 10.1007/s00262-013-1500-0.
[87] S. H. Hsieh *et al.*, « Galectin-1, a novel ligand of neuropilin-1, activates VEGFR-2 signaling and modulates the migration of vascular endothelial cells », *Oncogene*, vol. 27, nº 26, p. 3746-3753, juin 2008, doi: 10.1038/sj.onc.1211029.
[88] M.-H. Wu, N.-W. Ying, T.-M. Hong, W.-F. Chiang, Y.-T. Lin, et Y.-L. Chen, « Galectin-1 induces vascular permeability through the neuropilin-1/vascular endothelial growth factor receptor-1 complex », *Angiogenesis*, vol. 17, nº 4, p. 839-849, oct. 2014, doi: 10.1007/s10456-014-9431-8.
[89] S. Rizzolio *et al.*, « Neuropilin-1-dependent regulation of EGF-receptor signaling », *Cancer Res.*, vol. 72, nº 22, p. 5801-5811, nov. 2012, doi: 10.1158/0008-5472.CAN-12-0995.
[90] S. Dutta *et al.*, « Neuropilin-2 Regulates Endosome Maturation and EGFR Trafficking to Support Cancer Cell Pathobiology », *Cancer Res.*, vol. 76, nº 2, p. 418-428, janv. 2016, doi: 10.1158/0008-5472.CAN-15-1488.
[91] Y. Cao *et al.*, « Neuropilin-1 upholds dedifferentiation and propagation phenotypes of renal cell carcinoma cells by activating Akt and sonic hedgehog axes », *Cancer Res.*, vol. 68, nº 21, p. 8667-8672, nov. 2008, doi: 10.1158/0008-5472.CAN-08-2614.

[92] Y. Cao *et al.*, « Neuropilin-2 promotes extravasation and metastasis by interacting with endothelial α5 integrin », *Cancer Res.*, vol. 73, n° 14, p. 4579-4590, juill. 2013, doi: 10.1158/0008-5472.CAN-13-0529.
[93] « GEPIA (Gene Expression Profiling Interactive Analysis) ». http://gepia.cancer-pku.cn/ (consulté le sept. 23, 2020).
[94] M. Sarris, K. G. Andersen, F. Randow, L. Mayr, et A. G. Betz, « Neuropilin-1 expression on regulatory T cells enhances their interactions with dendritic cells during antigen recognition », *Immunity*, vol. 28, n° 3, p. 402-413, mars 2008, doi: 10.1016/j.immuni.2008.01.012.
[95] B. Akkaya *et al.*, « Regulatory T cells mediate specific suppression by depleting peptide-MHC class II from dendritic cells », *Nat. Immunol.*, vol. 20, n° 2, p. 218-231, 2019, doi: 10.1038/s41590-018-0280-2.
[96] Y. Lepelletier *et al.*, « Immunosuppressive role of semaphorin-3A on T cell proliferation is mediated by inhibition of actin cytoskeleton reorganization », *Eur. J. Immunol.*, vol. 36, n° 7, p. 1782-1793, juill. 2006, doi: 10.1002/eji.200535601.
[97] S. Schellenburg, A. Schulz, D. M. Poitz, et M. H. Muders, « Role of neuropilin-2 in the immune system », *Mol. Immunol.*, vol. 90, p. 239-244, 2017, doi: 10.1016/j.molimm.2017.08.010.
[98] S. Curreli, Z. Arany, R. Gerardy-Schahn, D. Mann, et N. M. Stamatos, « Polysialylated neuropilin-2 is expressed on the surface of human dendritic cells and modulates dendritic cell-T lymphocyte interactions », *J. Biol. Chem.*, vol. 282, n° 42, p. 30346-30356, oct. 2007, doi: 10.1074/jbc.M702965200.
[99] A. Rey-Gallardo, C. Delgado-Martín, R. Gerardy-Schahn, J. L. Rodríguez-Fernández, et M. A. Vega, « Polysialic acid is required for neuropilin-2a/b-mediated control of CCL21-driven chemotaxis of mature dendritic cells and for their migration in vivo », *Glycobiology*, vol. 21, n° 5, p. 655-662, mai 2011, doi: 10.1093/glycob/cwq216.
[100] A. Casazza *et al.*, « Impeding macrophage entry into hypoxic tumor areas by Sema3A/Nrp1 signaling blockade inhibits angiogenesis and restores antitumor immunity », *Cancer Cell*, vol. 24, n° 6, p. 695-709, déc. 2013, doi: 10.1016/j.ccr.2013.11.007.
[101] X.-J. Chen *et al.*, « The role of the hypoxia-Nrp-1 axis in the activation of M2-like tumor-associated macrophages in the tumor microenvironment of cervical cancer », *Mol. Carcinog.*, vol. 58, n° 3, p. 388-397, 2019, doi: 10.1002/mc.22936.
[102] J. D. Cherry, J. A. Olschowka, et M. K. O'Banion, « Neuroinflammation and M2 microglia: the good, the bad, and the inflamed », *J. Neuroinflammation*, vol. 11, p. 98, juin 2014, doi: 10.1186/1742-2094-11-98.
[103] M. D. Caponegro, R. A. Moffitt, et S. E. Tsirka, « Expression of neuropilin-1 is linked to glioma associated microglia and macrophages and correlates with unfavorable prognosis in high grade gliomas », *Oncotarget*, vol. 9, n° 86, p. 35655-35665, nov. 2018, doi: 10.18632/oncotarget.26273.
[104] N. M. Stamatos *et al.*, « Changes in polysialic acid expression on myeloid cells during differentiation and recruitment to sites of inflammation: role in phagocytosis », *Glycobiology*, vol. 24, n° 9, p. 864-879, sept. 2014, doi: 10.1093/glycob/cwu050.
[105] S. Roy *et al.*, « Macrophage-Derived Neuropilin-2 Exhibits Novel Tumor-Promoting Functions », *Cancer Res.*, vol. 78, n° 19, p. 5600-5617, 01 2018, doi: 10.1158/0008-5472.CAN-18-0562.
[106] M. Leclerc *et al.*, « Regulation of antitumour CD8 T-cell immunity and checkpoint blockade immunotherapy by Neuropilin-1 », *Nat. Commun.*, vol. 10, n° 1, p. 3345, 26 2019, doi: 10.1038/s41467-019-11280-z.
[107] S. Sakaguchi, N. Sakaguchi, M. Asano, M. Itoh, et M. Toda, « Immunologic self-tolerance maintained by activated T cells expressing IL-2 receptor alpha-chains (CD25). Breakdown of a single mechanism of self-tolerance causes various autoimmune diseases », *J. Immunol. Baltim. Md 1950*, vol. 155, n° 3, p. 1151-1164, août 1995.
[108] W. Hansen *et al.*, « Neuropilin 1 deficiency on CD4+Foxp3+ regulatory T cells impairs mouse melanoma growth », *J. Exp. Med.*, vol. 209, n° 11, p. 2001-2016, oct. 2012, doi: 10.1084/jem.20111497.

[109] L. M. Ellis, « The role of neuropilins in cancer », *Mol. Cancer Ther.*, vol. 5, nº 5, p. 1099-1107, mai 2006, doi: 10.1158/1535-7163.MCT-05-0538.
[110] E. Morin *et al.*, « VEGF receptor-2/neuropilin 1 trans-complex formation between endothelial and tumor cells is an independent predictor of pancreatic cancer survival », *J. Pathol.*, vol. 246, nº 3, p. 311-322, 2018, doi: 10.1002/path.5141.
[111] S. Rizzolio et L. Tamagnone, « Multifaceted role of neuropilins in cancer », *Curr. Med. Chem.*, vol. 18, nº 23, p. 3563-3575, 2011, doi: 10.2174/092986711796642544.
[112] Y. Mumblat, O. Kessler, N. Ilan, et G. Neufeld, « Full-Length Semaphorin-3C Is an Inhibitor of Tumor Lymphangiogenesis and Metastasis », *Cancer Res.*, vol. 75, nº 11, p. 2177-2186, juin 2015, doi: 10.1158/0008-5472.CAN-14-2464.
[113] S. Niland et J. A. Eble, « Neuropilin: Handyman and Power Broker in the Tumor Microenvironment », *Adv. Exp. Med. Biol.*, vol. 1223, p. 31-67, 2020, doi: 10.1007/978-3-030-35582-1_3.
[114] B. Palodetto *et al.*, « SEMA3A partially reverses VEGF effects through binding to neuropilin-1 », *Stem Cell Res.*, vol. 22, p. 70-78, 2017, doi: 10.1016/j.scr.2017.05.012.
[115] M. J. Gray *et al.*, « Therapeutic targeting of neuropilin-2 on colorectal carcinoma cells implanted in the murine liver », *J. Natl. Cancer Inst.*, vol. 100, nº 2, p. 109-120, janv. 2008, doi: 10.1093/jnci/djm279.
[116] S. Zhang *et al.*, « Vascular endothelial growth factor regulates myeloid cell leukemia-1 expression through neuropilin-1-dependent activation of c-MET signaling in human prostate cancer cells », *Mol. Cancer*, vol. 9, p. 9, janv. 2010, doi: 10.1186/1476-4598-9-9.
[117] T.-M. Hong *et al.*, « Targeting neuropilin 1 as an antitumor strategy in lung cancer », *Clin. Cancer Res. Off. J. Am. Assoc. Cancer Res.*, vol. 13, nº 16, p. 4759-4768, août 2007, doi: 10.1158/1078-0432.CCR-07-0001.
[118] L. Zhang *et al.*, « VEGF-A/Neuropilin 1 Pathway Confers Cancer Stemness via Activating Wnt/β-Catenin Axis in Breast Cancer Cells », *Cell. Physiol. Biochem. Int. J. Exp. Cell. Physiol. Biochem. Pharmacol.*, vol. 44, nº 3, p. 1251-1262, 2017, doi: 10.1159/000485455.
[119] P. Hamerlik *et al.*, « Autocrine VEGF-VEGFR2-Neuropilin-1 signaling promotes glioma stem-like cell viability and tumor growth », *J. Exp. Med.*, vol. 209, nº 3, p. 507-520, mars 2012, doi: 10.1084/jem.20111424.
[120] C. Gong *et al.*, « Stimulation of medulloblastoma stem cells differentiation by a peptidomimetic targeting neuropilin-1 », *Oncotarget*, vol. 9, nº 20, p. 15312-15325, mars 2018, doi: 10.18632/oncotarget.24521.
[121] C.-A. Wang, J. C. Harrell, R. Iwanaga, P. Jedlicka, et H. L. Ford, « Vascular endothelial growth factor C promotes breast cancer progression via a novel antioxidant mechanism that involves regulation of superoxide dismutase 3 », *Breast Cancer Res. BCR*, vol. 16, nº 5, p. 462, oct. 2014, doi: 10.1186/s13058-014-0462-2.
[122] A. L. Elaimy et A. M. Mercurio, « Convergence of VEGF and YAP/TAZ signaling: Implications for angiogenesis and cancer biology », *Sci. Signal.*, vol. 11, nº 552, 16 2018, doi: 10.1126/scisignal.aau1165.
[123] H. L. Goel *et al.*, « GLI1 regulates a novel neuropilin-2/α6β1 integrin based autocrine pathway that contributes to breast cancer initiation », *EMBO Mol. Med.*, vol. 5, nº 4, p. 488-508, avr. 2013, doi: 10.1002/emmm.201202078.
[124] U. Yaqoob *et al.*, « Neuropilin-1 stimulates tumor growth by increasing fibronectin fibril assembly in the tumor microenvironment », *Cancer Res.*, vol. 72, nº 16, p. 4047-4059, août 2012, doi: 10.1158/0008-5472.CAN-11-3907.
[125] P. N. Matkar *et al.*, « Novel regulatory role of neuropilin-1 in endothelial-to-mesenchymal transition and fibrosis in pancreatic ductal adenocarcinoma », *Oncotarget*, vol. 7, nº 43, p. 69489-69506, oct. 2016, doi: 10.18632/oncotarget.11060.
[126] T. Shan *et al.*, « Prometastatic mechanisms of CAF-mediated EMT regulation in pancreatic cancer cells », *Int. J. Oncol.*, vol. 50, nº 1, p. 121-128, janv. 2017, doi: 10.3892/ijo.2016.3779.

[127] W. Cheng *et al.*, « NRP-1 expression in bladder cancer and its implications for tumor progression », *Tumour Biol. J. Int. Soc. Oncodevelopmental Biol. Med.*, vol. 35, n° 6, p. 6089-6094, juin 2014, doi: 10.1007/s13277-014-1806-3.
[128] H. Zhu, H. Cai, M. Tang, et J. Tang, « Neuropilin-1 is overexpressed in osteosarcoma and contributes to tumor progression and poor prognosis », *Clin. Transl. Oncol. Off. Publ. Fed. Span. Oncol. Soc. Natl. Cancer Inst. Mex.*, vol. 16, n° 8, p. 732-738, août 2014, doi: 10.1007/s12094-013-1141-y.
[129] D. Yin *et al.*, « Clinical significance of neuropilin-2 expression in laryngeal squamous cell carcinoma », *Am. J. Otolaryngol.*, vol. 41, n° 4, p. 102540, août 2020, doi: 10.1016/j.amjoto.2020.102540.
[130] A. Borkowetz *et al.*, « Neuropilin-2 is an independent prognostic factor for shorter cancer-specific survival in patients with acinar adenocarcinoma of the prostate », *Int. J. Cancer*, vol. 146, n° 9, p. 2619-2627, 01 2020, doi: 10.1002/ijc.32679.
[131] C. Hu, P. Zhu, Y. Xia, K. Hui, M. Wang, et X. Jiang, « Role of the NRP-1-mediated VEGFR2-independent pathway on radiation sensitivity of non-small cell lung cancer cells », *J. Cancer Res. Clin. Oncol.*, vol. 144, n° 7, p. 1329-1337, juill. 2018, doi: 10.1007/s00432-018-2667-8.
[132] J. S. Wey *et al.*, « Overexpression of neuropilin-1 promotes constitutive MAPK signalling and chemoresistance in pancreatic cancer cells », *Br. J. Cancer*, vol. 93, n° 2, p. 233-241, juill. 2005, doi: 10.1038/sj.bjc.6602663.
[133] M. J. Stanton *et al.*, « Autophagy control by the VEGF-C/NRP-2 axis in cancer and its implication for treatment resistance », *Cancer Res.*, vol. 73, n° 1, p. 160-171, janv. 2013, doi: 10.1158/0008-5472.CAN-11-3635.
[134] C. Zheng *et al.*, « Semaphorin3F down-regulates the expression of integrin alpha(v)beta3 and sensitizes multicellular tumor spheroids to chemotherapy via the neuropilin-2 receptor in vitro », *Chemotherapy*, vol. 55, n° 5, p. 344-352, 2009, doi: 10.1159/000232449.
[135] S. Rizzolio *et al.*, « Neuropilin-1 upregulation elicits adaptive resistance to oncogene-targeted therapies », *J. Clin. Invest.*, vol. 128, n° 9, p. 3976-3990, 31 2018, doi: 10.1172/JCI99257.
[136] S. Rizzolio *et al.*, « Downregulating Neuropilin-2 Triggers a Novel Mechanism Enabling EGFR-Dependent Resistance to Oncogene-Targeted Therapies », *Cancer Res.*, vol. 78, n° 4, p. 1058-1068, 15 2018, doi: 10.1158/0008-5472.CAN-17-2020.
[137] E. Van Cutsem *et al.*, « Bevacizumab in combination with chemotherapy as first-line therapy in advanced gastric cancer: a biomarker evaluation from the AVAGAST randomized phase III trial », *J. Clin. Oncol. Off. J. Am. Soc. Clin. Oncol.*, vol. 30, n° 17, p. 2119-2127, juin 2012, doi: 10.1200/JCO.2011.39.9824.
[138] V. Napolitano et L. Tamagnone, « Neuropilins Controlling Cancer Therapy Responsiveness », *Int. J. Mol. Sci.*, vol. 20, n° 8, avr. 2019, doi: 10.3390/ijms20082049.
[139] W.-C. Liang *et al.*, « Function blocking antibodies to neuropilin-1 generated from a designed human synthetic antibody phage library », *J. Mol. Biol.*, vol. 366, n° 3, p. 815-829, févr. 2007, doi: 10.1016/j.jmb.2006.11.021.
[140] C. D. Weekes *et al.*, « A phase I study of the human monoclonal anti-NRP1 antibody MNRP1685A in patients with advanced solid tumors », *Invest. New Drugs*, vol. 32, n° 4, p. 653-660, août 2014, doi: 10.1007/s10637-014-0071-z.
[141] A. Patnaik *et al.*, « A Phase Ib study evaluating MNRP1685A, a fully human anti-NRP1 monoclonal antibody, in combination with bevacizumab and paclitaxel in patients with advanced solid tumors », *Cancer Chemother. Pharmacol.*, vol. 73, n° 5, p. 951-960, mai 2014, doi: 10.1007/s00280-014-2426-8.
[142] B. A. Appleton *et al.*, « Structural studies of neuropilin/antibody complexes provide insights into semaphorin and VEGF binding », *EMBO J.*, vol. 26, n° 23, p. 4902-4912, nov. 2007, doi: 10.1038/sj.emboj.7601906.
[143] A. Starzec *et al.*, « Antiangiogenic and antitumor activities of peptide inhibiting the vascular endothelial growth factor binding to neuropilin-1 », *Life Sci.*, vol. 79, n° 25, p. 2370-2381, nov. 2006, doi: 10.1016/j.lfs.2006.08.005.

[144] L. Tirand *et al.*, « A peptide competing with VEGF165 binding on neuropilin-1 mediates targeting of a chlorin-type photosensitizer and potentiates its photodynamic activity in human endothelial cells », *J. Control. Release Off. J. Control. Release Soc.*, vol. 111, nº 1-2, p. 153-164, mars 2006, doi: 10.1016/j.jconrel.2005.11.017.
[145] H. Benachour *et al.*, « Multifunctional Peptide-conjugated hybrid silica nanoparticles for photodynamic therapy and MRI », *Theranostics*, vol. 2, nº 9, p. 889-904, 2012, doi: 10.7150/thno.4754.
[146] M. Richard *et al.*, « Carbohydrate-based peptidomimetics targeting neuropilin-1: Synthesis, molecular docking study and in vitro biological activities », *Bioorg. Med. Chem.*, vol. 24, nº 21, p. 5315-5325, 01 2016, doi: 10.1016/j.bmc.2016.08.052.
[147] A. K. Puszko *et al.*, « Neuropilin-1 peptide-like ligands with proline mimetics, tested using the improved chemiluminescence affinity detection method », *MedChemComm*, vol. 10, nº 2, p. 332-340, févr. 2019, doi: 10.1039/c8md00537k.
[148] H. Jia *et al.*, « Characterization of a bicyclic peptide neuropilin-1 (NP-1) antagonist (EG3287) reveals importance of vascular endothelial growth factor exon 8 for NP-1 binding and role of NP-1 in KDR signaling », *J. Biol. Chem.*, vol. 281, nº 19, p. 13493-13502, mai 2006, doi: 10.1074/jbc.M512121200.
[149] A. Jarvis *et al.*, « Small molecule inhibitors of the neuropilin-1 vascular endothelial growth factor A (VEGF-A) interaction », *J. Med. Chem.*, vol. 53, nº 5, p. 2215-2226, mars 2010, doi: 10.1021/jm901755g.
[150] J. Powell *et al.*, « Small Molecule Neuropilin-1 Antagonists Combine Antiangiogenic and Antitumor Activity with Immune Modulation through Reduction of Transforming Growth Factor Beta (TGFβ) Production in Regulatory T-Cells », *J. Med. Chem.*, vol. 61, nº 9, p. 4135-4154, 10 2018, doi: 10.1021/acs.jmedchem.8b00210.
[151] A. Starzec, M. A. Miteva, P. Ladam, B. O. Villoutreix, et G. Y. Perret, « Discovery of novel inhibitors of vascular endothelial growth factor-A-Neuropilin-1 interaction by structure-based virtual screening », *Bioorg. Med. Chem.*, vol. 22, nº 15, p. 4042-4048, août 2014, doi: 10.1016/j.bmc.2014.05.068.
[152] « ChemBridge | About Us | Company Overview ». https://www.chembridge.com/about/ (consulté le sept. 23, 2020).
[153] W.-Q. Liu *et al.*, « Synthesis and structure-activity relationship of non-peptidic antagonists of neuropilin-1 receptor », *Bioorg. Med. Chem. Lett.*, vol. 24, nº 17, p. 4254-4259, sept. 2014, doi: 10.1016/j.bmcl.2014.07.028.
[154] W.-Q. Liu *et al.*, « NRPa-308, a new neuropilin-1 antagonist, exerts in vitro anti-angiogenic and anti-proliferative effects and in vivo anti-cancer effects in a mouse xenograft model », *Cancer Lett.*, vol. 414, p. 88-98, 01 2018, doi: 10.1016/j.canlet.2017.10.039.
[155] E. Brachet *et al.*, « Synthesis, 3D-structure and stability analyses of NRPa-308, a new promising anti-cancer agent », *Bioorg. Med. Chem. Lett.*, vol. 29, nº 24, p. 126710, 15 2019, doi: 10.1016/j.bmcl.2019.126710.
[156] A. Dumond et G. Pagès, « Neuropilins, as Relevant Oncology Target: Their Role in the Tumoral Microenvironment », *Front. Cell Dev. Biol.*, vol. 8, p. 662, 2020, doi: 10.3389/fcell.2020.00662.
[157] A. Dumond, L. Demange, et G. Pagès, « Les neuropilines - Des cibles pertinentes pour améliorer le traitement des cancers », *médecine/sciences*, vol. 36, nº 5, Art. nº 5, mai 2020, doi: 10.1051/medsci/2020080.
[158] L. M. Ellis, « The role of neuropilins in cancer », *Mol. Cancer Ther.*, vol. 5, nº 5, p. 1099-1107, mai 2006, doi: 10.1158/1535-7163.MCT-05-0538.
[159] D. Hanahan et R. A. Weinberg, « The Hallmarks of Cancer », *Cell*, vol. 100, nº 1, p. 57-70, janv. 2000, doi: 10.1016/S0092-8674(00)81683-9.
[160] D. Hanahan et R. A. Weinberg, « Hallmarks of Cancer: The Next Generation », *Cell*, vol. 144, nº 5, p. 646-674, mars 2011, doi: 10.1016/j.cell.2011.02.013.
[161] L. S. Cooley *et al.*, « A multi-layered systems approach for renal cell carcinoma », Cancer Biology, preprint, janv. 2020. doi: 10.1101/2020.01.13.904235.

[162] T. Murayama et N. Gotoh, « Patient-Derived Xenograft Models of Breast Cancer and Their Application », *Cells*, vol. 8, n° 6, juin 2019, doi: 10.3390/cells8060621.
[163] A. Patel, S. Cohen, R. Moret, G. Maresh, G. C. Gobe, et L. Li, « Patient-derived xenograft models to optimize kidney cancer therapies », *Transl. Androl. Urol.*, vol. 8, n° Suppl 2, p. S156-S165, mai 2019, doi: 10.21037/tau.2018.11.04.
[164] C. J. Veinotte, G. Dellaire, et J. N. Berman, « Hooking the big one: the potential of zebrafish xenotransplantation to reform cancer drug screening in the genomic era », p. 10, 2014.
[165] Z. I. Stryker, M. Rajabi, P. J. Davis, et S. A. Mousa, « Evaluation of Angiogenesis Assays », *Biomedicines*, vol. 7, n° 2, mai 2019, doi: 10.3390/biomedicines7020037.
[166] N. A. Lokman, A. S. F. Elder, C. Ricciardelli, et M. K. Oehler, « Chick Chorioallantoic Membrane (CAM) Assay as an In Vivo Model to Study the Effect of Newly Identified Molecules on Ovarian Cancer Invasion and Metastasis », *Int. J. Mol. Sci.*, vol. 13, n° 8, p. 9959-9970, août 2012, doi: 10.3390/ijms13089959.

APPENDICES

Appendix 1. ccRCC treatments' chemical structure.

Type of inhibitor	Name	Structure
Antibodies	Bevacizumab	
Tyrosine-kinase inhibitors	Sorafenib	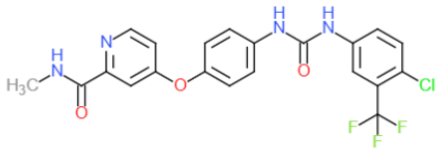
	Sunitinib	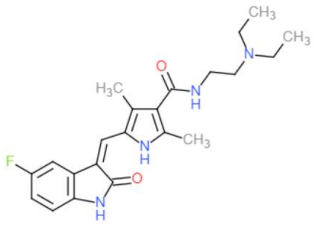
	Pazopanib	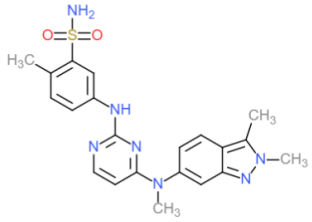
	Cabozantinib	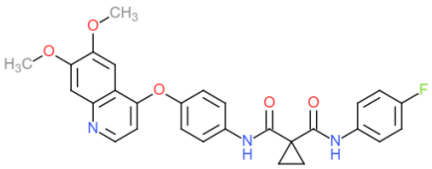
	Lenvatinib	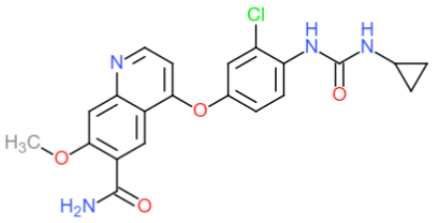
	Axitinib	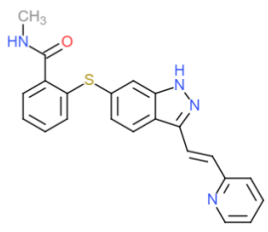

mTOR inhibitor	Temsirolimus	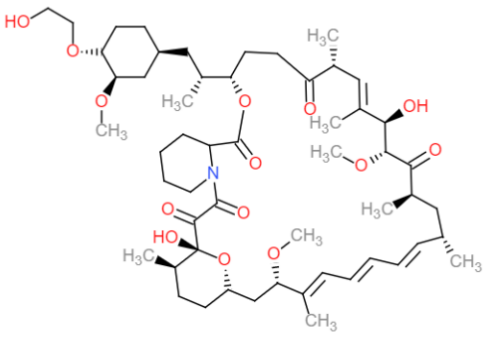
	Everolimus	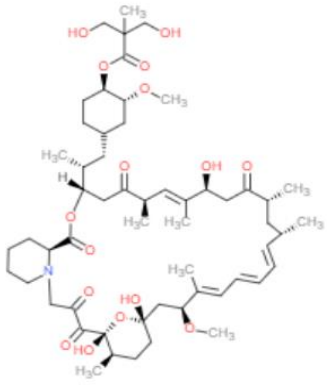
Immunotherapies (Antibodies)	Nivolumab (anti PD-1)	
	Pembrolizumab (anti PD-1)	
	Ipilimumab (anti CTLA-4)	
	Avelumab (anti PD-L1)	

Appendix 2. NRPs inhibitors' chemical structure.

Type of inhibitor	Name	Structure
Antibodies	MNRP-1685A	
Peptides and pseudo peptides	ATWLPPR	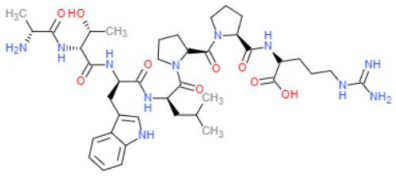
	Lys(hArg)-AA^2-AA^3-Arg	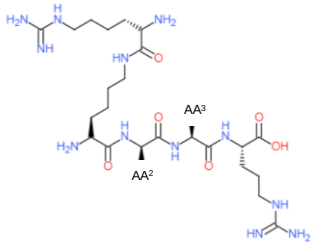
	with:	**AA^2:** Dab (Diaminobutyric acid) 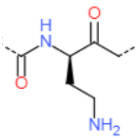 **AA^3:** ΔPro 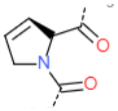 Oic (Octahydroindole) 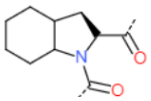
	EG3287	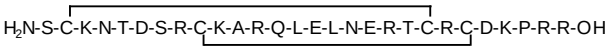
	EG00229	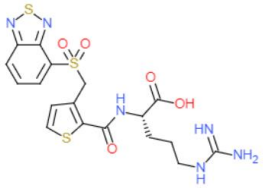
	EG01377	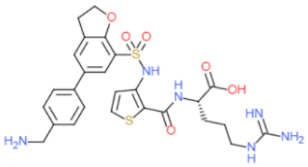

Non-peptidic inhibitors	Chembridge compound 7739526	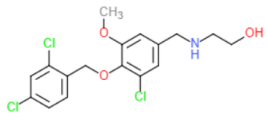
	NRPa-47	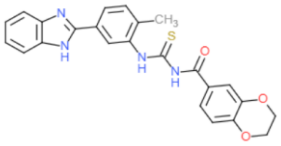
	NRPa-48	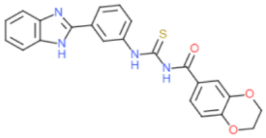
	NRPa-308	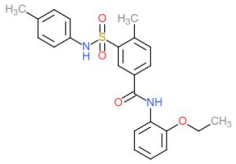

Appendix 3. Article 3.

The combination of bevacizumab/Avastin and erlotinib/Tarceva is relevant for the treatment of metastatic renal cell carcinoma: the role of a synonymous mutation of the EGFR receptor. *Theranostics.* 2020.

Renaud Grépin, Mélanie Guyot, **Aurore Dumond**, Jérôme Durivault, Damien Ambrosetti, Jean-François Roussel, Florence Dupré, Hervé Quintens and Gilles Pagès.

Ivyspring International Publisher

Theranostics

2020; 10(3): 1107-1121. doi: 10.7150/thno.38346

Research Paper

The combination of bevacizumab/Avastin and erlotinib/Tarceva is relevant for the treatment of metastatic renal cell carcinoma: the role of a synonymous mutation of the EGFR receptor

Renaud Grépin[1], Mélanie Guyot[2], Aurore Dumond[1], Jérôme Durivault[1], Damien Ambrosetti[3], Jean-François Roussel[4], Florence Dupré[4], Hervé Quintens[5] and Gilles Pagès[2] ✉

1. Centre Scientifique de Monaco, Biomedical Department, 8 Quai Antoine Ier, MC-98000 Monaco, Principality of Monaco.
2. University Cote d'Azur, Institute for research on cancer and aging of Nice (IRCAN) CNRS UMR 7284/ INSERM U 1081 3
3. Department of Pathology, Nice University Hospital, University of Nice Sophia Antipolis.
4. Centre Hospitalier Princesse Grace, Pathology department, Monaco.
5. Centre Hospitalier Princesse Grace, Urology department, Monaco.

✉ Corresponding author: Gilles Pagès: gpages@unice.fr

Received: 2019.07.11; Accepted: 2019.08.14; Published: 2020.01.01

Abstract

Metastatic clear cell renal cell carcinomas (mRCC) over-express the vascular endothelial growth factor (VEGF). Hence, the anti-VEGF antibody bevacizumab/Avastin (BVZ) combined with interferon alpha (IFN) was approved for the treatment of mRCC. However, approval was lost in July 2016 due to the absence of sustained efficacy. We previously showed that BVZ accelerates tumor growth in experimental models of mRCC in mice, results in part explained by down-regulation of the phospho tyrosine phosphatase receptor kappa (PTPRκ) in tumor cells. The epidermal growth factor receptor (EGFR) is a direct target of PTPRκ. Its down-regulation leads to constitutive activation of EGFR, an observation which prompted us to test the effect of the EGFR inhibitor erlotinib/Tarceva (ERLO) in addition to BVZ/IFN. The influence of the long non-coding RNA, EGFR-AS1, on ERLO efficacy was also addressed.

Methods: The effect of BVZ/IFN/ERLO was tested on the growth of experimental tumors in nude mice. The presence of germline mutation in the EGFR was evaluated on cell lines and primary RCC cells. *In vitro* translation and transfections of expression vectors coding the wild-type or the EGFR mutated gene in HEK-293 cells were used to test the role of EGFR mutation of the ERLO efficacy. Correlation between EGFR/EGFR-AS1 expression and survival was analyzed with an online available data base (TCGA).

Results: Tumor growth was strongly reduced by the triple combination BVZ/IFN/ERLO and linked to reduced levels of pro-angiogenic/pro-inflammatory cytokines of the ELR+CXCL family and to subsequent inhibition of vascularization, a decreased number of lymphatic vessels and polarization of macrophages towards the M1 phenotype. Cells isolated from surgical resection of human tumors presented a range of sensitivity to ERLO depending on the presence of a newly detected mutation in the EGFR and to the presence of EGFR-AS1.

Conclusions: Our results point-out that the BVZ/IFN/ERLO combination deserves testing for the treatment of mRCC that have a specific mutation in the EGFR.

Introduction

Before the development of anti-angiogenic therapies (AAT), the outcome of mRCC was poor. The first treatment approved for mRCC was the humanized monoclonal antibody bevacizumab/

Avastin (BVZ) in combination with the standard treatment interferon alpha (IFN), the only treatment that showed a modest efficacy [1]. These drugs are aimed at asphyxiating the tumors, so they should be curative but the results of pivotal clinical trials were disappointing and gave only an increase in the time to progression and in the quality of life without a major improvement in overall survival [2, 3]. The reasons for this poor efficacy depend on compensative mechanisms that allow tumor cells to escape drug-mediated cell death. Acquisition of dependence on alternative signaling pathways favoring cell proliferation and invasion has been described including the c-MET [4] and the neuropilin (NRP1/NRP2) [5, 6] pathways. Myeloid cells have also been involved in the refractoriness to AAT [7]. The presence of redundant pro-angiogenic factors is also one of the causes of relapse to treatments targeting the VEGF/VEGFR pathway especially the ELR+CXCL pro-angiogenic/pro-inflammatory cytokines [8, 9]. Identification of markers of response to treatment is an important challenge and may favor the discovery of new potent therapeutic targets [10, 11]. The epidermal growth factor receptor (EGFR) is over-expressed in mRCC probably via EGR-1 dependent activation of its promoter [12]. The hypoxia-inducible factors 1, 2 (HIF-1, 2) are constitutively active in the majority of mRCC because of frequent loss of function of the von Hippel-Lindau gene that stimulates the expression of the transforming growth factor α (TGF- α), an activator of the EGFR pathway [13]. Our previous results showed that the pressure of selection exerted by BVZ induced down-regulation of the phospho tyrosine phosphatase receptor kappa (PTPRκ), a natural inhibitor of EGFR activity resulting in the acquisition of increased proliferation of tumor cells [9]. These cells were driven by over-activation of EGFR as attested by the level of phosphorylation and of the subsequent activation of the ERK/MAP kinase and PI3 kinase/AKT pathways. *In vitro*, the EGFR inhibitor erlotinib/Tarceva (ERLO), which is approved for the treatment of lung cancers harboring specific mutations in EGFR, strongly inhibited proliferation of cells derived from BVZ-resistant tumors [9]. These results paved the way for experiments dedicated to evaluating the relevance of combinations of ERLO/BVZ/IFN to prevent acquired resistance and to improve the current therapeutic practices. The present study highlights the molecular mechanisms associated with the efficacy of combined treatments in experimental mRCC in mice and the relevance of their use in a specific fraction of patients.

Materials and methods

Cell lines

The Ethics departments of the University hospital, the Cancer Centre (Centre Antoine Lacassagne), Nice, France and the Princess Grace Hospital of Monaco approved this study and participants provided their written informed consent. Cells were isolated from tumors as previously described [14]. RCC4, 786-O and A498 cells were from the American Type Culture Collection and were cultured in the same defined medium.

RNA extraction and RT-PCR

Quantitative PCR (qPCR) experiments were performed after cell passage 11. One microgram of total RNA was used for reverse transcription, using the QuantiTect Reverse Transcription kit (QIAGEN, Hilden, Germany), with blend of oligo(dT) and random primers to prime first-strand synthesis. For real-time PCR, we used the master mix plus for SYBR assay (Eurogentec, Liege, Belgium). The PCR conditions were 10 minutes at 95°C followed by 40 cycles 15 seconds at 95°C, 1 minute at 60°C. The sequences of the different couples of oligo-nucleotides are detailed in supplementary Table 1.

Antibodies

The following antibodies were used for immuno-blotting: anti-phospho ERK 1,2 and anti-tubulin (Sigma St Louis, MO), anti-phospho S6 Kinase, total anti-EGFR/HER1 and anti-pEGFR/ HER1 (Cell Signaling, Cambridge, UK) and anti ERKs (Santa Cruz Biotechnology, Santa Cruz, CA references sc 93).

Immuno-fluorescence

Tumor sections were handled as described previously [9]. Sections were incubated with anti-mouse LYVE-1 polyclonal (Ab 14817, 1:200; Abcam, Cambridge, MA, USA) or monoclonal anti-α-smooth muscle actin Sigma (αSMA A2547, 1:1000; Sigma, France), and rat monoclonal anti-mouse CD31 (clone MEC 13.3, 1:1000; BD Pharmingen, Franklin Lakes, NJ, USA) antibodies.

Measurement of hemoglobin and cytokines

Frozen tumor tissues were homogenized using a Precellys tissue homogenizer (Bertin, Montigny-le-Bretonneux, France) in cell extraction buffer (Biosource, Villebon sur Yvette, Belgium). The intra-tumor hemoglobin content, CXCL cytokines, VEGF and VEGFC were measured as previously described [9].

Tumor xenograft experiment

Five million 786-O or A498 cells were injected subcutaneously into the flank of 5-week-old nude (nu/nu) female mice (Janvier). The tumor volume was determined with a caliper (v ¼ L _ l2 _ 0.5). When the tumor reached 100 mm3, mice were treated twice a week with control or ERLO (50 mg/kg) or BVZ (B, 7.5 mg/kg) plus IFN (9MIU) plus or minus ERLO (50 mg/kg).

This study was carried out in strict accordance with the recommendations in the Guide for the Care and Use of Laboratory Animals. Our experiments were approved by our internal ethic committee.

Transfection experiments

The assay was performed as already described [15] in duplicate with different amounts of pcDNA4 vector carrying the wild-type and the variant EGFR sequence (two independent preparations for each construct). At the same time, 300 ng of pGL3 luciferase expression plasmids were co-transfected as an independent control of the transfection efficiency in each well. The transfection efficiency was calculated from the luciferase counts normalized to the amount of protein. Only cells that showed the same degree of transfection efficiency (difference < 20%) were analyzed.

Statistical analysis

Statistical analyses were two-sided and were performed using R-2.12.2 for Windows. Statistical comparisons were performed using the Student *t*-test or Wilcoxon test for quantitative data.

Results

ERLO exerts a strong cytostatic and cytotoxic effect that depends on the mRCC cell line and inhibits the production of pro-angiogenic cytokines

Activation of the EGFR pathway in response to BVZ was demonstrated previously in experimental mRCC in mice [9]. However, the intrinsic sensitivity to EGFR inhibitors of mRCC cells was poorly investigated. Therefore, we evaluated sensitivity using two model cell lines, 786-O and A498 cells. We obtained a dose-dependent decrease in the proliferation rate with both cell lines. The maximal reduction was of 60% and 33% for 786-O and A498 cells, respectively for the highest ERLO concentration (10 μM). Regardless of the ERLO concentration, the percentage of dead cells was equivalent (10% and 2% for 786-O and A498 cells, respectively, **Figure 1A-B**). Therefore, ERLO is cytostatic rather than cytotoxic and the cytostatic effect was stronger for 786-O cells. ERLO induced dose-dependent inhibition of EGF production by 786-O cells whereas this was not modified in A498 cells (**Figure 1C**). Therefore, the more potent effect of ERLO on cell proliferation observed for 786-O cells may be explained by inhibition of an EGF/EGFR autocrine pathway. Consistent with this, the phosphorylated/active form of EGFR (pEGFR) was dose-dependently inhibited by ERLO in 786-O cells. In A498 cells, the EGFR levels were higher compared to 786-O cells and ERLO had no incidence on pEGFR, which remained low whether or not ERLO was present, as compared to basal levels in 786-O cells (**Figure 1D** and **Figure S1**). We observed a decrease in the activity of the ERK/MAP kinase proliferation pathway for both cell lines. However, the ERK activity was lower and was more strongly inhibited by ERLO in 786-O cells. The AKT activity (pAKT) was high and was inhibited by ERLO in 786-O cells but almost undetectable in A498 cells. This result may explain the differential effect exerted by ERLO on proliferation for the two independent cell lines (**Figure 1D** and **Figure S1**).

Gefitinib, another EGFR inhibitor used to treat lung cancers [16], or cetuximab, a monoclonal antibody against EGFR, reduced the production of VEGF and CXCL8 in different cancer cells, which may explain their therapeutic efficacy [17, 18]. Therefore, the effect of EGFR inhibition on secreted cytokines involved in angiogenesis was evaluated. ERLO, even at a low concentration (1 μM), inhibited VEGF production in 786-O cells but this was not modified in A498 cells (**Figure 1E**). The opposite result was observed for CXCL8 (dose-dependent inhibition in A498 cells and no effect in 786-O cells, **Figure 1F**). These results suggest that ERLO may indirectly inhibit angiogenesis through decreased production of pro-angiogenic factors by tumor cells.

Combining BVZ/IFN with ERLO inhibited the growth of experimental mRCC in mice

Considering that activation of the EGFR pathway is one of the causes of relapse when on anti-angiogenic treatment with BVZ [9], we tested the effect of the combination of BVZ/IFN, one of the first approved anti-angiogenic therapies [19], with the EGFR inhibitor ERLO on the growth of two experimental mRCC tumor cell lines 786-O and A498 cells in mice. INF was used in this model to be consistent with the previously approved combination administered to the patients. Tumor growth was equivalent in the control and the BVZ/IFN groups for 786-O cells while transient inhibition was observed for A498 cells. These results reflect the intrinsic or acquired resistance observed in patients [19]. ERLO alone had a modest effect on tumor growth and

relapse was observed after 45 days of treatment with 786-O cells. This observation is consistent with the results of clinical trials showing the lack of anti-tumor activity associated with anti-EGFR treatments [20, 21]. However, a sustained inhibitory effect was observed for A498 cells suggesting that inhibition of the EGFR pathway may hold some benefit depending on the genetic characteristics of the tumor. The triple association BVZ/IFN/ERLO was the most efficacious showing strong inhibition of tumor growth with 786-O and A498 cells although the effect of the triple combination was equivalent to ERLO alone for the latter cells (**Figure 2A-C**). These results highlight the differences in response to AAT and EGFR pathway–targeting treatments, which probably reflects tumor heterogeneity [22] or different subclasses of kidney tumors (clear cell (786-O) or papillary (A498) carcinomas [23]).

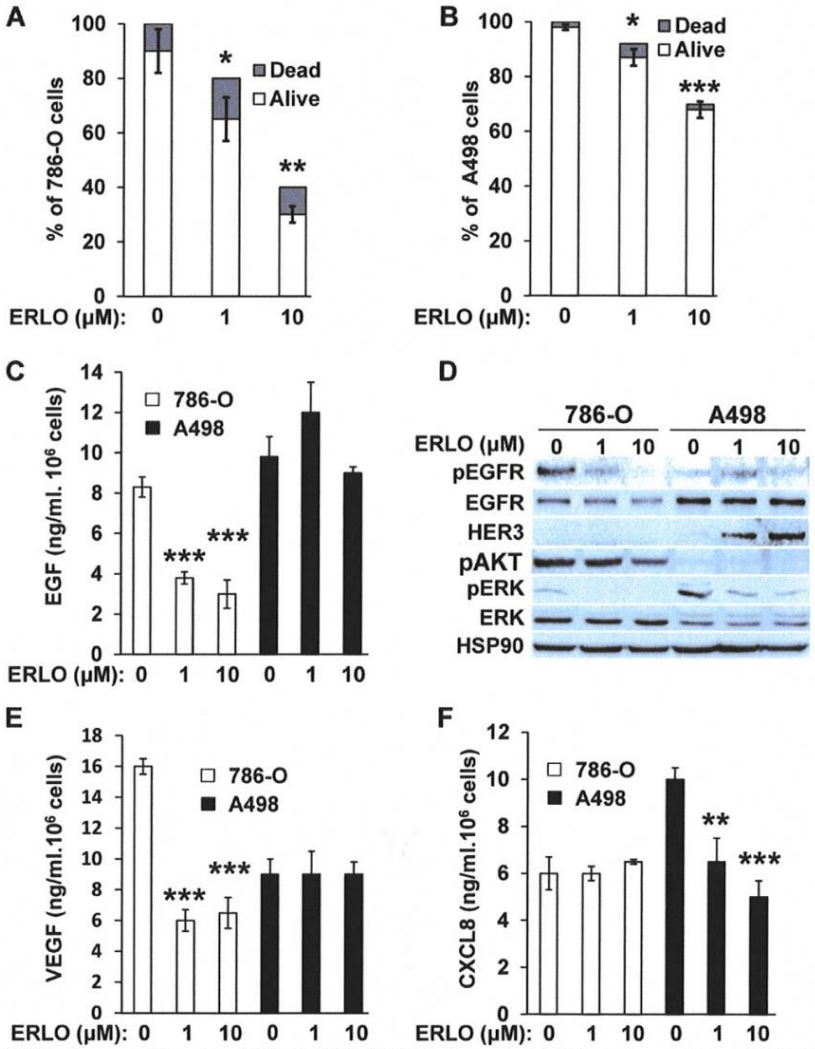

Figure 1. 786-O and A498 cells present different sensitivities to ERLO. (A) 786-O cells were treated with increasing concentrations of ERLO. The percentage of live and dead cells is indicated. *p<0.05; **p<0.01. **(B)** A498 cells were treated with increasing concentrations of ERLO. The percentage of live and dead cells is indicated. * p < 0.05; *** p < 0.001. **(C)** 786-O or A498 cells were treated with increasing concentrations of ERLO. EGF levels were evaluated in cell supernatants by ELISA. *** p < 0.001. **(D)** 786-O or A498 cells were treated with increasing concentrations of ERLO and were evaluated for the presence of total and active form of EGF receptor (EGFR/pEGFR), HER3, the total and active form of ERK (ERK/pERK) and the active form of AKT (pAKT) by immuno-blotting. HSP90 is shown as a loading control. **(E)** 786-O or A498 cells were treated with increasing concentrations of ERLO. VEGF levels were evaluated in cell supernatants by ELISA. *** p < 0.001. **(F)** 786-O or A498 cells were treated with increasing concentrations of ERLO. CXCL8 levels were evaluated in cell supernatants by ELISA. ** p < 0.01; *** p < 0.001.

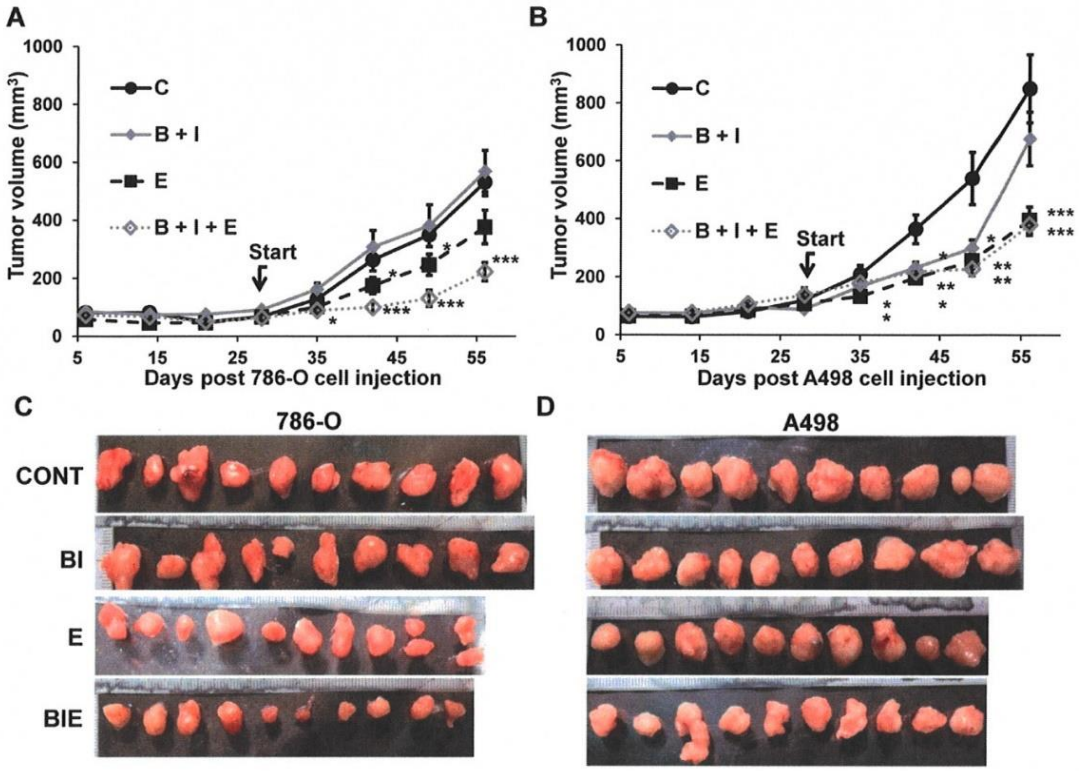

Figure 2. The role of the BVZ/IFN and ERLO combination on RCC xenograft tumor growth. (A) 5.10^6 cells 786-O cells were subcutaneously injected into nude mice. Seven days after injections all mice developed tumors. 31 days after cell injection (start treatment), mice were treated twice a week with control or ERLO (E, 50 mg/kg) or BVZ (B, 7.5 mg/kg) plus IFN (I, 9MIU) plus or minus ERLO (50 mg/kg). The tumor volume is presented as the means ± s.d. ($n = 10$). Statistical differences to the untreated mice are shown: *p <0.05; *** p<0.001. **(B)** Same experiment as described in a but using A498 cells. * p < 0.05; ** p< 0.01; *** p< 0.001. * p < 0.05; *** p < 0.001. **(C)** Images of the 786-O tumors at the end of the experiments. **(D)** Images of A498 tumors at the end of the experiment.

BVZ/IFN/ERLO strongly reduced tumor vessel density and prevented the development of lymphatic vessels

We showed previously that BVZ alone stimulated experimental tumor growth. This unexpected result correlated with tumor vessel normalization and the development of a lymphatic network shown in the literature to be involved in tumor cell dissemination [9, 24]. Considering these observations, we hypothesized that the triple combination may eradicate blood vessels and may prevent the development the lymphatics. The number of blood vessels decreased for 786-O tumors treated with BVZ/IFN and ERLO (**Figure 3A** and **Figure S2A**) but was not different for A498 tumors (**Figure 3C** and **Figure S2B**). However, these treatments increased the number of vessels (CD31 positive) lined with αSMA-positive cells, a pattern of vessel normalization (**Figure 3A-C** and **Figure S2A-B**). The triple combination decreased the number of blood vessels but also increased coverage with αSMA labelled cells for 786-O and A498 tumors (**Figure 3A-C** and **Figure S2A-B**). The amount of tumor hemoglobin was significantly decreased for only the triple combination suggesting that the treatment reduced tumor perfusion and/or hemorrhagic vessels (**Figure 3E**). As previously reported, BVZ stimulated the development of a lymphatic network in 786-O tumors [9]. A similar result was observed when BVZ was coupled with IFN for 786-O and A498 tumors although lymphatic vessels were already present in A498 tumors in untreated mice (**Figure 3B-D** and **Figure S2A-B**). ERLO stimulated the development of lymphatics for both tumor model systems. However, the triple combination strongly reduced the BVZ/IFN- or ERLO-dependent development of the lymphatic network for both model systems (**Figure 3B-D** and **Figure S2A-B**) and the basal level of lymphatics for the A498 tumors. These results suggest that the triple combination inhibited tumor growth partly by inhibiting the formation of blood and lymphatic networks.

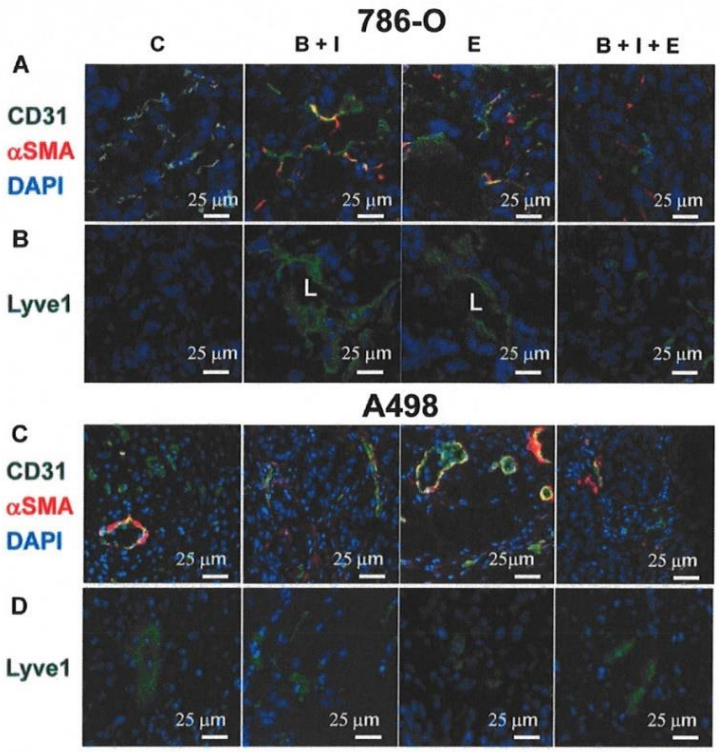

Hemoglobin (mg/ml/µg protein)	C	B + I	E	B + I + E
786-O tumors	552	634	580	402 (***)
A498 tumors	954	783	818	612 (**)

Figure 3. The BVZ/IFN/ERLO combination decreased the tumor blood vessel density and prevented/inhibited the development of lymphatic vessels. The tumor vasculature in each experimental group was detected by immuno-staining for CD31 (endothelial cells, green) and α-SMA i (pericytes, red); **(A)** 786-O cell model; **(C)** A498 cell model. LYVE-1 immuno-staining (green) shows lymphatic endothelial cells. Lymphatic vessels with lumens (L) are indicated. **(B)** 786-O model; **(D)** A498 model. Tumor sections were counterstained with 40,6-diamidino-2-phenylindole (DAPI) (nucleus, blue). **(E)** The intra-tumor amount of hemoglobin (Hg), a global read out of the blood supply, is given for both model systems and for the different experimental conditions.

Analysis of genes related to tumor angiogenesis and lymphangiogenesis, cell proliferation, immune tolerance and polarization of macrophages

To understand the better efficacy of BVZ/IFN/ERLO, we investigated the genes involved in the adaptation of cancer cells (proliferation genes) and cells of the tumor environment (immune tolerance, macrophages, pro/anti-angiogenic genes) to a given treatment. **Table 1** summarizes the modifications to the mRNA analyzed by qPCR or proteins analyzed by ELISA. First, gene expression differed for the two cell lines highlighting the importance of the tumor genetic background. However, some genes were consistently modified by the different treatments in both cell lines. PTPRκ mRNA levels were decreased by BVZ [9], but were up-regulated by BVZ/IFN in 786-O and A498 cells. Strikingly, inhibition of EGFR by ERLO induced PTPRκ only in A498 tumors. However, PTPRκ levels were decreased by the triple combination. These results suggest that the association of IFN with BVZ prevented compensatory activation of proliferation pathways mediated by a decrease in PTPRκ. However, concomitant inhibition of the VEGF and EGFR pathways resulted in down-regulation of PTPRκ. Human EGFR levels were increased by BVZ/IFN in both cell lines indicating that the compensatory mechanisms linked to VEGF/VEGFR inhibition involved the EGFR pathway. Induction of EGFR in cells of the microenvironment was also observed in response to ERLO with both cell lines

indicating that EGFR inhibition was compensated by over-expression of the receptor. In both cell lines, the inhibition of the EGFR pathway was also compensated by over-expression of EGF by tumor cells only for the triple combination. The colony stimulating factor 1 and its receptor (CSF1/CSF1R) were then investigated since CSF1R is highly expressed in RCC cells because of chromosome 5q22qter amplification [25, 26]. The triple combination inhibited CSF1R expression in both cell lines suggesting that the treatment indirectly targeted an autocrine proliferation pathway. Our previous observation showed that BVZ had no effect on expression of its target VEGF produced either by tumor cells or cells of the microenvironment [9]. Unfortunately, the triple combination stimulated VEGF expression by tumor cells in both model systems. Moreover, VEGFC, a key player involved in metastatic dissemination via the lymphatics, was enhanced by the triple combination in both model systems. Increased VEGFC expression was consistent with the presence of lymphatic vessels observed in **Figure 2B-D**. The expression of angiogenic factors redundant for VEGF was suspected to promote BVZ resistance [9]. The CXCL family of cytokines was investigated because of its involvement in RCC aggressiveness, as we previously shown [8, 9]. The CXCL family of cytokines is divided into pro- and anti-angiogenic members. Only CXCL5 and CXCL7, two pro-angiogenic members, are consistently down- and up-regulated in both cell lines, respectively by the triple combination. The inflammatory context is a key player in adaptation to treatment. CD45 a tumor-infiltrating leukocyte gene was increased in 786-O tumors treated with BVZ/INF. F4/80 macrophage gene was also up-regulated by BVZ/INF or BVZ/INF /ERLO for the 786-O model and down-regulated for the triple combination in A498 tumors. The polarization of macrophages is particularly important for treatment adaptation [27]. Only the triple combination consistently down-regulated expression markers of M2 macrophages (arginase and CD206) in the two tumor models. Finally, immune tolerance was investigated because of the efficacy of anti-programmed death ligand (PDL1) antibody treatment, especially for the most aggressive tumors [28]. PDL1 was only detected in 786-O cells and BVZ/IFN and BVZ/IFN/ERLO strongly induced its expression. This finding is in agreement with the clinical activity of the BVZ plus atezolizumab (anti-PDL1) combo [29]. According to these differences, we attempted to quantify the good and bad prognostic markers. We gave a score of 1 for a good prognostic marker, a score of -1 for a bad marker and 0 for unchanged or undetected markers.

The best score (3) was obtained with BVZ/IFN treatment whereas the worst score (-3) was assigned to ERLO treatment of 786-O cells. For the A498 cells BVZ/IFN or ERLO generated the best scores. Surprisingly, triple treatment did not give the best score although tumor growth was strongly impaired. These results suggest that the triple association may select tumor cells with a more aggressive phenotype that are kept in check by the drugs.

Cells derived from mice tumors treated with BVZ/IFN/ERLO are still sensitive to ERLO

The different treatments generated a wide range of profiles of tumor growth. Therefore, we hypothesized that due to the selection pressure exerted by the different drugs, tumor cells acquired specific genotypic/phenotypic profiles. Thus, we analyzed their proliferation after amplification and selection from the tumors, as previously described [9]. The proliferation rates forty-eight hours after seeding of cells from control, BVZ/IFN and ERLO 786-O treated-tumors were low or similar (125, 175 and 160 %, respectively, **Figure 4A**).

However, cells from BVZ/IFN/ERLO 786-O treated-tumors proliferated three times more than those from control tumors (350 %, **Figure 4A**), which reflected their strong level of EGF production (**Table 1**). The proliferation rates of A498 cells extracted from the different tumors were higher than that of 786-O cells (200 %) whereas they were lower for parental cells (**Figure S4**). However, they were similar whatever the treatment (**Figure 4B**). In these cells, the intra-tumor levels of human/mouse EGF and EGFR varied according to the treatment (**Table 1**). We showed previously that exposure to BVZ sensitized resistant cells to ERLO because of PTPRκ down-regulation [9]. Consistently, 786-O and A498 cells from BVZ/IFN tumors were more sensitive to ERLO than cells from control tumors (28 % versus 43
% inhibition for 786-O cells and 17 % versus 32 % for A498 cells). This result is also consistent with increased expression of EGFR in both model systems. 786-O cells from ERLO tumors were still highly sensitive to ERLO (40 % inhibition) whereas A498/ERLO cells became insensitive (only 7 % inhibition). This result is consistent with increased expression of EGF in 786-O cells and its down-regulation in A498 cells (**Table 1**). Cells from triple-treated tumors were still sensitive to ERLO whatever the model. This persistent response to ERLO was linked to increased expression of EGF in both model systems (**Table 1** and **Figure 4A-B**). Hence, the chronic inhibition of the EGF/EGFR proliferation pathway is consistent with the *in vivo* efficacy of the triple combination.

Table 1. Analysis of pro-angiogenic/pro-lymphangiogenic/pro-inflammatory genes/proteins in tumors from mice treated with ERLO, BVZ/INF or BVZ/INF/ERLO.

qPCR	786-O				A498			
	Control	BVZ/INF	ERLO	BVZ/INF + ERLO	Control	BVZ/INF	ERLO	BVZ/INF + ERLO
Housekeeping genes								
36B4	100	100	100	100	100	100	100	100
m-36B4	100	100	100	100	100	100	100	100
Proliferation genes								
PTPRκ	100	289 (***)	88	54 (***)	100	185 (**)	156 (**)	33 (**)
EGFR	100	158 (*)	116	133	100	172 (**)	210 (**)	82
m-EGFR	100	313 (*)	222 (**)	96	100	106	151 (*)	156 (*)
CSF1	100	467 (**)	72	104	100	159	39 (**)	75
CSF1R	100	43 (*)	50 (*)	26 (**)	100	71	73	59 (*)
m-CSF1	100	17 (**)	242 (***)	135	100	27 (***)	44 (**)	50 (*)
m-CSF1R	100	122	110	81	undetected			
Immune tolerance gene								
PDL1	100	1332 (***)	130	768 (**)	undetected			
Tumor-infiltrating leukocyte gene								
m-CD45	100	205 (**)	76	101	100	113	96	76
Macrophage gene								
m-F4/80	100	300 (***)	140	388 (***)	100	91	87	58 (***)
Macrophage M1 specific genes								
m-iNOS	100	93	121	104	100	127	80	75
m-IL6	100	110	73	127	100	107	78	70
Macrophage M2 specific genes								
m-ARG1	100	8 (***)	334 (***)	19 (***)	100	139 (*)	143 (**)	55 (***)
m-CD206	100	38 (***)	644 (***)	59 (*)	100	74	104	52 (*)
Pro/anti-angiogenesis genes								
IL6	100	99	146	33 (*)	undetected			
CXCL5	100	100	309 (**)	49 (*)	100	74 (**)	52 (***)	80 (**)
CXCL4	100	394 (***)	73	119	undetected			
CXCL10	100	87	166 (*)	216 (*)	undetected			
ELISA (pg/mg)	786-O				A498			
	Control	BVZ/INF	ERLO	BVZ/INF + ERLO	Control	BVZ/INF	ERLO	BVZ/INF + ERLO
hVEGF	2065	2280	3192 (**)	3287 (**)	1646	1945	2591 (**)	2620 (***)
mVEGF	2395	2214	1755 (*)	2007	2108	2206	1431 (**)	1930
hVEGF-C	63,5	56,4	50,2	102.1 (**)	43,1	46,2	53,1	84.7 (**)
hEGF	221	264 (**)	272 (**)	711 (***)	173	192	128 (**)	294 (**)
mEGF	697	766	363 (**)	683	267	313	286 (*)	468 (**)
CXCL1	376	267 (*)	302	289 (*)	238	300	333	349
CXCL7	26,4	29	34.4 (*)	38.4 (**)	25,8	25,8	31.7 (*)	32.6 (*)
CXCL8	2560	1620 (***)	1659 (**)	2019 (**)	1835	1675	1503 (*)	1765
Good		8	5	8		3	7	5
Bad		-5	-8	-6		-2	-6	-7
Score		3	-3	2		1	1	-2

The percentage expression of the different genes evaluated by qPCR and the amounts of cytokines detected by ELISA are shown. The indication "m" stands for mouse genes. If not indicated the genes are human ones. For the measured genes, the reference values (100) correspond to the content of a given gene in tumors of the placebo-treated mice. The amounts of cytokine in tumor extracts are given in picograms (pg) or nanograms (ng) per milligrams (mg) of total protein. The statistically significant differences are shown. * $p < 0.05$: ** $p < 0.01$:*** $p < 0.001$. A good prognostic marker is presented in black characters on a grey background; a poor prognostic marker is presented in white characters on a black background and markers with no significant modification are presented in black characters on a white background. The number of good or bad prognostic markers and the markers that are not influenced by a given treatment are shown. A score of +1 is given to a good prognostic marker whereas a score of -1 is given to a poor prognostic marker. The final score corresponds to the addition of good and poor prognostic markers. For 786-O cells, BVZ/INF and BVZ/INF/ERLO treatments gave positive scores (3 and 2 respectively) with the highest number of good prognostic indicators (8), whereas ERLO gave a negative score (-3) with the highest number of bad prognostic factors (-8). For A498 cells, BVZ/INF/ERLO treatment gave the worst score (-2) with the highest number of poor prognostic indicators (-7), whereas BVZ/INF and ERLO gave equivalent positive scores (1) with the highest number of good prognostic indicators for ERLO (7).

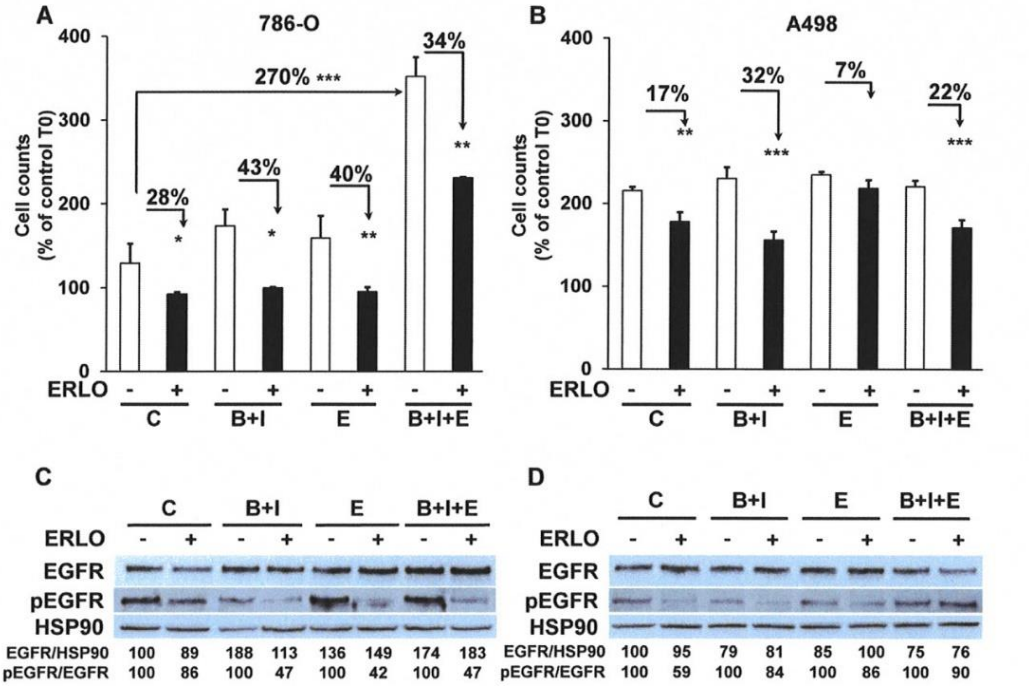

Figure 4. The capacity to proliferate and the sensitivity to ERLO of cells from experimental tumors. (A) The capacity to proliferate of 786-O cells isolated from three independent tumors from each group was tested using the MTT assay (C cells from untreated mice; B+I; cells from BVZ/IFN-treated mice; B+I+E; cells from BVZ/IFN/ERLO-treated mice) in the absence (-) or presence (+) of ERLO. **(B)** The proliferative capacity of A498 cells isolated from three independent tumors for each group in the absence (-) or presence of ERLO was tested using MTT assays. For both cell types, results are presented as the mean fold increase ± s.d. Statistical differences in the fold increase of tumor cells isolated from control mice were taken as reference values. * $p < 0.05$; ** $p < 0.01$; *** $p < 0.001$. **(C)** Representative 786-O cells from the four experimental groups were tested for the presence of the total and active form of EGFR (EGFR/pEGFR) in the absence (-) or presence (+) of ERLO (10 μM). HSP90 is shown as a loading control. Quantification of the relative level of EGFR (EGFR/HSP90) and pEGFR (pEGFR/EGFR) is shown. The reference values (100%) correspond to the levels of EGFR and pEGFR in cells of tumors derived from untreated mice in the absence of ERLO. **(D)** Equivalent experiments as described in **c** for the A498 model.

We then analyzed the level and activity of EGFR and the sensitivity to ERLO of signaling pathways involved in cell proliferation (ERK/MAP Kinase and PI3Kinase/AKT). Total EGFR levels were increased following treatment of the 786-O model system and were slightly decreased in the A498 model. Basal levels of the phosphorylated/active form of EGFR (pEGFR) decreased in 786-O and A498 cells after BVZ/IFN treatment. This result is consistent with increased levels of PTPRκ (**Table 1** and **Figure 4C-D**). However, the decreased level of PTPRκ in cells from the triple-treated tumors resulted in a modest increase in basal pEGFR levels for both systems. ERLO inhibited pEGFR in the different cells for both cellular models except for A498 cells from the triple-treated tumors. This result reflects an alternative mechanism of EGFR activation probably through the increased expression of EGF by cells of the microenvironment (**Table 1**). Inhibition of the EGFR activity correlated with inhibition of ERK and preferentially with the AKT activity (**Figure S3A-B**). However, the persistence of ERK and AKT activity independently of the EGFR activity reflects activation of alternative proliferation pathways independent of the EGF/EGFR pathway after chronic exposure to treatments.

Primary cells present a different sensitivity to ERLO

We showed previously that treatment response to AAT, especially to the current reference treatment sunitinib, was equivalent in metastatic patients and in primary cells derived from the patients' surgically removed tumor [14]. In equivalent experiment BVZ had only a modest effect on tumor cell *in vitro*. The sensitivity to ERLO can be assessed on primary cells as well to propose this alternative treatment in case of resistance to sunitinib. The half-maximal inhibitory concentration (IC50) for ERLO and for sunitinib, is reported in **Table 2** for our reference 786-O and A498 cell lines and the already described primary cells [14]. Three primary cell cultures were derived from metastatic tumors (CC, M, TF). Some cells were sensitive to both treatments (sunitinib, ERLO; 786-O, CC), to only sunitinib (A498, M) or to none of these treatments (TF). Only one primary culture (CC) was

more sensitive to ERLO compared to 786-O cells (IC50 1.65 lower). M and TF cells presented a 2.2 and a 2.3-fold higher IC50 for ERLO compared to 786-O cells. To explain the relative sensitivity to ERLO of the primary cultures, we compared their relative amount of EGFR to that of our reference cell lines 786-O and A498. We also added an additional cell line obtained from the ATCC, RCC4 cells. A498 cells expressed the highest amounts of mRNA and protein (**Figure S5A-C**). EGFR mRNA levels in 786-O cells are 50% and 25% percent those of RCC4 and A498 cells respectively. However, EGFR protein levels in 786-O cells are 20% and 6.6% percent those of RCC4 and A498 cells respectively. Of note ERLO did not influence the EGFR level (**Figure S5B-C**). This discrepancy for 786-O cells may be related to the high levels of a long non-coding EGFR antisense mRNA (EGFR-AS1) already described as a marker of poor prognosis in RCC [30] and which modulates ERLO efficacy in head and neck carcinoma [31]. EGFR-AS1 mRNA levels were the highest and EGFR mRNA levels were the lowest in 786-O cells (**Figure S5D**). The relationship between EGFR/EGFR-AS1 levels and tumor aggressiveness was evaluated by using the online available data of the TCGA. EGFR is overexpressed in RCC from non-metastatic (M0) and metastatic (M1) patients as compared to healthy tissue. Surprisingly, EGFR levels decreased in tumors from metastatic patients (compared M0 to M1) (**Figure S6A**). Over-expression of EGFR was indicative of a longer overall survival (OS) for M0 patients ($p = 0.00209$) whereas an inversion of this trend was observed for M1 patients although it did not reach statistical significance ($p = 0.107$, **Figure S6B-C**). In M1 patients, overexpression of EGFR was correlated to a shorter progression-free survival (PFS, $p = 0.0241$) and a trend was observed for a shorter disease-free survival (DFS, $p = 0.0609$) (**Figure S6D-E**). EGFR-AS1 is also overexpressed in RCC from M0 and M1 patients as compared to healthy tissues. No statistically significant difference was observed between M0 or M1 tumors (**Figure S7A**). High EGFR-AS1 levels were correlated with a shorter OS in M1 patients ($p = 0.0468$) and a trend was observed in M0 patients although non-significant ($p = 0.121$) (**Figure S7B-C**). However, high EGFR-AS1 levels were associated with a longer DFS in M0 patients ($p = 0.0145$) and a shorter PFS in M1 patients ($p = 0.0434$) (**Figure S7D-E**). Hence, in M0 patients a mirror image of the role of EGFR and EGFR-AS1 on OS and DFS was observed with an unexpected beneficial role of EGFR on OS. However, EGFR and EGFR-AS1 were systematically associated with shorter OS and DFS in M1 patients. These results are consistent with the pejorative role of EGFR and the relevance of its inhibition in metastatic patients.

A silent mutation of EGFR correlated with EGFR levels and ERLO sensitivity

EGFR levels and its activity varied from tumor to tumor, a situation that may explain the general failure to ERLO in clinical trials. In lung cancers, for which ERLO is routinely used, EGFR protein levels and activity, that are crucial for ERLO efficacy, are never assessed before ERLO treatment. Moreover, ERLO is efficient for lung tumors but only if EGFR has mutations in the kinase domain [16, 32]. To determine whether specific mutation(s) may explain the relative expression and the difference in sensitivity to ERLO of cell lines and primary cultures, we performed exome sequencing of the *EGFR* gene. The different mutations/deletions determining ERLO sensitivity in lung cancers were not detected in RCC cells [16, 32]. We detected a single-nucleotide polymorphism (SNP) that modifies the codon corresponding to glutamine from CAG to a CAA (NM_005228; G 2618 to A, rs1050171), a mutation described in osteosarcoma [33] and in head and neck tumors [31, 34]. RCC4 cells are wild-type (CAG codon) on both alleles, 786-O cells are heterozygous and A498 cells are homozygous for the mutation (CAA on both alleles, **Figure 5A**). The corresponding amino acid is located within the kinase domain (Q 787). This specific mutation modifies a frequently used codon for Q to a rare codon (CAG, frequent codon for Q, 73% to rare codon CAA (27%)). In addition to the differences in mRNA levels, this result may explain the difference in the total amounts of EGFR detected in the different cell lines and their sensitivity to ERLO (Supplementary Fig. S5). We then derived primary cultures from additional surgically removed tumors. 3 out of 31 primary cells (9.7%) were wild-type, 13 out of 31 (41.9%) were heterozygous and 15 out of 31 (48.4%) were homozygous for the silent mutation. We also derived primary cultures from the normal renal tissue for the corresponding patients. Normal cells were carrying the mutation suggesting its presence in the germinal state. This result was consistent with the allele distribution of this SNP in the European population (https://www.ncbi.nlm.nih.gov/SNP/snp_ref.cgi?rs=1050171).

Sensitivity to ERLO was tested in the different primary cells. The IC50 for ERLO was the lowest for cells with the heterozygous mutation and the highest for the cells with the homozygous mutation and intermediate for wild-type cells (**Figure 5B**). The differences in ERLO sensitivity were confirmed using another specific EGFR inhibitor: AZD3759 (**Figure 5C**). Considering these results, we investigated whether the G2618A mutation could be responsible for the discrepancy between the mRNA and protein

levels observed in the different cell lines. We hypothesized that a higher efficiency of translation of mRNA carrying the A mutation occurs. To functionally test this hypothesis, we performed an *in vitro* transcription and translation assay using an EGFR construct for both the wild-type and the mutated allele. The wild-type construct was translated less efficiently than the mutant (**Figure 5D**). To confirm these results, HEK293 cells expressing very low EGFR levels were transfected with expression vectors coding for the wild-type or the mutated EGFR. A luciferase construct was co-transfected as a control for transfection efficiency as already described [15]. Comparing only samples with the same transfection efficiency, we found that the wild-type EGFR plasmid produced a lower amount of protein (**Figure 5E**). These results strongly suggest that patients carrying an homozygous wild-type genotype express the highest levels of EGFR.

Table 2. Sensitivity of the primary cells to the different treatments.

	CELL LINES		PRIMARY CELLS		
	786-O	A498	CC	M	TF
Sunitinib	6± 1	6 ± 0.3	4.1 ± 0.3	4 ± 0.5	11.3 ± 0.8
Erlotinib	5.3 ± 0.9	9± 0.5	3.2 ± 0.1	11.5 ± 1.2	12.2 ± 2

The IC50 for the different drugs ± SD is shown. 786-O cells are sensitive to sunitinib and erlotinib and serve as the reference. We considered the cells to be sensitive to a drug if the concentration giving 50% inhibition of cell proliferation (IC50) was lower than or equal to the IC50 in 786-O cells and was considered resistant if the IC50 was higher than for 786-O cells. CC, M and TF cells were derived from tumors of metastatic patients. When cells are sensitive to a given treatment, the value is presented on a white background but if cells are insensitive it is on a black background.

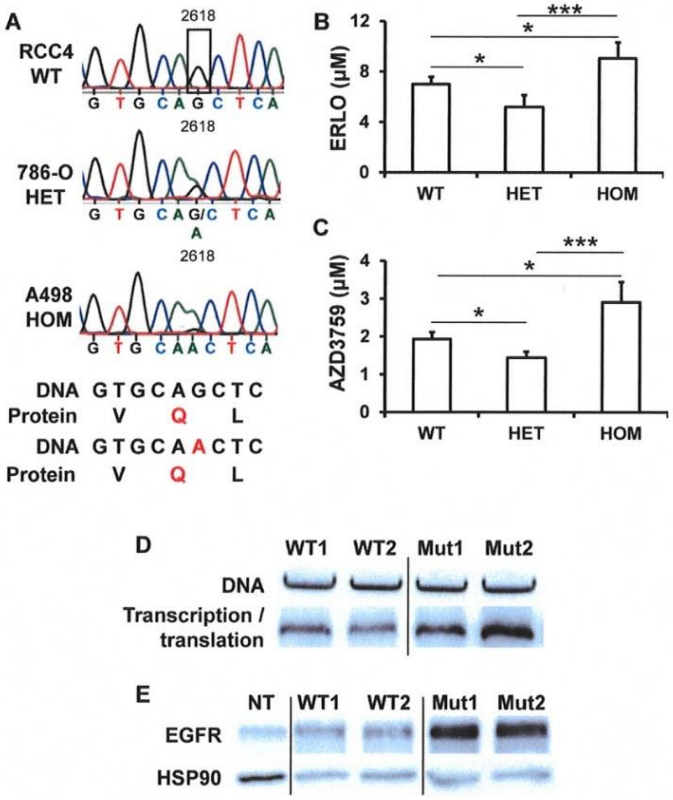

Figure 5. The presence of a silent mutation in the kinase domain of EGFR is indicative of ERLO efficacy. **(A)** Sequence chromatogram analysis of the EGFR coding region of genomic DNA obtained from RCC4, 786-O and A498 cells. **(B)** The IC50 for ERLO of the different primary cells wild-type (WT) heterozygous (HET) or homozygous (HOM) for the G 2618 A mutation was tested by MTT assays. * $p < 0.05$; *** $p < 0.001$. **(C)** Equivalent experiments as described in **(B)** for AZD3759 compound. **(D)** *In vitro* transcription and translation of two independent wild-type (WT1, WT2) and mutated (Mut1, Mut2) EGFR expression plasmids. Upper panel: equal amounts of DNA were used for *in vitro* reactions, and the quality of the plasmids was verified on agarose gels colored with ethidium bromide. Lower panel: proteins resulting from the *in vitro* transcription/translation reaction were analyzed by immuno-blotting. **(E)** 200 ng of two independent expression vectors carrying wild-type (WT1, WT2) and mutated (Mut1, Mut2) EGFR expression plasmids were transfected into HEK293 and total protein lysates were analyzed by immune-blotting. Comparison between samples was performed after the calculation of the transfection efficiency. HSP90 is shown as a loading control.

Discussion

The presence of high amounts of EGFR in mRCC cells suggested that EGFR inhibitors may have a potent therapeutic effect. A phase II clinical trial with the EGFR pharmacological inhibitor [21] and a phase I/II clinical trial using EGFR-directed antibodies gave disappointing results [35] on RCC, but the BVZ/ERLO combination appeared promising for hereditary renal cell cancer and sporadic papillary renal cell carcinoma (clinical trial NCT01130519 [36]). Both clinical trials on RCC did not associate EGFR inhibitors with the previously FDA-approved combination of BVZ and IFN. While remaining cautious, the differences between the results of the clinical trials and our preclinical models suggest that IFN enhances the therapeutic effect of BVZ and ERLO. The recent development of immune checkpoint inhibitors for kidney cancer strongly suggests that IFN, the first generation of immuno-therapies, is a key player for combined treatment and should be associated with anti-EGFR inhibitors for a maximal effect.

To gain insight into the related molecular mechanisms, we scrutinized the different pathways that were involved in relapse on treatment with BVZ in our previous study [9]: modification to the network of blood and lymphatic vessels, compensation by redundant angiogenic factors, selection of more aggressive tumor cells and adaptation to the microenvironment. Our previous study highlighted the strong impact of BVZ on the normalization of the vascular network and the development of a VEGFC-dependent lymphatic network. In the present study, a striking difference between ERLO and BVZ/IFN treatments, alone or in combination was observed for both networks. Whereas single treatment normalized the blood vessels and stimulated the development of a lymphatic network, the triple combination was associated with a decrease in the number of blood vessels, an increase in α-SMA labelled cells and the presence of fewer or equivalent numbers of Lyve-1 positive cells. Despite the stabilization of tumor growth, the presence of lymphatic vessels [37] and α-SMA-labelled tumor associated fibroblasts [38, 39] were described as indicative of further tumor evolution. The pressure of selection mediated by the treatment, stimulated VEGFC expression by human tumor cells. Such differences are implicated in mechanisms of resistance [40]. VEGFC-dependent induction by a treatment may also serve to define the best concentration of a drug that avoids such compensatory mechanisms.

Our current study was based on the BVZ-mediated decrease of PTPRκ, down-regulator of EGFR activity. However, BVZ/IFN increased PTPRκ levels. Hence, IFN indirectly decrease the activity of EGFR and other tyrosine kinase receptors that are PTPRκ targets (PDGFR, cMET, insulin receptor). EGFR is not only expressed by tumor cells but also by endothelial cells and the EGF/EGFR pathway participates in processes of tumor vascularization [41]. Induction of human or mouse EGF and/or EGFR with single treatment with ERLO or BVZ/IFN may explain the increase in the number of mature blood vessels.

The decrease of CSF1R amounts with the triple treatment argues strongly for a reduction in tumor growth since the CSF1/CSF1R pathway exerts an autocrine proliferation loop in RCC and CSF1R is indicative of poor prognosis [42]. Moreover, the EGF produced by tumor cells stimulated the secretion of CSF1 by cells of the microenvironment, which amplified proliferation of tumor cells [42]. Any decrease in EGF or CSF1 will prevent tumor growth, a situation encountered with only the triple combination.

Triple treatment also played a prominent role on the polarization of macrophages that can alternate between pro-inflammatory (M1) and pro-tumorigenic (M2) phenotypes [43]. Whereas M1 markers were not affected, M2 markers were down-regulated with BVZ/IFN/ERLO for the 786-O and A498 cellular models. M2 macrophages have been implicated in increased angiogenesis [44]. Hence, down-regulation of M2 macrophages may explain the decrease in micro-vessel density in tumors with BVZ/IFN/ERLO. The M2 phenotype is stimulated by the CSF1 pathway [45], which is consistent with the upregulation of M2 markers in the presence of ERLO.

The prognostic score we generated for the different combinations, was not indicative of the ideal treatment and differed for the two tumor models. These results suggest that these treatments may be efficient but need to be used with caution depending on specific genetic characteristics. Cells isolated from tumors exposed to triple treatment showed a higher ability to proliferate in only one model. However, the cells were still sensitive to ERLO in both models. This result suggests that ERLO must be maintained to prevent acceleration of tumor growth.

The increase in PDL1, which participates in evasion of immune surveillance [46], is not in favor of the use of the triple combination. Since treatments targeting the PD-1/PDL1 axis have been approved for the treatment of mRCC [47], it may be used at relapse when on the triple combination. However, despite expression of PDL1 by tumor cells, the presence of IFN may still induce proliferation of cytotoxic T lymphocytes and may maintain immune surveillance.

EGFR inhibitors are currently used for the treatment of lung cancers, but treatment is efficient only if the receptor has specific mutations in the kinase domain [16, 32]. Moreover, a mutation that antagonizes the efficacy of the major EGFR inhibitor ERLO was recently discovered [48]. Although the presence of these mutations depends on the cancer types, they are very rare in mRCC [49]. A specific mutation of the kinase domain of EGFR was recently described in mRCC but in another position than that described in the literature [50]. The discovery of a specific mutation in EGFR in mRCC may constitute a predictive marker of sensitivity/resistance to EGFR inhibitors to increase the treatment arsenal in case of therapeutic impasse. However, we were troubled by the differences between *in vivo* and *in vitro* results (better efficacy of ERLO for the A498 model *in vivo* and better efficacy of ERLO for the 786-O model *in vitro*). This discrepancy may be explained by the ability of the different tumor cells to shape the microenvironment. As illustrated in Table 1, human and mouse EGFR is induced by ERLO in the A498 model but only mouse EGFR is induced in the 786-O model. Human EGF is induced in the 786-O model and mouse EGF is induced in the A498 model. Hence, it is reasonable to think that the growth of A498 tumors is more addicted to the EGF/EGFR pathway and therefore more sensitive to ERLO.

Another possibility is the difference in perfusion (measurement of hemoglobin levels) of the 786-O versus the A498 model. Strikingly, the hemoglobin in A498 tumors is twice that of 786-O tumors. Therefore, ERLO may have a better access to tumor cells in the A498 model.

Finally, the EGFR genotype status is unknown in nude mice and may mitigate the relative efficacy of ERLO. Nevertheless, these experiments aimed at demonstrating the relevance of adding EGFR inhibitors to the previously approved BVZ/IFN treatment. Since the mutation appears as germinal, we can estimate that the triple combination would be more efficient for patients with a heterozygous genotype.

The analysis of genome sequences in cancer revealed that silent mutations can control the speed of mRNA translation, mRNA folding, pre-mRNA splicing, and through translational pausing, the folding of proteins [51]. Moreover, mRNA containing CAG codons are less translated than those with the CAA codon. Hence, silent mutations are driver mutations for tumor development and constitute predictive markers of resistance to a given treatment [15]. The G2618A mutation modifies a frequently used codon for Q to a rare codon. Its presence in the germinal state suggests that the patients with kidney cancers carrying a homozygous mutation (A/A) are intrinsically resistant to EGFR inhibitors. However, the opposite situation was observed for patients with head and neck cancers (higher sensitivity to ERLO if A/A), a phenotype depending on the degradation of the long non-coding RNA EGFR-AS1 [31]. The A/A genotype destabilizes the EGFR-AS1 resulting in EGFR inhibitors sensitivity in head and neck tumors. On the contrary, EGFR-AS1 levels are the lowest in homozygous wild-type (G/G) RCC cells. Strikingly, EGFR-AS1 expression is very low and it is not correlated to survival in head and neck tumors (TCGA analysis), which is exactly the contrary in RCC. The regulation of protein expression in heterozygous cells remains unclear and was a not addressed in the seminal paper of Tan and colleagues on head and neck cancers [31]. The presence of the mutation (A/A) creates a high affinity binding site for miR219. Such an interaction may also lower mRNA translation in heterozygous RCC cells and increased sensitivity to EGFR inhibitors. Hence, the A/A mutation and the presence of miR219 may serve as a rheostat for down-regulating EGFR levels. This mechanism is consistent with the tumor suppressor role of miR219 [52]. Surprisingly, EGFR-AS1 was recently described as an indicator of shorter overall and disease-free survival in a cohort of Chinese patients [30]. The inverse situation we observed for Caucasian patients of the TCGA needs further evaluation.

In conclusion, EGFR is a relevant therapeutic target for mRCC in combination with anti-angiogenic treatment but only in the presence of a relevant mutation, different to those described in lung cancer. Association of first-generation immunotherapy with IFN should be revisited because of the associated debilitating side effects and new associations with immune checkpoint inhibitors may have a strong therapeutic impact.

Supplementary Material Supplementary figures and tables.
http://www.thno.org/v10p1107s1.pdf

Acknowledgements

This work was supported by the French association for cancer research (ARC), the Fondation de France, the French National Institute for Cancer Research (INCA, SUNITRES contract), the Agence Nationale de la Recherche (ANR), The Centre Scientifique de Monaco (Call for clinical research projects), the Ligue Nationale contre le Cancer (Equipe labellisée 2019), the "Conseil Général des Alpes Maritimes", the association "Cordon de Vie" directed by Mrs Fabienne Mourou and the Fondation

François Xavier Mora.

We thank Mr Nicolas Rijo and Dr Hervé Raps for the management of patient samples, Dr Baharia Mograbi, Dr Patrick Brest, Dr Agnès Paquet and Dr Bernard Mari for helpful discussions, Dr Nicola Nottet for bioinformatic analysis, and Dr MChristiane Brahimi-Horn for editorial assistance.

Competing Interests

The authors have declared that no competing interest exists.

References

1. Escudier B, Pluzanska A, Koralewski P, Ravaud A, Bracarda S, Szczylik C, et al. Bevacizumab plus interferon alfa-2a for treatment of metastatic renal cell carcinoma: a randomised, double-blind phase III trial. Lancet. 2007; 370: 2103-11.
2. Escudier B, Porta C, Bono P, Powles T, Eisen T, Sternberg CN, et al. Randomized, controlled, double-blind, cross-over trial assessing treatment preference for pazopanib versus sunitinib in patients with metastatic renal cell carcinoma: PISCES Study. J Clin Oncol. 2014; 32: 1412-8.
3. Motzer RJ, Hutson TE, Cella D, Reeves J, Hawkins R, Guo J, et al. Pazopanib versus sunitinib in metastatic renal-cell carcinoma. N Engl J Med. 2013; 369: 722-31.
4. Sennino B, Ishiguro-Oonuma T, Wei Y, Naylor RM, Williamson CW, Bhagwandin V, et al. Suppression of tumor invasion and metastasis by concurrent inhibition of c-Met and VEGF signaling in pancreatic neuroendocrine tumors. Cancer Discov. 2012; 2: 270-87.
5. Cao Y, Hoeppner LH, Bach S, E G, Guo Y, Wang E, et al. Neuropilin-2 promotes extravasation and metastasis by interacting with endothelial alpha5 integrin. Cancer Res. 2013; 73: 4579-90.
6. Cao Y, E G, Wang E, Pal K, Dutta SK, Bar-Sagi D, et al. VEGF exerts an angiogenesis-independent function in cancer cells to promote their malignant progression. Cancer Res. 2012; 72: 3912-8.
7. Shojaei F, Wu X, Qu X, Kowanetz M, Yu L, Tan M, et al. G-CSF-initiated myeloid cell mobilization and angiogenesis mediate tumor refractoriness to anti-VEGF therapy in mouse models. Proc Natl Acad Sci U S A. 2009; 106: 6742-7.
8. Grepin R, Guyot M, Giuliano S, Boncompagni M, Ambrosetti D, Chamorey E, et al. The CXCL7/CXCR1/2 axis is a key driver in the growth of clear cell renal cell carcinoma. Cancer Res. 2014; 74: 873-83.
9. Grepin R, Guyot M, Jacquin M, Durivault J, Chamorey E, Sudaka A, et al. Acceleration of clear cell renal cell carcinoma growth in mice following bevacizumab/Avastin treatment: the role of CXCL cytokines. Oncogene. 2012; 31: 1683-94.
10. Garcia-Cenador MB, Lopez-Novoa JM, Diez J, Garcia-Criado FJ. Effects and mechanism of organ protection by cardiotrophin-1. Curr Med Chem. 2013; 20: 246-56.
11. Garcia-Donas J, Esteban E, Leandro-Garcia LJ, Castellano DE, del Alba AG, Climent MA, et al. Single nucleotide polymorphism associations with response and toxic effects in patients with advanced renal-cell carcinoma treated with first-line sunitinib: a multicentre, observational, prospective study. Lancet Oncol. 2011; 12: 1143-50.
12. Nishi H, Nishi KH, Johnson AC. Early Growth Response-1 gene mediates up-regulation of epidermal growth factor receptor expression during hypoxia. Cancer Res. 2002; 62: 827-34.
13. de Paulsen N, Brychzy A, Fournier MC, Klausner RD, Gnarra JR, Pause A, et al. Role of transforming growth factor-alpha in von Hippel--Lindau (VHL)(-/-) clear cell renal carcinoma cell proliferation: a possible mechanism coupling VHL tumor suppressor inactivation and tumorigenesis. Proc Natl Acad Sci U S A. 2001; 98: 1387-92.
14. Grepin R, Ambrosetti D, Marsaud A, Gastaud L, Amiel J, Pedeutour F, et al. The relevance of testing the efficacy of anti-angiogenesis treatments on cells derived from primary tumors: a new method for the personalized treatment of renal cell carcinoma. PLoS ONE. 2014; 9: e89449.
15. Griseri P, Bourcier C, Hieblot C, Essafi-Benkhadir K, Chamorey E, Touriol C, et al. A synonymous polymorphism of the Tristetraprolin (TTP) gene, an AU-rich mRNA-binding protein, affects translation efficiency and response to Herceptin treatment in breast cancer patients. Hum Mol Genet. 2011; 20: 4556-68.
16. Paez JG, Janne PA, Lee JC, Tracy S, Greulich H, Gabriel S, et al. EGFR mutations in lung cancer: correlation with clinical response to gefitinib therapy. Science. 2004; 304: 1497-500.
17. Ciardiello F, Caputo R, Bianco R, Damiano V, Fontanini G, Cuccato S, et al. Inhibition of growth factor production and angiogenesis in human cancer cells by ZD1839 (Iressa), a selective epidermal growth factor receptor tyrosine kinase inhibitor. Clin Cancer Res. 2001; 7: 1459-65.
18. Ciardiello F, Troiani T, Bianco R, Orditura M, Morgillo F, Martinelli E, et al. Interaction between the epidermal growth factor receptor (EGFR) and the vascular endothelial growth factor (VEGF) pathways: a rational approach for multi-target anticancer therapy. Ann Oncol. 2006; 17 Suppl 7: vii109-14.
19. Escudier B, Bellmunt J, Negrier S, Bajetta E, Melichar B, Bracarda S, et al. Phase III trial of bevacizumab plus interferon alfa-2a in patients with metastatic renal cell carcinoma (AVOREN): final analysis of overall survival. J Clin Oncol. 2010; 28: 2144-50.
20. Rowinsky EK, Schwartz GH, Gollob JA, Thompson JA, Vogelzang NJ, Figlin R, et al. Safety, pharmacokinetics, and activity of ABX-EGF, a fully human anti-epidermal growth factor receptor monoclonal antibody in patients with metastatic renal cell cancer. J Clin Oncol. 2004; 22: 3003-15.
21. Drucker B, Bacik J, Ginsberg M, Marion S, Russo P, Mazumdar M, et al. Phase II trial of ZD1839 (IRESSA) in patients with advanced renal cell carcinoma. Invest New Drugs. 2003; 21: 341-5.
22. Gerlinger M, Rowan AJ, Horswell S, Larkin J, Endesfelder D, Gronroos E, et al. Intratumor heterogeneity and branched evolution revealed by multiregion sequencing. N Engl J Med. 2012; 366: 883-92.
23. Brodaczewska KK, Szczylik C, Fiedorowicz M, Porta C, Czarnecka AM. Choosing the right cell line for renal cell cancer research. Mol Cancer. 2016; 15: 83.
24. Dufies M, Giuliano S, Ambrosetti D, Claren A, Ndiaye PD, Mastri M, et al. Sunitinib Stimulates Expression of VEGFC by Tumor Cells and Promotes Lymphangiogenesis in Clear Cell Renal Cell Carcinomas. Cancer Res. 2017; 77: 1212-26.
25. Behbahani TE, Thierse C, Baumann C, Holl D, Bastian PJ, von Ruecker A, et al. Tyrosine kinase expression profile in clear cell renal cell carcinoma. World J Urol. 2012; 30: 559-65.
26. Soares MJ, Pinto M, Henrique R, Vieira J, Cerveira N, Peixoto A, et al. CSF1R copy number changes, point mutations, and RNA and protein overexpression in renal cell carcinomas. Mod Pathol. 2009; 22: 744-52.
27. Szade A, Grochot-Przeczek A, Florczyk U, Jozkowicz A, Dulak J. Cellular and molecular mechanisms of inflammation-induced angiogenesis. IUBMB Life. 2015; 67: 145-59.
28. Escudier B, Sharma P, McDermott DF, George S, Hammers HJ, Srinivas S, et al. CheckMate 025 Randomized Phase 3 Study: Outcomes by Key Baseline Factors and Prior Therapy for Nivolumab Versus Everolimus in Advanced Renal Cell Carcinoma. Eur Urol. 2017.
29. McDermott DF, Huseni MA, Atkins MB, Motzer RJ, Rini BI, Escudier B, et al. Clinical activity and molecular correlates of response to atezolizumab alone or in combination with bevacizumab versus sunitinib in renal cell carcinoma. Nat Med. 2018; 24: 749-57.
30. Wang A, Bao Y, Wu Z, Zhao T, Wang D, Shi J, et al. Long noncoding RNA EGFR-AS1 promotes cell growth and metastasis via affecting HuR mediated mRNA stability of EGFR in renal cancer. Cell Death Dis. 2019; 10: 154.
31. Tan DSW, Chong FT, Leong HS, Toh SY, Lau DP, Kwang XL, et al. Long noncoding RNA EGFR-AS1 mediates epidermal growth factor receptor addiction and modulates treatment response in squamous cell carcinoma. Nat Med. 2017; 23: 1167-75.
32. Lynch TJ, Bell DW, Sordella R, Gurubhagavatula S, Okimoto RA, Brannigan BW, et al. Activating mutations in the epidermal growth factor receptor underlying responsiveness of non-small-cell lung cancer to gefitinib. N Engl J Med. 2004; 350: 2129-39.
33. Do SI, Jung WW, Kim HS, Park YK. The expression of epidermal growth factor receptor and its downstream signaling molecules in osteosarcoma. Int J Oncol. 2009; 34: 797-803.
34. Taguchi T, Tsukuda M, Imagawa-Ishiguro Y, Kato Y, Sano D. Involvement of EGFR in the response of squamous cell carcinoma of the head and neck cell lines to gefitinib. Oncol Rep. 2008; 19: 65-71.
35. Motzer RJ, Amato R, Todd M, Hwu WJ, Cohen R, Baselga J, et al. Phase II trial of antiepidermal growth factor receptor antibody C225 in patients with advanced renal cell carcinoma. Invest New Drugs. 2003; 21: 99-101.
36. Srinivasan R, Su D, Stamatakis L, Siddiqui MM, Singer E, Shuch B, et al. Mechanism based targeted therapy for hereditary leiomyomatosis and renal cell cancer (HLRCC) and sporadic papillary renal cell carcinoma: interim results from a phase 2 study of bevacizumab and erlotinib. European Journal of Cancer. 2014; 50, Supplement 6: 8.
37. Belsante M, Darwish O, Youssef R, Bagrodia A, Kapur P, Sagalowsky AI, et al. Lymphovascular invasion in clear cell renal cell carcinoma--association with disease-free and cancer-specific survival. Urol Oncol. 2014; 32: 30 e23-8.
38. Criscitiello C, Esposito A, Curigliano G. Tumor-stroma crosstalk: targeting stroma in breast cancer. Curr Opin Oncol. 2014; 26: 551-5.
39. Sonpavde G, Willey CD, Sudarshan S. Fibroblast growth factor receptors as therapeutic targets in clear-cell renal cell carcinoma. Expert Opin Investig Drugs. 2014; 23: 305-15.
40. Ebos JM, Lee CR, Kerbel RS. Tumor and host-mediated pathways of resistance and disease progression in response to antiangiogenic therapy. Clin Cancer Res. 2009; 15: 5020-5.
41. Schreier B, Gekle M, Grossmann C. Role of epidermal growth factor receptor in vascular structure and function. Curr Opin Nephrol Hypertens. 2014; 23: 113-21.
42. Menke J, Kriegsmann J, Schimanski CC, Schwartz MM, Schwarting A, Kelley VR. Autocrine CSF-1 and CSF-1 receptor coexpression promotes renal cell carcinoma growth. Cancer Res. 2012; 72: 187-200.

43. Mantovani A, Allavena P, Sica A, Balkwill F. Cancer-related inflammation. Nature. 2008; 454: 436-44.
44. Lin EY, Pollard JW. Tumor-associated macrophages press the angiogenic switch in breast cancer. Cancer Res. 2007; 67: 5064-6.
45. Lin EY, Nguyen AV, Russell RG, Pollard JW. Colony-stimulating factor 1 promotes progression of mammary tumors to malignancy. J Exp Med. 2001; 193: 727-40.
46. Massari F, Santoni M, Ciccarese C, Santini D, Alfieri S, Martignoni G, et al. PD-1 blockade therapy in renal cell carcinoma: Current studies and future promises. Cancer Treat Rev. 2015; 41: 114-21.
47. Motzer RJ, Tannir NM, McDermott DF, Aren Frontera O, Melichar B, Choueiri TK, et al. Nivolumab plus Ipilimumab versus Sunitinib in Advanced Renal-Cell Carcinoma. N Engl J Med. 2018; 378: 1277-90.
48. Kobayashi S, Boggon TJ, Dayaram T, Janne PA, Kocher O, Meyerson M, et al. EGFR mutation and resistance of non-small-cell lung cancer to gefitinib. N Engl J Med. 2005; 352: 786-92.
49. Wheler JJ, Falchook GS, Tsimberidou AM, Hong DS, Naing A, Piha-Paul SA, et al. Aberrations in the epidermal growth factor receptor gene in 958 patients with diverse advanced tumors: implications for therapy. Ann Oncol. 2013; 24: 838-42.
50. Pflueger D, Sboner A, Storz M, Roth J, Comperat E, Bruder E, et al. Identification of molecular tumor markers in renal cell carcinomas with TFE3 protein expression by RNA sequencing. Neoplasia. 2013; 15: 1231-40.
51. Supek F, Minana B, Valcarcel J, Gabaldon T, Lehner B. Synonymous mutations frequently act as driver mutations in human cancers. Cell. 2014; 156: 1324-35.
52. Sun X, Xu M, Liu H, Ming K. MicroRNA-219 is downregulated in non-small cell lung cancer and inhibits cell growth and metastasis by targeting HMGA2. Mol Med Rep. 2017; 16: 3557-64.

Appendix 4. Review 1.

Les Neuropilines, des cibles pertinentes pour améliorer le traitement des cancers. *Médecine/sciences.* 2020.

Aurore Dumond, Luc Demange and Gilles Pagès.

médecine/sciences 2020 ; 36 : 487-96

Les neuropilines

Des cibles pertinentes pour améliorer le traitement des cancers

Aurore Dumond[1], Luc Demange[2], Gilles Pagès[1,3]

> Une angiogenèse exacerbée est une des caractéristiques (« *hallmarks* ») du cancer, définies par Hanahan et Weinberg[1]. Cependant, le ciblage de la voie de signalisation du VEGF (*vascular endothelial growth factor*) ou de ses récepteurs a montré ses limites thérapeutiques. Après un bénéfice thérapeutique indéniable pour les patients, les tumeurs récidivent après quelques mois, et deviennent généralement métastatiques et incurables. Les neuropilines 1 et 2 (NRP1, 2) dont l'activité a été décrite initialement dans le système nerveux, stimulent de nombreuses fonctions impliquées dans l'agressivité tumorale, notamment la prolifération cellulaire, l'angiogenèse et la lymphangiogenèse, ainsi que la tolérance immunitaire. Ainsi, une surexpression de NRP1 ou 2 dans de nombreuses tumeurs, est corrélée à une survie courte des patients. Cette revue a pour objectif de décrire les mécanismes d'action impliqués dans la stimulation de NRP1 et NRP2 et de faire le point sur les stratégies thérapeutiques en études précliniques ou en essais de phase précoces chez des patients atteints de différents cancers. <

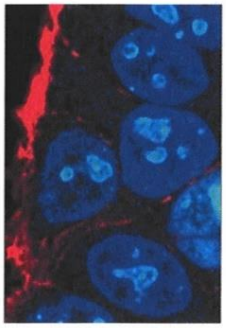

[1]Centre scientifique de Monaco, Département de biologie médicale, 8 quai Antoine Ier, MC-98000 Monaco, Principauté de Monaco.
[2]Université de Paris, CiTCoM, UMR 8038 CNRS, Faculté de Pharmacie, 4 avenue de l'Observatoire, F-75006 Paris, France.
[3]Université Côte d'Azur, Institut de recherche sur le cancer et le vieillissement de Nice, CNRS UMR 7284 ; Inserm U1081, Centre Antoine Lacassagne, 33 avenue de Valombrose, 06189 Nice, France.
gpages@unice.fr

Les neuropilines

Organisation génomique et structure protéique

Les neuropilines (NRP) sont des glycoprotéines membranaires de type-1[2] d'une taille de 130-140 kDa. Deux protéines de la même famille, NRP1 et NRP2, codées par des gènes différents positionnés sur deux chromosomes (10p12 pour NRP1 et 2q34 pour NRP2), partagent 44 % d'homologie de séquence. Elles sont composées d'un domaine extracellulaire N-terminal, d'un domaine transmembranaire et d'un domaine cytoplasmique de 43-44 acides aminés. La partie extracellulaire comprend cinq domaines : a1, a2, b1, b2 et c. La partie cytoplasmique ne contient pas de domaine de signalisation mais un motif PDZ[3] et un triplet d'acides aminés SEA (sérine, acide glutamique, alanine). Le domaine PDZ permet la formation et la stimulation des complexes de signalisation. Les domaines membranaire et cytoplasmique sont impliqués dans la dimérisation de récepteurs. Des formes solubles de NRP1 et NRP2 (sNRP1, sNRP2) dépourvues des domaines transmembranaires et cytoplasmiques et une isoforme de NRP2 sans motif SEA sont issues d'épissages alternatifs *(Figure 1)*.

L'invalidation des gènes *NRP*

L'invalidation du gène *NRP1* entraîne des anomalies du développement cardiaque et du développement des réseaux vasculaires et nerveux. Ces déficiences conduisent à une létalité embryonnaire entre 10 et 12,5 jours [1]. La surexpression de *NRP1* est également létale pour les embryons d'environ 12,5 jours, provoquant des malformations cardiaques [2].

L'absence du gène *NRP2* n'est pas létale mais une diminution des vaisseaux lymphatiques et des défauts du système nerveux ont été observés chez les animaux invalidés (KO) [3].

Les souris doublement invalidées pour *NRP1* et *NRP2* présentent des anomalies vasculaires plus graves. Les embryons, qui meurent à

Vignette (Photo © Inserm-Delapierre, Patrick).

[1] L'article de D. Hanahan D et R.A. Weinberg, publié en 2000 dans *Cell* [40] est un article majeur décrivant les caractéristiques distinctives des cancers. Il sera complété par les mêmes auteurs en 2011 [41].

[2] Ancrée dans la membrane par une hélice α hydrophobe.

[3] PDZ est un acronyme reprenant le nom des trois protéines dans lesquelles le motif a été initialement décrit : *Post-synaptic density protein 95* (PSD-95), *drosophila disc large tumor suppressor* (Dlg1) et *zona occludens 1* (ZO-1).

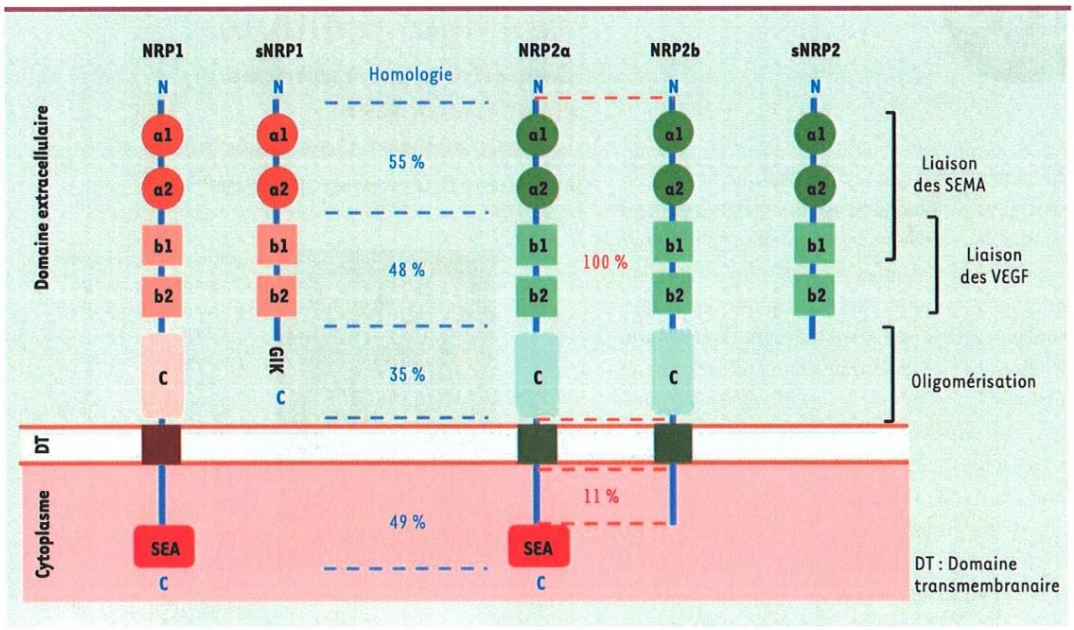

Figure 1. *Structures des domaines de NRP1 et NRP2 et variants d'épissage.* Le domaine extracellulaire comprend deux domaines CUB (a1/a2) (complément 1r/s, Uegf - protéine embryonnaire de l'oursin - et BMP1), deux domaines d'homologie aux facteurs de coagulation V/VIII (b1/b2), et un domaine MAM (homologue à la protéase méprine, à l'antigène A5, et à la tyrosine phosphatase récepteur μ et κ) (c). Les domaines de liaison de SEMA3A et VEGF sont indiqués. Les formes solubles (sNRP1 and sNRP2) ont un domaine extracellulaire tronqué et sont dépourvues des domaines transmembranaires et cytosoliques. Deux formes de NRP2 issues d'un épissage alternatif sont représentées. La partie intracellulaire de ces formes ne présente que 11 % d'homologie. Le pourcentage d'homologie des différents domaines (extracellulaire membranaire et cytosolique) est indiqué. Les domaines C-terminaux de NRP1 et NRP2a contiennent une séquence de liaison (SEA) à la protéine à domaine PDZ GPIC (ou synectine) [5, 6] (adapté de [8]).

8,5 jours du développement embryonnaire [4], présentent de grandes zones avasculaires et des interstices entre les vaisseaux sanguins.

Les ligands et interacteurs des NRP

Les NRP sont apparemment dépourvues de capacités de signalisation intrinsèque en raison de l'absence de domaine catalytique intracellulaire. Elles exercent donc leur activité principalement en tant que corécepteurs. Néanmoins, le court domaine intracellulaire des NRP se lie à la synectine, une protéine à domaine PDZ, également appelée GIPC1 (*GAIP-interacting protein C terminus, member 1*) [5, 6]. L'interaction entre NRP et GIPC1 créerait une plateforme moléculaire permettant le recrutement de petites protéines G, Ras, Rac1 ou RhoA, à la membrane, à l'origine de la stimulation des voies de signalisation auxquelles participent ERK (*extracellular signal-regulated kinases*) et AKT (protéine kinase B) [7].

Les NRP ayant fixé un ligand forment un hétérodimère avec le récepteur qui lui est spécifique. Cinq familles de récepteurs de spécificités différentes interagissent avec les NRP (voir plus loin). Dans le cas de dimères de ligands, les NRP peuvent également interagir entre elles formant des homo- ou des hétérodimères de NRP. Elles se lient alors à des dimères de récepteurs partenaires formant un complexe qui induit une signalisation intracellulaire spécifique.

Sémaphorines et plexines

Les NRP ont été décrites initialement comme des récepteurs neuronaux liant les sémaphorines (SEMA), une famille de protéines (sept classes ont été décrites) dont le rôle est de guider la croissance des axones. Les NRP, *via* leurs domaines a1, a2, b1 et b2, interagissent avec les plexines, les récepteurs spécifiques des SEMA [8]. C'est cette liaison qui conduit à l'activation des voies de signalisation impliquées dans le développement, le guidage axonal et dans l'immunité. NRP1 se lie préférentiellement à SEMA3A et NRP2 à SEMA3C ou SEMA 3F [8].

VEGF et VEGFR

Le gène *VEGF* (*vascular endothelial growth factor*) comprend 8 exons. Les exons 1 à 5 correspondent à des domaines de la protéine impliqués dans la liaison à

ses récepteurs (les VEGFR1 et VEGFR2) tandis que les domaines codés par les exons 7 et 8 se lient à NRP1 et NRP2. Les différents épissages des exons 6, 7 et 8 du gène génèrent deux familles distinctes d'isoformes de la protéine. Les isoformes correspondant à l'exon 8a sont pro-angiogéniques tandis que les isoformes provenant de l'exon 8b sont anti-angiogéniques [9]. Quatre formes prédominantes de VEGF existent : le VEGF121, le VEGF189, le VEGF206 et, surtout, le VEGF165 qui est le plus abondant et le plus actif dans de nombreux cancers. Il se lie préférentiellement à NRP1 (avec un Kd de 0,2nM) plutôt qu'à NRP2 (pour lequel le Kd est de 5nM).

La liaison du VEGF165 à NRP1 conduit à la formation d'un complexe associant les récepteurs VEGFR1 et VEGFR2. Cette association entre les VEGFR et NRP1 amplifie le signal induit par le VEGF165 et stimule ainsi l'angiogenèse. NRP2 lie le VEGF165 et le VEGFC, le principal facteur de lymphangiogenèse. Il s'associe aux récepteurs VEGFR2 et VEGFR3 pour stimuler l'angiogenèse et la lymphangiogenèse. La liaison entre ces VEGFR et NRP2 repose sur les domaines b1 et b2 de la protéine NRP. Les VEGFR peuvent également être activés par les VEGF, indépendamment des NRP. La liaison du VEGF à NRP1 induit la migration cellulaire et stimule l'angiogenèse sans intervention des VEGFR. À noter que les NRP solubles (sNRP) sont des compétiteurs pour la liaison du VEGF au NRP1 membranaire.

Une surexpression des VEGF a été observée dans la plupart des cancers humains. L'étude de la stimulation des NRP par le VEGF semble donc pertinente dans un contexte thérapeutique.

HGF et cMET

La signalisation induite par la fixation du facteur de croissance hépatocytaire (HGF) à son récepteur (cMET) régule la survie, la prolifération et la migration des cellules endothéliales. La liaison de HGF à cMET joue également un rôle important dans la progression tumorale. En s'associant à cMET, NRP1 amplifie l'invasion tumorale induite par HGF. La liaison d'HGF à cMET inhibe l'apoptose et favorise la tolérance immunitaire, en interagissant avec le ligand de mort programmé 1 (PD-L1) [10]. NRP1 stimulerait ainsi la croissance tumorale en inhibant l'immunité antitumorale.

TGF-β1 et TGF-βR

La fixation du TGFβ1 (*transforming growth factor beta 1*) à son récepteur, le TGFβR, stimule la voie de signalisation impliquant SMAD2 et SMAD3, régule la transition épithélio-mésenchymateuse (TEM) et promeut la progression et l'invasion tumorale. NRP1 fixe le TGFβ par son domaine b1 et interagit avec les récepteurs TGFβR1, 2 et 3. La signalisation qui en résulte stimule l'angiogenèse indépendamment du VEGFR2. Le complexe TGFβ/NRP1/TGFβR promeut également l'activité des lymphocytes T régulateurs et donc la tolérance immunitaire.

PDGF et PDGFR

La liaison du PDGF (*platelet-derived growth factor*) à son récepteur (le PDGFR) induit une signalisation qui stimule la prolifération et la différenciation cellulaires. Il existe quatre formes de PDGF : PDGFA, B, C et D, qui s'homo- ou s'hétéro-dimérisent et se fixent sur les récepteurs PDGFRα ou β, des récepteurs tyrosine kinase qui s'autophosphorylent après liaison de leur ligand. Selon l'isoforme de PDGF, le récepteur s'homo- ou s'hétéro-dimérise, conduisant à trois combinaisons entre les deux formes du récepteur : αα, αβ ou ββ. La liaison du PDGF au PDGFR active les MAPK (*mitogen-activated protein kinases*) et la voie impliquant la phosphoinositide 3-kinase (PI3K). NRP1 s'associe au PDGFR lié au PDGF, amplifiant ainsi les voies de signalisation qui sont induites.

FGF et FGFR2

La fixation du FGF (*fibroblast growth factor*) au récepteur FGFR2 induit la migration et la prolifération cellulaires. Cet axe de signalisation est majeur pour la prolifération des cellules endothéliales et donc pour l'angiogenèse. En s'associant au FGFR2, les NRP jouent un rôle clé dans l'amplification des signaux qui sont induits par le FGF.

La voie de signalisation Hedgehog

La voie de signalisation Hedgehog est impliquée dans l'embryogenèse et, chez l'adulte, dans la réparation tissulaire. Son activation stimule la prolifération et la différenciation cellulaires. Sa sur- ou sous-expression est à l'origine du développement de cancers. Dans des cellules de cancers du rein à cellules claires (ccRCC), la réduction de l'expression de *NRP1* (par shARN[4]) permet de diminuer celle de *sonic hedgehog* (SHH)[5] et de son activateur transcriptionnel Gli1 (*glioma-associated oncogene homolog 1*). L'inhibition de la voie de signalisation impliquant SHH force la différenciation des cellules tumorales [11].

Rôles des NRP dans le système immunitaire *(Tableau I)*

Les cellules dendritiques

Ces cellules sont recrutées au site où un antigène est présent. En réponse, elles subissent une maturation qui leur permet de migrer vers les organes lymphoïdes afin d'activer les lymphocytes T naïfs et induire la réponse immunitaire primaire spécifique de l'antigène. NRP1, qui est exprimé par les cellules dendritiques matures et par les lymphocytes T naïfs, permet l'adhérence des deux cellules par une interaction homophilique (NRP1/NRP1). NRP1 participe donc à l'activation de la réponse immunitaire primaire. NRP1, exprimé à la surface des lymphocytes T, peut également interagir avec SEMA3A

[4] Petits ARN en épingle à cheveux : ils permettent de réduire l'expression d'un gène par interférence.

[5] L'une des trois protéines impliquées dans la voie de signalisation Hedgehog. Les deux autres sont DHH (*desert Hedgehog homolog*) et IHH (*indian Hedgehog homolog*).

	Cellules dendritiques	Macrophages	Lymphocytes T cytotoxiques	Lymphocytes T auxiliaires	Cellules NKT	Lymphocytes T régulateurs
NRP1	+ (Interaction avec les lymphocytes T naïfs) – (Interaction avec les lymphocytes T activés)	+ (Migration vers les zones hypoxiques) – (Interaction avec les lymphocytes T régulateurs)	+ (Reconnaissance de l'antigène) ?	+ (Différenciation des lymphocytes B)	?	+ (Interaction avec les cellules dendritiques) –
NRP2	+ (Migration vers les ganglions lymphatiques)	+ (Induction de la phagocytose)	?	?	?	– (Inhibition de la migration des lymphocytes T)

Tableau I. *Le rôle des NRP dans le système immunitaire.* La présence de NRP1 ou NRP2 sur chaque cellule du système immunitaire est mentionnée. Un rôle immunostimulant est indiqué par +, un rôle immunosuppresseur par –. L'absence de détermination de la présence de NRP est mentionnée par ? (le ? correspond en fait, au fait que le rôle d'activateur du système immunitaire ou immunosuppressif de NRP1 ou 2 sur ces cellules n'a pas encore été décrit et pas l'absence de détermination de la présence de NRP).

qui est présent sur les cellules dendritiques et les lymphocytes T, ce qui inhibe l'activation et la prolifération de ces derniers et donc induit une tolérance immunitaire [12].

Les cellules dendritiques peuvent avoir pour origine les monocytes circulants. La différenciation de ces monocytes en cellules dendritiques s'accompagne d'une augmentation d'expression de NRP2 [13]. La sialylation de NRP2 protègerait en fait les cellules dendritiques lors de leur migration vers les ganglions lymphatiques. Dans les ganglions, l'acide polysialique porté par NRP2 sera éliminé, permettant aux cellules dendritiques d'activer les lymphocytes T [14].

Les macrophages

Les macrophages jouent un rôle prépondérant dans la surveillance immunitaire, l'élimination des débris cellulaires et la présentation antigénique aux lymphocytes. Deux types de macrophages ont été distingués : les macrophages de type M1 qui sont pro-inflammatoires et les macrophages de type M2, pro-angiogéniques, immunosuppressifs et donc pro-tumoraux, notamment dans les tissus qui sont hypoxiques. L'hypoxie induit l'expression de SEMA3A par les cellules tumorales. Elles peuvent alors interagir avec NRP1 qui est exprimé par les macrophages, en association avec les récepteurs de SEMA3A, les plexines A1 et A4, également exprimés par les macrophages. Les macrophages associés aux tumeurs (TAM) sont retenus dans les zones hypoxiques où ils exercent leur rôle pro-tumoral. La diminution de l'expression de NRP1 par les macrophages se traduit par une limitation de la localisation de ces TAM dans les zones périphériques de la tumeur qui sont normoxiques, ce qui supprime le caractère pro-tumoral de ces cellules [15]. Dans la microglie (constituée de cellules macrophagiques au niveau du cerveau), NRP1 joue un rôle immunosuppresseur en favorisant la différenciation des cellules vers un phénotype de type M2. Une interaction homophilique (NRP1/NRP1) entre cellules microgliales et lymphocytes T régulateurs provoque une libération de TGF-β et une immunosuppression. L'expression de NRP1 par les macrophages associés aux gliomes (GAM) provoque ainsi une réponse pro-tumorale. Son inhibition réduit la croissance tumorale et induit une polarisation des cellules vers le type M1, antitumoral [16].

L'expression de *NRP2* augmente lors de la différenciation des monocytes en macrophages [13] à proximité des zones d'inflammation, ce qui se traduit par une augmentation de la capacité de phagocytose des cellules. À noter que la sialylation de NRP2 réduit la capacité de phagocytose des macrophages [17].

Les lymphocytes T

Les lymphocytes T cytotoxiques (T $CD8^+$) détruisent les cellules infectées présentant un peptide antigénique issu du pathogène associé à une molécule du complexe majeur d'histocompatibilité (CMH) de classe I. L'expression de NRP1 est augmentée à la surface des lymphocytes T $CD8^+$ effecteurs et mémoires, et favorise la reconnaissance de l'antigène [8]. Néanmoins, le rôle exact de NRP1 dans ce contexte reste inconnu.

Les lymphocytes T auxiliaires (T $CD4^+$) produisent de l'interleukine 2 et de l'interféron gamma qui stimulent la prolifération des lymphocytes T et B. NRP1 est exprimé par les lymphocytes T $CD4^+$. Il permet, par ailleurs, la maturation des lymphocytes B [8].

Les lymphocytes T régulateurs (Treg) sont essentiels à la prévention des maladies auto-immunes. NRP1 maintient ces fonctions grâce à son interaction avec SEMA4A, exprimée par les cellules dendritiques. Cette

liaison stabilise en effet les lymphocytes Treg en recrutant PTEN (homologue de phosphatase et tensine) et en inhibant la phosphorylation d'Akt. L'expression de NRP1 par les lymphocytes Treg permet leur migration vers les tumeurs où ils jouent un rôle immunosuppresseur. La liaison homophilique des molécules NRP1 exprimées par les cellules dendritiques induit une tolérance immunitaire [8].

L'expression de *NRP2* est amplifiée dans les lymphocytes T $CD4^+/CD8^+$ mais elle est moins importante sur les lymphocytes T qui n'expriment que CD8 ou que CD4. L'interaction entre NRP2, SEMA3F et la plexine A1, inhibe la migration des lymphocytes T immatures.

Les cellules NKT (*natural killer T*) représentent un lien entre immunité innée et immunité adaptative. Activées, elles sont capables de détruire leur cible cellulaire et produisent des cytokines anti- et pro-inflammatoires. Le rôle de NRP1 exprimé par ces cellules reste inconnu [8].

Les NRP ont donc différents rôles dans le système immunitaire. Ils interviennent dans les capacités de migration des cellules, dans leur interaction avec d'autres cellules mais aussi dans la régulation de leur réponse immunitaire.

Rôles des NRP dans le cancer

La surexpression des NRP, généralement synonyme d'agressivité, est souvent observée dans les carcinomes, les mélanomes, les glioblastomes, les leucémies, et les lymphomes. Dans des modèles expérimentaux de cancer du poumon, la réduction de l'expression de *NRP1* diminue la migration, l'invasion cellulaire et le nombre de métastases [18]. Dans des modèles de cancer du côlon, la surexpression de *NRP2* stimule la progression tumorale et sa réduction inhibe la tumorigenèse et augmente l'apoptose [19]. Dans le cas du carcinome du rein à cellules claires (ccRCC), la diminution de l'expression de *NRP1* réduit la migration, l'invasion et la tumorigenèse [11], et de celle de *NRP2* diminue l'extravasation cellulaire dans le réseau lymphatique et la dissémination métastatique [20].

Les inhibiteurs de NRP : des approches rationnelles aux cribles multi-étapes

Du fait de leurs rôles dans l'angiogenèse, la lymphangiogenèse, la tumorigenèse et dans le système immunitaire, les NRP sont devenues des cibles pertinentes dans le traitement du cancer et, notamment, dans le traitement du carcinome du rein ccRCC, un des cancers les plus vascularisés. Un anticorps monoclonal, le MNRP-1685A, qui cible NRP1, est en cours d'essais cliniques [21] et plusieurs inhibiteurs chimiques des NRP (petites molécules, peptides, etc.) sont en phases préclinique ou clinique.

Le MNRP-1685A

Le MNRP-1685A (vésencumab) est un anticorps monoclonal humanisé spécifique des domaines extracellulaires b1 et b2 de NRP1 : il inhibe son interaction avec le VEGF. Il a été obtenu par *phage display* (une méthode de sélection d'anticorps fondée sur l'expression aléatoire par des bactériophages de fragments d'anticorps ou de peptides multiples) [22]. Dans des modèles précliniques, ses effets se sont révélés être marginaux sur la croissance tumorale. Ils sont plus importants en présence d'un anticorps spécifique du VEGF [23]. L'anticorps anti-NRP1 diminue l'intégrité vasculaire en réduisant le nombre de péricytes. Il rend ainsi les vaisseaux sanguins plus sensibles aux anticorps anti-VEGF. Le MNRP1685A a été testé dans deux essais cliniques de phase Ia et Ib, seul ou en combinaison avec un anticorps monoclonal humanisé anti-VEGF, le bévacizumab (Avastin®), dans un ensemble de tumeurs solides en échec thérapeutique [21, 24]. Le traitement a été bien toléré au cours des essais en escalade de doses, avec néanmoins quelques effets indésirables, qui ont été atténués par une prémédication par dexaméthasone. Une protéinurie élevée observée chez les patients ayant reçu l'association des deux anticorps a été rédhibitoire pour poursuivre les essais cliniques. Une augmentation d'expression de NRP1 peut néanmoins résulter d'une adaptation aux traitements, notamment dans les cancers de la prostate [25]. Il est donc important d'évaluer la pertinence d'une fenêtre thérapeutique d'administration des anticorps anti-NRP1 et de développer d'autres outils thérapeutiques plus performants.

Bases structurales pour définir des inhibiteurs chimiques de NRP1 et de NRP2

Plusieurs structures cristallines de la tuftsine (le tétrapeptide – TKPR – qui mime l'extrémité C-terminale du VEGF), du VEGF et du VEGFC, en interaction avec leur domaine de liaison à NRP1 et NRP2, ont été résolues par diffraction aux rayons X [26]. Les extrémités C-terminale de la tuftsine et du VEGF se lient aux domaines b1 et b2 des NRP, par l'intermédiaire de l'arginine en position terminale. Des liaisons hydrogène impliquent également plusieurs acides aminés de cette zone de fixation. En effet, l'asparagine en position 320 (Asp-320) établit deux liaisons hydrogène avec le motif guanidinium de la chaîne latérale de l'arginine. De même, les tyrosines Tyr-353, Thr-349 et la sérine Ser-346 interagissent avec le motif carboxyle terminal. La poche de fixation accueillant l'arginine en position C-terminale est conservée entre NRP1 et NRP2.

Le VEGFC est secrété sous la forme d'une pro-protéine qui est inactive. Elle subit une protéolyse de ses extrémités N- et C-terminales qui lui permet d'acquérir son activité biologique. La protéolyse en C-terminale libère en effet une extrémité basique contenant deux arginines (SIIRR) qui permet sa liaison aux NRP. Ainsi, seule la forme protéolysée de VEGFC interagit avec NRP2 et le stabilise. La résolution de la structure de VEGFC protéolysé, cristallisé avec les domaines b1 et b2 de NRP2, révèle une liaison similaire à celle décrite pour l'interaction entre le VEGF et NRP1.

La sélectivité de NRP1 pour le VEGF, et celle de NRP2 pour le VEGFC, ne reposent donc pas sur des différences structurales touchant les poches de fixation de l'arginine présentes dans ces deux isoformes. Cependant, deux liaisons hydrogène supplémentaires, qui s'établissent entre l'acide glutamique en position 154 (Glu-154) du VEGF et la thréonine Thr-299, spécifiques de NRP1 (absentes de NRP2), sont importantes pour cette sélectivité. Il est donc possible de cibler sélectivement NRP1 par des pseudo-peptides.

L'heptapeptide A7R et ses dérivés

Le peptide ATWLPPR (A7R) est le premier peptide inhibant l'interaction entre le VEGF et les NRP qui a été identifié par *phage display* *(Figure 2A)*. A7R bloque la fixation de VEGF radiomarqué (^{125}I-VEGF) sur le VEGFR2. Il inhibe la prolifération de cellules endothéliales (HUVEC) et bloque la croissance de tumeurs expérimentales du sein en affectant la vascularisation tumorale [27]. L'arginine C-terminale, la leucine en position 4 et les prolines en position 5 et 6 (LPRR) sont essentielles à son efficacité. Le groupement carboxyle (-COOH) de l'arginine est sous sa forme acide libre, et la torsion du squelette formé par ces quatre acides aminés est similaire celle prise par le squelette de la partie C-terminale du VEGF.

La partie N-terminale du peptide a été modifiée afin de permettre son marquage par du ^{99m}Tc (Technétium 99 m), en introduisant un motif *S*-benzoyle-mercaptoacétique. Contrairement au peptide original, le radio-peptide ne se fixe pas à NRP2, révélant l'existence d'interactions entre l'extrémité N-terminale du peptide et la protéine. Des versions stables *in vivo* d'A7R ont été développées pour des applications en photothérapie dynamique [28] ou en imagerie par résonance magnétique [29].

Peptido-mimétiques glycosylés

Des peptido-mimétiques dérivés d'A7R et rigidifiés à l'aide d'un motif carbohydrate remplaçant la séquence LPRR ont été développés [30] *(Figure 2B)*. Le peptido-mimétique le plus puissant intègre un motif phénylsulfonamide et une arginine. Il inhibe l'interaction du VEGF avec NRP1, et altère la tubulogenèse. Sa stabilité au sein du site de fixation du VEGF dans NRP1 repose non seulement sur un réseau dense de liaisons hydrogène, impliquant en particulier son motif guanidinium et l'Asp-320 de NRP1, mais également une interaction $\pi - \pi$ [6] ou cation–π impliquant son noyau phénylsulfonamide.

Pentapeptides rigidifiés

Des pseudo-peptides ramifiés de séquence générale Lys(hArg)-AA^2-AA^3-Arg^7 ont également été réalisés [31]. Les premières structures décrites possédaient une proline en position AA^3. L'interaction entre ces pseudo-peptides et NRP1 repose sur des liaisons hydrogène établies entre la partie Lys(hArg) du peptide et le carboxylate de l'Asp-320 de la protéine. La partie centrale de la séquence, les résidus AA^2 et AA^3, interviennent également dans la liaison. Différentes optimisations ont été réalisées, en remplaçant la proline en position AA^3 par certains de ses isostères[8] conventionnels *(Figure 2C)*. Sa substitution par la 3,4-déhydroproline (ΔPro) ou par l'octahydroindole (Oic) induit une stabilité métabolique du peptide qui augmente son affinité pour NRP1. Ces molécules sont en cours de développement. Des petits peptides cycliques dérivés d'A7R, plus résistants *in vivo* que les peptides linéaires, ont également été synthétisés [31].

L'EG3287 et ses dérivés

Le groupe de Zachary et Selwood à Londres (*University College London*) développe des inhibiteurs pseudo-peptidiques de NRP1 sur la base de la structure du domaine C-terminal du VEGF. Ces chercheurs se sont focalisés sur le sous-domaine structural défini par les acides aminés compris entre la Ser-138 et l'Arg-165 du VEGF, caractérisé par l'existence de deux ponts disulfures, une hélice-α et un coude β. Le peptide bicyclique correspondant à cette séquence, l'EG3287, a été synthétisé en 2006 *(Figure 3A)* [32]. Il inhibe l'interaction entre le VEGF et des cellules endothéliales porcines exprimant NRP1. Une optimisation structurale de l'EG3287 a permis d'obtenir, en 2010, un nouveau « *hit* », baptisé EG00229 [33]. Celui-ci présente un motif guanidinium, qui mime l'arginine C-terminale de VEGF, et un motif sulfonamide relié par un cœur thiophène *(Figure 3B)*. La structure chimique de cette molécule s'éloigne de celle des peptides conventionnels, mais elle en conserve cependant certains éléments de similitude (en particulier le motif guanidinium).

La structure cristallographique du complexe formé entre NRP1 et l'EG00229 montre que le peptide se superpose à la tuftsine dans la poche de fixation de l'arginine [34]. Sa fonction guanidinium établit des liaisons hydrogène avec l'Asp-320 et la Ser-149 de NRP1. L'EG00229 interfère avec la liaison de VEGF radiomarqué ([^{125}I]-VEGF) aux cellules endothéliales porcines, et inhibe l'interaction entre le VEGF et les cellules de carcinome humain de prostate DU145 qui surexpriment NRP1. Il réduit la viabilité de cellules de carcinome pulmonaire, et augmente les effets cytotoxiques du paclitaxel et du 5-fluorouacil, des chimiothérapies de première ligne utilisées dans différents cancers.

L'EG01377, décrit par la même équipe en 2018, ne se lie pas à NRP2, ce qui en fait un inhibiteur sélectif de NRP1 *(Figure 3C)*. Ce peptide inhibe la migration de cellules endothéliales humaines (HUVEC), la formation de microtubules induite par du VEGF, et la croissance de sphéroïdes générés à partir de cellules de mélanome stimulées par du VEGF [35].

[6] Liaison formée par recouvrement orbitalaire latéral entre les deux atomes.

[7] AA signifiant un acide aminé et le chiffre en exposant, sa position.

[8] De formes et encombrements comparables.

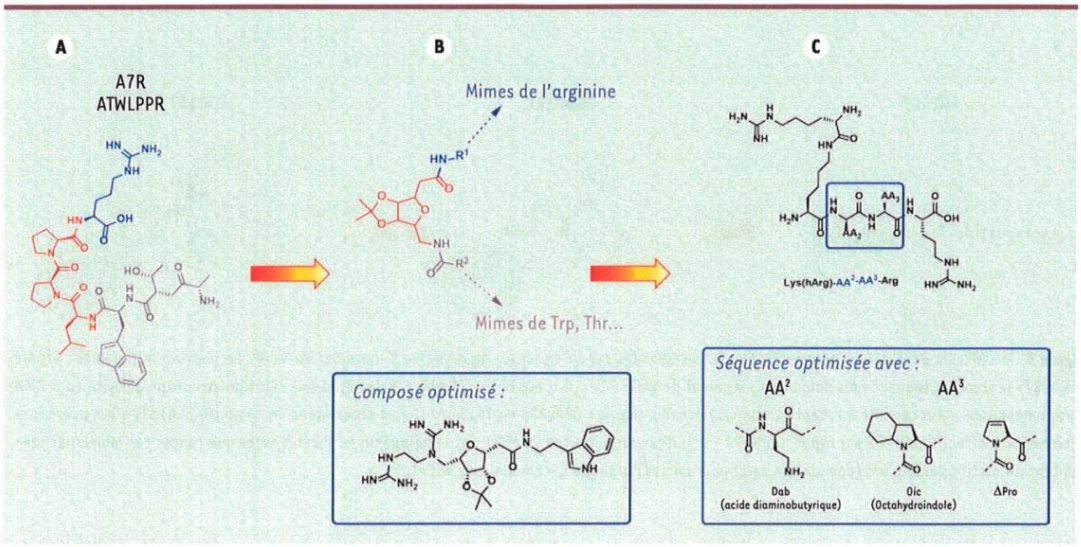

Figure 2. *Inhibiteurs peptidiques et pseudo-peptidiques dérivés de l'heptapeptide ATWLPPR (A7R). A.* Structure chimique de l'heptapeptide, identifié par phage display. Des peptides dérivés de A7R plus stables (introduction de liaison peptidiques réduites) ont été développés pour des applications en photothérapie [28] ou pour l'imagerie par résonance magnétique [29]. *B.* Première série de pseudo-peptides dérivés de A7R [30]. Dans cette série, un motif carbohydrate vient mimer la séquence LPP du peptide A7R. La molécule la plus prometteuse bloque l'interaction entre VEGF165 et NRP1 avec une IC_{50} de 39 µM. *C.* Nouvelle génération de pseudo-peptides rigidifiés [31] présentant des IC_{50} de l'ordre de 15-25 µM.

Les inhibiteurs non peptidiques sélectionnés par criblage multi-étapes

Les criblages multi-étapes, qui incluent un crible virtuel, utilisent d'importantes banques de composés afin d'identifier des molécules possédant des structures originales interagissant avec leurs cibles avec une forte affinité. Deux cribles portant sur NRP1 ont exploré une banque de 500 000 composés disponibles *via* la *ChemBridge Compound Collection*[9]. Le champ d'investigation a été réduit à 300 000 composés par l'utilisation du logiciel FAF-Drug2 qui permet d'exclure des molécules présentant des propriétés toxiques et/ou de mauvais profils pharmacologiques.

Identification du composé ChemBridge ID : 7739526, non testé *in vivo*

Les *dockings* (ou arrimages moléculaires)[10] modélisés à partir de la structure cristallographique obtenue par interaction de NRP1 avec la tuftsine (code PDB : 2ORZ)[11] ont permis aux équipes de B. Villoutreix et G. Perret (Lille) d'identifier 508 molécules potentiellement capables d'interagir avec NRP1. Leur capacité d'inhibition de la liaison entre le VEGF165 et NRP1 a été examinée (à une concentration de 100 µM) faisant émerger 7 *hits* (inhibition supérieure à 40 %). Une nouvelle étape de crible *in silico*, destinée à identifier de nouveaux produits présentant des similarités structurales avec les 7 *hits* initiaux, a été réalisée, révélant de nouveaux candidats qui ont également été testés pour leur pouvoir inhibiteur. Ce processus a été répété une troisième fois. Le meilleur composé obtenu par cette approche (ChemBridge ID : 7739526) présente une capacité d'inhibition de la liaison du VEGF165 à NRP1 comparable à celle de la tuftsine [36]. Cette molécule ne contient pas de fonction guanidinium. La prédiction de liaison suggère que l'hydrogène du motif hydroxyle de la molécule établit une liaison hydrogène avec l'Asp-320 de NRP1 et que la Glu-348 de la protéine établit une liaison hydrogène avec l'oxygène de la fonction éther reliant les deux noyaux aromatiques. Les effets de ces composés sur les cellules n'ont pas été examinés.

NRPa-47 et NRPa-308, deux antagonistes non peptidiques de NRP1 actifs *in vivo*

Dans ce crible multi-étapes réalisé par les équipes de C. Garbay, M. Montes et O. Hermine (Paris), le crible virtuel a été réalisé en utilisant pour modèle le co-cristal NRP1/tuftsine et les logiciels Surflex-dock et ICM-VLS, pour la modélisation. Une liste consensus de 3 000 composés-candidats, des petites molécules dépourvues de

[9] https://www.chembridge.com/about/

[10] Méthode de modélisation permettant de définir à partir de deux structures modélisées la meilleure configuration spatiale aboutissant à une interaction optimale.

[11] La banque de données sur les protéines *Protein Data Bank* ou PDB est une collection de données sur la structure tridimensionnelle de macromolécules biologiques.

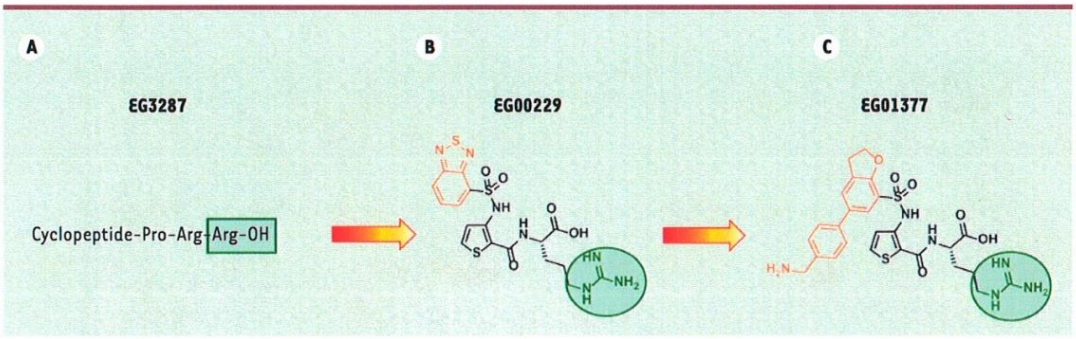

Figure 3. *Inhibiteurs peptidiques et pseudo-peptidiques fondés sur la structure du domaine C-terminal du VEGF.* Le peptide initialement étudié (EG3287) reprend la séquence du domaine C-Terminal de VEGF [32]. Il a été optimisé grâce à des étude de relation structure-activité (par RMN notamment), ce qui a conduit à l'identification du pseudo-peptide EG00229 en 2010 [33]. Plus récemment, le composé EG01377 s'est avéré être un inhibiteur sélectif de NRP1 par rapport à NRP2 [34]. Il possède *in vitro* un effet anti-angiogénique. Il est à noter que toutes ces molécules présentent un motif guanidinium (encadré en vert) pour mimer l'arginine C-terminale de VEGF165.

motifs peptidiques a émergé. L'analyse de leurs *dockings* avec NRP1 a permis de retenir 1 317 molécules qui ont été testées *in vitro*. Les tests fonctionnels réalisés sur des cellules endothéliales (crible cellulaire) ont réduit la liste à 158 candidats puis 56 molécules ont été retenues pour leur capacité à inhiber l'interaction entre le VEGF165 et NRP1 lors d'une étape de crible moléculaire. La détermination sur des cellules humaines de cancer mammaire (MDA-MB-231) des concentrations inhibitrices (IC_{50}) de ces 56 composés, a permis d'identifier deux molécules, NRPa-47 et NRPa-308, comme étant les plus prometteuses [37-39]. Ces deux candidats présentent des IC_{50} sub-micromolaires sur des cellules endothéliales et de cancer du sein *(Figure 4)*.

Le NRPa-47 présente un noyau benzimidazole connecté à un noyau benzodioxane par un bras espaceur carboxythiourée. Cette molécule est dépourvue de motif guanidinium, et l'atome d'azote du benzimidazole interagit avec l'Asp-320 de NRP1 *via* une liaison hydrogène. Le soufre du bras espaceur et l'un des atomes d'oxygène du benzodioxane établissent des liaisons hydrogène avec les résidus de la poche de liaison de NRP1 (Tyr-297 pour le soufre ; Tyr-353 et Thr-349 pour l'oxygène). Ce *docking* a permis d'optimiser la structure de cet antagoniste et d'identifier ainsi le NRPa-48 comme étant un nouvel inhibiteur de NRP1. Ce dernier composé présente des activités antiprolifératives comparables à celles du produit parent.

Le NRPa-308 possède trois noyaux aromatiques. La prédiction par *docking* suggère que le noyau portant l'éther d'éthyle s'insère profondément dans la poche de fixation de l'arginine, et interagit par *π-stacking*[12] et/ou interactions hydrophobes avec les noyaux aromatiques des Tyr-297 et Tyr-353. Cette prédiction suggère que l'oxygène de l'amide et l'azote du sulfonamide du NRPa-308 établissent des liaisons hydrogène avec le Trp-301 et la Glu-348 de NRP1.

Sur des lignées de carcinome du rein à cellules claires, le NRPa-308 exerce des effets antiprolifératifs marqués. Il est moins toxique pour des cellules isolées de tissus sains que le traitement de référence de ces cancers, le sunitinib : il possède donc un indice de sélectivité supérieur à celui du sunitinib.

NRPa-47, NRPa-48 et NRPa-308 exercent une activité anti-angiogénique et réduisent la mobilité des cellules endothéliales. Ils sont cytotoxiques sur plusieurs lignées cellulaires cancéreuses résistantes. NRPa-47 et NRPa-308 ralentissent la croissance de tumeurs expérimentales du sein chez la souris, prolongent la survie des animaux et retardent la formation de métastases. Ces molécules réduisent la vascularisation des tumeurs sans induire de toxicité aiguë. Des résultats récents suggèrent que le NRPa-308 est internalisé par les cellules tumorales [39]. Le mécanisme du franchissement de la membrane cellulaire n'est cependant pas élucidé, mais il pourrait dépendre de l'activité de transporteur des NRP.

Conclusion

Les cancers très vascularisés comme ceux du rein, du sein, du poumon, du côlon ou de la sphère ORL (oto-rhino-laryngologique) sont des modèles intéressants pour le développement de thérapies anti-angiogéniques. Actuellement, les traitements ciblant la voie VEGF/VEGFR sont administrés dans les cancers métastatiques du côlon et du rein. Leurs effets restent cependant transitoires pour la majorité des patients. Le ciblage d'autres acteurs pertinents de la vascularisation tumorale représente toujours un défi pour lutter plus efficacement contre ces pathologies. Dans cette revue, nous avons révélé le rôle majeur des NRP dans l'agressivité de nombreux cancers. Leur surexpression

[12] Interaction attractive et non covalente entre deux noyaux aromatiques.

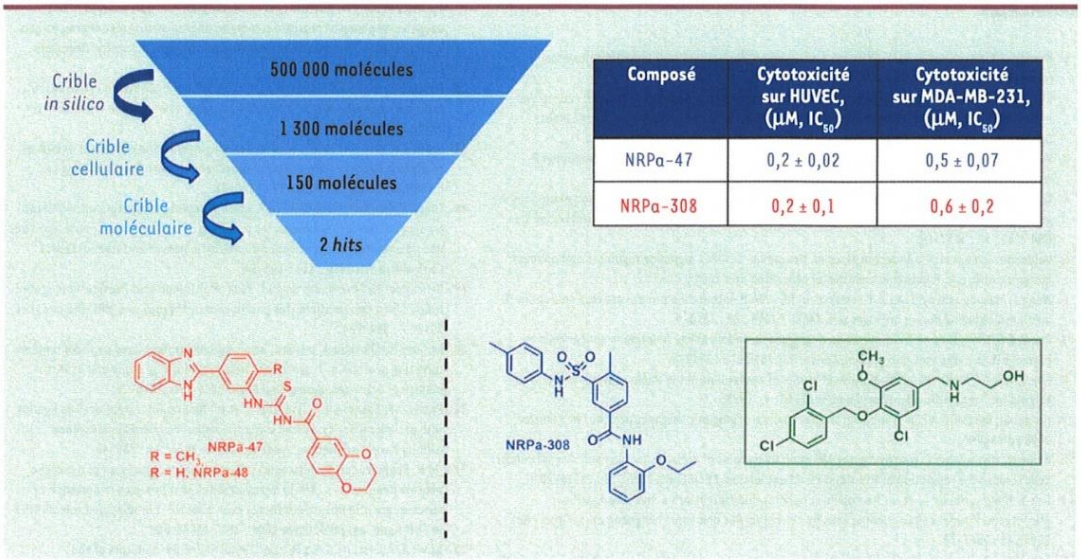

Composé	Cytotoxicité sur HUVEC, (μM, IC_{50})	Cytotoxicité sur MDA-MB-231, (μM, IC_{50})
NRPa-47	0,2 ± 0,02	0,5 ± 0,07
NRPa-308	0,2 ± 0,1	0,6 ± 0,2

Figure 4. ***Inhibiteurs non peptidiques sélectionnés par crible multi-étapes.*** Cette approche, qui combine des étapes de cribles *in silico* de bibliothèques de produits commerciaux puis des tests cellulaires et moléculaires, a permis d'identifier les premiers inhibiteurs non peptidiques de NRP1 actifs *in vivo* (les composés NRPa-47, NRPa-48 et NRPa-308) et ne présentant pas de toxicité avérée chez les animaux traités [36-38]. Le rationnel du crible est représenté en haut à gauche et les effets cellulaires en haut à droite. Ces composés ont été récemment resynthétisés par les chimistes, et leur optimisation structurale est en cours (amélioration des paramètres pharmaco-chimiques, de leur efficacité biologique, etc.). Il a également été prouvé récemment qu'une certaine fraction de NRPa-308 pénètre à l'intérieur des cellules tumorales [39]. Le composé identifié (ChemBridge ID : 7739526) est représenté dans l'encart vert [35] ; ce composé n'a pas fait l'objet d'étude *in vivo* à notre connaissance. Il est intéressant de noter qu'aucunes des molécules identifiées par cribles multi-étapes, bien que sélectionnées pour leur affinité avec la poche de fixation de NRP-1 avec le VEGF165, ne possède de motif guanidinium mimant l'arginine C-terminale.

est synonyme d'angiogenèse et de lymphangiogenèse exacerbée et est donc de mauvais pronostic. Leur rôle dans les réponses immunitaires innée et adaptive suppose leur implication importante dans l'immunité antitumorale. NRP1 joue un rôle antitumoral dans les étapes précoces de la tumorigenèse, mais dans des tumeurs de stade avancé, il devient pro-tumoral et immunosuppresseur. Le rôle de NRP2 dans le système immunitaire n'a pas été encore totalement déterminé.

Les NRP représentent donc des cibles pertinentes pour traiter différents cancers mais la cinétique d'administration de drogues capables de les inhiber doit être considérée avec prudence. De nombreuses molécules peptidiques ou biologiques qui ciblent les NRP et dont l'efficacité a été testée *in vitro* et *in vivo*, ont été développées. Le rôle spécifique de NRP1 et NRP2 reste encore à élucider afin que leur ciblage produise un effet thérapeutique optimal. ◊

SUMMARY

Neuropilins: relevant therapeutic targets to improve the treatment of cancers

Exacerbated angiogenesis is one of the hallmarks of cancer defined by Hanahan and Weinberg. However, targeting the signaling pathway of the "Vascular Endothelial Growth Factor (VEGF)" or its receptors has shown its therapeutic limits. Despite short term benefits for patients, tumors always relapse and generally become metastatic and incurable. Neuropilins 1 and 2 (NRP1, 2) whose activity was originally described in the nervous system, stimulate many parameters involved in tumor aggressiveness including cell proliferation, angiogenesis and lymphangiogenesis, and immune tolerance. Thus, an overexpression of NRP1 or 2 in many tumors, is correlated with a short survival of the patients. The purpose of this review is to describe the mechanisms of action involved in stimulating NRP1, 2 and to take stock of therapeutic strategies in preclinical studies or in early phase trials in patients with different cancers. ◊

REMERCIEMENTS

Les auteurs remercient pour leur soutien la Société Helsinn, la Ligue nationale contre le cancer (Équipe labellisée en 2019), l'Institut national du cancer (contrat : VEGFIL et SunitRES), la Fondation de France, le Programme européen FP7 - Marie Curie Intra-European grant (Contrat : VELYMPH), la Fondation François Xavier Mora, et la Cancéropole PACA.

LIENS D'INTÉRÊT

Les auteurs déclarent n'avoir aucun lien d'intérêt concernant les données publiées dans cet article.

RÉFÉRENCES

1. Kawasaki T, Kitsukawa T, Bekku Y, *et al.* A requirement for neuropilin-1 in embryonic vessel formation. *Development* 1999 ; 126 : 4895-902.
2. Kitsukawa T, Shimono A, Kawakami A, *et al.* Overexpression of a membrane protein, neuropilin, in chimeric mice causes anomalies in the cardiovascular system, nervous system and limbs. *Development* 1995 ; 121 : 4309-18.
3. Yuan L, Moyon D, Pardanaud L, *et al.* Abnormal lymphatic vessel development in neuropilin 2 mutant mice. *Development* 2002 ; 129 : 4797-806.
4. Takashima S, Kitakaze M, Asakura M, *et al.* Targeting of both mouse neuropilin-1 and neuropilin-2 genes severely impairs developmental yolk sac and embryonic angiogenesis. *Proc Natl Acad Sci USA* 2002 ; 99 : 3657-62.
5. Valdembri D, Caswell PT, Anderson KI, *et al.* Neuropilin-1/GIPC1 signaling regulates alpha5beta1 integrin traffic and function in endothelial cells. *PLoS Biol* 2009 ; 7 : e25.
6. Wang L, Mukhopadhyay D, Xu X. C terminus of RGS-GAIP-interacting protein conveys neuropilin-1-mediated signaling during angiogenesis. *FASEB J* 2006 ; 20 : 1513-5.
7. Cao Y, E G, Wang E, *et al.* VEGF exerts an angiogenesis-independent function in cancer cells to promote their malignant progression. *Cancer Res* 2012 ; 72 : 3912-8.
8. Roy S, Bag AK, Singh RK, *et al.* Multifaceted role of neuropilins in the immune system: potential targets for immunotherapy. *Front Immunol* 2017 ; 8 : 1228.
9. Harper SJ, Bates DO. VEGF-A splicing: the key to anti-angiogenic therapeutics? *Nat Rev Cancer* 2008 ; 8 : 880-7.
10. Balan M, Mier y Teran E, Waaga-Gasser AM, *et al.* Novel roles of c-Met in the survival of renal cancer cells through the regulation of HO-1 and PD-L1 expression. *J Biol Chem* 2015 ; 290 : 8110-20.
11. Cao Y, Wang L, Nandy D, *et al.* Neuropilin-1 upholds dedifferentiation and propagation phenotypes of renal cell carcinoma cells by activating Akt and sonic hedgehog axes. *Cancer Res* 2008 ; 68 : 8667-72.
12. Lepelletier Y, Moura IC, Hadj-Slimane R, *et al.* Immunosuppressive role of semaphorin-3A on T cell proliferation is mediated by inhibition of actin cytoskeleton reorganization. *Eur J Immunol* 2006 ; 36 : 1782-93.
13. Schellenburg S, Schulz A, Poitz DM, Muders MH. Role of neuropilin-2 in the immune system. *Mol Immunol* 2017 ; 90 : 239-44.
14. Curreli S, Arany Z, Gerardy-Schahn R, *et al.* Polysialylated neuropilin-2 is expressed on the surface of human dendritic cells and modulates dendritic cell-T lymphocyte interactions. *J Biol Chem* 2007 ; 282 : 30346-56.
15. Casazza A, Laoui D, Wenes M, *et al.* Impeding macrophage entry into hypoxic tumor areas by Sema3A/Nrp1 signaling blockade inhibits angiogenesis and restores antitumor immunity. *Cancer Cell* 2013 ; 24 : 695-709.
16. Cherry JD, Olschowka JA, O'Banion MK. Neuroinflammation and M2 microglia: the good, the bad, and the inflamed. *J Neuroinflammation* 2014 ; 11 : 98.
17. Stamatos NM, Zhang L, Jokilammi A, *et al.* Changes in polysialic acid expression on myeloid cells during differentiation and recruitment to sites of inflammation: role in phagocytosis. *Glycobiology* 2014 ; 24 : 864-79.
18. Hong TM, Chen YL, Wu YY, *et al.* Targeting neuropilin 1 as an antitumor strategy in lung cancer. *Clin Cancer Res* 2007 ; 13 : 4759-68.
19. Gray MJ, Van Buren G, Dallas NA, *et al.* Therapeutic targeting of neuropilin-2 on colorectal carcinoma cells implanted in the murine liver. *J Natl Cancer Inst* 2008 ; 100 : 109-20.
20. Cao Y, Hoeppner LH, Bach S, *et al.* Neuropilin-2 promotes extravasation and metastasis by interacting with endothelial alpha5 integrin. *Cancer Res* 2013 ; 73 : 4579-90.
21. Weekes CD, Beeram M, Tolcher AW, *et al.* A phase I study of the human monoclonal anti-NRP1 antibody MNRP1685A in patients with advanced solid tumors. *Invest New Drugs* 2014 ; 32 : 653-60.
22. Liang WC, Dennis MS, Stawicki S, *et al.* Function blocking antibodies to neuropilin-1 generated from a designed human synthetic antibody phage library. *J Mol Biol* 2007 ; 366 : 815-29.
23. Pan Q, Chanthery Y, Liang WC, *et al.* Blocking neuropilin-1 function has an additive effect with anti-VEGF to inhibit tumor growth. *Cancer Cell* 2007 ; 11 : 53-67.
24. Patnaik A, LoRusso PM, Messersmith WA, *et al.* A Phase Ib study evaluating MNRP1685A, a fully human anti-NRP1 monoclonal antibody, in combination with bevacizumab and paclitaxel in patients with advanced solid tumors. *Cancer Chemother Pharmacol* 2014 ; 73 : 951-60.
25. Tse BWC, Volpert M, Ratther E, *et al.* Neuropilin-1 is upregulated in the adaptive response of prostate tumors to androgen-targeted therapies and is prognostic of metastatic progression and patient mortality. *Oncogene* 2017 ; 36 : 3417-27.
26. Parker MW, Xu P, Li X, Vander Kooi CW. Structural basis for selective vascular endothelial growth factor-A (VEGF-A) binding to neuropilin-1. *J Biol Chem* 2012 ; 287 : 11082-9.
27. Starzec A, Vassy R, Martin A, *et al.* Antiangiogenic and antitumor activities of peptide inhibiting the vascular endothelial growth factor binding to neuropilin-1. *Life Sci* 2006 ; 79 : 2370-81.
28. Tirand L, Frochot C, Vanderesse R, *et al.* A peptide competing with VEGF165 binding on neuropilin-1 mediates targeting of a chlorin-type photosensitizer and potentiates its photodynamic activity in human endothelial cells. *J Control Release* 2006 ; 111 : 153-64.
29. Benachour H, Seve A, Bastogne T, *et al.* Multifunctional Peptide-conjugated hybrid silica nanoparticles for photodynamic therapy and MRI. *Theranostics* 2012 ; 2 : 889-904.
30. Richard M, Chateau A, Jelsch C, *et al.* Carbohydrate-based peptidomimetics targeting neuropilin-1: synthesis, molecular docking study and in vitro biological activities. *Bioorg Med Chem* 2016 ; 24 : 5315-25.
31. Puszko AK, Sosnowski P, Tymecka D, *et al.* Neuropilin-1 peptide-like ligands with proline mimetics, tested using the improved chemiluminescence affinity detection method. *Medchemcomm* 2019 ; 10 : 332-40.
32. Jia H, Bagherzadeh A, Hartzoulakis B, *et al.* Characterization of a bicyclic peptide neuropilin-1 (NP-1) antagonist (EG3287) reveals importance of vascular endothelial growth factor exon 8 for NP-1 binding and role of NP-1 in KDR signaling. *J Biol Chem* 2006 ; 281 : 13493-502.
33. Jarvis A, Allerston CK, Jia H, *et al.* Small molecule inhibitors of the neuropilin-1 vascular endothelial growth factor A (VEGF-A) interaction. *J Med Chem* 2010 ; 53 : 2215-26.
34. Powell J, Mota F, Steadman D, *et al.* Small molecule neuropilin-1 antagonists combine antiangiogenic and antitumor activity with immune modulation through reduction of transforming growth factor beta (TGFbeta) production in regulatory T-cells. *J Med Chem* 2018 ; 61 : 4135-54.
35. Starzec A, Miteva MA, Ladam P, *et al.* Discovery of novel inhibitors of vascular endothelial growth factor-A-Neuropilin-1 interaction by structure-based virtual screening. *Bioorg Med Chem* 2014 ; 22 : 4042-8.
36. Liu WQ, Megale V, Borriello L, *et al.* Synthesis and structure-activity relationship of non-peptidic antagonists of neuropilin-1 receptor. *Bioorg Med Chem Lett* 2014 ; 24 : 4254-9.
37. Liu WQ, Lepelletier Y, Montes M, *et al.* NRPa-308, a new neuropilin-1 antagonist, exerts in vitro anti-angiogenic and anti-proliferative effects and in vivo anti-cancer effects in a mouse xenograft model. *Cancer Lett* 2018 ; 414 : 88-98.
38. Borriello L, Montes M, Lepelletier Y, *et al.* Structure-based discovery of a small non-peptidic Neuropilins antagonist exerting in vitro and in vivo anti-tumor activity on breast cancer model. *Cancer Lett* 2014 ; 349 : 120-7.
39. Brachet E, Dumond A, Liu WQ, *et al.* Synthesis, 3D-structure and stability analyses of NRPa-308, a new promising anti-cancer agent. *Bioorg Med Chem Lett* 2019 ; 29 : 126710.
40. Hanahan D, Weinberg RA. The hallmarks of cancer. *Cell* 2000 ; 100 : 57-70.
41. Hanahan D, Weinberg RA. Hallmarks of cancer: the next generation. *Cell* 2011 ; 144 : 646-74.

TIRÉS À PART

G. Pagès

Appendix 5. Review 2.

Neuropilins, as relevant oncology target: their role in the tumoral microenvironment. *Frontiers in Cell and Developmental Biology.* 2020.

Aurore Dumond and Gilles Pagès.

frontiers in Cell and Developmental Biology

REVIEW
published: 17 July 2020
doi: 10.3389/fcell.2020.00662

Neuropilins, as Relevant Oncology Target: Their Role in the Tumoral Microenvironment

Aurore Dumond[1]* *and Gilles Pagès*[1,2]*

[1] *Medical Biology Department, Centre Scientifique de Monaco, Monaco, Monaco,* [2] *Inserm U1081, CNRS UMR 7284, Centre Antoine Lacassagne, Institut de Recherche sur le Cancer et le Vieillissement de Nice, Université Côte d'Azur, Nice, France*

Angiogenesis is one of the key mechanisms involved in tumor growth and metastatic dissemination. The vascular endothelial growth factor (VEGF) and its receptors (VEGFR) represent one of the major signaling pathways which mediates angiogenesis. The VEGF/VEGFR axis was intensively targeted by monoclonal antibodies or by tyrosine kinase inhibitors to destroy the tumor vascular network. By inhibiting oxygen and nutrient supply, this strategy was supposed to cure cancers. However, despite a lengthening of the progression free survival in several types of tumors including colon, lung, breast, kidney, and ovarian cancers, modest improvements in overall survival were reported. Anti-angiogenic therapies targeting VEGF/VEGFR are still used in colon and ovarian cancer and remain reference treatments for renal cell carcinoma. Although the concept of inhibiting angiogenesis remains relevant, new targets need to be discovered to improve the therapeutic index of anti-VEGF/VEGFR. Neuropilin 1 and 2 (NRP1/2), initially described as neuronal receptors, stimulate angiogenesis, lymphangiogenesis and immune tolerance. Moreover, overexpression of NRPs in several tumors is synonymous of patients' shorter survival. This article aims to overview the different roles of NRPs in cells constituting the tumor microenvironment to highlight the therapeutic relevance of their targeting.

Keywords: neuropilins, tumor microenvironment, oncology, immunology, cancers

OPEN ACCESS

Edited by:
Lucas Treps,
VIB-KU Leuven Center for Cancer Biology, Belgium

Reviewed by:
Luca Tamagnone,
Institute for Cancer Research and Treatment (IRCC), Italy
Andrea Casazza,
CoBioRes Nv Biotech, Belgium

***Correspondence:**
Aurore Dumond
adumond@centrescientifique.mc
Gilles Pagès
gpages@unice.fr;
gilles.pages@unice.fr

Specialty section:
This article was submitted to Molecular and Cellular Oncology, a section of the journal Frontiers in Cell and Developmental Biology

Received: *13 May 2020*
Accepted: *01 July 2020*
Published: *17 July 2020*

Citation:
Dumond A and Pagès G (2020) Neuropilins, as Relevant Oncology Target: Their Role in the Tumoral Microenvironment. Front. Cell Dev. Biol. 8:662. doi: 10.3389/fcell.2020.00662

GENERALITIES ON THE NEUROPILINS

Genomic Organization and Protein Structure

The Neuropilins are type-1 membrane glycoproteins of 130–140 kDa. Two proteins of the same family, Neuropilin 1 and 2 (NRP1 and NRP2), coded by two different genes on independent chromosomes (10p12 for NRP1 and 2q34 for NRP2), share 44% of sequence homology. They are composed of a N-terminal extracellular domain, a transmembrane domain and a cytoplasmic domain of 43–44 amino acids. The extracellular domain comprises five subdomains: a1, a2, b1, b2, and c. The cytoplasmic part does not contain a signaling domain but has a PDZ domain and a triplet of amino acids "serine, glutamic acid, alanine (SEA)." The PDZ domain enables the formation and the stimulation of signaling complexes. The membrane and cytoplasmic parts are implicated in the receptors' dimerization. Soluble forms of NRP1 and NRP2 (sNRP1, sNRP2) without transmembrane and without cytoplasmic domain and an isoform of NRP2 without the SEA amino acid triplet are formed after alternative splicing.

The Phenotype of Knock-Out Mice

NRP1 gene invalidation (KO) induces defects in vascular, nervous, and cardiac network and leads to an embryonic lethality between 10 and 12.5 days (Kawasaki et al., 1999). The overexpression of NRP1 is lethal for embryos of about 12.5 days with cardiac defects (Kitsukawa et al., 1995).

NRP2 KO is not lethal but a diminution of lymphatic vessels and some abnormalities during the neural development are observed (Yuan et al., 2002).

Mice with a double NRP1 and NRP2 KO present more severe vascular abnormalities and embryos die at 8.5 days (Takashima et al., 2002) with the presence of important avascular zones and of some gaps between the blood vessels.

NRP Ligands

The NRPs bind to specific ligands and form heterodimers with five families of receptors. The dimerized ligands bind to the NRP homo- or heterodimers and to partner receptors dimers to form a complex which induces a specific intracellular signal. The sNRP are competitive forms for the binding of vascular endothelial growth factor (VEGF) to the membrane NRP1.

SEMA3/Plexin

The NRPs were first described as neuronal receptors binding the semaphorins (SEMA, seven classes described) which constitute a family of proteins that guide axons growth and are involved in cell apoptosis, migration and tumor suppression. SEMA3C is involved in endothelial cell apoptosis, it inhibits pathological angiogenesis and it promotes invasion and metastasis in cancers. SEMA3A is an angiogenesis inhibitor, that is less expressed during tumor development. Indeed, it controls pericytes recruitment to vessels (Niland and Eble, 2019). Neuropilins form a complex with SEMA receptors, the plexins. The binding of the SEMA on NRP is established through the a1, a2, b1, and b2 domains (Roy et al., 2017). The ternary complex between NRPs, SEMAs and the plexins enhances signal transduction during development, axon guidance and immunity. NRP1 binds preferentially to SEMA3A and NRP2 to SEMA3C or 3F (Roy et al., 2017). SEMA3E/PlexinD1 pathway is involved in the initial development of axon tracts in the forebrain and in the establishment of functional neuronal networks. Some axons expressed plexinD1 but not NRP1, in this case SEMA3E acts as a repellant. When neurons express plexinD1 and NRP1, SEMA3E is an attractant (Chauvet et al., 2007). The extracellular part of NRP1 is sufficient in inducing the attractive axonal guidance. PlexinD1 is necessary for SEMA3E's effects on axonal guidance. However, NRP1 is necessary to control the gating response of SEMA3E to induce a repulsive or attractive axon growth (Chauvet et al., 2007). According to the major role played by the NRP1/SEMA3E signaling in neurodevelopment, any defect may be related to neural disorder as it was suggested in a mouse model of schizophrenia (Daoust et al., 2014).

VEGF/VEGFR

The VEGF gene is composed of eight exons. Exons 1–5 are implicated in the binding to vascular endothelial growth factor receptors (VEGFR) and exons 7 and 8 in the binding to NRP1 and NRP2 (Guyot and Pages, 2015). The differential splicings of exon 6, 7 and 8 induce two distinct families of isoforms. Isoforms with the exon 8a are pro-angiogenic and isoforms with exon 8b are anti-angiogenic (Harper and Bates, 2008). Four predominant forms of VEGF exist: VEGF121, VEGF189, VEGF206 and the more abundant and active in many cancers, the VEGF165. The VEGF165 binds preferentially to NRP1 (Kd = 0.2 nM) as compared to NRP2 (Kd = 5 nM).

In healthy people, VEGFs are involved in wound healing and vascular homeostasis. However, VEGFs promote tumor angiogenesis and lymphangiogenesis and high levels of VEGFs expression are synonymous of poor prognosis in cancers. NRP1 binds the VEGF165 and the receptors VEGFR1 and 2. VEGF binding stimulates this pathway leading to increased angiogenesis. NRP2 binds the VEGF165 and VEGFC, the main lymphangiogenic factor, and forms a complex with the receptors VEGFR2 or VEGFR3 to stimulate angiogenesis and lymphangiogenesis. The binding occurs through the NRPs' b1 and b2 domains. VEGFR activation by the VEGF does not require the NRP. However, in some tumors, VEGFRs are absent and NRP1 induce cell migration and angiogenesis in a VEGFR-independent manner. VEGF binding to NRP1, independently of VEGFR, activates RhoA and Ras, two effectors of different signaling pathways (Niland and Eble, 2019).

Thus, the stimulation of NRP by the VEGF is highly relevant in a therapeutic context.

PlGF/VEGFR

Placenta growth factor (PlGF) belongs to the VEGFs family and binds to VEGFR1 but not to VEGFR2. It was initially described as a placenta produced homodimeric protein. Three isoforms are initiated from alternative splicing: PlGF1, PlGF2, and PlGF3. PlGF2 is the only form containing exon 6, which codes for an heparin binding domain (Migdal et al., 1998). PlGF2 binds to NRP1 through amino acids encoded by exon 6 and exon 7 and PlGF1 through amino acids encoded by exon 7 (Migdal et al., 1998). In breast cancer, PlGF1 and NRP1 overexpression is correlated to a poor prognosis and PlGF2 is overexpressed in cancer tissues as compared to normal tissue (Escudero-Esparza et al., 2010). The PlGF/NRP pathway is implicated in tumor growth, angiogenesis, migration, and metastasis for melanoma cancers even in the absence of VEGFRs (Pagani et al., 2016). PlGF is also a relevant target in retinal diseases resistant to anti-VEGF therapies (Van Bergen et al., 2019). In the Sonic Hedgehog subgroup of medulloblastoma, PlGF binds to NRP1 leading to mitogen activated protein kinase (MAPK) signaling activation, tumor growth and dissemination (Snuderl et al., 2013). Moreover, the PlGF/NRP signaling pathway plays a key role in resistance to anti-angiogenic therapies (Pagani et al., 2016).

HGF/cMET

The signaling pathway induced by the hepatocyte growth factor (HGF) and its receptor (cMET) regulates endothelial cell survival, proliferation and migration. HGF/cMET complex plays an important role in tumor progression. NRP1, by binding to cMET, induces tumor invasion. As HGF/cMET inhibits apoptosis and promotes immune tolerance by interacting with the programmed

death ligand 1 (PD-L1) (Balan et al., 2015), the stimulation of this signaling pathway by NRP1 promotes tumor growth by inhibiting the antitumor immunity.

TGFβ1/TGFβRs

TGFβ1/TβRs stimulates the SMAD2/3 signaling pathway, which is involved in physiological development, host immunity, inflammation and in tumor progression, and invasion. TGFβ also promotes cancer progression and metastasis (Chaudhary et al., 2014). TGFβ binds to NRP1 via its b1 domain and forms a complex with TGFβ receptors I–III. Activation of this signaling pathway stimulates angiogenesis in a VEGFR2-independent manner. NRP1/TGFβ/TGFβR also promotes T regulatory lymphocytes activity and immune tolerance.

PDGF/PDGFR

The increased expression of PDGF and its receptors on tumor vasculature promotes pathological angiogenesis (Chaudhary et al., 2014). This signaling pathway also induces cell proliferation, differentiation, and epithelial to mesenchymal transition (Niland and Eble, 2019). Four PDGF variant exist: PDGFA, B, C, and D. These ligands bind to the tyrosine-kinase receptors PDGRFα or β. Depending on the ligand, the receptors will homo- or hetero-dimerize giving three possible combinations: αα, αβ, or ββ. PDGF-stimulated PDGFRs activate MAPK and PI3K signaling pathways. NRP1 forms a complex with PDGF and PDGFR amplifying their respective downstream signaling pathways.

FGF/FGFR2

FGF/FGFR2 complex induces cell migration and proliferation. This axis is key for endothelial cell proliferation and subsequent angiogenesis. By forming a complex with the FGFR2, the NRPs play a key role in amplifying its signaling pathways and consequently these biological phenomena.

Galectins

Galectins, part of the family of β-galactoside-binding proteins, are involved in cell-cell and cell-matrix interactions. Galectin-1 (Gal-1) induces tumor-associated HuVEC proliferation and migration, by enhancing VEGFA effects, and HuVEC adhesion. Gal-1 exerts these effects through VEGFR2 phosphorylation enhanced by Gal-1/NRP1 binding (Hsieh et al., 2008). The activation of NRP1/VEGFR1-dependent AKT signal by Gal-1 decreases endothelial-cadherin cell-cell junctions and increases the vascular permeability (Wu et al., 2014).

EGF/EGFR

Epidermal growth factor receptor (EGFR) is a monomeric transmembrane protein. EGFR mutations were described in several forms of cancers, such as breast or lung cancers and it is overexpressed in numerous tumors. EGFR activation stimulates AKT signaling. NRP1 extracellular domain is necessary for EGFR-endocytosis and AKT-dependent cancer cell viability and tumor growth. Hence, reduced expression of NRP1 limits EGFR endocytosis (Rizzolio et al., 2012). Furthermore, NRP2 is required, through WDFY1 (WD-repeat and FYVE-domain-containing protein 1), to activate EGFR endocytosis in cancer cells and to maintain EGFR activities (Dutta et al., 2016).

Hedgehog Signaling Pathway

This pathway is involved in embryogenesis and in adult's tissue healing. Its activation induces cell proliferation and differentiation. Its overexpression or downregulation induces cancer development and the epithelial-mesenchymal transition (EMT). NRPs are major regulators of the Hedgehog signaling pathway. A feedback loop exists between NRP1 and Hedgehog; Hedgehog signaling induces NRP1 expression, which promotes activation of Hedgehog targeted gene (Niland and Eble, 2019). A down-regulation of NRP1 by shRNA in ccRCC cell lines reduces sonic hedgehog (SHH) and its activator Gli1 expressions. SHH signaling pathway inhibition promotes tumor cell differentiation (Cao et al., 2008).

Integrins

NRPs also interacts with integrins. The intercellular interaction between integrins α5β1 and α9β1 expressed on endothelial cells and NRP2 expressed on tumor and endothelial cells increases tumor spreading and metastasis through and integrin-dependent mechanism (Cao et al., 2013; Alghamdi et al., 2020).

THE ROLE OF NEUROPILINS IN THE IMMUNE SYSTEM (FIGURE 1)

Dendritic Cells

They are recruited to the tumor site. After their contact with the antigen, they are maturated, which enables them to migrate to the lymphoid organs to activate naïve T cells and to induce the primary immune response. Two types of dendritic cells (DCs) exists: (i) myeloid DCs (mDCs) that present the antigen to T cells; (ii) plasmacytoid DCs (pDCs), generally involved in immune suppression. Activated pDCs have an antigen presenting capacity, they also activate T cells but to a lesser extent as compared to mDCs.

NRP1 is expressed on mature DC and on naïve T cells. This enables NRP1/NRP1 homophilic interaction and the formation of an immunological synapse between these two cell types. Thus, NRP1 mediates the primary immune response activation by promoting antigen presentation by DCs through this synapse (Sarris et al., 2008; Akkaya et al., 2019). NRP1 regulate cytoskeleton rearrangements allowing their transmigration to the lymphatics and lymphoid tissues to activate T cells. However, at a late stage of T cell activation, SEMA3A is secreted. By its interaction with NRP1 expressed on T cells, it disrupts the formation of the immunological synapse with the DC resulting in reduced T cell activation and immune tolerance (Lepelletier et al., 2006).

NRP2 expression increases during the differentiation from monocytes to dendritic cells (Schellenburg et al., 2017). Its sialylation protects DC during their migration to lymph nodes. In the lymph nodes, the polysialic acid is eliminated of NRP2 and DC activate T cells (Curreli et al., 2007; Rey-Gallardo et al., 2011).

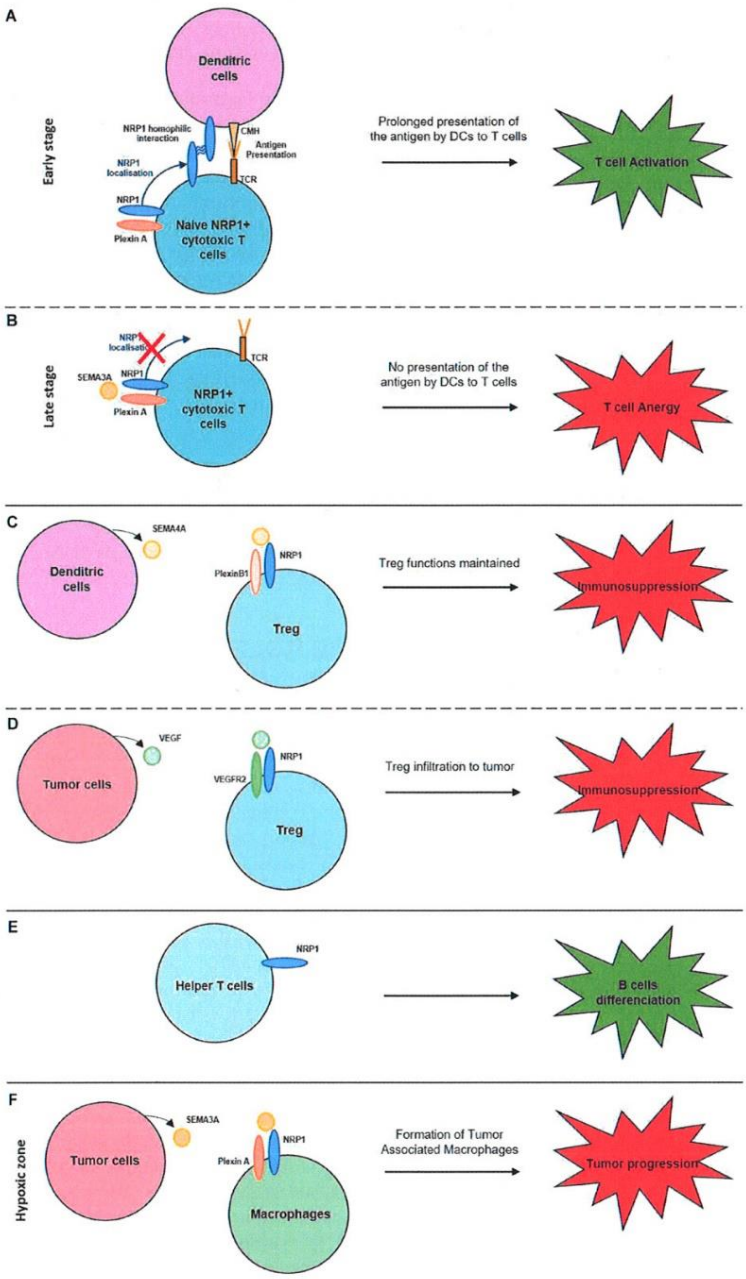

FIGURE 1 | Role of NRPs in the activation or suppression of the immune system. **(A)** NRP1 homophilic interaction enhances the interaction between naive cytotoxic T cells and dendritic cells inducing a prolonged antigen presentation and so T cell activation. **(B)** Expression of SEMA3A by mature cytotoxic T cells inhibits NRP1 localisation and induces T cell anergy. **(C)** Interaction between NRP1, expressed by Treg cells, with SEMA4A, expressed by dendritic cells maintain Treg functions. **(D)** Interaction between NRP1, expressed by Treg cells, with VEGF, expressed by tumor cells, enable Treg cells infiltration into the tumor and induce an immunosuppression. **(E)** NRP1+ helper T cells induce B cells differentiation to activate their immune response. **(F)** Interaction between NRP1, expressed by macrophages, with SEMA3A, expressed by tumor cells, induce the formation of tumor associated macrophages (TAM) and so a tumor progression.

Macrophages

They play a key role in immune surveillance, in cellular debris elimination and in antigen presentation. M1 macrophages are pro-inflammatory and M2 are pro-angiogenic, immunosuppressive, thus pro-tumoral particularly in hypoxic zones. Hypoxia induces SEMA3A expression on tumoral cells. It interacts with NRP1, and their receptors plexin A1 and A4, expressed on macrophages. Tumor-associated macrophages (TAM) reside in the hypoxic zones where they exert their pro-tumoral role. If NRP1 expression decreases, TAM remain in the normoxic peripheric zones of the tumor resulting in the suppression of their pro-tumoral role (Casazza et al., 2013; Chen et al., 2019). In the microglia, NRP1 plays an immune suppressive role by inducing a M2 phenotype. A NRP1/NRP1 homophilic interaction with the helper T cells induces immune suppression. NRP1 expression on glioma-associated macrophages (GAM) induces a pro-tumoral response. NRP1 inhibition reduces tumor growth and a macrophages polarization to an anti-tumoral role (Cherry et al., 2014; Caponegro et al., 2018).

NRP2 expression increases during the differentiation of monocytes to macrophages (Schellenburg et al., 2017) next to inflammatory zones to induce phagocytosis. NRP2 sialylation reduces phagocytosis capacity of the macrophages (Stamatos et al., 2014; Roy et al., 2018), thus NRP2+ M2 macrophages promote tumor progression (Niland and Eble, 2019).

T Cells

They are responsible of the adaptative immune response required for the control and the elimination of pathogenic agents and of tumor cells. Any dysfunctions in their development or activation induce auto-immune diseases and cancers. NRP1 is upregulated on active T cells (Chaudhary et al., 2014). Four types of T cells exist.

Cytotoxic T Cells (T CD8+)

They destroy the infected cells presenting the specific antigen through the class I major histocompatibility complex (MHC). The NRP1 expression is increased on CD8+ effective and memory T cells and promotes the antigen recognition (Roy et al., 2017). However, the exact NRP1 role in this context is unknown. NRP1 expression also correlates with PD1 expression on CD8+ T cells. Thus, NRP1 might represent a relevant biomarker to determine the efficacy of anti-PD1 immunotherapies. Indeed, patients with non-small cell lung cancer invaded with PD1-positive CD8+ T cells are highly responsive to anti-PD1 immunotherapies and present a longer survival (Leclerc et al., 2019).

Helper T Cells (T CD4+)

They are not cytotoxic but produce interleukin 2 and interferon gamma. These cytokines stimulate T and B cell proliferation. NRP1 is expressed on CD4+ T cells and induces B cells differentiation (Roy et al., 2017). Induction of NRP1 on regulatory T cells (Bruder et al., 2004) and on CD4+ T cells (Campos-Mora et al., 2019) induces immunosuppressive functions *in vivo*.

NKT Cells

They constitute a link between innate and adaptative immunity. Once activated, they lyse the targets and produce anti- and pro-inflammatory cytokines. NRP1 role on these NKT cells is unknown (Roy et al., 2017).

Regulatory T Cells (Treg)

Tregs play a role in immune homeostasis, allergic responses, auto-immune diseases, tumor immunity, and graft rejection. Their accumulation in tumors induces cancer progression and immune suppression (Sakaguchi et al., 1995). NRP1 is overexpressed by activated Tregs and promote their immunosuppressive role. NRP1 expression maintains the Tregs functions through the binding to SEMA4A, expressed by dendritic cells. NRP1/SEMA4A binding stabilizes the Treg by recruiting PTEN (Phosphatase and tensin homolog) and by inhibiting AKT phosphorylation. NRP1 expression on Treg induces their migration to the tumors where they play an immune-suppressive role (Hansen et al., 2012) by secreting IL-10 and IL-35, an anti-inflammatory cytokine. NRP1 expressed by Tregs are also attracted to tumors expressing VEGF where NRP1 acts as a VEGF co-receptor. The stimulation by VEGF, enhances T regs infiltration to tumors and an immunosuppressive response (Hansen et al., 2012).

CD4+/CD8+ T cells over-express NRP2 but NRP2 expression is lower on T cells expressing only CD8 or only CD4. The interaction between NRP2, SEMA3F and plexinA1 inhibits immature T cell migration.

Thus, the NRP have different roles in the immune system either in cell migration, cell-cell interaction or in the regulation of the immune response.

ROLES IN CANCER

Neuropilins expression level correlates with tumor growth, invasiveness, angiogenesis, and poor prognosis. NRPs over-expression is often observed in carcinoma, melanoma, glioblastoma, leukemia, and lymphoma in which NRPs exert diverse functions.

Functions of Neuropilins in Cancer

To grow over a few millimeters tumors turn into a pro-angiogenic environment that induces the formation of new blood vessels from the existing vascular network. This new vascular network surrounding the tumor, supplies oxygen and nutrients needed for tumors growth. Tumor cells, cells from the microenvironment and NRPs expressed on both cell types influence tumor angiogenesis (Niland and Eble, 2019). The roles of NRP1 in the growth and invasiveness of prostate, colorectal, kidney, lung, breast, ... human cancers have been confirmed with animal studies showing that exacerbated angiogenesis and a poor prognosis is correlated with NRP1 expression (Ellis, 2006). Only in pancreatic cancers, a high expression of NRP1 correlates with reduced vascularized areas, decreased tumor growth, and improved survival (Morin et al., 2018).

Expression of NRP2 is mostly correlated to tumor progression. In most cancers, the co-expression of NRP1 and NRP2 stimulates tumor growth and invasiveness (Rizzolio and Tamagnone, 2011). SEMA3C, which binds to NRP1 and NRP2 with equivalent affinity, inhibits tumor lymphangiogenesis by targeting immature vessels sprouting. However, its cleaved form, p65-SEMA3C, stimulates tumor lymphangiogenesis and metastatic dissemination of cancer cells expressing NRP2 (Mumblat et al., 2015).

Neuropilin 1 expression on tumor cells enhances cell viability, proliferation, migration, metastasis and favors cancer cell stemness. Since NRP1 promotes EMT through different pathways (TGF-β, Hedgehog, HGF...), which explains NRP1's pro-tumoral role.

Neuropilin 1 is expressed on breast cancer cells, and its interaction with VEGF165 inhibits apoptosis. Such inhibition is counteracted by SEMA3B (Ellis, 2006). SEMA3F competes with VEGF in binding to the NRPs and blocks breast cancer cell migration. However, SEMA3F decreases membrane E-cadherin, which promotes cell metastasis (Ellis, 2006). SEMA3A expressed on endothelial cells, antagonizes VEGF effects and correlates with a good prognosis (Niland and Eble, 2020). It is generally lost during tumor progression (Niland and Eble, 2019). In a VEGFA+/SEMA3A+ environment, NRP1 binds preferentially SEMA3A (Palodetto et al., 2017). Cells with a higher VEGF expression as compared to SEMA3A expression have promigratory characteristics.

In colon cancer, NRP1 expression correlates with increased vessel number and poor prognosis, while NRP2 over-expression stimulates tumor progression and the down-regulation of NRP2 expression inhibits tumorigenesis and increases apoptosis (Gray et al., 2008). In prostate cancer, elevated NRP1 levels stimulated by VEGF inhibit tumor cell apoptosis and angiogenesis and are synonymous of shorter survival. In ccRCC, NRP1 down-regulation reduces migration, invasion, and tumorigenesis (Cao et al., 2008), and NRP2 down-regulation decreases cell extravasation in the lymphatic network and the metastatic spread (Cao et al., 2013). NRP1 expression down-regulation in experimental model of lung cancer reduces cell migration, invasion, and metastasis (Hong et al., 2007).

Role in Cancer Stem Cells

A tumor is composed of cells differing in their morphology, their capacity to proliferate and to form metastasis and in their resistance to therapeutic agents. Among these different cells, only cancer stem cells (CSCs) are able to initiate a new primary tumor or metastasis. CSCs are cells that self-renew and that induce the heterogeneous aspect of the tumors. CSCs are resistant to chemo-and radiotherapy. As NRPs are less expressed in epithelial tissues compared to carcinomas, NRPs might play a role in stemness.

The role of the VEGFs/NRPs pathways have been studied in the triple negative breast cancer cell line MDA-MB-231 and the hormone sensitive MCF-7 cell line. While MDA-MB-231 have stemness characteristics MCF-7 cells have low stemness properties. In these cells, the level of stemness was correlated to the expression of VEGF and NRP1 (Zhang et al., 2017). Down-regulation of VEGF and NRP1 in MDA-MB-231 cells and overexpression of VEGF and NRP1 in MCF-7 cells confirmed that the VEGF/NRP1 signaling pathway is instrumental in driving stemness properties of breast cancer cells (Zhang et al., 2017). The VEGFC/NRP2 pathway is also involved in breast cancer stemness (Wang et al., 2014). The VEGF/NRP2 pathways stimulates stemness through activation of the YAP/TAZ signaling (Elaimy and Mercurio, 2018). This pathway also mediates homologous recombination by stimulating Rad51 expression leading to resistance to platinum chemotherapy in triple negative breast cancers (Elaimy et al., 2019). The NRP2/α6β1 integrin interaction activates the focal adhesion kinase (FAK) involved in tumorigenesis and associated to aggressive tumors (Goel et al., 2013). Furthermore, the VEGF/NRP1 pathway induces CSCs in breast cancers by activating the Wnt/β-catenin pathway (Zhang et al., 2017), which is involved in the induction of CSCs. The implication of VEGF/NRP1 pathway was also highlighted in glioma stem cells (Hamerlik et al., 2012) and in medulloblastoma stem cells (Gong et al., 2018).

Role in Cancer-Associated Fibroblasts

Fibroblasts are part of the tumor microenvironment and become myofibroblasts (normal activated fibroblasts) under tumoral conditions. By interacting with fibronectin, myofibroblasts promote fibronectin fibril assembly, and tumor growth through α5β1 integrin (Yaqoob et al., 2012). Fibronectin fibril assembly is regulated determinant of matrix stiffness involved in tumor progression. NRP1 induces integrin function by binding to fibronectin and by activating the intracellular kinase c-Abl (Yaqoob et al., 2012). Indeed, NRP1 intracellular domain stimulates c-Abl that activates small GTPases (Rac or Rho). These GTPases promote α5β1 integrin function and so increase fibronectin binding and assembly (Yaqoob et al., 2012). The NRP1 extracellular domain is O-linked glycosylated via the serine 612 residue, which increases NRP1 binding to fibronectin resulting in enhanced fibronectin and α5β1 integrin interaction (Yaqoob et al., 2012). Thus, NRP1 intra- and extracellular domains, through the activation of c-Abl and α5β1 integrin, increase fibronectin fibril assembly contributing to matrix stiffness and tumor progression and invasiveness. Furthermore, cancer-associated fibroblasts (CAFs) are one of the most expressed cells in the tumor microenvironment, and the principal source of TGFβ1. NRP1/TGFβ1 interaction stimulates endothelial-mesenchymal transition (EndMT), an important source of CAFs (Matkar et al., 2016). Finally, CAFs also promotes tumor migration and invasion by inducing EMT of cancers cells (Shan et al., 2017). This EMT induction is carried out through Hedgehog signaling. As above described, NRP1 is a major regulator of Hedgehog signaling. Thus, NRP1 expressed on CAF might also stimulate EMT which increases tumor cell migration and invasion worse prognosis.

Prognostic Role of NRP1 and NRP2 Pathways

Neuropilins correlate with poor prognosis in many cancers. Here are some examples. NRP1 is overexpressed in bladder cancer and correlates with poor prognosis (Cheng et al., 2014). In osteosarcoma, NRP1 is a prognostic factor of shorter progression-free (PFS) and overall survival (OS) (Zhu et al., 2014). NRP2 contributes to laryngeal squamous cell carcinoma progression and could serve as a new therapeutic target for this type of cancer (Yin et al., 2020). In prostate adenocarcinoma, NRP2 is a marker of bad prognosis (Borkowetz et al., 2020). Some activator of the NRP2 pathway including VEGFC were described as markers of good prognosis in non-metastatic kidney cancers but of poor prognosis in metastatic kidney cancers (Ndiaye et al., 2019). Thus, the level of expression of NRP2 and their partners, has to be determined to adapt a specific therapeutic strategy in tumors at different steps of their development.

Role in the Therapeutic Response

Resistances to targeted therapies are often related to the activation of alternative tyrosine-kinase receptors-mediated signaling pathways. As above described, NRPs interact with several tyrosine kinase receptors and enhance their activity.

Resistance to Chemo- and Radiotherapies

Radio- and chemotherapy are widely used to treat cancers.

A high expression of NRP1 in non-small cell lung cancer cells increases radio-resistance through an ABL-1-mediated up-regulation of RAD51 expression (Hu et al., 2018). In pancreatic cancer, NRP1 increases resistance to gemcitabine and 5-fluorouracil by activating the MAPK signaling pathway (Wey et al., 2005).

The NRP2/VEGFC pathway activates autophagy through the inhibition of mTOR complex 1 activity which helps cancer cells to survive following treatment (Stanton et al., 2013). NRP2 overexpression, induced by SEMA3F in adenocarcinoma, decreases integrin $\alpha v\beta 3$ and enhances cell sensitivity to chemotherapy (Zheng et al., 2009).

In some cancers, NRP targeted drug decreases resistance to chemo/radiotherapies.

Resistance to Targeted Therapies

In pancreatic ductal adenocarcinoma (PDAC), an increase of active integrin $\beta 1$ activates AKT signaling and resistance to cetuximab, an anti-EGFR monoclonal antibody (Kim et al., 2017). NRP1-dependent JNK signaling leads to the overexpression of EGFR and IGF1R, which induces resistance to BRAF (melanoma targeted therapy), HER2 (breast cancer targeted therapy) and MET (stomach and lung carcinomas therapy) inhibitors (Rizzolio et al., 2018b).

Neuropilin 2 overexpression decreases EGFR expression and resistance to MET-targeted therapies (Rizzolio et al., 2018a).

Thus, NRPs have become interesting biomarkers to determine the patients' responsiveness to radio- or chemotherapies or to targeted therapies. Indeed, patients with low NRP1 expression present a better OS than patients with high level of NRP1 (Van Cutsem et al., 2012; Napolitano and Tamagnone, 2019).

Again, combination of targeted therapies to NRP1 inhibitors increase the effects of therapies and reduces resistance.

CONCLUSION

Angiogenesis is one of the key mechanisms involved in cancer growth and dissemination. Anti VEGF were approved in combination with standard chemotherapies. Despite an improvement of progression free survival in several types of tumors by anti VEGF treatments, increases in OS were reported. The elevated expression in tumor, endothelial, and immune cells, makes NRP1 and 2 new relevant oncology targets to improve the treatment of cancers. This review describes the different roles and the expression level of NRPs in the different cells constituting the tumor microenvironment. NRPs form holoreceptors with many different receptors and, thus, are involved in many biological phenomena: angiogenesis, lymphangiogenesis, cell proliferation, migration, invasion, and tumor growth. Moreover, NRPs are expressed by several immune cells, in which they exert an activating or inhibiting role on the immune response. In many cancers, NRPs over-expression is synonymous of poor prognosis. This review highlights the implication of NRPs in several hallmarks of cancer and the relevance of targeting the NRPs for the treatment of cancers. Several molecules targeting NRPs are in development: (i) anti-NRP1 antibodies such as the MNRP1685A that has to be optimized to improve the therapeutic window and to decrease its toxic effects; (ii) cyclic, rigid or pseudo-peptides developed by optimizing the sequence ATWLPPR, mimicking the VEGF C-terminal domain interacting with NRP1; (iii) non-peptidic inhibitors such as NRPa-308 that exerts anti-cancer effects in triple negative breast cancer (Liu et al., 2018) and which is currently tested in ccRCC.

Despite these different therapeutic pathways, NRPs targeting must be improved to fight cancers that can benefit the most of these treatments. The antagonist role of NRPs as beneficial or detrimental markers depending on tumor stage suggests cautiousness before administration of anti NRPs treatments.

AUTHOR CONTRIBUTIONS

AD and GP were equally responsible for all parts of the manuscript. Both authors contributed to the article and approved the submitted version.

FUNDING

The authors acknowledge funding from Helsinn Company. This work was supported by the Fondation de France, the Ligue Nationale contre le Cancer (Equipe Labellisée 2019), the National Institute of Cancer (INCA, SUNITRES), the National Agency for Research (ANR, TARMAC), and the FX Mora and Flavien Foundations.

REFERENCES

Akkaya, B., Oya, Y., Akkaya, M., Al Souz, J., Holstein, A. H., Kamenyeva, O., et al. (2019). Regulatory T cells mediate specific suppression by depleting peptide-MHC class II from dendritic cells. *Nat. Immunol.* 20, 218–231. doi: 10.1038/s41590-018-0280-2

Alghamdi, A. A. A., Benwell, C. J., Atkinson, S. J., Lambert, J., Johnson, R. T., and Robinson, S. D. (2020). NRP2 as an emerging angiogenic player; promoting endothelial cell adhesion and migration by regulating recycling of alpha5 integrin. *Front. Cell Dev. Biol.* 8:395. doi: 10.3389/fcell.2020.00395

Balan, M., Teran, M. Y. E., Waaga-Gasser, A. M., Gasser, M., Choueiri, T. K., Freeman, G., et al. (2015). Novel roles of c-Met in the survival of renal cancer cells through the regulation of HO-1 and PD-L1 expression. *J. Biol. Chem.* 290, 8110–8120. doi: 10.1074/jbc.m114.612689

Borkowetz, A., Froehner, M., Rauner, M., Conrad, S., Erdmann, K., Mayr, T., et al. (2020). Neuropilin-2 is an independent prognostic factor for shorter cancer-specific survival in patients with acinar adenocarcinoma of the prostate. *Int. J. Cancer* 146, 2619–2627. doi: 10.1002/ijc.32679

Bruder, D., Probst-Kepper, M., Westendorf, A. M., Geffers, R., Beissert, S., Loser, K., et al. (2004). Neuropilin-1: a surface marker of regulatory T cells. *Eur. J. Immunol.* 34, 623–630. doi: 10.1002/eji.200324799

Campos-Mora, M., Contreras-Kallens, P., Galvez-Jiron, F., Rojas, M., Rojas, C., Refisch, A., et al. (2019). CD4+Foxp3+T regulatory cells promote transplantation tolerance by modulating effector CD4+ T Cells in a neuropilin-1-dependent manner. *Front. Immunol.* 10:882. doi: 10.3389/fimmu.2019.00882

Cao, Y., Hoeppner, L. H., Bach, S., Guangqi, E., Guo, Y., Wang, E., et al. (2013). Neuropilin-2 promotes extravasation and metastasis by interacting with endothelial alpha5 integrin. *Cancer Res.* 73, 4579–4590. doi: 10.1158/0008-5472.can-13-0529

Cao, Y., Wang, L., Nandy, D., Zhang, Y., Basu, A., Radisky, D., et al. (2008). Neuropilin-1 upholds dedifferentiation and propagation phenotypes of renal cell carcinoma cells by activating Akt and sonic hedgehog axes. *Cancer Res.* 68, 8667–8672. doi: 10.1158/0008-5472.can-08-2614

Caponegro, M. D., Moffitt, R. A., and Tsirka, S. E. (2018). Expression of neuropilin-1 is linked to glioma associated microglia and macrophages and correlates with unfavorable prognosis in high grade gliomas. *Oncotarget* 9, 35655–35665. doi: 10.18632/oncotarget.26273

Casazza, A., Laoui, D., Wenes, M., Rizzolio, S., Bassani, N., Mambretti, M., et al. (2013). Impeding macrophage entry into hypoxic tumor areas by Sema3A/Nrp1 signaling blockade inhibits angiogenesis and restores antitumor immunity. *Cancer Cell* 24, 695–709. doi: 10.1016/j.ccr.2013.11.007

Chaudhary, B., Khaled, Y. S., Ammori, B. J., and Elkord, E. (2014). Neuropilin 1: function and therapeutic potential in cancer. *Cancer Immunol. Immunother.* 63, 81–99. doi: 10.1007/s00262-013-1500-0

Chauvet, S., Cohen, S., Yoshida, Y., Fekrane, L., Livet, J., Gayet, O., et al. (2007). Gating of Sema3E/PlexinD1 signaling by neuropilin-1 switches axonal repulsion to attraction during brain development. *Neuron* 56, 807–822. doi: 10.1016/j.neuron.2007.10.019

Chen, X. J., Wu, S., Yan, R. M., Fan, L. S., Yu, L., Zhang, Y. M., et al. (2019). The role of the hypoxia-Nrp-1 axis in the activation of M2-like tumor-associated macrophages in the tumor microenvironment of cervical cancer. *Mol. Carcinog.* 58, 388–397. doi: 10.1002/mc.22936

Cheng, W., Fu, D., Wei, Z. F., Xu, F., Xu, X. F., Liu, Y. H., et al. (2014). NRP-1 expression in bladder cancer and its implications for tumor progression. *Tumour Biol.* 35, 6089–6094. doi: 10.1007/s13277-014-1806-3

Cherry, J. D., Olschowka, J. A., and O'banion, M. K. (2014). Neuroinflammation and M2 microglia: the good, the bad, and the inflamed. *J. Neuroinflam.* 11:98. doi: 10.1186/1742-2094-11-98

Curreli, S., Arany, Z., Gerardy-Schahn, R., Mann, D., and Stamatos, N. M. (2007). Polysialylated neuropilin-2 is expressed on the surface of human dendritic cells and modulates dendritic cell-T lymphocyte interactions. *J. Biol. Chem.* 282, 30346–30356. doi: 10.1074/jbc.m702965200

Daoust, A., Bohic, S., Saoudi, Y., Debacker, C., Gory-Faure, S., Andrieux, A., et al. (2014). Neuronal transport defects of the MAP6 KO mouse - a model of schizophrenia - and alleviation by Epothilone D treatment, as observed using MEMRI. *Neuroimage* 96, 133–142. doi: 10.1016/j.neuroimage.2014.03.071

Dutta, S., Roy, S., Polavaram, N. S., Stanton, M. J., Zhang, H., Bhola, T., et al. (2016). Neuropilin-2 Regulates Endosome Maturation and EGFR trafficking to support cancer cell pathobiology. *Cancer Res.* 76, 418–428. doi: 10.1158/0008-5472.can-15-1488

Elaimy, A. L., Amante, J. J., Zhu, L. J., Wang, M., Walmsley, C. S., Fitzgerald, T. J., et al. (2019). The VEGF receptor neuropilin 2 promotes homologous recombination by stimulating YAP/TAZ-mediated Rad51 expression. *Proc. Natl. Acad. Sci. U.S.A.* 116, 14174–14180. doi: 10.1073/pnas.1821194116

Elaimy, A. L., and Mercurio, A. M. (2018). Convergence of VEGF and YAP/TAZ signaling: Implications for angiogenesis and cancer biology. *Sci. Signal.* 11:eaau1165. doi: 10.1126/scisignal.aau1165

Ellis, L. M. (2006). The role of neuropilins in cancer. *Mol. Cancer Ther.* 5, 1099–1107. doi: 10.1158/1535-7163.mct-05-0538

Escudero-Esparza, A., Martin, T. A., Douglas-Jones, A., Mansel, R. E., and Jiang, W. G. (2010). PGF isoforms, PLGF-1 and PGF-2 and the PGF receptor, neuropilin, in human breast cancer: prognostic significance. *Oncol. Rep.* 23, 537–544.

Goel, H. L., Pursell, B., Chang, C., Shaw, L. M., Mao, J., Simin, K., et al. (2013). GLI1 regulates a novel neuropilin-2/alpha6beta1 integrin based autocrine pathway that contributes to breast cancer initiation. *EMBO Mol. Med.* 5, 488–508. doi: 10.1002/emmm.201202078

Gong, C., Valduga, J., Chateau, A., Richard, M., Pellegrini-Moise, N., Barberi-Heyob, M., et al. (2018). Stimulation of medulloblastoma stem cells differentiation by a peptidomimetic targeting neuropilin-1. *Oncotarget* 9, 15312–15325. doi: 10.18632/oncotarget.24521

Gray, M. J., Van Buren, G., Dallas, N. A., Xia, L., Wang, X., Yang, A. D., et al. (2008). Therapeutic targeting of neuropilin-2 on colorectal carcinoma cells implanted in the murine liver. *J. Natl. Cancer Inst.* 100, 109–120. doi: 10.1093/jnci/djm279

Guyot, M., and Pages, G. (2015). VEGF splicing and the role of VEGF splice variants: from physiological-pathological conditions to specific Pre-mRNA splicing. *Methods Mol. Biol.* 1332, 3–23. doi: 10.1007/978-1-4939-2917-7_1

Hamerlik, P., Lathia, J. D., Rasmussen, R., Wu, Q., Bartkova, J., Lee, M., et al. (2012). Autocrine VEGF-VEGFR2-Neuropilin-1 signaling promotes glioma stem-like cell viability and tumor growth. *J. Exp. Med.* 209, 507–520. doi: 10.1084/jem.20111424

Hansen, W., Hutzler, M., Abel, S., Alter, C., Stockmann, C., Kliche, S., et al. (2012). Neuropilin 1 deficiency on CD4+Foxp3+ regulatory T cells impairs mouse melanoma growth. *J. Exp. Med.* 209, 2001–2016. doi: 10.1084/jem.20111497

Harper, S. J., and Bates, D. O. (2008). VEGF-A splicing: the key to anti-angiogenic therapeutics? *Nat. Rev. Cancer* 8, 880–887. doi: 10.1038/nrc2505

Hong, T. M., Chen, Y. L., Wu, Y. Y., Yuan, A., Chao, Y. C., Chung, Y. C., et al. (2007). Targeting neuropilin 1 as an antitumor strategy in lung cancer. *Clin. Cancer Res.* 13, 4759–4768. doi: 10.1158/1078-0432.ccr-07-0001

Hsieh, S. H., Ying, N. W., Wu, M. H., Chiang, W. F., Hsu, C. L., Wong, T. Y., et al. (2008). Galectin-1, a novel ligand of neuropilin-1, activates VEGFR-2 signaling and modulates the migration of vascular endothelial cells. *Oncogene* 27, 3746–3753. doi: 10.1038/sj.onc.1211029

Hu, C., Zhu, P., Xia, Y., Hui, K., Wang, M., and Jiang, X. (2018). Role of the NRP-1-mediated VEGFR2-independent pathway on radiation sensitivity of non-small cell lung cancer cells. *J. Cancer Res. Clin. Oncol.* 144, 1329–1337. doi: 10.1007/s00432-018-2667-8

Kawasaki, T., Kitsukawa, T., Bekku, Y., Matsuda, Y., Sanbo, M., Yagi, T., et al. (1999). A requirement for neuropilin-1 in embryonic vessel formation. *Development* 126, 4895–4902.

Kim, Y. J., Jung, K., Baek, D. S., Hong, S. S., and Kim, Y. S. (2017). Co-targeting of EGF receptor and neuropilin-1 overcomes cetuximab resistance in pancreatic ductal adenocarcinoma with integrin beta1-driven Src-Akt bypass signaling. *Oncogene* 36, 2543–2552. doi: 10.1038/onc.2016.407

Kitsukawa, T., Shimono, A., Kawakami, A., Kondoh, H., and Fujisawa, H. (1995). Overexpression of a membrane protein, neuropilin, in chimeric mice causes anomalies in the cardiovascular system, nervous system and limbs. *Development* 121, 4309–4318.

Leclerc, M., Voilin, E., Gros, G., Corgnac, S., De Montpreville, V., Validire, P., et al. (2019). Regulation of antitumour CD8 T-cell immunity and checkpoint blockade immunotherapy by Neuropilin-1. *Nat. Commun.* 10:3345.

Lepelletier, Y., Moura, I. C., Hadj-Slimane, R., Renand, A., Fiorentino, S., Baude, C., et al. (2006). Immunosuppressive role of semaphorin-3A on T cell proliferation is mediated by inhibition of actin cytoskeleton reorganization. *Eur. J. Immunol.* 36, 1782–1793. doi: 10.1002/eji.200535601

Liu, W. Q., Lepelletier, Y., Montes, M., Borriello, L., Jarray, R., Grepin, R., et al. (2018). NRPa-308, a new neuropilin-1 antagonist, exerts in vitro anti-angiogenic and anti-proliferative effects and in vivo anti-cancer effects in a mouse xenograft model. *Cancer Lett.* 414, 88–98. doi: 10.1016/j.canlet.2017.10.039

Matkar, P. N., Singh, K. K., Rudenko, D., Kim, Y. J., Kuliszewski, M. A., Prud'homme, G. J., et al. (2016). Novel regulatory role of neuropilin-1 in endothelial-to-mesenchymal transition and fibrosis in pancreatic ductal adenocarcinoma. *Oncotarget* 7, 69489–69506. doi: 10.18632/oncotarget.11060

Migdal, M., Huppertz, B., Tessler, S., Comforti, A., Shibuya, M., Reich, R., et al. (1998). Neuropilin-1 is a placenta growth factor-2 receptor. *J. Biol. Chem.* 273, 22272–22278.

Morin, E., Sjoberg, E., Tjomsland, V., Testini, C., Lindskog, C., Franklin, O., et al. (2018). VEGF receptor-2/neuropilin 1 trans-complex formation between endothelial and tumor cells is an independent predictor of pancreatic cancer survival. *J. Pathol.* 246, 311–322. doi: 10.1002/path.5141

Mumblat, Y., Kessler, O., Ilan, N., and Neufeld, G. (2015). Full-Length Semaphorin-3C Is an Inhibitor of Tumor Lymphangiogenesis and Metastasis. *Cancer Res.* 75, 2177–2186. doi: 10.1158/0008-5472.can-14-2464

Napolitano, V., and Tamagnone, L. (2019). Neuropilins controlling cancer therapy responsiveness. *Int. J. Mol. Sci.* 20:2049. doi: 10.3390/ijms20082049

Ndiaye, P. D., Dufies, M., Giuliano, S., Douguet, L., Grepin, R., Durivault, J., et al. (2019). VEGFC acts as a double-edged sword in renal cell carcinoma aggressiveness. *Theranostics* 9, 661–675. doi: 10.7150/thno.27794

Niland, S., and Eble, J. A. (2019). Neuropilins in the context of tumor vasculature. *Int. J. Mol. Sci.* 20:639. doi: 10.3390/ijms20030639

Niland, S., and Eble, J. A. (2020). Neuropilin: handyman and power broker in the tumor microenvironment. *Adv. Exp. Med. Biol.* 1223, 31–67. doi: 10.1007/978-3-030-35582-1_3

Pagani, E., Ruffini, F., Antonini Cappellini, G. C., Scoppola, A., Fortes, C., Marchetti, P., et al. (2016). Placenta growth factor and neuropilin-1 collaborate in promoting melanoma aggressiveness. *Int. J. Oncol.* 48, 1581–1589. doi: 10.3892/ijo.2016.3362

Palodetto, B., Da Silva Santos Duarte, A., Rodrigues Lopes, M., Adolfo Corrocher, F., Marconi Roversi, F., Soares Niemann, F., et al. (2017). SEMA3A partially reverses VEGF effects through binding to neuropilin-1. *Stem Cell Res.* 22, 70–78. doi: 10.1016/j.scr.2017.05.012

Rey-Gallardo, A., Delgado-Martin, C., Gerardy-Schahn, R., Rodriguez-Fernandez, J. L., and Vega, M. A. (2011). Polysialic acid is required for neuropilin-2a/b-mediated control of CCL21-driven chemotaxis of mature dendritic cells and for their migration in vivo. *Glycobiology* 21, 655–662. doi: 10.1093/glycob/cw\break{}q216

Rizzolio, S., Battistini, C., Cagnoni, G., Apicella, M., Vella, V., Giordano, S., et al. (2018a). Downregulating Neuropilin-2 Triggers a Novel Mechanism Enabling EGFR-Dependent Resistance to Oncogene-Targeted Therapies. *Cancer Res.* 78, 1058–1068. doi: 10.1158/0008-5472.can-17-2020

Rizzolio, S., Cagnoni, G., Battistini, C., Bonelli, S., Isella, C., Van Ginderachter, J. A., et al. (2018b). Neuropilin-1 upregulation elicits adaptive resistance to oncogene-targeted therapies. *J. Clin. Invest.* 128, 3976–3990. doi: 10.1172/jci99257

Rizzolio, S., Rabinowicz, N., Rainero, E., Lanzetti, L., Serini, G., Norman, J., et al. (2012). Neuropilin-1-dependent regulation of EGF-receptor signaling. *Cancer Res.* 72, 5801–5811. doi: 10.1158/0008-5472.can-12-0995

Rizzolio, S., and Tamagnone, L. (2011). Multifaceted role of neuropilins in cancer. *Curr. Med. Chem.* 18, 3563–3575. doi: 10.2174/092986711796642544

Roy, S., Bag, A. K., Dutta, S., Polavaram, N. S., Islam, R., Schellenburg, S., et al. (2018). Macrophage-derived neuropilin-2 exhibits novel tumor-promoting functions. *Cancer Res.* 78, 5600–5617. doi: 10.1158/0008-5472.can-18-0562

Roy, S., Bag, A. K., Singh, R. K., Talmadge, J. E., Batra, S. K., and Datta, K. (2017). Multifaceted role of neuropilins in the immune system: potential targets for immunotherapy. *Front. Immunol.* 8:1228. doi: 10.3389/fimmu.2017.01228

Sakaguchi, S., Sakaguchi, N., Asano, M., Itoh, M., and Toda, M. (1995). Immunologic self-tolerance maintained by activated T cells expressing IL-2 receptor alpha-chains (CD25). Breakdown of a single mechanism of self-tolerance causes various autoimmune diseases. *J. Immunol.* 155, 1151–1164.

Sarris, M., Andersen, K. G., Randow, F., Mayr, L., and Betz, A. G. (2008). Neuropilin-1 expression on regulatory T cells enhances their interactions with dendritic cells during antigen recognition. *Immunity* 28, 402–413. doi: 10.1016/j.immuni.2008.01.012

Schellenburg, S., Schulz, A., Poitz, D. M., and Muders, M. H. (2017). Role of neuropilin-2 in the immune system. *Mol. Immunol.* 90, 239–244. doi: 10.1016/j.molimm.2017.08.010

Shan, T., Chen, S., Chen, X., Lin, W. R., Li, W., Ma, J., et al. (2017). Prometastatic mechanisms of CAF-mediated EMT regulation in pancreatic cancer cells. *Int. J. Oncol.* 50, 121–128. doi: 10.3892/ijo.2016.3779

Snuderl, M., Batista, A., Kirkpatrick, N. D., Ruiz De Almodovar, C., Riedemann, L., Walsh, E. C., et al. (2013). Targeting placental growth factor/neuropilin 1 pathway inhibits growth and spread of medulloblastoma. *Cell* 152, 1065–1076. doi: 10.1016/j.cell.2013.01.036

Stamatos, N. M., Zhang, L., Jokilammi, A., Finne, J., Chen, W. H., El-Maarouf, A., et al. (2014). Changes in polysialic acid expression on myeloid cells during differentiation and recruitment to sites of inflammation: role in phagocytosis. *Glycobiology* 24, 864–879. doi: 10.1093/glycob/cwu050

Stanton, M. J., Dutta, S., Zhang, H., Polavaram, N. S., Leontovich, A. A., Honscheid, P., et al. (2013). Autophagy control by the VEGF-C/NRP-2 axis in cancer and its implication for treatment resistance. *Cancer Res.* 73, 160–171. doi: 10.1158/0008-5472.can-11-3635

Takashima, S., Kitakaze, M., Asakura, M., Asanuma, H., Sanada, S., Tashiro, F., et al. (2002). Targeting of both mouse neuropilin-1 and neuropilin-2 genes severely impairs developmental yolk sac and embryonic angiogenesis. *Proc. Natl. Acad. Sci. U.S.A.* 99, 3657–3662. doi: 10.1073/pnas.022017899

Van Bergen, T., Etienne, I., Cunningham, F., Moons, L., Schlingemann, R. O., Feyen, J. H. M., et al. (2019). The role of placental growth factor (PlGF) and its receptor system in retinal vascular diseases. *Prog. Retin. Eye Res.* 69, 116–136. doi: 10.1016/j.preteyeres.2018.10.006

Van Cutsem, E., De Haas, S., Kang, Y. K., Ohtsu, A., Tebbutt, N. C., Ming Xu, J., et al. (2012). Bevacizumab in combination with chemotherapy as first-line therapy in advanced gastric cancer: a biomarker evaluation from the AVAGAST randomized phase III trial. *J. Clin. Oncol.* 30, 2119–2127. doi: 10.1200/jco.2011.39.9824

Wang, C. A., Harrell, J. C., Iwanaga, R., Jedlicka, P., and Ford, H. L. (2014). Vascular endothelial growth factor C promotes breast cancer progression via a novel antioxidant mechanism that involves regulation of superoxide dismutase 3. *Breast Cancer Res.* 16:462.

Wey, J. S., Gray, M. J., Fan, F., Belcheva, A., Mccarty, M. F., Stoeltzing, O., et al. (2005). Overexpression of neuropilin-1 promotes constitutive MAPK signalling and chemoresistance in pancreatic cancer cells. *Br. J. Cancer* 93, 233–241. doi: 10.1038/sj.bjc.6602663

Wu, M. H., Ying, N. W., Hong, T. M., Chiang, W. F., Lin, Y. T., and Chen, Y. L. (2014). Galectin-1 induces vascular permeability through the neuropilin-1/vascular endothelial growth factor receptor-1 complex. *Angiogenesis* 17, 839–849. doi: 10.1007/s10456-014-9431-8

Yaqoob, U., Cao, S., Shergill, U., Jagavelu, K., Geng, Z., Yin, M., et al. (2012). Neuropilin-1 stimulates tumor growth by increasing fibronectin fibril assembly in the tumor microenvironment. *Cancer Res.* 72, 4047–4059. doi: 10.1158/0008-5472.can-11-3907

Yin, D., Guo, L., Li, S., Tuerdi, A., Yang, X., Tang, Q., et al. (2020). Clinical significance of neuropilin-2 expression in laryngeal squamous cell carcinoma. *Am. J. Otolaryngol.* 41, 102540.

Yuan, L., Moyon, D., Pardanaud, L., Breant, C., Karkkainen, M. J., Alitalo, K., et al. (2002). Abnormal lymphatic vessel development in neuropilin 2 mutant mice. *Development* 129, 4797–4806.

Zhang, L., Wang, H., Li, C., Zhao, Y., Wu, L., Du, X., et al. (2017). VEGF-A/neuropilin 1 pathway confers cancer stemness via activating

wnt/beta-catenin axis in breast cancer cells. *Cell Physiol. Biochem.* 44, 1251–1262. doi: 10.1159/000485455

Zheng, C., Zhou, Q., Wu, F., Peng, Q., Tang, A., Liang, H., et al. (2009). Semaphorin3F down-regulates the expression of integrin alpha(v)beta3 and sensitizes multicellular tumor spheroids to chemotherapy via the neuropilin-2 receptor in vitro. *Chemotherapy* 55, 344–352. doi: 10.1159/000232449

Zhu, H., Cai, H., Tang, M., and Tang, J. (2014). Neuropilin-1 is overexpressed in osteosarcoma and contributes to tumor progression and poor prognosis. *Clin. Transl. Oncol.* 16, 732–738. doi: 10.1007/s12094-013-1141-y

Conflict of Interest: The authors declare that the research was conducted in the absence of any commercial or financial relationships that could be construed as a potential conflict of interest.

Appendix 6. Patent: New anti-VEGFC antibodies and uses thereof.

The present invention concerns new anti-VEGFC antibodies and their uses, in particular in the prevention and treatment of cancers and disorders characterized by undesirable lymphatic endothelial cell migration and/or proliferation.

Inventors: Gilles Pagès, Renaud Grépin and Aurore Dumond.

Form 1002 - 1: Public inventor(s)

Designation of inventor

User reference: B75798EPD40245
Application No:

Public

	Inventor	
	Name:	PAGES, Mr. Gilles
	Address:	37, boulevard du Larvotto 98000 MONACO Monaco
	The applicant has acquired the right to the European patent:	As employer
	Inventor	
	Name:	GREPIN, Mr. Renaud
	Address:	36 rue Lucien Faure Appartement B91 Batiment Allure 33300 BORDEAUX France
	The applicant has acquired the right to the European patent:	Under agreement:
	Inventor	
	Name:	DUMOND, Ms. Aurore
	Address:	34 avenue Jean Médecin Bat B 06000 NICE France
	The applicant has acquired the right to the European patent:	Under agreement:

Signature(s)

Place:	**Rennes**
Date:	**20 March 2020**
Signed by:	**/Armelle LEONARD/**
Association:	**REGIMBEAU**
Representative name:	**Armelle LEONARD**
Capacity:	**(Representative)**

Europäisches Patentamt | European Patent Office | Office européen des brevets

Acknowledgement of receipt

We hereby acknowledge receipt of your request for grant of a European patent as follows:

Submission number	1000496977	
Application number	EP20305296.4	
File No. to be used for priority declarations	EP20305296	
Date of receipt	20 March 2020	
Your reference	B75798EPD40245	
Applicant	CENTRE NATIONAL DE LA RECHERCHE SCIENTIFIQUE (CNRS)	
Country	FR	
Title	New anti-VEGFC antibodies and uses thereof	
Documents submitted	package-data.xml	ep-request.xml
	application-body.xml	ep-request.pdf (5 p.)
	SPECEPO-1.pdf\B75798 texte depot.pdf (41 p.)	SPECEPO-2.pdf\B75798 FIGURES DEPOT.pdf (5 p.)
	SEQLTXT.txt\B75798D75798_Projet Patentin_ST25.txt	f1002-1.pdf (1 p.)
Submitted by	EMAIL=bomer@regimbeau.eu,CN=Francoise BOMER,O=CABINET REGIMBEAU,C=FR	
Method of submission	Online	
Date and time receipt generated	20 March 2020, 16:28:05 (CET)	
Official Digest of Submission	E2:ED:B4:BA:D7:29:16:CA:50:DB:39:4D:04:80:C9:9B:06:CA:9A:9A	

/INPI, section dépôt/